



University of HUDDERSFIELD

University of Huddersfield Repository

Buj, David

KLOTHO PROTEINS KLO-1 AND KLO-2 INTERACT WITH DAF-2/DAF-16 PATHWAY TO REGULATE ENERGY METABOLISM, STRESS RESISTANCE AND AGEING

Original Citation

Buj, David (2019) KLOTHO PROTEINS KLO-1 AND KLO-2 INTERACT WITH DAF-2/DAF-16 PATHWAY TO REGULATE ENERGY METABOLISM, STRESS RESISTANCE AND AGEING. Doctoral thesis, University of Huddersfield.

This version is available at <http://eprints.hud.ac.uk/id/eprint/34852/>

The University Repository is a digital collection of the research output of the University, available on Open Access. Copyright and Moral Rights for the items on this site are retained by the individual author and/or other copyright owners. Users may access full items free of charge; copies of full text items generally can be reproduced, displayed or performed and given to third parties in any format or medium for personal research or study, educational or not-for-profit purposes without prior permission or charge, provided:

- The authors, title and full bibliographic details is credited in any copy;
- A hyperlink and/or URL is included for the original metadata page; and
- The content is not changed in any way.

For more information, including our policy and submission procedure, please contact the Repository Team at: E.mailbox@hud.ac.uk.

<http://eprints.hud.ac.uk/>

**KLOTHO PROTEINS KLO-1 AND KLO-2 INTERACT
WITH DAF-2/DAF-16 PATHWAY TO REGULATE
ENERGY METABOLISM, STRESS RESISTANCE
AND AGEING**

DAVID BUJ

A thesis submitted to the University of Huddersfield in partial fulfilment of the requirements for the degree
of Doctor of Philosophy

The University of Huddersfield

January 2019

Copyright statement

- i. The author of this thesis (including any appendices and/or schedules to this thesis) owns any copyright in it (the "Copyright") and s/he has given The University of Huddersfield the right to use such copyright for any administrative, promotional, educational and/or teaching purposes.
- ii. Copies of this thesis, either in full or in extracts, may be made only in accordance with the regulations of the University Library. Details of these regulations may be obtained from the Librarian. This page must form part of any such copies made.
- iii. The ownership of any patents, designs, trademarks and any other intellectual property rights except for the Copyright (the "Intellectual Property Rights") and any reproductions of copyright works, for example graphs and tables ("Reproductions"), which may be described in this thesis, may not be owned by the author and may be owned by third parties. Such Intellectual Property Rights and Reproductions cannot and must not be made available for use without the prior written permission of the owner(s) of the relevant Intellectual Property Rights and/or Reproductions

Abstract

Klotho was originally identified in mice presenting multiple age-related traits and shortened lifespan due to disruption of α -Klotho gene. β -Klotho was identified later, and it shares sequence and structural similarity and characteristics with α -Klotho. Klotho proteins are involved in the regulation of multiple signalling pathways due to being key regulators of endocrine fibroblast growth factor (FGF19, -21 and -23) signalling and participating in insulin/insulin like growth factor signalling (IIS). *Caenorhabditis elegans* has a simpler metabolism and reduced amount of paralog proteins than mammals, therefore reducing the complexity of the metabolic interactions. Hence *C. elegans* was used in this study to assess the role of Klothos for physiology of ageing and stress responses.

C. elegans klo-1 and *klo-2* are the gene orthologs of mammalian α - and β -Klotho and encode for proteins with only one KL domain rather than the two that form the mammalian Klotho. The effects of genetic deletions of *klo-1* and *klo-2* were assessed in *C. elegans*. In addition, *klo-1* and *klo-2* genetic mutations were studied in combinations with *daf-2/insulin receptor* and *daf-16/foxo* hypomorphic mutations. *klo-2* deficiency (*klo-2(ok1862)* mutation) significantly extended lifespan and improved resistance to heat stress. Both parameters were further improved in double mutants of *klo-2(ok1862)* and *daf-2(e1370)*. Synergy between *klo-1(ok2925)* and *daf-2(e1370)* also induced extended lifespan. *klo-1* deficiency alone was able to improve survival to oxidative stress. In addition, a trend was observed in progeny reduction, delayed development time and impaired lipid metabolism in *klo-1* and *klo-2* mutant worms. All alterations caused by *klo-1*, *klo-2* and *daf-2* alone or in combination were suppressed by *daf-16(mu86)* mutation.

The phenotypic effects observed in the mutant worms suggest that KLO-1 and KLO-2 regulate DAF-2/InsR pathway directly or indirectly through FGFR pathway. Both pathways are highly dependent of the activity of DAF-16, which will explain the dependency of KLO-1 and KLO-2 on functional DAF-16.

Table of Contents

Abstract.....	3
Table of Contents	4
List of Figures	12
List of Tables	16
Dedications and Acknowledgements	18
List of abbreviations.....	19
1 Introduction.....	21
1.1 Obesity and lifespan: a global health challenge	21
1.2 Klotho proteins	22
1.3 Endocrine fibroblast growth factors.....	24
1.4 Klotho interaction with FGF and FGFR.....	25
1.5 β -Klotho interacts with FGF19 to regulate cholesterol metabolism	26
1.6 Klotho interaction with FGF23 to control osmoregulation	27
1.7 β -Klotho role in regulation of energy homeostasis.....	28
1.7.1 β -Klotho and FGF21	28
1.7.2 β -Klotho and IIS	29

1.8	Klotho and stress resistance	32
1.9	<i>Caenorhabditis elegans</i> as a model organism.....	33
1.10	<i>C. elegans</i> Klotho proteins, KLO-1 and KLO-2	36
1.11	Sterol metabolism in <i>C. elegans</i>	37
1.12	Insulin signalling and ageing in <i>C. elegans</i>	39
1.13	Aim of present study.....	40
2	Materials and methods	41
2.1	<i>C. elegans</i> strains	41
2.2	Media	42
2.2.1	Nematode growth media	42
2.2.2	Bacteria growth media.....	42
2.2.3	Physiological solutions	42
2.2.4	Worm freezing media	43
2.3	Maintenance of <i>C. elegans</i>	43
2.4	Freezing and recovery of <i>C. elegans</i> stocks.....	43
2.5	Strain construction	44
2.6	Viable progeny Assay	45
2.7	Feeding behaviour	45

2.8	Lifespan Assays	46
2.9	Health status of adult worms.....	47
2.10	Stress assays	47
2.10.1	Oxidative stress assay survival	47
2.10.2	Oxidative stress induction of GFP reporter genes.....	47
2.10.3	Heat stress.....	48
2.10.4	Physiological Stress Assay.....	48
2.11	Development time.....	49
2.12	Dauer formation assay	49
2.13	Starvation.....	49
2.14	Microscopy.....	50
2.14.1	Microscopy of fixed animals	50
2.14.2	Microscopy of living animals.....	50
2.15	Lipid Staining	51
2.15.1	Sudan Black B	51
2.15.2	Oil-red-O staining.....	51
2.15.3	Nile red	52
2.16	Quantification of worm movement.....	52

2.17	Pumping rate	53
2.18	Molecular Biology methods	53
2.18.1	<i>C. elegans</i> genotyping	53
2.18.2	RNA extraction.....	54
2.18.3	RT-PCR	55
2.18.4	Cloning.....	56
2.18.5	Sequencing.....	56
3	Results.....	57
3.1	Klotho regulation of ageing	57
3.1.1	<i>C. elegans</i> Klotho orthologs, KLO-1 and KLO-2, interact with insulin/IGF-1 pathway to regulate worm lifespan	57
3.1.1.1	Effect of glucose on lifespan of Klotho mutant <i>C. elegans</i>	59
3.1.2	Analysis of progeny number	63
3.1.2.1	Progeny of Klotho mutant worms	63
3.1.2.2	Interaction between Klotho and insulin /IGF-1 pathway to control brood size	65
3.1.2.3	Glucose activates insulin /IGF-1 pathway to control brood size.....	67
3.1.3	Development time from egg to adult.....	69
3.1.3.1	Effect of glucose on development time	71

3.1.4	Cause of premature adult death	75
3.2	Health of <i>Klotho</i> mutant worms.....	78
3.2.1	Morphology and functionality of the pharynx in <i>Klotho</i> mutant worms	78
3.2.2	Movement of worms as an indicator of food sensitivity and metabolic rate	81
3.2.3	Healthy worms moving at 16 and 28 days of adult life	82
3.2.4	Cysts in <i>Klotho</i> mutant worms	86
3.2.4.1	Presence of cysts and malformation of digestive tract	86
3.2.4.2	The development of seam cells.....	88
3.3	Stress resistance.....	88
3.3.1	Oxidative stress	88
3.3.1.1	Survival on exposure to high concentration of paraquat	89
3.3.1.2	Superoxide dismutase gene expression is not altered in <i>Klotho</i> mutants upon oxidative stress response.	91
3.3.1.2.1	psod-3::GFP expression on larvae grown in the presence of paraquat	91
3.3.1.2.2	psod-3::GFP expression in adults stressed with paraquat for 30 minutes	94
3.3.2	Heat stress.....	96
3.3.2.1	Temperature dependent dauer formation of <i>Klotho</i> mutants	96
3.3.2.1.1	Dauer formation at 27 °C for 72 h (genetic deletion of <i>klo-2</i> induces dauer formation at 27 °C)	96

3.3.2.1.2	klo-2(ok1862) induces dauer formation at 25 °C	99
3.3.2.1.3	Dauer formation at 23 °C and 20 °C	100
3.3.2.2	Resistance to heat stress of larvae	104
3.3.2.2.1	Lethality at 27 °C of non-dauer larvae	104
3.3.2.2.2	Survival of L4 larvae from a heat shock at 37 °C.....	107
3.3.3	Response to osmotic stress caused by ion depletion	109
3.4	Klotho as a regulator of lipid metabolism and starvation	112
3.4.1	Starvation effect on expression of Klotho gene reporter	113
3.4.2	Lipid quantification	115
3.4.2.1	Nile red	115
3.4.2.2	Oil-red-O (ORO)	117
3.4.3	Expression of target proteins of DAF-16, involved in lipid homeostasis	117
3.4.3.1	atgl-1::GFP expression	117
3.4.3.2	fat-7::GFP expression is altered in Klotho mutant worms	119
3.4.4	Klotho regulation of cholesterol metabolism.....	121
3.4.4.1	Cholesterol depletion shortens lifespan of wild type and lifespan Klotho defective worms 121	
3.4.4.2	Cholesterol depletion effect on viable progeny sizebrood size	123

4 Discussion	128
4.1 Klotho regulation of ageing	128
4.1.1 KLO-1 and KLO-2 in the regulation of lifespan.....	128
4.1.2 <i>Effect of glucose on lifespan</i>	136
4.1.3 Extended lifespan of <i>daf-2</i> and <i>klo-2</i> double mutants is not caused by a reduced brood size or retarded development	137
4.1.4 Glucose increases production of viable progeny.....	139
4.2 Health of <i>Klotho</i> mutant worms.....	141
4.2.1 Klotho effect in food behaviour does not depend on motility.....	141
4.2.2 Klotho and DAF-2 act synergistically to increase healthspan and affect egg laying.....	142
4.3 Stress resistance.....	144
4.3.1 <i>klo-2</i> controls dauer formation independently of <i>daf-2</i> , but dependent of <i>klo-1</i>	144
4.3.2 KLO-2 acts synergistically with DAF-2 to regulate heat stress response in a KLO-1 dependent manner	147
4.3.3 KLO-1 controls the response to oxidative stress independently of DAF-2, but dependent on KLO-2	148
4.4 Klotho as regulator of lipid metabolism and starvation	152
4.4.1 Klotho proteins are needed for the utilization of lipids as energy source during fasting	152
4.4.2 Relation between <i>Klotho</i> and lipid metabolism proteins ATGL-1 and FAT-7.....	153

4.4.3	Klotho proteins help the worms to use cholesterol.....	155
4.5	Final conclusions and summary.....	157
	Bibliography.....	164
	Appendix 1.....	180
	Appendix 2.....	182
	Appendix 3.....	183

Words: 44,216

List of Figures

Figure 1 Schematic representation of human and worm <i>Klotho</i> proteins.....	23
Figure 2 Schematic representation of FGFR1 protein.....	26
Figure 3 Summary of metabolic interactions described.....	32
Figure 4 α - and β -Klotho interact with FGFs (FGF19, -21 and -23) and Insulin pathways to regulate energy and ion metabolism.....	32
Figure 5 <i>C. elegans</i> . Schematic drawing of a hermaphrodite (around 1mm).....	34
Figure 6 Conservation of the FGF/FGFR/Klotho interaction in human and <i>C. elegans</i>	35
Figure 7 β -Klotho is involved in the cross-talk interaction between FGF and IIS pathways to regulate cholesterol metabolism.	38
Figure 8 Diagram of a 5cm NGM plate with two different food sources: <i>E. coli</i> HB101 (HB) and <i>E. coli</i> OP50 (OP50).	46
Figure 9 Effect of <i>klo-1(ok2925)</i> , <i>klo-2(ok1862)</i> , <i>daf-2(e1370)</i> and <i>daf-16(mu86)</i> mutations on lifespan depending on media conditions (control or 2% glucose).....	63
Figure 10 Mean progeny of worms grown in standard NGM at 20 °C.....	64
Figure 11 Mean progeny of worms grown on control NGM or on 2 % glucose NGM at 20 °C.	66
Figure 12 Percentage of fully developed adult worms at 72 h (A), 84 h (B) and 96 h (C) after egg hatching.....	75
Figure 13 Percentage of censored worms in lifespan assay presented in the Figure 9 and Table 2...	77

Figure 14 Pharynx morphology of young adult worms.	78
Figure 15 Pumping rate (pumps / 30 seconds) \pm 95 % C.I. of N2 wild type, <i>klo-1(ok2925)</i> , <i>klo-2(ok1862)</i> and <i>klo-2(ok1862); klo-1(ok2925)</i> double mutant worms at 24 h, 48 h and 72 h of development..	79
Figure 16 Pumping rate (pumps / 30 seconds) \pm 95 % C.I. of N2 wild type, <i>klo-1(ok2925)</i> , <i>klo-2(ok1862)</i> and <i>daf-2(e1370)</i> <i>Klotho</i> mutant worms at one day of adult life (10 worms per strain).	80
Figure 17 Worm motility at different temperatures and upon temperature upshift.	82
Figure 18 Worms with <i>daf-2 (e1370)</i> mutation are healthier for longer time.	84
Figure 19 Assessment of digestive tract of wild type and <i>klo-2 (ok1862); klo-1 (ok2925)</i> worms at embryo and larvae stages.	87
Figure 20 Survival of L4 larvae in 300 mM paraquat after 9 h.	89
Figure 21 <i>psod-3::GFP</i> expression in L3 stage worms grown in NGM with or without 0.25 mM paraquat.	92
Figure 22 <i>psod-3::GFP</i> expression in larvae grown 48 h on NGM with or without 0.25 mM paraquat.	93
Figure 23 <i>psod-3::GFP</i> expression.	95
Figure 24 Dauer formation at 27°C.	97
Figure 25 Dauer formation at 25 °C.	99
Figure 26 Dauer formation at 23 °C and 20 °C.	102
Figure 27 Dead larvae at 27 °C.	105
Figure 28 Survival of <i>Klotho</i> mutants at 37 °C.	108

Figure 29 Percentage of adult worms at different time points (time 0 h corresponds to time of egg been lay).....	111
Figure 30 Expression of <i>pklo-1::RFP</i> and <i>pklo-2::GFP</i>	114
Figure 31 Lipid staining and quantification.....	116
Figure 32 Expression of <i>ATGL-1::GFP</i>	118
Figure 33 Expression and quantification of <i>fat-7::GFP</i>	121
Figure 34 Effect of cholesterol depletion.....	122
Figure 35 Explanation of the selected animals from worms grown in depleted (0 mM) cholesterol NGM for progeny quantification assay.	124
Figure 36 Mean progeny of N2 wild type and <i>klo-2(ok1862); klo-1(ok2925)</i> double mutant worms grown in standard NGM (+ control) or 0 mM cholesterol NGM.	126
Figure 37 Proposed model of protein interactions between <i>kLO-1</i> , <i>KLO-2</i> , <i>DAF-2</i> and <i>DAF-16</i> , including an unknown ageing mediator protein called “Protein X”, which leads to alterations of lifespan.....	130
Figure 38 Proposed model of protein interactions between <i>kLO-1</i> , <i>KLO-2</i> , <i>DAF-2</i> and <i>DAF-16</i> , including an unknown ageing mediator protein called “Protein X”, which leads to alterations of lifespan.....	133
Figure 39 Proposed model of interactions between <i>KLO-1</i> and glucose in the regulation of IIS pathway.	137
Figure 40 Phenotypic observations and proposed model for regulation of thermotolerance and thermogenesis.....	146
Figure 41 Proposed model of protein interactions between <i>KLO-1</i> , <i>KLO-2</i> , <i>DAF-2</i> and <i>DAF-16</i> , including an unknown mediator protein called “Oxidative stress activator”.	150

Figure 42 Human and worm metabolism of cholesterol. 156

Figure 43 Summary of metabolic interactions described. 163

List of Tables

Table 1 Primer sets to genotype <i>klo-1(ok2925)</i> , <i>klo-2(ok1862)</i> , <i>daf-2(e1370)</i> and <i>daf-16(mu86)</i>	54
Table 2 Mean lifespan of worms maintained in standard or 2 % glucose NGM.	61
Table 3 Mean progeny \pm 95 % C.I. of wild type, <i>klo-1(ok2925)</i> , <i>klo-2(ok1862)</i> and double mutant <i>klo-2(ok1862); klo-1(ok2925)</i> worms.	65
Table 4 Mean progeny \pm 95 % C.I. of wild type, <i>daf-2(e1370)</i> mutants, <i>daf-2(e1370) klo-2(ok1862); klo-1(ok2925)</i> mutants and <i>daf-16(mu86); daf-2(e1370) klo-2(ok1862); klo-1(ok2925)</i> mutant worms.....	68
Table 5 Percentage of adults at different time points of development in standard conditions (NGM) and in 2 % glucose.	72
Table 6. Healthy animals at 16 and 28 days of adult life.	85
Table 7 Survival of worms in 300 mM paraquat.....	90
Table 8. Values of <i>psod-3::GFP</i> expression in larvae grown in NGM with or without 0.25 mM paraquat for 48 h.	93
Table 9. <i>psod-3::GFP</i> values of one day old adult worms treated with 100 mM paraquat for 30 min followed by 3 hours recovery in standard NGM with food.	94
Table 10 Percentage of animals entering dauer state at 27 °C.	98
Table 11 Percentage of animals entering dauer state at 25 °C.	100
Table 12 Percentage of animals entering dauer state at 23 °C and 20 °C.	103
Table 13 Percentage of dead larvae after 72 h at 27 °C.....	106

Table 14 Percentage of living animals after 8 h incubation at 37 °C.	109
Table 15 Percentage of adult worms at 60 and 72 h of development in standard conditions (NGM) or ion depleted NGM (0 mM Ca ²⁺ , 0 mM Mg ²⁺ and 0 mM K ⁺).....	112
Table 16 Lifespan is reduced in cholesterol depleted NGM.	122
Table 17 Mean progeny ± 95 % C.I. of wild type and <i>klo-2(ok1862)</i> ; <i>klo-1(ok2925)</i> worms grown in standard NGM or 0 mM cholesterol NGM.....	127
Table 18 Main phenotypic alterations observed	159

Dedications and Acknowledgements

I am very thankful to all the people that help me during these years of hard work. Thanks to everyone in the University of Huddersfield, to the technicians for their support and their patience with me, to my postgraduate colleagues and especially to my supervisor. I am very pleased that I had a supervisor that was always available and friendly, and at the same time was pushing me for the best. Thank you Tarja, you have worked so hard to make this thesis possible. Thank you!

I want to thank my friends for these great years and family for their support and education. I want to thank my wife for the constant support too, for the extraordinary constant efforts she made to take care of our family while I was working on this thesis. Gracias cariño, este trabajo es de los dos.

Finally, I want to thank the Ballester family that took care of my wife and I since we arrived at Huddersfield. I am especially thankful to the father, Pedro, for all the motivation and support. I will always remember our daily conversation on the way to work. I also want to remember his son, my friend Pedrito, who is taking care of us all from heaven. Pedrito, this work is dedicated to you.

List of abbreviations

1,25(OH)₂D - 1,25-dihydroxycholecalciferol

ADAM - A Disintegrin and Metalloproteinase

akt-1 – RAC-alpha serine/threonine-protein kinase also known as PKB

AMPK – adenosine monophosphate-activated protein kinase

C. elegans - *Caenorhabditis elegans*

Cyp24 - 24-hydroxylase

Cyp27b1 - 1 α -hydroxylase

CYP7A1 - cholesterol 7 alpha-hydroxylase

DA - dafachronic acid

DAF – abnormal dauer formation

DAF-12- worm homolog to mammal FXR

DAF16 - worm homolog to mammal FOXO

DAF-18 - worm homolog to mammal PTEN

DAF-2 - worm homolog to mammal InsR

ERK – extracellular signal-regulated kinase

FGF - Fibroblast growth factor

FGFR - Fibroblast growth factor Receptor

FXR – farnesoid-X receptor

FOXO - Forkhead box protein O1

hsKlotho - Human spliced Klotho

IGF-1 - Insulin-like growth factor-1

InsR - Insulin/IGF-1 receptor

IIS - Insulin/IGF-1 signalling

LKB1 - liver kinase B1, also known as serine/threonine kinase 11 (STK11)

MAPK – mitogen activated protein kinase

PGC-1 α - Peroxisome proliferator-activated receptor gamma coactivator 1-alpha

PI3-K - phosphatidylinositol 3-kinase

PIP2 - phosphatidylinositol (3,4)-bisphosphate

PIP3 - phosphatidylinositol (3,4,5)-trisphosphate

PKB - protein kinase B

PPAR - Peroxisome proliferator-activated receptor gamma

PTEN - phosphatidylinositol-3,4,5-trisphosphate 3-phosphatase)

SIRT1 - Sirtuin 1, also known as NAD-dependent deacetylase sirtuin-1

TRPV5 - transient receptor potential ion channel

1 Introduction

1.1 Obesity and lifespan: a global health challenge

All living organisms depend on appropriate nutrition for health, growth and function. Genetic or physiological disturbances in the processing of nutrients (food) lead to metabolic disorders including obesity, which is a growing health problem.

Between 1993 and 2012 the proportion of obese adults in England increased from 13.2% to 24.4% among men and from 16.4% to 25.1% among women (Lifestyles statistics team, 2014). During that time period, the proportion of overweight adults (including obese) increased from 57.6% to 66.6% among men and from 48.6% to 57.2% among women (Lifestyles statistics team, 2014). The number of obese children also increased from 17.5% in 2006/07 to 18.9% in 2011/12 (Lifestyles statistics team, 2014).

Obesity increases the risk of life-threatening diseases such as type II diabetes, heart disease, certain types of cancers and stroke. It is estimated that in England more than 34,000 deaths a year are caused by obesity which represents 7 % of all deaths (Lifestyles statistics team, 2014). The principle cause of obesity is too high energy intake compared to energy expenditure, because excess calories are stored as fat.

Intake of excess amount of food increases glucose levels in blood abnormally and in consequence the production of insulin is incremented to induce the absorption of glucose mainly by the liver, muscle and adipose tissue. Higher than normal amounts of circulating insulin induce over-activation of insulin/insulin-like growth factor 1 (IGF-1) receptor (InsR) and an increased activity of insulin/IGF-1 signalling (IIS) pathway, which makes it possible to store high quantity of energy as lipids. The result is an increased lipid storage leading to overweight and obesity (Klip & Pâquet, 1990; Kulkarni et al., 1999; Pan et al., 1997; Saltiel & Kahn, 2001).

The repetitive over-activation of InsR may lead to insulin resistant state called type II diabetes (Kulkarni et al., 1999; Saltiel & Kahn, 2001). Therefore, overweight and obesity disorders increase the risk of developing diabetes. For example, the probability to develop type II diabetes is 13 times higher in obese women as compared to not obese women (Lifestyles statistics team, 2014).

IIS pathway is evolutionary conserved and regulates growth, development and lifespan (Taniguchi, Emanuelli, & Kahn, 2006). Alterations in IIS are associated with growth dysfunctions, cancer, insulin resistance, obesity and diabetes (Lindhurst et al., 2012). Increased activity of IIS pathway also induces premature ageing (Blüher, Kahn, & Kahn, 2003; Gottlieb & Ruvkun, 1994).

Recently, a protein called Klotho was discovered to modulate ageing and energy metabolism too (Kuro-o et al., 1997; Yamamoto et al., 2005). Moreover, Klotho protein has been shown to interact with IIS (Yamamoto et al., 2005). In this thesis the role of Klotho in ageing, development, reproduction, energy and ion metabolism will be assessed.

1.2 Klotho proteins

There are three Klotho proteins, α -Klotho, β -Klotho and γ -Klotho which are type I single pass transmembrane proteins (Iglesias, Selgas, Romero, & Diez, 2012; Ito et al., 2000; Kharitonov, 2009; Kuro-o et al., 1997). α -Klotho was originally identified in a mouse strain with *α -Klotho* disrupted gene (Kuro-o et al., 1997). This mouse presented multiple age-related traits and shortened lifespan (Kuro-o et al., 1997). β -Klotho was identified later and it shares structural identity and characteristics with α -Klotho (Ito et al., 2000). β -Klotho deficient mutant mice have no obvious abnormalities (normal lifespan), however, they have altered bile acid metabolism (Ito et al., 2005; Kurosu et al., 2007).

α - and β -Klotho proteins are expressed in different tissues. α -Klotho is expressed mostly in the kidney and the brain of young and adult mice (Kuro-o et al., 1997). β -Klotho is predominantly expressed in the

liver and pancreas of adult mice (Ito et al., 2000). During mouse embryonic development, β -Klotho is highly expressed in the gut, yolk, liver, pancreas, and white and brown adipose tissues (Ito et al., 2000); in contrast, α -Klotho expression is not detected during early embryonic development (Kuro-o et al., 1997).

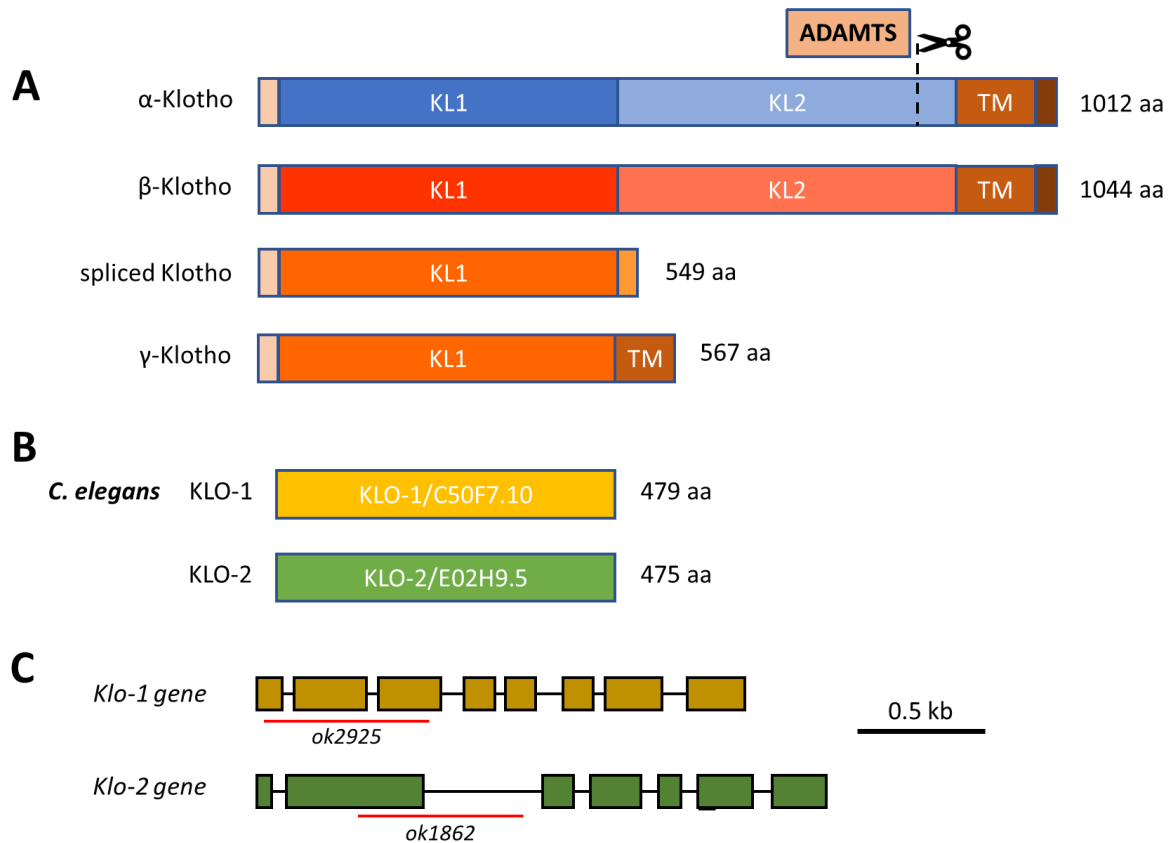


Figure 1 Schematic representation of human and worm *Klotho* proteins

A: Human α - and β -Klotho proteins are 1012 and 1044 amino acids long respectively and consists of a short cytoplasmic tail (dark brown), transmembrane domain (light brown), two Klotho domains (KL1 and KL2) and a signal peptide (beige). KL1 and KL2 domains have 32 - 34 % sequence identity between them. Vertebrate α -Klotho can be cleaved by ADAM10 and ADAM17 (scissors), producing a shorter soluble α -Klotho protein without transmembrane domain. Alternative splicing of human α -Klotho mRNA produces 549-amino acid protein consisting of KL1 domain (spliced Klotho). Similar to alternatively spliced α -Klotho, there is γ -Klotho which consists mainly of KL-1 domain with a shorter transmembrane domain. B: *C. elegans* has two Klothos, KLO-1 and KLO-2 which consist of a single kl domain of 479 and 475 amino acids (aa) respectively. D: schematic structure representing *C. elegans Klotho* orthologs *klo-1* (C50F7.10) and *klo-2* (E02H9.5). Boxes represent exons and black lines represent introns. Underlined in red are the *klo-1* deletion *ok2925* and *klo-2* deletion *ok1862*.

In humans, the two Klotho paralogs are 41.2 % identical and both share homology to family 1 glycosidases (Ito et al., 2000). Around 1000 amino acids constitute the vertebrate α -Klotho and β -Klotho proteins and they consist of a signal peptide on the amino terminus, two Klotho domains (KL1 and KL2) with a 32 - 34 % sequence identity between them, a transmembrane domain and a small cytoplasmic domain (Figure 1) (Matsumura et al., 1998; Shiraki-Iida et al., 1998). Vertebrate Klothos can be cleaved by the A Disintegrin and Metalloproteinase ADAM10 and ADAM17, which cut the extracellular domain from the membrane domain allowing the soluble Klotho protein to circulate in the bloodstream (Bloch et al., 2009; Chen, Podvin, Gillespie, Leeman, & Abraham, 2007; Kurosu et al., 2005). Also, the human Klotho mRNA can be alternatively spliced, producing a secreted protein of 549-amino acids which mainly consists of the KL1 domain (Matsumura et al., 1998; Shiraki-Iida et al., 1998)). Moreover, there is another protein called γ -Klotho (567 amino acids long) which consists of KL-1 domain and a shorter transmembrane domain (Ito, Fujimori, Hayashizaki, & Nabeshima, 2002; Trošt, Peña-Ilopis, Koirala, & Stojan, 2015). However, little is known about the function of γ -Klotho (Figure 1).

α -Klotho has been shown to reduce lifespan by different mechanisms. α -Klotho and β -Klotho interact with a subfamily of fibroblast growth factors (FGFs), the FGF19 subfamily consisting of FGF19, -21 and -23, to regulate mineral and energy homeostasis (Berglund et al., 2009; Inagaki et al., 2005; Lin, Wang, Blackmore, & Desnoyers, 2007; Nishimura, Nakatake, Konishi, & Itoh, 2000; Polanska, Edwards, Fernig, & Kinnunen, 2011; Wu et al., 2007; X. Wu et al., 2008; Xie et al., 1999). The cross-talk between Klotho and IIS pathway is another way in which Klotho regulates energy homeostasis and, in consequences, lifespan too (Chen et al., 2007; Kurosu et al., 2005; Unger, 2006).

1.3 Endocrine fibroblast growth factors

In vertebrates, α -Klotho and β -Klotho have been shown to regulate the interaction between FGF19 subfamily of FGFs (also known as the endocrine FGFs) and their cognate FGF receptors (FGFRs)

(Iglesias et al., 2012; Kharitonov, 2009). These endocrine FGFs (FGF19, 21 and 23 in humans) do not readily bind to FGFRs and need α -Klotho and β -Klotho as cofactors (Iglesias et al., 2012; Kharitonov, 2009) to bind and signal through their canonical FGFRs.

The endocrine FGFs normally have very low affinities to canonical FGFRs and to heparan sulphate co-receptors and thus remain in circulation (Eswarakumar, Lax, & Schlessinger, 2005; Kurosu et al., 2006; Razzaque & Lanske, 2007). Tissue-specific expression of α - and β -Klotho provides specific sites of action for these endocrine FGFs (Kharitonov et al., 2008; Kurosu et al., 2006; Lin et al., 2007). Specifically, FGF21 requires β -Klotho to bind FGFR to mediate energy metabolism (Kharitonov et al., 2008), and FGF23 requires α -Klotho to mediate phosphate and calcium metabolism in the bone-kidney axis (Kurosu et al., 2006; Urakawa et al., 2006). FGF19 can utilize either α - or β -Klotho as co-receptor (Lin et al., 2007; Wu et al., 2007) or can bind and activate the FGFR4 without the help of Klotho co-factors (Wu et al., 2007; X. Wu et al., 2008; Xie et al., 1999).

Although all three endocrine FGFs are able to act through same FGFRs in any part of the body, each of them have a specific physiological role: FGF19 is involved in cholesterol metabolism and bile acid (BA) synthesis, FGF21 plays an important role in lipid and glucose homeostasis and FGF23 regulates phosphate and calcium homeostasis ((Inagaki et al., 2005; Nishimura et al., 2000); for a review see (Kharitonov, 2009)).

1.4 Klotho interaction with FGF and FGFR

α -Klotho binds to FGFR to create a new site for FGF23 C-terminal tail, while β -Klotho binds FGF19/FGF21 C-terminal tail and the FGFR independently with two distinct binding sites (Goetz et al., 2012). At least in the case of FGFR1, α - and β -Klotho bind to the third immunoglobulin Ig domain III (Goetz et al., 2012). Binding of FGF/Klotho/FGFR complex causes FGFR dimerization and triggers autophosphorylation and activation of the FGFR tyrosine kinase domains (Eswarakumar et al., 2005;

Lemmon & Schlessinger, 2010). Tyrosine autophosphorylation controls the protein tyrosine kinase activity of the receptor but also serves as a mechanism for assembly and recruitment of intracellular signalling complexes (Lemmon & Schlessinger, 2010).

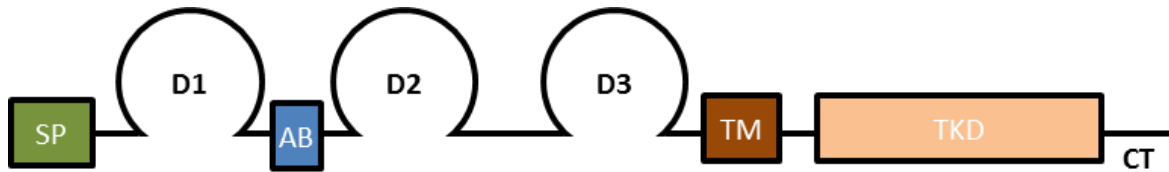


Figure 2 Schematic representation of FGFR1 protein.

Signal peptide (SP), acidic box (AB), immunoglobulin like domains (D1–3), transmembrane domain (TM), tyrosine kinase domains (TKD), and C-terminal tail (CT) are shown. Adapted from (Miraoui, Dwyer, & Pitteloud, 2011)

1.5 β -Klotho interacts with FGF19 to regulate cholesterol metabolism

Human FGF19 is highly expressed in the gut and in mice, over-expression of its mouse homolog, FGF15, reveals decreased levels of plasma glucose, triglycerides, total cholesterol, and liver fat content, as well as decreased levels of insulin, leptin, glucagon and IGF-1 ((Tomlinson et al., 2002) for review see (Kharitonov, 2009)). This is caused by the interaction of FGF19 with FGFR4/ β -Klotho to suppress bile acid synthesis and hepatocyte proliferation (A. L. Wu et al., 2011).

FGF19/FGFR4/ β -Klotho complex activation leads to phosphorylation of the extracellular signal-regulated kinase (ERK1/2) which in turn inhibits cholesterol 7 α -hydroxylase (CYP7A1) so that cholesterol cannot be metabolised into bile acid and other sterols (Tomiya et al., 2010; A. L. Wu et al., 2011).

1.6 Klotho interaction with FGF23 to control osmoregulation

In α -Klotho deficient mice (Kuro-o et al., 1997), overproduction of 1,25(OH)₂D (1,25-dihydroxycholecalciferol, the active metabolite of vitamin D) and altered calcium and phosphate ion homeostasis are the major cause of the ageing like phenotype (Tsujikawa, Kurotaki, Fujimori, Fukuda, & Nabeshima, 2003).

FGF23 interacts with α -Klotho in the kidney and controls serum levels of 1,25(OH)₂D by regulating the metabolising enzymes of vitamin D, 1 α -hydroxylase (Cyp27b1) and 24-hydroxylase (Cyp24) (Urakawa et al., 2006). FGF23 was discovered while screening genetic alterations causing autosomal dominant hypophosphatemic rickets (T Shimada et al., 2001; White et al., 2000, 2001). FGF23 knockout animals present high levels of Ca²⁺, phosphate and vitamin D levels in the plasma, and ectopic calcification of soft tissues, alterations in bone mineralization and shortened lifespan (Takashi Shimada et al., 2004) phenocopying α -Klotho deficient mice (Kuro-o et al. 1997). High expression of α -Klotho in the kidney reconstitutes FGFR1(IIIc) into the specific receptor for FGF23, targeting the tissue for FGF23 renal action (Urakawa et al., 2006).

It has been suggested that α -Klotho may have glycosidase activity (Kuro-o et al., 1997; Tohyama et al., 2004) and is able to modulate glycans on transient receptor potential ion channel (TRPV5) in human and mouse cells *in vitro* (Chang et al., 2005). TRPV5 is a Ca²⁺ channel that when mutated causes alterations in the homeostasis of Ca²⁺, comparable to those observed in α -Klotho-deficient mice (Cha et al., 2008; Chang et al., 2005).

1.7 β -Klotho role in regulation of energy homeostasis

1.7.1 β -Klotho and FGF21

FGF21 regulates energy homeostasis by enhancing the efficiency and functionality of mitochondria through the activation of 5'AMP-activate protein kinase (AMPK) and sirtuin 1 (SIRT1) (Chau, Gao, Yang, Wu, & Gromada, 2010). In vertebrates, FGF21 interacts with β -Klotho and FGFR1c or FGFR4 to phosphorylate ERK1/2 which activates liver kinase B1 (LKB1; a serine/threonine kinase) and subsequently AMPK. Activation of AMPK increases the cellular levels of NAD⁺, which in turn activates SIRT1. Activated SIRT1 induces the activity of proteins like forkhead box O (FOXO), farnesoid X receptor (FXR), heat-shock factor 1 (HSF-1) and peroxisome proliferator-activated receptor gamma coactivator 1-alpha (PGC-1 α) among others, which enhances mitochondrial function and oxidative capacity (Chau et al., 2010; Westerheide, Anckar, Stevens Jr., Sistonen, & Morimoto, 2009) .

It has been proposed that tissue-specific expression of β -Klotho could be targeting the tissue-specific action of FGF21 (Kharitonov et al., 2008), although FGF21 can act independently of β -Klotho in mouse adipose tissue (Tomiyama et al., 2010). FGF21 is secreted from liver upon fasting and acts on white adipose tissue to promote glucose uptake and lipolysis (Inagaki et al., 2007; Kharitonov et al., 2005). These effects almost mirror the ones observed for FGF19 (Coskun et al., 2008; Kharitonov et al., 2005), probably because both FGFs use the same cofactor, β -Klotho, suggesting there could an overlap in the functions of FGF21 and -19 *in vivo*.

FGF21 expression in the white adipose tissue is induced after feeding (Badman et al., 2007; Muise et al., 2008). Pharmacological administration of recombinant FGF21 protein to diabetic mice and rhesus monkeys strongly enhances insulin sensitivity, decreases plasma glucose and triglycerides, preserves pancreatic beta-cell functions and improves resistance to diet-induced and age-induced weight gain and fat accumulation (Foltz et al., 2012; Kharitonov et al., 2005). Administration of FGF21 to obese/overweight humans with type 2 diabetes reduced body weight and increased IGF1 and triglyceride levels (Talukdar, Zhou, et al., 2016) similar to those observed in obese mice and monkeys.

In obese mice (ob/ob mutants), recombinant FGF21 starts reducing plasma glucose 4h after administration, but the half-life of FGF21 is only 0.7 - 1.1 hours, which means that FGF21 is no longer in circulation when the effect takes place (Kharitonov et al., 2005). This suggests that FGF21 induces the transcription of target genes which then promote the uptake of glucose.

In humans, FGF21 is related to attenuation of catecholamine-stimulated (but not basal) lipolysis in fat cells expressing β -Klotho (Kharitonov et al., 2008; Ogawa et al., 2007). Concentrations of FGF21 in circulation are significantly elevated in obese rodents responding poorly to exogenous FGF21 (Hale et al., 2012), suggesting that obesity could be an FGF21-resistant state (Fisher et al., 2011). These results together with those on fasting physiology suggest that FGF21 gene expression responds to both fasting and feeding and may be induced in nutritional crisis, including starvation and overfeeding (Uebanso et al., 2011). However, studies analysing the response of FGF21 to weight loss in humans have shown controversial findings (Dong et al., 2015; Gaich et al., 2013).

The capacity of FGF21/ β -Klotho/FGFR complex to regulate glucose and lipid metabolism makes it an important target for treatment of obesity and diabetes and FGF21 is currently in clinical trials (Dong et al., 2015; Gaich et al., 2013). But the regulation of FGF21 in whole metabolism has a negative effect on bone mineral balance. Recent assays show that long term treatment of diabetic patients with FGF21 could enhance bone loss often associated with diabetes (Wei et al., 2012). Better understanding of the regulatory effect of β -Klotho in this pathway would be beneficial for developing new treatments for obesity and diabetes.

1.7.2 β -Klotho and IIS

IIS signalling is composed by a highly integrated network that regulates development and metabolism (Taniguchi et al., 2006). Insulin activates the insulin receptor (IR) which phosphorylates insulin receptor substrate (IRS) proteins to activate two main signalling pathways. The first one is the phosphatidylinositol 3-kinase (PI3K)-AKT/protein kinase B (PKB) pathway, which is the signalling

cascade responsible for the vast majority of metabolic actions of insulin. The second pathway is the Ras-mitogen-activated protein kinase (MAPK), which is involved in gene regulation and interacts with the PI3K pathway to regulate cell growth and differentiation (Avruch, 1998).

Lifespan alterations are also observed in Klotho mutant mice. Reduction-of-function and loss-of-function mutations of α -Klotho in mice produced a lifespan shortening and mice over-expressing α -Klotho have longer lifespan and have less progeny (Kuro-o et al., 1997; Kurosu et al., 2005). The same effects on lifespan and progeny were observed in mice with a reduction of insulin function.

FGF21 has a potent effect on glucose uptake in adipocytes (Kharitonkov et al., 2005). The sensitization of insulin action is considered to be the major mechanism by which FGF21 reduces high levels of plasmatic glucose. Insulin can also impact the FGF21 pathway, making a physiological crosstalk between these two molecules possible (Berglund et al., 2009). FGF21 has been postulated as regulator of glucose metabolism by inducing glucose transporter 1 (GLUT1) (Kharitonkov et al., 2005), while insulin is known to activate GLUT4 translocation (Avruch, 1998).

FGF21 and insulin pathways have Klotho as a direct or indirect modulator of their interaction with their respective receptors (Chau et al., 2010; Chen et al., 2007; Unger, 2006; Westerheide et al., 2009). It has been shown that Klotho defective mice are extremely sensitive to insulin, while mice overexpressing Klotho are insulin-resistant (Kuro-o, 2010). In vivo, insulin increases serum levels of Klotho protein, which in turn inhibits insulin signalling (Chen et al., 2007; Matsumura et al., 1998). Insulin enhances the activity of ADAM7 and ADAM10 to cleave α and β -Klotho from the membrane (Chen et al., 2007). Then, higher concentrations of soluble Klotho inhibit autophosphorylation of Insulin/IGF-1 Receptor and the association with PI3K and AKT-1 thus downregulating IIS (Chen et al., 2007; Kurosu et al., 2005; Unger, 2006).

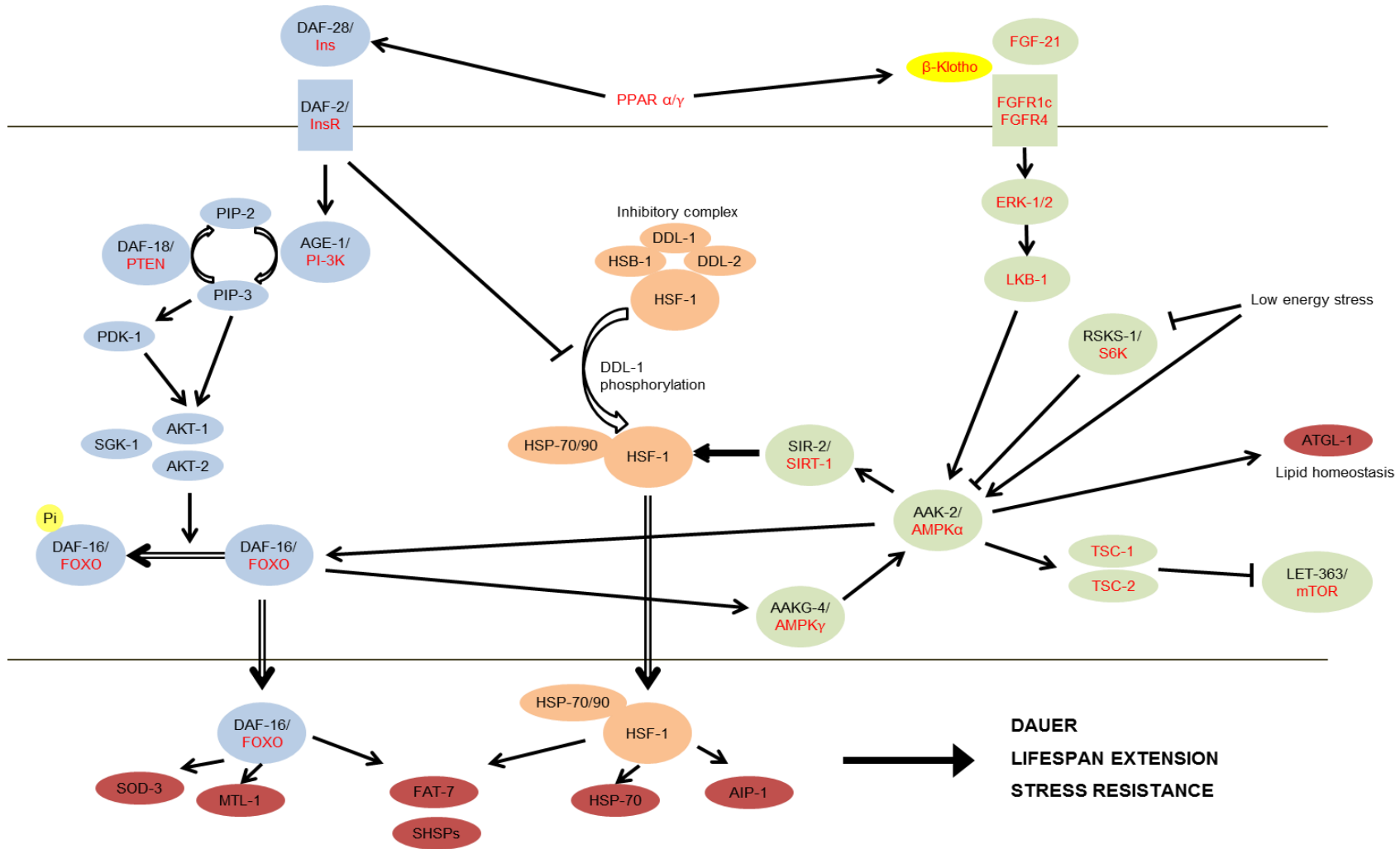


Figure 3 Summary of main proteins involved in insulin and FGF metabolism.

Proteins involved in IIS pathway are coloured in blue and proteins downstream β -Klotho/FGF/FGFR interaction are coloured in green. Protein names in red font refer to mammalian proteins and in black font to *C. elegans* proteins. Both IIS and FGF pathways regulate DAF-16/FOXO activity and the transcription of multiple DAF-16 target genes (coloured in garnet). HSF-1 could also be activated by proteins downstream FGF signalling to induce transcription of multiple genes, and together with DAF-16 could cause dauer formation, lifespan extension or stress resistance.

1.8 Klotho and stress resistance

α -Klotho regulates IIS pathway by suppressing the phosphorylation of insulin/IGF-1 receptor (Kurosu et al., 2005). α -Klotho is therefore inhibiting the phosphorylation of FOXO and promoting FOXO entering the nucleus and to upregulate the transcription of SOD2, conferring more resistance to oxidative stress (Yamamoto et al., 2005).

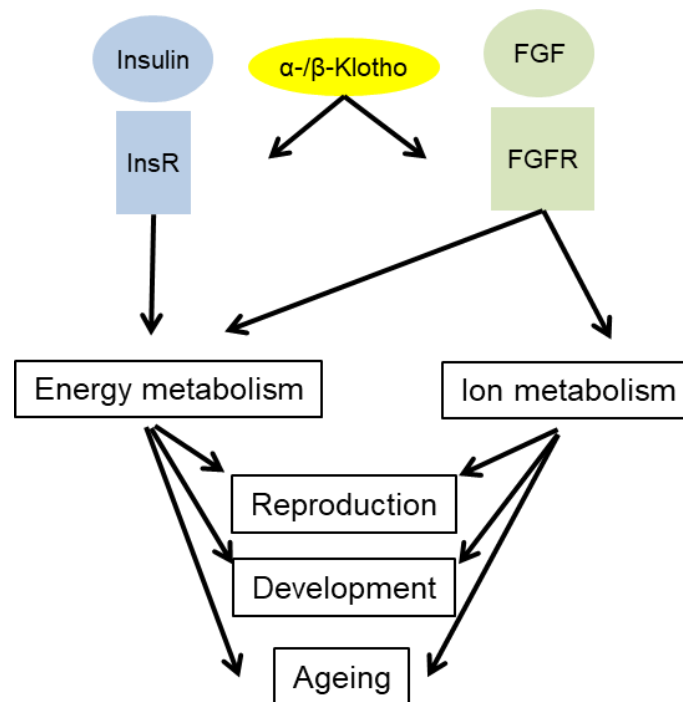


Figure 4 α - and β -Klotho interact with FGFs (FGF19, -21 and -23) and Insulin pathways to regulate energy and ion metabolism.

β -Klotho also has a role in regulating the resistance to stress by enhancing the interaction of FGF21 with FGFR1c or FGFR4, which activates AMPK α (Chau et al., 2010). This leads to the expression of stress resistance genes by direct activation of FOXO or by activation of HSF-1 through SIRT-1 (Chau et al., 2010; Westerheide et al., 2009) .

1.9 *Caenorhabditis elegans* as a model organism

Because α - and β -Klotho are involved in the regulation of multiple physiological and metabolic pathways the use of an organism with relatively simpler metabolism, reduced genetic redundancy and genetic tractability to study Klotho function *in vivo* is very useful. This is why the nematode *Caenorhabditis elegans* was used as model organism in this thesis.

After a decade from his first thoughts, in 1974 Sydney Brenner published four manuscripts including one entitled 'The genetics of *Caenorhabditis elegans*' (Brenner, 1974) to explain the methodology for using *C. elegans* as a model organism. Almost twenty-five years later, in 1998, the *Caenorhabditis elegans* consortium completed the sequence of the 100 Mb genome of this tiny and free living nematode, which contains 20,444 protein-coding genes, becoming the first animal to have its full genome sequenced (Spieth, Lawson, Davis, Williams, & Howe, 2014; The *C. elegans* sequencing consortium, 1998).

Main reasons why *C. elegans* is a good model organism are that worms are cheap to maintain, there are males and self-fertilizing hermaphrodites, they are small in size (1mm long when adults) and they have large broods (~300 eggs /adult worm), they have short life cycle of 3 days at 20 °C, their cell number and development are invariant and their transparency allows for cell and tissue visualization, and the use of fluorescent markers to study *in vivo* processes (L Avery & You, 2012; Chalfie, Tu, Euskirchen, Ward, & Prasher, 1994; Corsi, Wightman, & Chalfie, 2015).

The success of *C. elegans* as a model organism can be attributed to the highly conserved genes from worms to humans. Several human disorders and diseases are caused by mutations in genes with homologies in *C. elegans* (Culetto & Sattelle, 2000). For 60 to 80 % of human genes there is an orthologous gene in the *C. elegans* genome (Kaletta & Hengartner, 2006) and orthologous sequences have been found in *C. elegans* for around 40 % of the genes associated to human diseases (Culetto & Sattelle, 2000; Silverman et al., 2009). These genomic homologies make the discoveries in *C. elegans* relevant to study of human health, diseases and disorders.

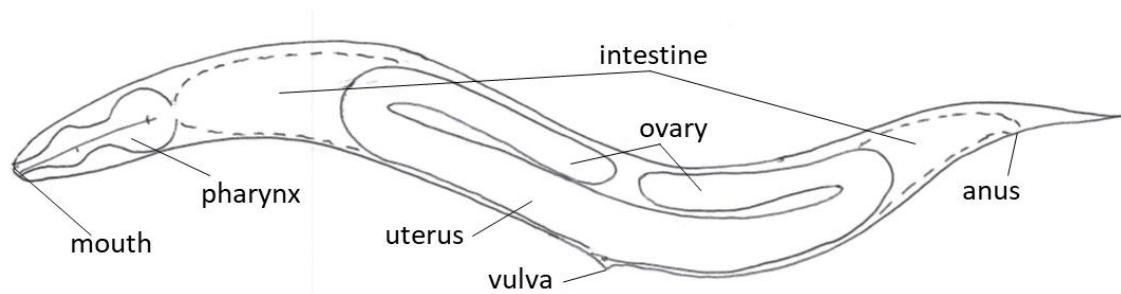


Figure 5 *C. elegans*. Schematic drawing of a hermaphrodite (around 1mm).

Specifically, *C. elegans* is an excellent model to study insulin-like signalling. Partial loss of IIS has pleiotropic effects including altered response to stress and extended lifespan (Gottlieb & Ruvkun, 1994). In worms, IIS also controls the dauer phenotype (Gottlieb & Ruvkun, 1994) which is an arrested developmental variant that occurs in response to stressful environmental conditions (overcrowding, starvation or elevated temperatures) (Cassada & Russell, 1975). Identification of dauer formation constitutive (*Daf-c*) and defective (*Daf-d*) mutant worms has helped to identify the IIS pathway components and to understand the importance of the signalling cascade (Gottlieb & Ruvkun, 1994; Hu, 2007; Malone & Thomas, 1994). *C. elegans* has only one insulin-like receptor, DAF-2, which has been extensively studied using a wide range of mutant alleles (Gems et al., 1998; Patel et al., 2008). Different *daf-2* reduction of function alleles demonstrates that reduced IIS pathway activity leads to worms entering dauer stage under conditions in which wild type worms would continue with the normal

developmental process. For example, all *daf-2(e1370)* (reduced tyrosine kinase activity) mutant worms enter dauer stage at 25 °C while wild type worms continue growing (Gottlieb & Ruvkun, 1994).

C. elegans is also a well-established genetic model organism to assess Klotho/FGFR signalling *in vivo* without genetic redundancy (for review see (Polanska, Fernig, & Kinnunen, 2009)). *C. elegans* has a single ortholog of the four mammalian *fgfrs*, *egl-15* (DeVore, Horvitz, & Stern, 1995), and two orthologs of the 22 vertebrate *fgf* genes, *egl-17* (Burdine, Chen, Kwok, & Stern, 1997) and *let-756* (Roubin et al., 1999). Recently, *klo-1* and *klo-2* genes have been identified in *C. elegans* as the orthologs for the vertebrate α - and β -Klothos (Figure 1) (Polanska et al., 2011).

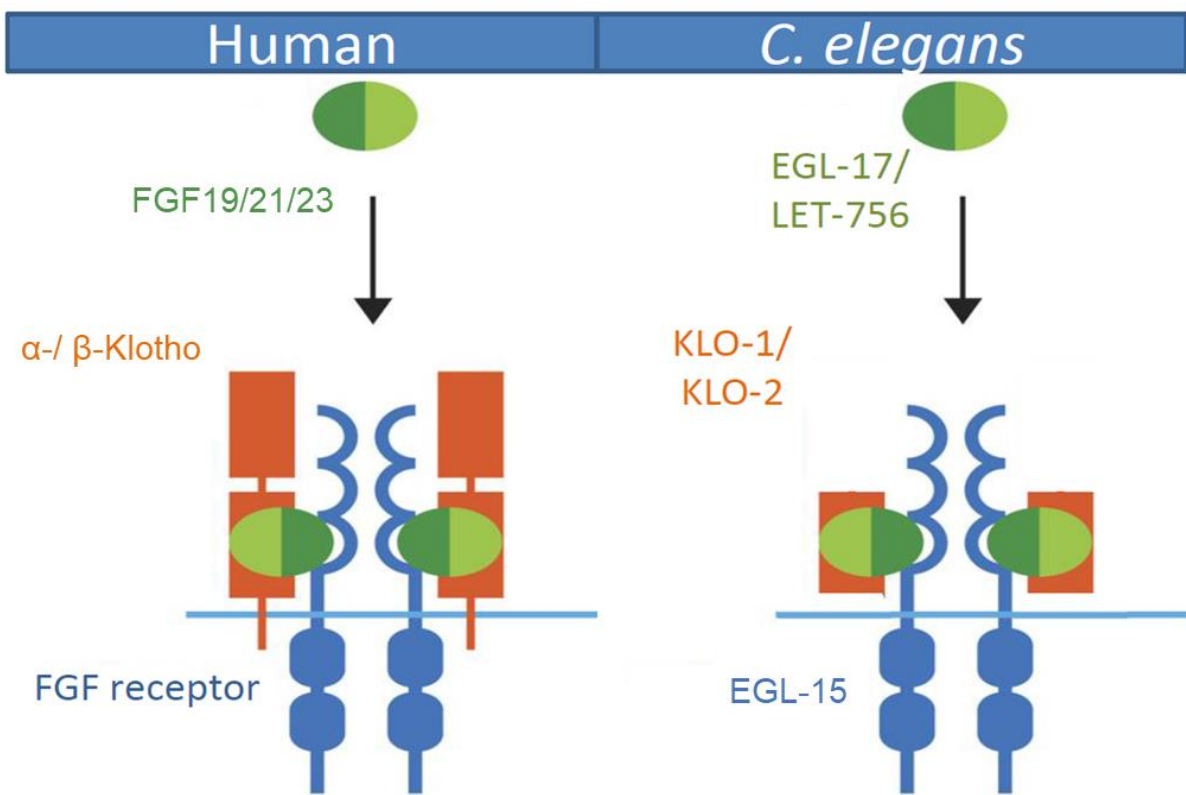


Figure 6 Conservation of the FGF/FGFR/Klotho interaction in human and *C. elegans*.

Although the complexity of the FGF/FGFR/Klotho signalling system is reduced in *C. elegans*, the morphogen and endocrine functions of FGFs are retained in parallel (Polanska et al., 2011). EGL-15/FGFR signalling regulates both the development and the function of the excretory system. *klo-1* and *klo-2* are specifically expressed in organs involved in osmoregulation and metabolism in *C. elegans* (Polanska et al., 2011). EGL-15 regulates *klo-1* expression, EGL-15 associates biochemically with KLO-1 and abnormal levels of EGL-15 or KLO-1 lead to defects in osmoregulation and sensitivity to physiological stress (Polanska et al., 2011).

1.10 *C. elegans* Klotho proteins, KLO-1 and KLO-2

The predicted KLO-1 protein in *C. elegans* is 479 amino acids and the sequence identity with the vertebrate α -Klotho and β -Klotho proteins is around 33 - 35 % and 29 - 30 % respectively (Polanska et al., 2011). The predicted KLO-2 protein is 475 amino acids and the sequence identity with the vertebrate Klotho and β -Klotho is 34 - 35 % and 33 - 34 % respectively (Polanska et al., 2011). The sequence identity of KLO-1 and KLO-2 to the first vertebrate Klotho domain (KL1) is around 33 - 35 % and only between 18 - 24% when compared with the KL2 domain (Figure 1) respectively (Polanska et al., 2011). Therefore, the function of KLO-1 and KLO-2 worm proteins is likely to be more similar to human γ -Klotho, which consists only of KL-1 domain. However, the function of γ -Klotho is not well known, so parallels can only be drawn to mammalian α - and β -Klotho.

Klotho orthologs are found in other Caenorhabditis species (*C. brenneri*, *C. remanei* and *C. brigssae*) and in Drosophila. *Klotho* genes of both, nematode and fly, encode proteins which are composed of a single KL domain without a transmembrane domain. From the phylogenetic analysis it is suggested that those single KL domain Klotho orthologs could be an ancestral form of the vertebrate Klotho (Figure 1; (Polanska et al., 2011)). Similarly to the nematode or fly Klothos, the mammalian *Klotho* genes could be alternatively spliced producing an isoform containing only one KL domain (Matsumura et al., 1998;

Shiraki-Iida et al., 1998). KLO-1 and KLO-2 lack a transmembrane domain and a putative secretion signal (Polanska et al., 2011) and the sub-cellular localisation is currently unknown.

klo-1 and *klo-2* expression partially overlap as both are expressed in the intestine, which is used to store lipid droplets because *C. elegans* do not have adipocytes. *klo-1* is also expressed in the excretory canal, while *klo-2* is also expressed in the hypodermis (Polanska et al., 2011). Together, these are the *C. elegans* organs involved in energy metabolism and osmoregulation. This suggests that the function of Klothos in the regulation of energy homeostasis and ion balance may be evolutionarily conserved from nematodes to mammals (Polanska et al., 2011).

Moreover, the role of KLO-1 and KLO-2 worm proteins in ageing process appears to be like the findings in mammals. Simultaneous RNAi downregulation of both KLO-1 and KLO-2 proteins reduces mean lifespan by 2 days (Château, Araiz, Descamps, & Galas, 2010). On the other hand, overexpression of *klo-1* (*klo-1* gain of function) in a wild type genetic background has been shown to prolong the mean lifespan by 1 to 2 days (Polanska et al., 2011).

There is also phenotypic evidence that worm *Klotho* proteins are involved in ion balance. Double mutant worms of *klo-1(ok2925)* and *klo-2(ok1862)* display a fluid homeostasis phenotype which consists in the presence of hollow cysts in 31 % of the animals (Xu et al., 2017). Some evidence suggests that these cysts are related to the role of KLO-1 protein in the development of the excretory canal (Polanska et al., 2011).

1.11 Sterol metabolism in *C. elegans*

In worms, cholesterol is metabolised by DAF-36 cholesterol 7-desaturase (homolog of mammalian CYP7A1 protein) into 7-dehydrocholesterol and downstream of the pathway, DAF-9 (homolog of mammalian CYP27A1/ACOX-2) produces sterol hormones such as gamravali, pregnenolone and

dafachronic acid (DA) that bind directly to DAF-12 (nuclear hormone receptor homologous to mammalian FXR) ((Matyash et al., 2004); for review see (Antebi, 2015)). The binding of a sterol to DAF-12 inhibits DAF-16 (sole orthologue to mammalian FOXO) entering the nucleus to induce dauer formation (Matyash et al., 2004). There is a negative feedback regulation by DAF-16 inducing the transcription of genes which in turn inhibit the synthesis of sterol hormones by DAF-9 or DAF-36 (Matyash et al., 2004; Tomiyama et al., 2010).

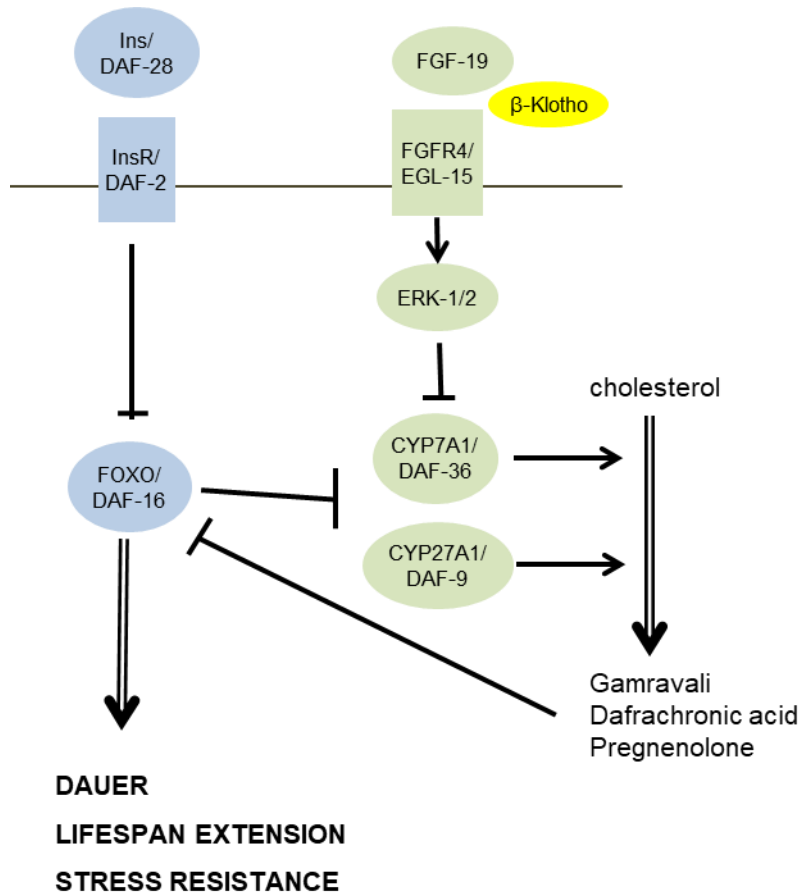


Figure 7 β -Klotho is involved in the cross-talk interaction between FGF and IIS pathways to regulate cholesterol metabolism.

Proteins are represented by coloured circles, indicating first the mammalian name of the protein and after the slash, the ortholog worm protein, if described.

Although nematodes are cholesterol auxotrophs, they need very small amounts of it to survive (Matyash et al., 2004). Worms grown in media without cholesterol are not affected until 2nd or 3rd generation, when

development is arrested (Matyash et al., 2004). This means that unlike in mammals, in *C. elegans* cholesterol does not play essential role in the stability of cell membrane structure (Matyash et al., 2001). Worms may regulate the properties of the membrane in response to temperature changes by alterations in the composition of phospholipids (Tanaka et al., 1996).

1.12 Insulin signalling and ageing in *C. elegans*

The vast majority of insulin actions are mediated by the PI3K-AKT/ PKB pathway. *C. elegans* DAF-2/INSR activation phosphorylates AGE-1 (homolog to mammalian PI3-K) which regulates the phosphorylation of PIP2 (phosphatidylinositol (3,4)-bisphosphate) into PIP3 (the trisphosphate form). This step is negatively regulated by DAF-18 (homolog to mammal PTEN (phosphatidylinositol-3,4,5-trisphosphate 3-phosphatase)) which dephosphorylates PIP3 into PIP2. PIP3 activates AKT/SGK (Brunet et al., 2001; Yamamoto et al., 2005) complex directly or mediated by PDK (Sharp & Bartke, 2005; Tatar, Bartke, & Antebi, 2003), and this activated complex phosphorylates DAF-16 /FOXO protein, which is arrested in the cytosol being unable to enter the nucleus to induce dauer stage, lifespan extension or stress resistance.

Reduction-of-function mutations in the genes encoding *daf-2/InsR*, insulin receptor substrates (IRS), and *age-1/PI3-kinase* increase longevity in *C. elegans*, and also in *Drosophila* (Bartke, 2008; Clancy et al., 2001; Kenyon, Chang, Gensch, Rudner, & Tabtiang, 1993). Similar results of extended lifespan have been found in mice lacking insulin receptor in adipose tissues (Blüher et al., 2003) and dwarf mice with impaired endocrine axis GH (growth hormone) - IGF-1 (Brown-Borg, Borg, Meliska, & Bartke, 1996). Previous studies have shown that *Klotho* inhibits insulin receptor autophosphorylation in cultured mammalian cells (Kurosu et al., 2005; Wolf et al., 2008) and represses directly or ligand-dependently the tyrosine kinase activity of DAF-2 in *C. elegans* (Château et al., 2010).

1.13 Aim of present study

The aim of this thesis is to study the role of KLO-1 and KLO-2 proteins in the regulation of energy and ion metabolism and stress resistance. The effect of genetic deletions of *klo-1* and *klo-2* will be assessed individually and in combination using *C. elegans* as a model organism.

Regulation of energy metabolism will be analysed in multiple parameters such as lifespan, development and fertility. The effect on ion metabolism will be assessed by studying adaptation response to ion depletion in the growth environment. Moreover, stress responses to heat and oxidative agents will be also assessed in genetic mutants of *klo-1* and *klo-2*.

2 Materials and methods

2.1 *C. elegans* strains

C. elegans strains were maintained at 20 °C unless stated otherwise essentially as described by (Brenner, 1974). Some strains were provided by the Caenorhabditis Genetics Center (CGC), which is funded by NIH Office of Research Infrastructure Programs (P40 OD010440). Wild type (wt) used in this thesis was N2 var. Bristol. In addition, the following strains, alleles and transgenes were used: GR1038 *daf-16(mu86)* LG I with a deletion of 11 kb in *daf-16* gene that removes nearly all of the winged-helix domain and ~1 kb upstream of the 5' UTR (Lin, Hsin, Libina, & Kenyon, 2001a), CB1370 *daf-2(e1370)* III which encodes for DAF-2 (P1465S) affecting the tyrosine kinase domain (Kimura, Tissenbaum, Liu, & Ruvkun, 1997), TC380 *klo-2(ok1862)* III with a deletion of 770 bp in *klo-2* gene (Polanska et al., 2011) (*C. elegans* Gene Knockout Consortium. WBPaper00041807), VC2175 *klo-1(ok2925)* IV with a deletion of 592 bp in *klo-1* gene (*C. elegans* Gene Knockout Consortium. WBPaper00041807) and BX113 *lin-15B&lin-15A(n765)* X; waEx15 [*fat-7::GFP* + *lin-15(+)*] maintained by picking non-multivulva worms which should be GFP+ (Brock, Browse, & Watts, 2006).

Integrated arrays included were: hJls67 [*atgl-1p::atgl-1::GFP* + *mec-7::RFP*] (Zhang et al., 2010), huls33 [*sod-3::GFP* + *rol-6(su1006)*] (Essers et al., 2005). rrls1 [*elt-2::GFP* + *unc-119(+)*] X and ncls13 [*ajm-1::GFP*] (Bulow, Boulin, & Hobert, 2004; Mohler, Simske, Williams-Masson, Hardin, & White, 1998). Extrachromosomal arrays included were: jtEx179 [*myo-2::GFP*; *pklo-1::mCherry*], jtEx129 [*pklo-2::GFP*; *ptph::mCherry*] and waEx15 [*fat-7::GFP* + *lin-15(+)*] (Brock et al., 2006).

Males were obtained by heat shock essentially as described (Brenner, 1974; Stiernagle, 2006). Briefly, four L4 hermaphrodites were heat shocked at 34 °C for 4 hours, which increases the rate of obtaining oocytes without chromosome X, therefore promotes the formation of males (X0). After 48 hours at 20

°C, plates were checked for males. To maintain males, eight male worms were mated with four L4 hermaphrodites.

2.2 Media

2.2.1 Nematode growth media

Nematode growth medium (NGM) agar consisted of 19.5 g of agar Bacteriological (OXOID), 3 g of NaCl and 2.5 g of tryptone (Fisher) per 975 ml of distilled H₂O. After autoclaving, 1 ml of cholesterol (Sigma) in EtOH (at 5mg/ml), 1 ml of 1 M CaCl₂, 1 ml of 1 M MgSO₄ and 25 ml of 1 M of potassium phosphate buffer (KPO₄ pH 6.0) were added per litre of NGM.

2.2.2 Bacteria growth media

LB agar consisted of 10 g of tryptone (Fisher), 5 g of yeast extract (Fisher), 10 g of NaCl and 15 g of agar Bacteriological (OXOID) per 1 litre of distilled H₂O. pH was adjusted to 7.5 using 1 M NaOH. The medium was autoclaved before use (Byerly, Cassada, & Russell, 1976).

B-Broth consisted of 10 g of tryptone (Fisher) and 5 g of NaCl per 1 litre of distilled H₂O and pH was adjusted to 7.0 using 1 M NaOH. The medium was autoclaved before use.

2.2.3 Physiological solutions

M9 buffer consisted of 40 mM Na₂HPO₄, 22 mM KH₂PO₄, 8.6 mM NaCl and 18.7 mM NH₄Cl in 5.8 g of Na₂HPO₄, 3 g of KH₂PO₄, 0.5 g of NaCl and 1 g of NH₄Cl per 1 litre of distilled H₂O. The medium was autoclaved before use.

10X PBS (phosphate buffered saline) consisted of 1.37 M NaCl, 26.8 mM KCl, 99.3 mM Na₂HPO₄ and 17.6 mM KH₂PO₄ in 1 litre of distilled H₂O. The pH was adjusted to 7.4 using 1 M NaOH and autoclaved.

2.2.4 Worm freezing media

Freezing media consisted of 5.85 g of NaCl, 6.8 g of Na₂HPO₄, 300 g of Glycerol (Sigma) and 5.6 ml of 1 M NaOH. Distilled H₂O was added to 1 litre final volume and autoclaved.

2.3 Maintenance of *C. elegans*

The methods related to *C. elegans* maintenance such as the preparation of bacterial food source, preparation of NGM plates and seeding of bacteria, the worm transferring technique and frequency, and the cleaning of contaminated worm stocks were done essentially as described by (Brenner, 1974)(Stiernagle, 2006).

2.4 Freezing and recovery of *C. elegans* stocks

Worms were collected in 500 µl of M9 buffer from plates full of L1 and L2 larvae, placed in a 1.5 ml Eppendorf tube and another 500 µl of Freezing Solution was added. The worms were then placed in a Styrofoam rack in the -80 °C freezer for gradual freezing.

For recovery, the worms were defrosted at room temperature and then placed on a new NGM plate. The first worms started to crawl again after some minutes (Stiernagle, 2006).

2.5 Strain construction

Standard genetic methods for *C. elegans* were used (Brenner, 1974). To obtain new strains with more than one gene mutation or to introduce arrays into different genetic backgrounds, the specific alleles were crossed by mating at standard maintenance conditions of 20 °C.

To make a *klo-2* and *klo-1* double mutant strain, four *klo-1(ok2925)* hermaphrodites at L4 stage were crossed with eight *klo-2(ok1862)* males. After 4 days, the F1 progeny was checked for males as an indication of successful mating; in positive case, sixteen F1 young hermaphrodites were placed individually on new NGM plates and allowed to lay F2 progeny.

Once the F2 was laid after 2 days, each F1 worm was placed in a PCR tube with 10 µl of lysis buffer for genotyping (see section 2.18.1). Confirmed heterozygous worms were selected for continuation. 48 F2 hermaphrodites were placed individually on new NGM plates and left for 2 days to lay the F3 progeny.

F2 hermaphrodites were genotyped as previously, and plates where the mother was homozygous *klo-2(ok1862); klo-1(ok2925)* mutant were kept. The F3 worms were genotyped to corroborate that they were mutant homozygous worms.

To study the effects of Klotho with Insulin/IGF-1 pathway, *klo-2(ok1862); klo-1(ok2925)* double mutant males were crossed with *daf-2(e1370)* mutant hermaphrodites and *daf-16(mu86)* mutant hermaphrodites as previously explained.

To introduce the GFP markers into Klotho mutants, *klo-2(ok1862) klo-1(ok2925)* double mutant males were crossed with the hermaphrodites of interest essentially as described before and the worms carrying the GFP reporter gene were selected each generation by fluorescent microscopy. *huls33[sod-3::GFP + rol-6(su1006)]* was followed by selecting roller worms (C.Mello, M.Kramer, Stinchcomb, & Ambros, 1991; Essers et al., 2005) and *waEx15 [fat-7::GFP + lin-15(+)]* array was followed by picking

no-Muv worms which could produce some Muv progeny (*lin-15B&lin-15A(n765)* X genotype) (Brock et al., 2006; Clark, Lu, & Horvitz, 1994).

Full list of strains obtained is provided in Appendix 1.

2.6 Viable progeny Assay

At L4 moult, animals were transferred to new NGM plates, only one L4 moult per plate. Age refers to days after L4 moult was first transferred to the new NGM plate. The day when L4 moult was transferred to new NGM plate constitutes the day 0 of NGM plate A. The worm started to lay eggs overnight and after 24 h this plate A was on Day 1 for those eggs and larvae on it. The adult mother worm was transferred to a new NGM plate, which was plate B on day 0, and left for the next 24 h to lay eggs. The number of eggs and larvae were counted on plate A day 1.

After another 24 hours, the adult worm was transferred again to a new NGM plate C day 0, and the number of eggs, L1 larvae, > L1 larvae and adults on plate A day 2 and plate B day 1 were counted. This procedure was repeated as many days as the adult laid eggs (5-7 days) (Polanska et al., 2011).

2.7 Feeding behaviour

The experiment was performed in standard NGM media plates incubated at 20 °C based on (Shtonda & Avery, 2006). L1 worms feeding on *E. coli OP50* were washed off the plates with M9 buffer and collected into a 1.5 ml Eppendorf tube. Worms were washed twice with M9 and 1 µl of worms was placed on the "X point" equidistant to *E. coli HB101* and *E. coli OP50* lawns. Number of worms outside

the food or on the different food lawns was assessed by counting the worms at different time points.

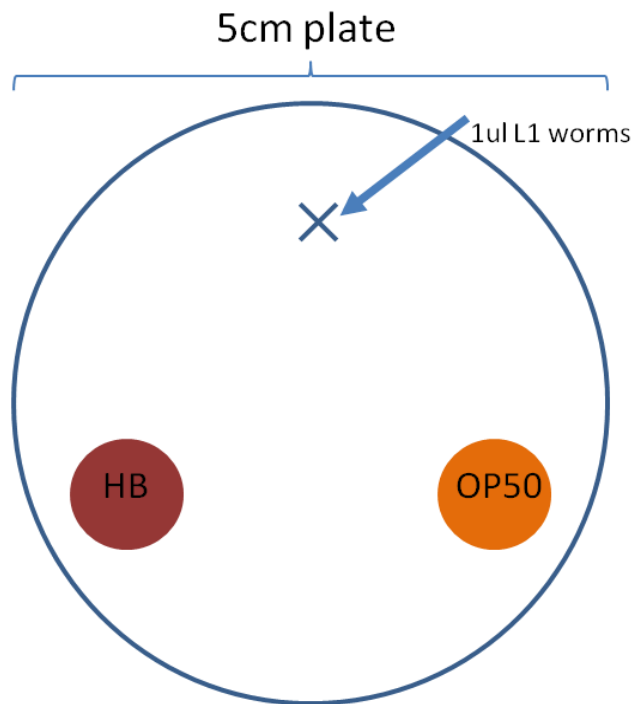


Figure 8 Diagram of a 5cm NGM plate with two different food sources: *E. coli* HB101 (HB) and *E. coli* OP50 (OP50).

“X” indicates the equidistant point from the food layers where the worms were placed.

2.8 Lifespan Assays

Lifespan assay was carried out at 20 °C on standard NGM plates with no 5-fluoro-2'-deoxyuridine (FUdR) added and live *E. coli* OP50 (Rooney et al., 2014). The lifespan of the animals was calculated from L4 to death. Animals were scored as dead when they did not move, pump, or respond to prodding. Animals that had crawled off the plate, had an “exploded” phenotype such that their gonad extruded out of the body through the vulva, or were egg-laying defective such that they accumulated hatched larvae inside the mother were censored at the time of the event. SPSS was used to analyse the data with Kaplan-Meier test, which includes censored worms into the analysis (Hsin & Kenyon, 1999).

2.9 Health status of adult worms

To test if lifespan elongation was also equivalent to longer healthy life, the worms were assessed for their ability to move at 16 and 28 days of adult life. Worms able to bend their body to move back and forward were counted as healthy, whereas the ones that were only able to move the pharynx were counted as old (adapted from (Keith, Amrit, Ratnappan, & Ghazi, 2014)).

2.10 Stress assays

2.10.1 Oxidative stress assay survival

Resistance to paraquat toxicity was tested according to (An & Blackwell, 2003) with some modifications. Young adult worms were transferred into 200 µl tubes (2 worms per tube) containing 30 µl of M9 with or without 300mM paraquat (SigmaAldrich, UK). Each trial consisted of 8 worms per strain in either paraquat or control M9. Worms were incubated at 20 °C and counted every hour for dead animals as ones not showing any pharyngeal pumping or bending movements. Animals that crawled away from the liquid or exploded were censored. SPSS program was used to analyse the data using Kaplan-Meier test (as explained before in Lifespan Assays method).

2.10.2 Oxidative stress induction of GFP reporter genes

Oxidative stress response to gene expression was assessed using *psod-3::GFP* reporter (Essers et al., 2005). Acute response to high paraquat concentration was performed essentially as described by (An & Blackwell, 2003). Around 80 one day old adult worms were transferred into 200 µl tubes containing 30 µl of M9 with or without 100 mM paraquat, and incubated for 30-60 min. Then worms were allowed to recover on food containing NGM plates for 3 h before microscopy.

Alternatively, as described by (Essers et al., 2005), 20-30 adult worms were transferred to new NGM plate containing 0.25 mM paraquat and allowed to lay eggs for 3-5 h. After 48 hours, larvae were collected to quantify GFP levels using Zeiss Axiomager Z1 equipped with Zeiss Axiocam MRm camera.

2.10.3 Heat stress

Response to heat stress was measured by exposing the worms to 37 °C, similar to described by (Keith et al., 2014). 30 age synchronised L4 larvae grown at 20 °C were transferred to preheated OP50 seeded NGM plates (one plate per strain) and incubated at 37 °C. Worm survival was monitored every hour for 9 hours. To minimise temperature changes, one single plate at a time was taken out of the incubator, worms were counted and placed back in the incubator within 2 minutes. Worms were counted as dead if they did not respond to gentle tapping, show pharyngeal pumping or bending movements. Relative resistance of each strain was compared by plotting a Kaplan-Meier survival curve, as explained for lifespan assay.

2.10.4 Physiological Stress Assay

Response to physiological stress under Ca^{2+} , Mg^{2+} and K^+ free conditions was assayed essentially as described previously (Teramoto, Lambie, & Iwasaki, 2005). Strains were grown in NGM plates at 20 °C for at least two generations before starting the experiment and until the plates were full of eggs. The eggs were then picked and placed in assay plates.

40 - 80 eggs were placed in each plate with different growth conditions. There were four different culture conditions of which three lacks one ion (Ca^{2+} , Mg^{2+} and K^+) and the fourth one was the normal NGM agar used as a positive control. The number of eggs, larvae and adults were counted every 12 hours until 110 hours of development.

2.11 Development time

10 adult worms were transferred to new NGM plates and allowed to lay eggs for 3 h before being removed from the plates. The plates were transferred to a 20 °C incubator and the number of larvae, dauers and adults were counted every 12 h until all worms reached adult stage.

2.12 Dauer formation assay

20 to 30 adult worms grown at 20 °C were transferred to a new NGM plate and allowed to lay eggs for 3 - 5 hours at 20 °C, after which the adults were removed. Then progeny was incubated at assay temperature (20 °C, 23 °C, 25 °C or 27 °C). Dauer and non-dauer worms were counted at 48 h and 72 h.

Dauers were distinguished by a radially constricted body and pharynx, and darkly pigmented intestine (Pierce et al., 2001).

2.13 Starvation

Age synchronised worms were washed from the plates with M9 or PBS buffer into conical tubes. Animals were allowed to settle by gravity and buffer was removed. To remove as much *E. coli* OP50 as possible, the worms were washed two more times with buffer. Worms were allowed to settle by gravity and, using a glass Pasteur pipette, transferred with the minimum amount of buffer to a new NGM plate without any food. Because some *E. coli* was transferred to the new plate, the starvation time wasn't started until 30 - 60 min later when all food was finished. After 3 - 12 h of fasting, worms were analysed in comparison with well-fed worms.

2.14 Microscopy

Fluorescence and DIC images were acquired using Zeiss AxioImager Z1 equipped with Zeiss AxioCam MRm camera and Zeiss Zen software. Images were cropped, adjusted and analysed using Zeiss Zen and/or Adobe Photoshop CC2015.

2.14.1 Microscopy of fixed animals

Paraformaldehyde fixed animals were mounted by placing 15 μ l of Mowiol on a microscope slide and pipetting 15 μ l of worms into the Mowiol drop. A coverslip was placed over and let it set for 30 minutes before worms were observed under microscope. Mowiol mounting medium was made by mixing 6 g of glycerol (Sigma), 2.4 g of Mowiol 4-88, 6 ml of H₂O, 12 ml of 0.2 M Tris-Cl (pH 8.5) and heating to 50 °C for 10 min with occasional mixing. For fluorescence detection, 0.625 g of DABCO (1,4-diazabicyclo-[2,2,2]-octane; SigmaAldrich) was added and Mowiol mounting medium was centrifuged at 5000g for 15 min, then aliquoted in 1 ml Eppendorf tubes and stored at -80 °C.

2.14.2 Microscopy of living animals

To observe live worms, 7 μ l of 30 mM Na-Azide in M9 buffer was added on 4% agarose (in H₂O) pad on microscope slide. The worms were transferred into the Na-Azide/M9 drop without damaging the agarose pad. A coverslip was placed on top and the worms were used directly for microscopy.

2.15 Lipid Staining

2.15.1 Sudan Black B

Sudan Black B staining was adapted from (E.-Y. Lee et al., 2009). Briefly, one day old adults synchronised by egg laying were washed from plates using 1 x PBS pH 7.4. To remove excess bacteria, worms were washed three times with 1x PBS and allowed to settle by gravity. Worms were fixed by resuspension in 500 μ l of 1 % PFA (paraformaldehyde) in PBS. Worms were permeabilised by freezing in liquid N₂ and thawing for three times. Worms were incubated on ice for 10 min before washing them with ice cold water three times. Worms were dehydrated using series of ethanol dilutions 25 %/ 50 %/ 70 % in ddH₂O. Worms were resuspended in 60 μ l of Sudan Black B (5 mg/ ml in 70 % ethanol, filtered through a 0.20 μ M pore) was added. The worms were incubated at room temperature for 30 minutes. Worms were washed three times by addition of 1 ml of 25 % ethanol and 10 min incubation at room temperature. Finally, worms were washed with ddH₂O, mounted on microscope slides with Mowiol mount media and imaged with a Zeiss Axiolmager Z1.

2.15.2 Oil-red-O staining

Oil-Red-O staining was carried out essentially as described by (O'Rourke, Soukas, Carr, & Ruvkun, 2009). Briefly, one day old adults synchronised by egg laying were washed from plates using 1 x PBS pH 7.4. To remove excess bacteria, worms were washed three times with 1x PBS and allowed to settle by gravity. Worms were permeabilised by resuspension in 120 μ l of PBS containing equal volume of 2x MRWB buffer with 2 % paraformaldehyde (PFA). 2x MRWB buffer is composed of 160 mM KCl, 40 mM NaCl, 14 mM Na₂EGTA, 1 mM spermidine-HCl (Sigma), 0.4 mM spermine (Sigma), 30 mM Na-PIPES pH 7.4, 0.2 % β -mercaptoethanol (Sigma). Worms were gently rocked for 1 h at room temperature (RT). Worms were allowed to settle by gravity, buffer was aspirated and, to remove PFA, worms were washed with 1x PBS. Worms were resuspended in 60 % isopropanol and incubated for 15 minutes at RT to dehydrate. Worms were allowed to settle, isopropanol was removed and 1 ml of freshly diluted 60 %

Oil-Red-O was added. Oil-Red-O (Sigma) stock solution was prepared by diluting 0.5 g into 100 ml of isopropanol, which had been equilibrated for several days, to 60 % with ddH₂O. The diluted Oil-Red-O was rocked for at least 1 h and then filtered through 0.45 or 0.22 µm-filter. Animals were incubated overnight in Oil-Red-O with rocking. Worms were allowed to settle; the dye was removed and 200 µL of 1x PBS 0.01 % Triton X-100 (Sigma) was added. Animals were mounted on microscope slides with Mowiol mount media and imaged with a Zeiss Axiolmager Z1.

2.15.3 Nile red

Nile Red (4,4-difluoro-5-methyl-4-bora-3a,4a-diaza-s-indacene-3-dodecanoic acid; SigmaAldrich) was used to visualise lipids in living nematodes. This compound is fluorescent and do not produce any adverse effects on *C. elegans*. Nile Red staining was carried out essentially as described previously (O'Rourke et al., 2009).

Briefly, *E. coli* OP50 was plated in normal NGM plates and allowed to grow for a few days. Then 100 µl of Nile Red solution (2.5 µg/ ml in PBS or M9 buffer) was added to the plate containing 6 ml of NGM (final concentration Nile Red was 41 ng/ ml). When the Nile Red solution was absorbed by the agar, 3 to 5 adult worms were placed in the plates and left to lay progeny. The worms born on NGM with Nile Red plates were collected at the desired developmental stage and observed alive in the Zeiss Axiolmager Z1 microscope.

2.16 Quantification of worm movement

Worm movement was quantified based on the principles described by (Shtonda & Avery, 2006), without the automated worm tracker. One worm was placed in a single agar plate containing a homogeneous lawn of *E. coli*. After 2 hours at 20 °C or 25 °C a photo was taken of the crawling path of the worm on

the bacterial lawn. At least 20 independent plates were analysed for each worm strain. Worm tracks were measured from captured images using Image J.

2.17 Pumping rate

The number of pharyngeal pumps was counted for 30 seconds at different developmental stages as described (Gaglia & Kenyon, 2009).

2.18 Molecular Biology methods

2.18.1 *C. elegans* genotyping

To confirm the genotype of the worms for one or more alleles, a single hermaphrodite was placed in a tube containing 10 µl of lysis buffer (containing 10 µl of proteinase K (10 mg/ml; Macherey-Nagel) in 1 ml of Worm Lysis Buffer containing (containing 50 mM KCl, 10 mM Tris pH 8.2, 2.5 mM MgCl₂ (Bioline), 0.45 % NP-40 (Sigma), 0.45 % Tween 20 (Sigma) and 0.01 % gelatine). Worms were then incubated at 60 °C for 45 minutes for lysing process and then at 95 °C for 15 minutes to inactivate the proteinase K.

The lysis reaction was used as a template in the PCR reaction using a set of three primers, one of them in the deleted region of the allele variant. This produced different size products depending of the allele variant.

Genotyping PCR reaction consisted of 1 X NH₄ buffer (Bioline), 2 mM MgCl₂ (Bioline), 200 µM of each dNTP (Bioline), 0.2 µM of each primer, 0.5 µl of Taq polymerase (homemade) and 3 µl of worm lysis as template in a total reaction volume of 25 µl.

Table 1 Primer sets to genotype klo-1(ok2925), klo-2(ok1862), daf-2(e1370) and daf-16(mu86).

allele	primers set	annealing temperature °C	amplified product size (bp)			
			wild type	bp	mutant	bp
ok1862	TK166,TK175,TK176	58	TK166,TK175	491	TK166,TK176	640
ok2925	TK263,TK264,TK265	62	TK263,TK264	443	TK263,TK265	659
e1370	TK314,TK315	60	TK314,TK315	872	TK314,TK315	872
mu86	TK311,TK312,TK313	60	TK311,TK312	772	TK311,TK313	984

DNA was amplified using an initial denaturation step at 94 °C for 2 minutes, followed by 35 cycles as denaturation at 94 °C for 20 seconds, annealing for 20 seconds with temperature depending on primers (Appendix 2) and primer extension at 72 °C for 45 - 60 seconds and one final extension at 72 °C for 5 minutes on a PCR machine (Applied Biosystems. Veriti 96 well thermal cycler). When the PCR reaction was finished, the samples were run on 1.8 % agarose gel until the bands were separated enough to observe the differences under UV light.

daf-2 and *daf-16* primer sequences were the same as used by (Love et al., 2010). *daf-2* genotype was verified using TK314 and TK315 primers to amplify a 872 bp DNA fragment. Wild type *daf-2* fragment contains a cut site for BlnI (5'...GC*TNAGC...3') which cuts the PCR product into 420 bp and 452 bp fragments. In e1370 mutation, BlnI cut site is altered and therefore the 872 bp PCR fragment is not cut. For digestion reaction, 1 U of BlnI (NEB) and 3 µl NEB CutSmart Buffer were added to 25µl PCR reaction, and then incubated for 1 h at 37 °C, and analysed on 1.8% agarose gel.

2.18.2 RNA extraction

For RNA purification, worms were collected from plates in M9 buffer and transferred into 1.5 µl Eppendorf tubes. The worms were centrifuged at 200g for 4 min, the supernatant was removed, and worms were washed twice with M9 buffer. 1 ml of Trizol (Invitrogen) was added and the worms in Trizol were dropped into liquid N₂ contained in a mortar. Worms were ground into powder using a pestle for 10 min. The worm powder was collected into a new tube and was incubated at room temperature for 5 min.

0.2 ml of chloroform (Sigma) was added for every 1 ml of Trizol, the worms were mixed for 15 seconds and immediately incubated at room temperature for 3 min. The worms were centrifuged at 12,000g for 15 min at 4 °C. The aqueous upper phase was collected into a new tube and 0.5 ml of 100 % isopropanol (Fisher) was added for every 1 ml of Trizol. The sample was incubated for 10 min at room temperature and centrifuged at 12,000g for 10 min at 4 °C. The supernatant was removed, and the pellet was washed with 1 ml of 75 % ethanol in DEPC H₂O per 1 ml Trizol, vortexed briefly and centrifuged at 7,500g for 5 min at 4 °C.

Supernatant was discarded, and the RNA pellet was air dried for 10 min at least. Dry pellet was resuspended in 20 µl RNase free H₂O and incubated at 55 °C for 10 min. RNA concentration was measured using DeNovix DS-11 UV-Vis Spectrophotometer.

2.18.3 RT-PCR

SuperScript® III One-Step RT-PCR System with Platinum® Taq High Fidelity DNA Polymerase (Invitrogen/LifeTechnologies) was used for the cDNA synthesis and amplification.

1 µg template RNA, 1 µl forward primer (10 µM), 1 µl reverse primer (10 µM) and 20.6 µl autoclaved distilled H₂O were added to 25 µl 2X Reaction Mix.

The reaction mix was incubated at 94 °C for 5 min and immediately placed on ice. 1 µl of RT/Taq HiFi Polymerase was added and RT-PCR was carried out on a PCR machine (Applied Biosystems. Veriti 96 well thermal cycler) as follows: (48 - 49.5) °C/ 45 min; 94 °C/ 2 min; [94 °C/ 20 s; (58 - 59.5) °C / 30 s; 72° C / 100 s] x 40 cycles; 72 °C / 10 min; 10 °C / hold. Primers pairs used for *klo-1* were TK280_klo1F (forward) and TK281_klo1R (reverse) and for *klo-2* were TK282_klo2F (forward) and TK283_klo2R (reverse). Primer sequences can be found in Appendix 2.

The samples were run on 0.8 % agarose gel containing SYBR Safe (Invitrogen) in TAE buffer at 85 V for 50 minutes. 5 µl of Hyperladder 1 kb (Bioline) was used as reference.

The gel was observed under UV light and the target bands corresponding to the desired amplified cDNAs were cut. The PCR products were purified from the gel using Qiagen PCR purification kit (Qiagen) method and eluted in 30 µl Elution Buffer (EB) provided by the kit.

2.18.4 Cloning

pCR™8/GW/TOPO® TA Cloning® Kit (Invitrogen/LifeTechnologies) was used to clone the RT-PCR fragment into pCR8/GW vector and transform into One Shot TOP10 Chemically Competent *E. coli* cells provided by the kit. The pCR8/GW plasmid contains resistance to spectinomycin (Sigma) allowing selection for *E. coli* cells containing a circular pCR8 plasmid with the insert.

Between 8-16 colonies formed on the LB + Spectinomycin (100 µg/ml) agar plates were picked into individual tubes containing LB + Spectinomycin (100 µg/ml) and grown overnight at 37 °C. Plasmid DNA was extracted using Qiaprep Miniprep kit (Qiagen) and stored at -20 °C.

Plasmid DNAs were digested with EcoR1 (NEB) and run on 0.8 % agarose gel.

2.18.5 Sequencing

Clones containing the cDNA sequences of *klo-1* and *klo-2* were sent for sequencing to Eurofins MWG Operon, (Germany).

3 Results

3.1 Klotho regulation of ageing

Klotho was first discovered in mouse as an ageing suppressor gene. Mice with a disruption of *Klotho* gene display phenotypes associated with ageing and have shorter lifespan than wild type mice (Kuro-o et al., 1997).

C. elegans has two orthologs of mammalian α - and β -*Klotho*, *klo-1* and *klo-2* (Polanska et al., 2011). The predicted mRNA sequences of both *klo-1* and *klo-2* were confirmed by sequencing the cDNA sequences obtained by RT-PCR.

3.1.1 *C. elegans* Klotho orthologs, KLO-1 and KLO-2, interact with insulin/IGF-1 pathway to regulate worm lifespan

In this thesis, the effect of genetic deletions of *klo-1(ok2925)* and *klo-2(ok1862)* in the regulation of ageing in *C. elegans* was studied for the first time.

Lifespan of worms was measured from young adult stage until death. Mean lifespan was calculated and log-rank test was used to analyse differences between different worm strains and media conditions.

In standard NGM, N2 wild type worms had a mean lifespan of 19.4 days and a maximum lifespan of 30 days (Figure 9). Mean lifespan was not altered by *klo-1(ok2925)* mutation (mean 18.8 days, maximum 29 days), but it was significantly extended in *klo-2(ok1862)* mutant worms, which have a mean lifespan of 20.5 days (p value 0.048; max lifespan 29 days; Table 2). Although *klo-2(ok1862); klo-1(ok2925)* double mutant worms have a slightly longer mean lifespan of 19.9 days (maximum 30 days), it is not significantly different to wild type (Figure 9A). Previously, RNAi to simultaneously knockdown both *klo-1* and *klo-2* in worms has been shown to result in a reduction of lifespan (Château et al., 2010) and the

results with the genetic deletion alleles were thus in discrepancy with the previous RNAi studies. To further investigate the role of *klo-1(ok2925)* and *klo-2(ok1862)* deletion mutations to worm lifespan, interactions with known ageing related genes were studied.

daf-2(e1370) is a partial loss-of-function mutation in the tyrosine kinase domain of the *C. elegans* insulin receptor, DAF-2, which doubles lifespan as compared to wild type worms (Kenyon et al., 1993). Here, *daf-2(e1370)* worms had a mean lifespan of 46.2 days, which is more than twice as long as the lifespan of wild type worms (Figure 9B). Lengthening of lifespan caused by DAF-2 downregulation was significantly increased in combination with *Klotho* mutations. Specifically, *daf-2(e1370)* mutation in conjunction with *klo-1* mutation extended mean lifespan by 3.5 days in comparison to *daf-2(e1370)* mutation alone (mean lifespan 49.7; p value 0.009; Table 2; Figure 9B). Even more pronounced increase in lifespan was seen in conjunction with *klo-2* mutation, with a mean lifespan of 58.8 days (Figure 9B). *daf-2*, *klo-2* and *klo-1* triple mutant worms had a mean lifespan of 54.8 days (Figure 9B), which is more than the lifespan of *daf-2; klo-1* double mutants but less than *daf-2 klo-2* double mutants (Table 2).

The maximum lifespan was more prolonged in *daf-2(e1370) klo-2(ok1862)* worms than in *daf-2(e1370)* worms, 92 and 65 days respectively (Table 2). Also, *daf-2(e1370); klo-1(ok2925)* double and *daf-2(e1370) klo-2(ok1862); klo-1(ok2925)* triple mutant worms had maximum lifespans of 81 and 90 days, which are longer than that of *daf-2(e1370)* worms (Figure 9B). Taken together these results suggest that genetic deletions of *klo-1* and *klo-2* further prolong lifespan in *daf-2(e1370)* mutant background with reduced insulin receptor signalling.

The lifespan prolonging effect caused by *daf-2(e1370)* is *daf-16* dependent (Kenyon et al., 1993). DAF-16 is the sole *C. elegans* forkhead box O/FOXO transcription factor and mediates the functions of DAF-2 in ageing and dauer formation (Kenyon et al., 1993). Consistent with previous findings (Murphy et al., 2003), *daf-16(mu86)* mutation significantly reduced lifespan, to a mean of 14.3 days (Figure 9C) compared to wild type *C. elegans* and also suppressed the lifespan extension of *daf-2(e1370)* from 46.2

days to 17.8 days in *daf-16(mu86); daf-2(e1370)* double mutant worms (Table 2; Figure 9C). *daf-16(mu86)* mutation also significantly reduced the mean lifespan of *Klotho* double mutants from 19.9 to 16.1 days (Table 2) and of *daf-2(e1370) klo-2(ok1862); klo-1(ok2925)* mutants from 54.8 to 18.4 days (Table 2).

Compared to wild type *C. elegans*, the mean lifespan of *daf-16(mu86); klo-2(ok1862); klo-1(ok2925)* triple mutant worms and of *daf-16(mu86); daf-2(e1370) klo-2(ok1862); klo-1(ok2925)* quadruple mutant worms was also significantly reduced (Table 2) to 16.1 and 18.4 days respectively (Figure 9D - E). Taken together, *daf-16(mu86)* was able to suppress the lifespan prolonging effects of *daf-2(e1370)*, *klo-2(ok1862)* and *klo-1(ok2925)* mutations.

3.1.1.1 Effect of glucose on lifespan of *Klotho* mutant *C. elegans*

Glucose has been shown to shorten lifespan by inhibiting the lifespan extending effects of *daf-2(e1370)* partial loss-of function mutation which activates DAF-16/FOXO transcription factor (Kimura et al., 1997; Lee, Murphy, & Kenyon, 2009). *daf-2(e1370)* worms cultured in 2 % glucose have similar lifespan to wild type (Lee et al., 2009). To assess the effect of glucose in *Klotho* mutant worms, animals were transferred to new NGM plates with or without 2 % glucose every two days until they stopped laying eggs. Lifespan was monitored until death, mean lifespan was calculated and log-rank test was used to test for significance as before.

Consistent with previously published data, glucose significantly reduced the mean lifespan of wild type worms from 19.4 to 16.6 days (Figure 9F) (Lee et al., 2009). Similarly, glucose shortened the lifespan of *klo-2(ok1862)* single mutants from 20.5 days to 17.7 days and of *klo-2(ok1862); klo-1(ok2925)* double mutants from 19.9 days to 17.6 days (Table 2). Intriguingly, addition of glucose had no effect on the mean lifespan of *klo-1(ok2925)* mutants (18.8 and 18.9 days), suggesting that *klo-1(ok2925)* mutants are insensitive to the presence of glucose.

The mean lifespan of *daf-2(e1370)* mutants grown in the presence of 2 % glucose was closer to that of wild type worms grown without glucose (22.8 and 19.4 days, respectively) as previously reported (Lee et al., 2009). Glucose also reduced the mean lifespan of *Klotho* mutants in *daf-2(e1370)* genetic background, but the effect was different for *klo-1* and *klo-2*. The mean lifespan of *daf-2(e1370); klo-1(ok2925)* double mutants was shortened from 49.7 to 28.1 days (Figure 9I), which is less pronounced than the effect of glucose on *daf-2(e1370)* alone (Table 2). Glucose shortened the mean lifespan of *daf-2(e1370) klo-2(ok1862)* double mutants from 58.8 to 28.6 days (Figure 9J) and of *daf-2(e1370) klo-2(ok1862); klo-1(ok2925)* triple mutant worms from 54.8 to 30.7 days (Figure 9K). In essence, glucose shortened the mean lifespan of *daf-2(e1370)* single mutants and of *daf-2(e1370) klo-2(ok1862)* double mutants by 51 %, whereas the effect on *daf-2(e1370) klo-1(ok2925)* double mutants and on *daf-2(e1370) klo-2(ok1862); klo-1(ok2925)* triple mutants was 43 % and 44 % less respectively. All these results suggest that worms with *klo-1(ok2925)* mutation are less affected by glucose.

Glucose did not affect mean lifespan of *daf-16(mu86)* animals (Figure 9C). However, glucose had a significant reduction on mean lifespan of *daf-16(mu86); daf-2(e1370)* mutants from 17.8 to 15.5 days (Figure 9C) and from 16.1 to 14.3 days of *daf-16(mu86); klo-2(ok1862); klo-1(ok2925)* (Figure 9D; Table 2). Finally, glucose did not affect the mean lifespan of *daf-16(mu86); daf-2(e1370) klo-2(ok1862); klo-1(ok2925)* quadruple mutants (Figure 9E). These results support the fact that *daf-2(e1370) klo-2(ok1862); klo-1(ok2925)* mutants were less affected by glucose than *daf-2(e1370)* mutants.

Table 2 Mean lifespan of worms maintained in standard or 2 % glucose NGM.

Control and glucose treated animals were grown in parallel, Maximum lifespan corresponds to the death age of the most long-lived worm. Number of animals observed equals the number of total animals minus the censored. Log-rank (Kaplan-Meier) test was performed to determine significant differences if p values are less than 0.05. First column from the right indicates the p-values of comparing N2 wild type in NGM to each worm strain and treatment.

Strain	Treatment	Mean Lifespan \pm SEM (days)	Maximum Lifespan (days)	Number of Animals Observed / Total Animals	P value against N2 wt in NGM
N2 wt	NGM	19.4 \pm 0.3	30	143 / 186	
	2 % glucose	16.6 \pm 0.3	29	135 / 280	<0.0001
<i>klo-1(ok2925)</i>	NGM	18.8 \pm 0.5	29	71 / 112	0.71
	2 % glucose	18.7 \pm 0.6	22	22 / 40	0.19
<i>klo-2(ok1862)</i>	NGM	20.5 \pm 0.4	29	70 / 100	0.048
	2 % glucose	17.7 \pm 0.5	20	23 / 37	0.008
<i>klo-2(ok1862); klo-1(ok2925)</i>	NGM	19.9 \pm 0.6	30	79 / 152	0.053
	2 % glucose	17.6 \pm 0.4	30	89 / 249	0.0002
<i>daf-2(e1370)</i>	NGM	46.2 \pm 1.0	65	121 / 159	0.0001
	2 % glucose	22.8 \pm 0.8	32	34 / 85	<0.0001
<i>daf-2(e1370); klo-1(ok2925)</i>	NGM	49.7 \pm 1.4	81	80 / 124	<0.0001
	2 % glucose	28.1 \pm 0.9	47	49 / 110	<0.0001
<i>daf-2(e1370) klo-2(ok1862)</i>	NGM	58.8 \pm 1.2	92	159 / 220	<0.0001
	2 % glucose	28.6 \pm 0.9	49	62 / 145	<0.0001
<i>daf-2(e1370) klo-2(ok1862); klo-1(ok2925)</i>	NGM	54.8 \pm 1.3	90	170 / 232	<0.0001
	2 % glucose	30.7 \pm 0.8	41	59 / 123	<0.0001
<i>daf-16(mu86)</i>	NGM	14.3 \pm 0.8	20	23 / 34	<0.0001
	2 % glucose	15.9 \pm 0.7	17	9 / 25	0.0003
<i>daf-16(mu86); daf-2(e1370)</i>	NGM	17.8 \pm 0.4	27	81 / 121	0.006
	2 % glucose	15.5 \pm 0.5	23	47 / 97	<0.0001
<i>daf-16(mu86); klo-2(ok1862); klo-1(ok2925)</i>	NGM	16.1 \pm 0.4	27	76 / 118	<0.0001
	2 % glucose	14.3 \pm 0.5	18	38 / 63	<0.0001
<i>daf-16(mu86); daf-2(e1370) klo-2(ok1862); klo-1(ok2925)</i>	NGM	18.4 \pm 0.4	28	96 / 162	0.038
	2 % glucose	17.4 \pm 0.7	20	16 / 30	0.01

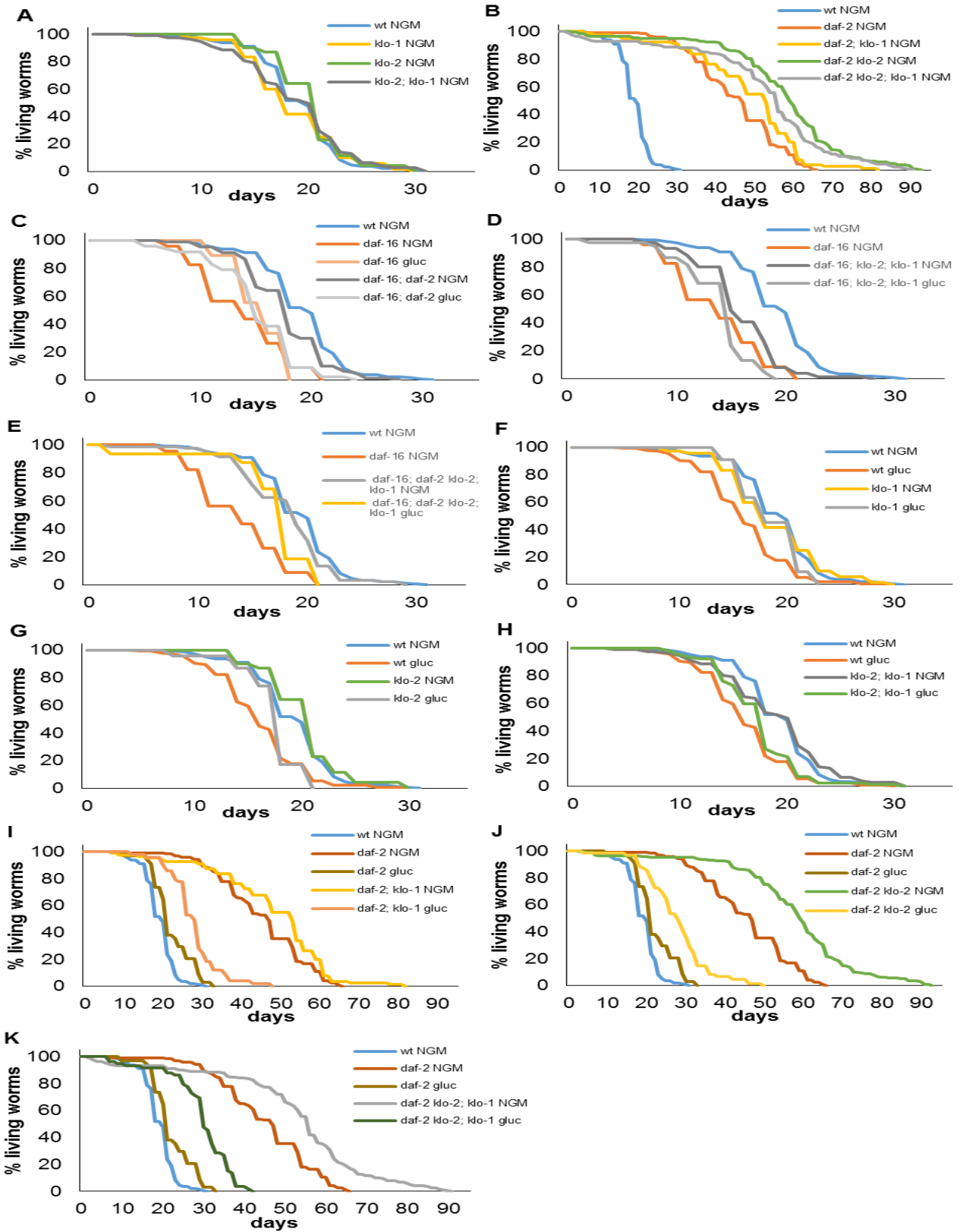


Figure 9 Effect of *klo-1(ok2925)*, *klo-2(ok1862)*, *daf-2(e1370)* and *daf-16(mu86)* mutations on lifespan depending on media conditions (control or 2% glucose).

N2 Bristol wild type (wt) was used as the control strain. The survival curves represent the sum of all animals examined in at least two independent experiments. The log-rank (Kaplan-Meier) test was used to test the hypothesis that the mean lifespans of different groups were equal. Total number of animals, mean lifespan \pm SEM (days), maximum lifespan and p values are presented in Table 2. A: *klo-2(ok1862)* mutants had a mean lifespan of one more day than wild type. B: *daf-2(e1370)* in conjunction with *Klotho* mutations elongated lifespan to three times longer than wild type. C: *daf-16(mu86)* worms had a shorter lifespan than wild type and were not affected by glucose. *daf-16(mu86); daf-2(e1370)* had a shorter lifespan than wild type but longer than *daf-16(mu86)* and glucose reduced their lifespan. D: *daf-16(mu86); klo-2(ok1862); klo-1(ok2925)* triple mutants had shorter lifespan than wild type and even shorter in the presence of glucose. E: The mean lifespan of *daf-16(mu86); daf-2(e1370) klo-2(ok1862); klo-1(ok2925)* and wild type worms were the same and were not affected by glucose. F: Glucose shortens the mean lifespan of wild type worms but not that of *klo-1(ok2925)* mutants. G,H: *klo-2(ok1862)* and *klo-1(ok2925); klo-2(ok1862)* mutant animals had a shorter mean lifespan in the presence of 2 % glucose. I: Glucose reduced mean lifespan of *daf-2(e1370)* to wild type value. *daf-2(e1370); klo-1(ok2925)* worms are less affected by glucose than *daf-2(e1370)* worms. J: *daf-2(e1370); klo-2(ok1862)* worms were equally affected by glucose than *daf-2(e1370)*, the lifespan was reduced by 51 % in both strains. K: Glucose reduced the mean lifespan of *daf-2(e1370); daf-2(e1370); klo-1(ok2925)* mutants by 44 %.

3.1.2 Analysis of progeny number

3.1.2.1 Progeny of *Klotho* mutant worms

Life history theory claims that the brood size, development and lifespan are related (Roff, 1992). This implies that reduced brood and extended lifespan are correlated, as is true for *daf-2(e1370)* mutants worms (Baxi, Ghavidel, Waddell, Harkness, & Carvalho, 2017; Ruaud, Katic, & Bessereau, 2011; Tissenbaum & Ruvkun, 1998).

To quantify the number of progeny of *Klotho* mutants, young adult worms were individually placed in new standard NGM plates and transferred to new NGM plates every 24 hours until they stopped laying eggs (5 to 8 days). The number of fertilised and unfertilised eggs (Narbonne, Maddox, & Labbe, 2015) was counted 24 h after the worm had been placed on the plate. The development of the fertilised eggs was followed every 24 hours to count for dead embryos, arrested larvae (larval arrested progeny which do not reach adult stage) and adults (viable progeny).

Worms were maintained at 20 °C, in which conditions wild type worms displayed a mean viable progeny of 266 ± 27 (95 % C.I.) worms. In these same conditions, *Klotho* mutant worms displayed similar mean

viable progeny numbers than wild type worms (Figure 10). The mean viable progeny of *klo-1(ok2925)* mutants was 243 ± 28 (95 % C.I.) worms, for *klo-2(ok1862)* mutants 298 ± 47 (95 % C.I.) worms and for *klo-2(ok1862); klo-1(ok2925)* double mutants 248 ± 45 (95 % C.I.) worms (Figure 10). Intriguingly, *klo-2(ok1862)* mutants produced significantly more viable progeny compared to *klo-1(ok2925)* mutants ($p = 0.02$; Table 3), however there was no significant difference to wild type.

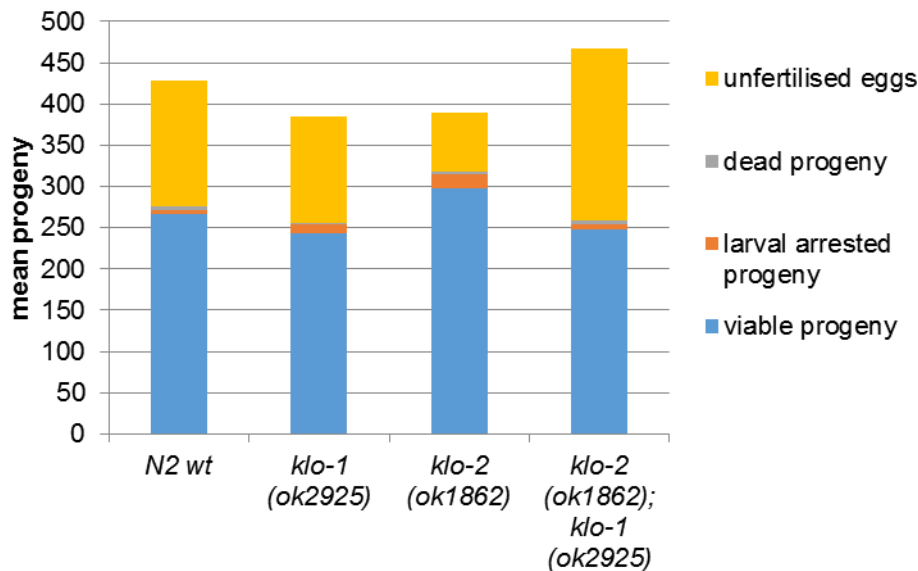


Figure 10 Mean progeny of worms grown in standard NGM at 20 °C.

5 worms per worm strain were included in this test. Total progeny consisted of viable progeny (blue bars), which were the worms that developed into fertile adults, larval arrested progeny (orange bars), which were the larvae that remained larvae after 5 days of development, dead progeny (grey bars), which were dead as embryos or larvae, and unfertilised eggs that were mostly laid after the 3rd day of laying period. Tukey's analysis results are shown in Table 3.

After 5 days of development, few worms were not developed into adults because they were arrested as larvae. The mean larval arrested progeny in wild type worms was only five worms, and significantly more were observed for *klo-1(ok2925)* and *klo-2(ok1862)* mutant genotypes, 12 and 17 larval arrested worms respectively (Table 3; Figure 10). No difference was observed in *klo-2(ok1862); klo-1(ok2925)* double mutant worms.

The amount of dead progeny was no more than five worms on average in any of the strains and the differences between strains could be caused by a simply miscounting of 1 – 2 worms (Table 3; Figure 10).

The mean unfertilised eggs laid by N2 wild type was 153 ± 105 (95 % C.I.), similar to 128 ± 61 (95 % C.I.) unfertilised eggs laid on average by *klo-1(ok2925)* mutants (Figure 10). The mean of unfertilised eggs was lower in *klo-2(ok1862)* and higher in *Klotho* double mutant worms as compared to wild type, 72 ± 64 (95 % C.I.) and 209 ± 77 (95 % C.I.) respectively (Figure 10). However, due to the high intrinsic variability in all strains, these differences were not statistically significant (Table 3).

Table 3 Mean progeny \pm 95 % C.I. of wild type, *klo-1(ok2925)*, *klo-2(ok1862)* and double mutant *klo-2(ok1862); klo-1(ok2925)* worms.

Tukey's analysis results are presented as p values against N2 wild type worms. N = number of mothers analysed. $\alpha = 0.05$

Strain	N	Viable progeny		Larval arrested progeny		Dead progeny		Unfertilised eggs	
		mean \pm 95 % C.I.	p value	mean \pm 95 % C.I.	p value	mean \pm 95 % C.I.	p value	mean \pm 95 % C.I.	p value
N2 wt	5	266 \pm 27		5 \pm 4		5 \pm 5		153 \pm 105	
<i>klo-1(ok2925)</i>	5	243 \pm 28	0.14	12 \pm 4	0.008	2 \pm 1	0.15	128 \pm 61	0.59
<i>klo-2(ok1862)</i>	5	298 \pm 47	0.14	17 \pm 10	0.01	2 \pm 4	0.35	72 \pm 64	0.11
<i>klo-2(ok1862); klo-1(ok2925)</i>	5	248 \pm 45	0.36	6 \pm 4	0.45	5 \pm 3	0.86	209 \pm 77	0.27

3.1.2.2 Interaction between *Klotho* and insulin /IGF-1 pathway to control brood size

Brood size was quantified in *daf-2(e1370)* single mutants, triple mutants of *daf-2(e1370) klo-2(ok1862); klo-1(ok2925)* and quadruple mutants of *daf-16(mu86); daf-2(e1370) klo-2(ok1862); klo-1(ok2925)* to analyse possible relationship of *Klotho* with insulin pathway on brood size. Worms were cultured in standard NGM and 2 % glucose NGM in parallel at 20 °C.

In this experiment, the mean viable progeny of N2 wild type worms grown on standard NGM was 241 ± 15 (95 % C.I.). The number of viable progeny was significantly less for *daf-2(e1370)* 100 ± 27 (95 % C.I.) as has been shown previously (Ruaud et al., 2011; Tissenbaum & Ruvkun, 1998) and for *daf-*

2(e1370) klo-2(ok1862); klo-1(ok2925) mutants 106 ± 21 (95 % C.I.) (Table 4; Figure 11). The reduction in viable progeny caused by *daf-2(e1370)* was completely restored to normal values in *daf-16(mu86); daf-2(e1370) klo-2(ok1862); klo-1(ok2925)* mutants with a viable progeny of 278 ± 260 (95 % C.I.) (Figure 11). However, most of the mothers became a bag of worms during the experiment and only the progeny of two quadruple mutant worms was included in the analysis.

A mean of 196 ± 104 (95 % C.I.) unfertilised eggs were laid by N2 wild type worms in standard NGM. In contrast, all the mutant worms laid significantly less unfertilised eggs than wild type (Figure 11). *daf-2(e1370)* and *daf-2(e1370) Klotho* mutants laid only two unfertilised eggs each on average, but in conjunction with *daf-16(mu86)* the quadruple mutants laid an average of 80 ± 25 (95 % C.I.) unfertilised eggs (Table 4; Figure 11).

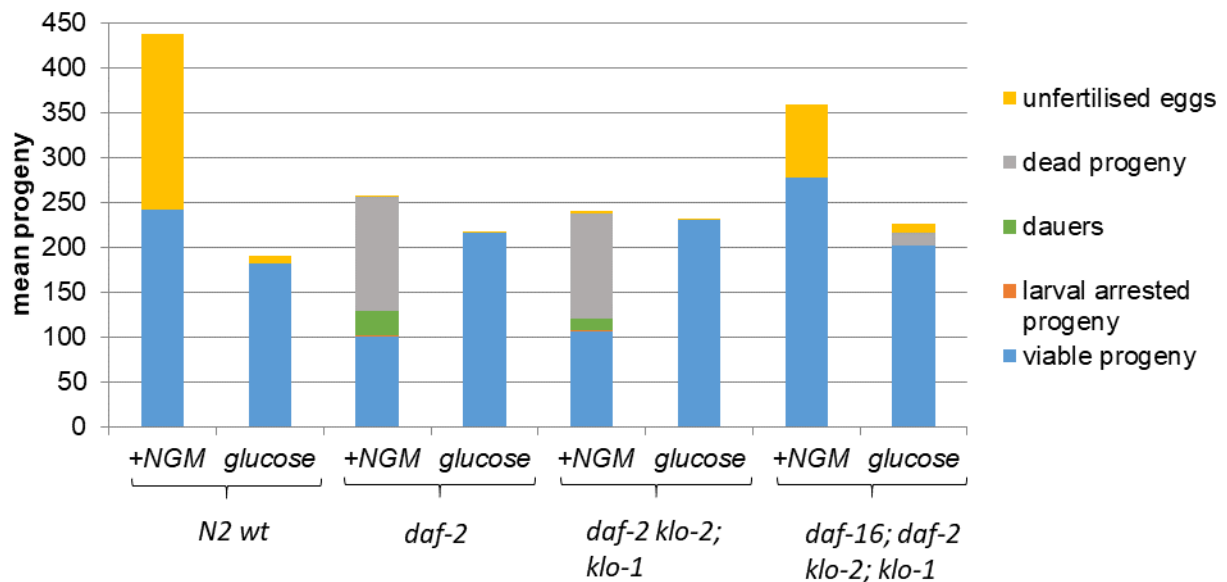


Figure 11 Mean progeny of worms grown on control NGM or on 2 % glucose NGM at 20 °C.

Total progeny consisted of viable progeny (blue bars), which were the worms that developed into fertile adults, larval arrested progeny (orange bars), which remained as larvae after 5 days of development, dauers (green bars), dead progeny (grey bars), which were dead as embryos or larvae, and unfertilised eggs (yellow bars) that were mostly laid after 3rd day of laying period. Tukey's analysis results are shown in Table 4.

All wild type fertilised eggs developed normally into viable adult progeny. In contrast, 27 ± 5 (95 % C.I.) of *daf-2(e1370)* progeny and 13 ± 7 (95 % C.I.) *daf-2(e1370) klo-2(ok1862); klo-1(ok2925)* progeny

became dauers (Figure 11). Also, both *daf-2(e1370)* and *daf-2(e1370) klo-2(ok1862); klo-1(ok2925)* triple mutants had a significant number of dead larvae, 126 ± 12 (95 % C.I.) and 117 ± 27 (95 % C.I.) of the total progeny respectively (Figure 11).

3.1.2.3 Glucose activates insulin /IGF-1 pathway to control brood size

The life history theory does not hold true for wild type *C. elegans* when the energy balance is altered, for example by supplementation with 2% glucose in the growth media. The addition of glucose to the growth medium reduced the mean lifespan of wild type worms (Figure 11). However, despite the shorter lifespan, they did not lay more progeny (Figure 11). Instead, glucose reduced the total number of eggs laid by N2 wild type worms from 437 to 191, and significantly reduced the number of viable progeny from 241 ± 15 (95 % C.I.) to 182 ± 39 (95 % C.I.) (Figure 11), in agreement with previously reported (Lee et al., 2009). The number of unfertilised eggs laid was also significantly reduced from 196 ± 104 (95 % C.I.) to 9 ± 18 (95 % C.I.) in the presence of glucose (Figure 11; Table 4).

daf-2(e1370) and *daf-2(e1370) klo-2(ok1862); klo-1(ok2925)* worms behaved very similarly in 2 % glucose NGM. Contrary to what was seen in wild type worms, both *daf-2(e1370)* and *daf-2(e1370) klo-2(ok1862); klo-1(ok2925)* mutants had significantly more viable progeny when 2% glucose was present, an increase from 100 ± 27 (95 % C.I.) to 216 ± 27 (95 % C.I.) and from 106 ± 21 (95 % C.I.) to 231 ± 19 (95 % C.I.), respectively (Figure 11; Table 4). The number of viable progeny in *daf-2(e1370) klo-2(ok1862); klo-1(ok2925)* triple mutants was also significantly higher than in wild type in the presence of 2 % glucose ($p = 0.02$; Figure 11). Glucose also completely suppressed dauer formation and abolished larval lethality in *daf-2(e1370)* and *daf-2(e1370) klo-2(ok1862); klo-1(ok2925)* mutant worms (Figure 11).

Table 4 Mean progeny \pm 95 % C.I. of wild type, *daf-2(e1370)* mutants, *daf-2(e1370) klo-2(ok1862)*; *klo-1(ok2925)* mutants and *daf-16(mu86)*; *daf-2(e1370) klo-2(ok1862)*; *klo-1(ok2925)* mutant worms.

Tukey's analysis results are presented as p values against N2 wild type worms and as also as the comparison of each worm strain on standard NGM versus on 2 % glucose NGM. $\alpha = 0.05$.

Strain	Treatment	N	viable progeny		Dauers		dead progeny			unfertilised eggs				
			mean \pm 95 % C.I.	p value against N2	p value NGM vs glucose	mean \pm 95 % C.I.	p value against N2	p value NGM vs glucose	mean \pm 95 % C.I.	p value against N2	p value NGM vs glucose	mean \pm 95 % C.I.	p value against N2	p value NGM vs glucose
N2 wt	+NGM	5	241 \pm 15			0 \pm 0			0 \pm 0			196 \pm 104		
	glucose	4	182 \pm 39	0.02		0 \pm 0	1.00		0 \pm 0	1.00		9 \pm 18	<0.0001	
<i>daf-2</i>	+NGM	5	100 \pm 27	<0.0001		27 \pm 5	<0.0001		126 \pm 12	<0.0001		2 \pm 3	<0.0001	
	glucose	5	216 \pm 27	0.69	<0.0001	0 \pm 0	1.00	<0.0001	0 \pm 0	1.00	<0.0001	1 \pm 2	<0.0001	1.00
<i>daf-2 klo-2; klo-1</i>	+NGM	7	106 \pm 21	<0.0001		13 \pm 7	<0.0001		117 \pm 27	<0.0001		2 \pm 3	<0.0001	
	glucose	9	231 \pm 19	0.99	<0.0001	0 \pm 0	1.00	<0.0001	0 \pm 0	1.00	<0.0001	0 \pm 1	<0.0001	1.00
<i>daf-16; daf-2 klo-2; klo-1</i>	+NGM	2	278 \pm 260	0.61		0 \pm 0	1.00		0 \pm 0	1.00		80 \pm 25	0.002	
	glucose	3	201 \pm 110	0.33	0.03	0 \pm 0	1.00	1.00	14 \pm 33	0.84	0.86	10 \pm 39	<0.0001	0.21

The negative effects of glucose on brood size and viability were restored when *daf-16(mu86)* mutation was introduced into *daf-2(e1370)* or *daf-2(e1370) klo-2(ok1862); klo-1(ok2925)* mutants. In the presence of 2 % glucose, quadruple mutant worms had, similar to wild type worms, a significant reduction of viable progeny from 278 ± 260 (95 % C.I.) to 201 ± 110 (95 % C.I.) and a significant reduction of unfertilised eggs laid from 80 ± 25 (95 % C.I.) to 10 ± 39 (95 % C.I.) (Figure 11).

Taken together, *Klotho* mutations in combination with *daf-2(e1370)* did not significantly alter the effects caused by *daf-2(e1370)* alone on total egg production (fertilised and unfertilised) or on viability. In the presence of glucose, there were no production of unfertilised eggs and no larval arrested progeny. Also, all four strains had similar mean viable brood size (Figure 11; Table 4).

3.1.3 Development time from egg to adult

According to the life history theory, it could be hypothesised that worms living longer and having less progeny would also develop slower into adults. To test this hypothesis, the number of adult worms was counted every 12 h to determine how different mutations affected development time from egg to adult. The time when the eggs were laid by mothers (about 300 min after first cleavage) was considered as time zero (0 h) of development. Percentage of adult worms was compared at 3 different time points 72 h, 84 h and 96 h.

At 72 hours, 63 % and at 84 h 99% of wild type worms have developed to reproductively mature adults (Figure 12A and B). Genetic deletion of both *klo-1* and *klo-2* slightly altered development time. At 72 h of development significantly less *klo-2(ok1862); klo-1(ok2925)* worms were adults (56 %). However, at 84 h 97 % of all *klo-2(ok1862); klo-1(ok2925)* double mutants had developed into adults and no difference was observed as compared to wild type worms (Figure 12A - B; Table 5). In contrast, *daf-2(e1370)* mutation caused a significant delay in development either on its own or in combination with *Klotho* mutations (Table 5 Table 5). None of the *daf-2(e1370)* mutants had developed to adults at 72 h or at 84 h of development (Figure 12A - B); instead they required 132 h to become adults. Similar

percentages of adults were seen for *daf-2; klo-1* and *daf-2; klo-2* double mutants and for *daf-2 klo-2; klo-1* triple mutants at 72 h and 84 h (Table 5; Figure 12A - B). Intriguingly, *klo-1(ok2925)* mutation further delayed development of *daf-2(e1370)* worms into adults at 96 h. At 96 h, 25 % of *daf-2* mutants were adults, compared to 7 % and 14 % of *daf-2; klo-1* and *daf-2 klo-2; klo-1* mutants, respectively (Figure 12; p value < 0.0001). This further developmental delay seemed to be specific to *klo-1* as there was no difference between *daf-2* single and *daf-2 klo-2* double mutants (25 and 29 % adults, respectively; p value = 0.8; Figure 12C Table 5).

daf-16(mu86) mutants had shorter lifespan and larger brood size than wild type. A faster development would be expected according to the life history theory, but *daf-16(mu86)* mutants initially display a larval developmental delay. At 72 h, 48 % of *daf-16(mu86)* worms have developed into adults, however, at 86 h there is no difference to wild type animals, and 100% of *daf-16(mu86)* mutants have become adults (Figure 12A - B; Table 5).

The development delay effect caused by *daf-2(e1370)* was inhibited by *daf-16(mu86)*. At 84h, almost all (99%) of *daf-16(mu86); daf-2(e1370)* mutants were adults (Figure 12B). Early larval development was again delayed, as at 72 h, 9 % of *daf-16(mu86); daf-2(e1370)* mutants were adults compared to 48 % of *daf-16(mu86)* (p value < 0.0001; Figure 12A Table 5).

Compared to *daf-16(mu86)* worms, the development of *daf-16(mu86); klo-2(ok1862); klo-1(ok2925)* worms was significantly slower, 38 % of adults at 72 h and 96 % of adults at 84 h (Figure 12A - B). However, *daf-16(mu86)* mutation was less able to suppress the developmental delay when in conjunction with *daf-2, klo-1* and *klo-2* mutations, and at 72 h of development, only 2 % of *daf-16(mu86); daf-2(e1370) klo-2(ok1862); klo-1(ok2925)* worms were adults (Figure 12.A).

3.1.3.1 Effect of glucose on development time

In the presence of glucose, development was accelerated in all strains tested (Figure 12; Table 5). Wild type worms and *klo-2(ok1862); klo-1(ok2925)* mutants developed faster when grown on 2 % glucose NGM, as the percentage of adults at 72 h increased from 63 to 89 % and from 56 to 78 % respectively (Figure 12; Table 5).

The effect of glucose on development was more significant in strains carrying *daf-2(e1370)* mutation. At 84 h of development the percentage of *daf-2(e1370)* adults increased from 0 to 12 % (Figure 12B) and at 96 h increased from 25 to 89 % (Figure 12C).

Similar to control conditions, development of *daf-2(e1370); klo-1(ok2925)* worms in glucose was slower than that of *daf-2(e1370)* worms. At 96 h of development 76 % of *daf-2(e1370); klo-1(ok2925)* mutants were adults (p value = 0.0001; Figure 12C). Glucose had no further effects on *daf-2(e1370) klo-2(ok1862)* worms compared to *daf-2(e1370)*, and the development time was the same in both strains (Figure 12; Table 5). However, glucose significantly accelerated the development of *daf-2(e1370) klo-2(ok1862); klo-1(ok2925)* triple mutant worms increasing the percentage of adults at 84 h to 49 % (p value < 0.0001; Figure 12B; Table 5Table 5).

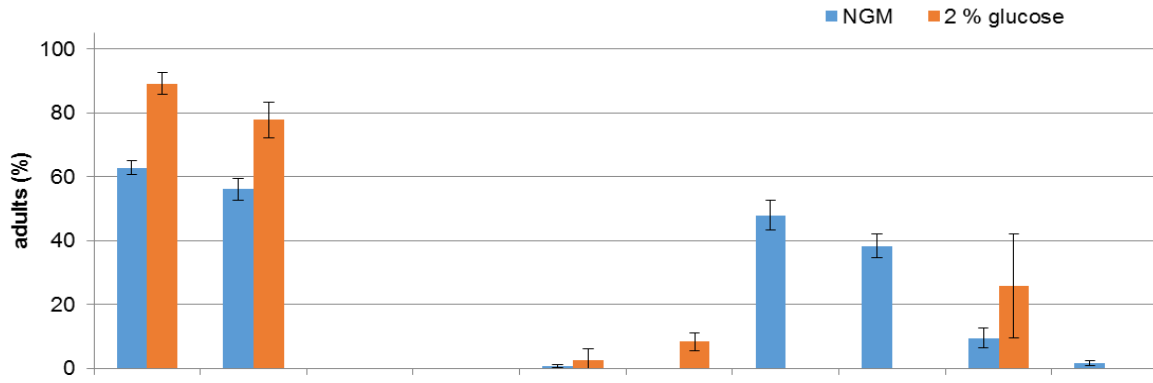
Table 5 Percentage of adults at different time points of development in standard conditions (NGM) and in 2 % glucose.

At least two independent experiments are shown. Data is presented for three different time points of development 72 h, 84 h and 96 h (time 0 h corresponds to time of eggs been laid). For each time point, the percentage of adults \pm 95 % C.I. was analysed with Tukey's test ($p = 0.05$) and the results are presented as p-values. Each strain was compared against wild type on NGM or each strain grown on NGM compared to 2 % glucose containing media.

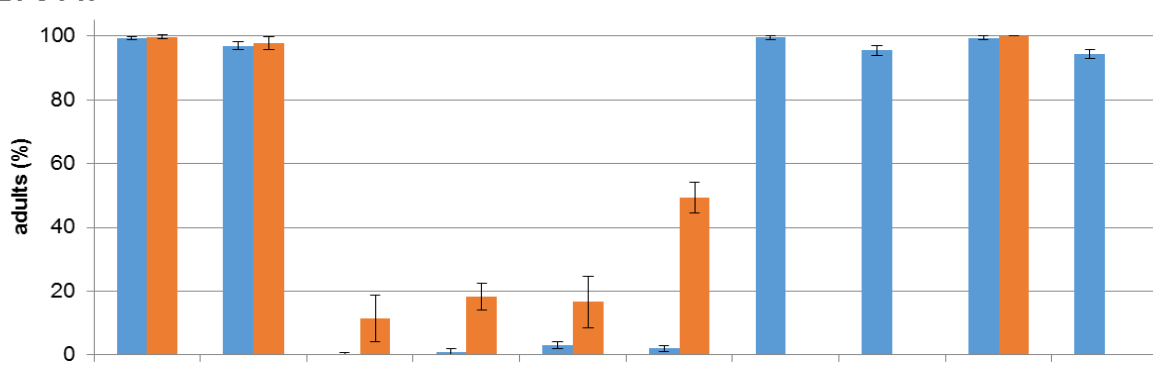
Strain	Treatment	N	72 h			84 h			96 h		
			adults (%) \pm 95 % C.I.	p-value against wt NGM	p-value NGM vs glucose	adults (%) \pm 95 % C.I.	p-value against wt NGM	p-value NGM vs glucose	adults (%) \pm 95 % C.I.	p-value against wt NGM	p-value NGM vs glucose
N2 wt	NGM	1771	63 \pm 2.3			99 \pm 0.4			99 \pm 0.3		
	Glucose	316	89 \pm 3.4	0.0000		100 \pm 0.6	1.0000		100 \pm 0.6	1.0000	
<i>klo-2(ok1862); klo-1(ok2925)</i>	NGM	786	56 \pm 3.5	0.0003		97 \pm 1.2	0.3556		98 \pm 1.1	0.9339	
	Glucose	207	78 \pm 5.7	0.0000	0.0000	98 \pm 2.0	0.9997	1.0000	98 \pm 1.9	1.0000	1.0000
<i>daf-2(e1370)</i>	NGM	418	0 \pm 0.0	0.0000		0 \pm 0.5	0.0000		25 \pm 4.3	0.0000	
	Glucose	113	0 \pm 0.0	0.0000	1.0000	12 \pm 7.2	0.0000	0.0007	89 \pm 6.0	0.0017	0.0000
<i>daf-2(e1370); klo-1(ok2925)</i>	NGM	446	0 \pm 0.0	0.0000		1 \pm 1.0	0.0000		7 \pm 2.8	0.0000	
	glucose	333	0 \pm 0.0	0.0000	1.0000	18 \pm 4.2	0.0000	0.0000	76 \pm 4.6	0.0000	0.0000
<i>daf-2(e1370) klo-2(ok1862)</i>	NGM	901	1 \pm 0.5	0.0000		3 \pm 1.1	0.0000		29 \pm 4.0	0.0000	
	glucose	80	3 \pm 3.5	0.0000	1.0000	17 \pm 8.1	0.0000	0.0000	89 \pm 6.9	0.0173	0.0000
<i>daf-2(e1370) klo-2(ok1862); klo-1(ok2925)</i>	NGM	895	0 \pm 0.0	0.0000		2 \pm 0.9	0.0000		14 \pm 2.7	0.0000	
	glucose	409	8 \pm 2.7	0.0000	0.0037	49 \pm 4.9	0.0000	0.0000	86 \pm 3.5	0.0000	0.0000
<i>daf-16(mu86)</i>	NGM	463	48 \pm 4.6	0.0000		100 \pm 0.6	1.0000		100 \pm 0.0	1.0000	
<i>daf-16(mu86); klo-2(ok1862); klo-1(ok2925)</i>	NGM	669	38 \pm 3.7	0.0000		96 \pm 1.6	0.0061		99 \pm 0.9	1.0000	
<i>daf-16(mu86); daf-2(e1370)</i>	NGM	358	9 \pm 3.1	0.0000		99 \pm 0.7	1.0000		99 \pm 0.7	1.0000	
	glucose	31	26 \pm 16.3	0.0000	0.4230	100 \pm 0.0	1.0000	1.0000	100 \pm 0.0	1.0000	1.0000

<i>daf-16(mu86); daf-2(e1370) klo-2(ok1862); klo-1(ok2925)</i>	NGM	1104	2 ± 0.7	0.0000	94 ± 1.4	0.0000	97 ± 1.1	0.8672
Total		9300						

A. 72 h



B. 84 h



C. 96 h

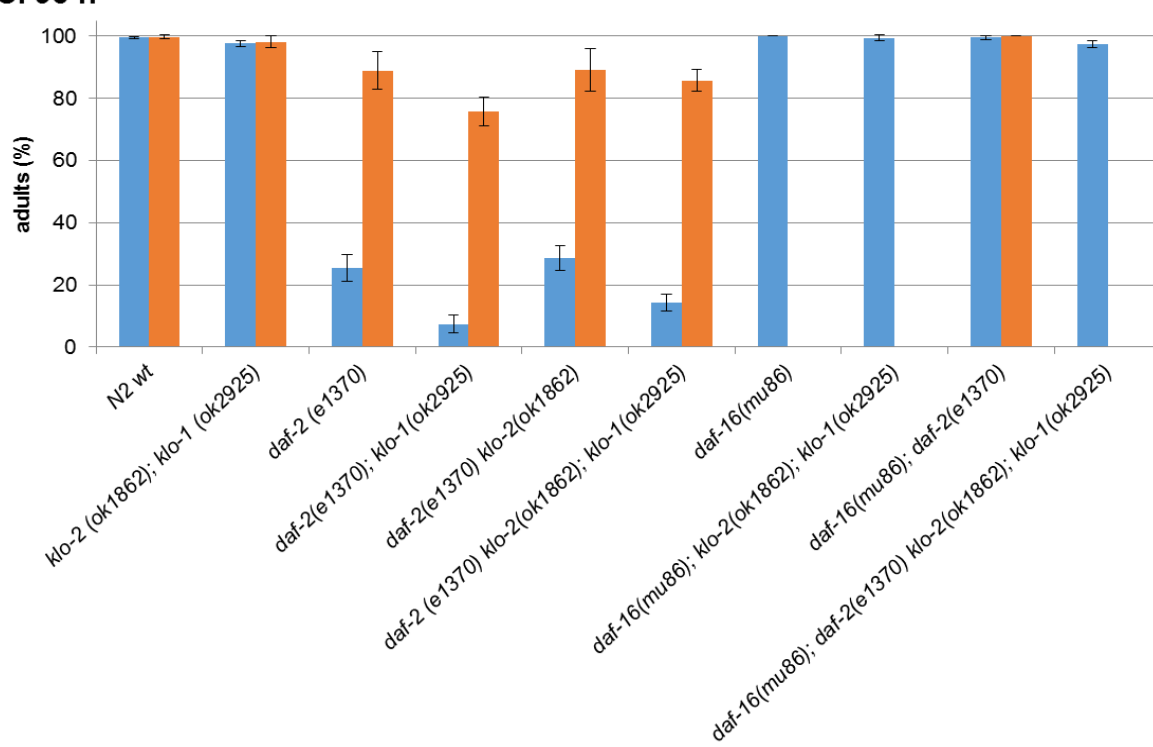


Figure 12 Percentage of fully developed adult worms at 72 h (A), 84 h (B) and 96 h (C) after egg hatching.

Each worm strain was grown in standard NGM (blue bars) or in 2 % glucose (orange bars), except three strains which have been grown in NGM+ only (*daf-16 (mu86)*, *daf-16 (mu86); klo-2(ok1862)*; *klo-1(ok2925)* and *daf-16 (mu86); daf-2(e1370) klo-2(ok1862)*; *klo-1(ok2925)*). Error bars represent 95 % C.I.. Tukey's test was used to analyse the data and is presented in Table 5.

3.1.4 Cause of premature adult death

Defects in egg-laying (egl phenotype) may lead to bag of worms in which the progeny hatches inside the mother and the larvae eat their way out of the mother, thereby killing it, and hence affecting the lifespan of the mother. In some occasions the worms crawl out of the plate while exploring their environment. Both of these events were accounted for when assessing lifespan. Worms were censored in the lifespan assays if they crawled off the plate, became bag of worms or exploded (internal organs were expelled through the vulva).

In the case of wild type *C. elegans*, 17 % of animals crawled off the plate (Figure 13A), 3 % died as bag of worms (Figure 13B) and none exploded (Figure 13C). *klo-1(ok2925)* and *klo-2(ok1862)* single mutants behaved similar to wild type and no differences were observed. In contrast, 33 % of *klo-2; klo-1* double mutant worms crawled off the plate, which was significantly more than wild type ($p = 0.01$; Figure 13A) and could indicate problems in food sensing or behavioural defects.

The percentages of *daf-2(e1370)* worms that crawled off, became bag of worms and exploded were very similar to wild type, but differences were found in worms carrying *Klotho* mutations in *daf-2(e1370)* genetic background.

daf-2(e1370) klo-2(ok1862) mutants crawled off the plate significantly less than wild type (3 %, $p = 0.01$; Figure 13A). *daf-2(e1370); klo-1(ok2925)* and *daf-2 Klotho* triple mutant crawled off the plate similar to wild type, however, a significantly higher percentage became bag of worms, 18% ($p = 0.006$ as compared to wild type; $p = 0.005$ as compared to *daf-2(e1370)* worms) and 17 % ($p = 0.005$ as compared to wild type; $p = 0.01$ as compared to *daf-2(e1370)* worms) respectively (Figure 13B). *klo-1(ok2925)* mutants produced the highest percentage of bag of worms, alone or in combination with *daf-2(e1370)*, which could suggest a

weak egg laying defective (egl) phenotype caused by *klo-1(ok2925)*. Also, 12 % of *daf-2(e1370) klo-2(ok1862); klo-1(ok2925)* triple mutants exploded, which was significantly higher percentage than that of wild type ($p < 0.0001$), double mutant *klo-2(ok1862); klo-1(ok2925)* or *daf-2(e1370)* worms (Figure 13C).

daf-16(mu86) mutation did not affect significantly the causes of death as compared to wild type. No differences were observed, either, in worms carrying *daf-16(mu86)* mutation in combination with *Klotho* or *daf-2* mutations. However, 10 % ($p < 0.0001$) of *daf-16(mu86); daf-2(e1370) klo-2(ok1862); klo-1(ok2925)* worms exploded, and together with *daf-2(e1370) klo-2(ok1862); klo-1(ok2925)* triple mutants, these two strains had a significant increase in the percentage of exploded worms (Figure 13C).

The presence of glucose increased the percentage of wild type worms that crawled outside the NGM, from 17 % to 36 % ($p = 0.01$; Figure 13A), but it did not affect the amount of worms that became bag of worms or exploded (Figure 13B - C). *Klotho* mutants were not affected by the presence of glucose and *daf-2(e1370)* mutants crawled off significantly more in 2 % glucose NGM than in standard NGM, 28 % and 10 % respectively ($p = 0.03$; Figure 13A).

Glucose had no effect on the number of bags of worms in any of the strains. However, glucose inhibited the exploded phenotype of *daf-2(e1370) Klotho* triple mutants and *daf-16(mu86); daf-2(e1370) Klotho* quadruple mutants (Figure 13C).

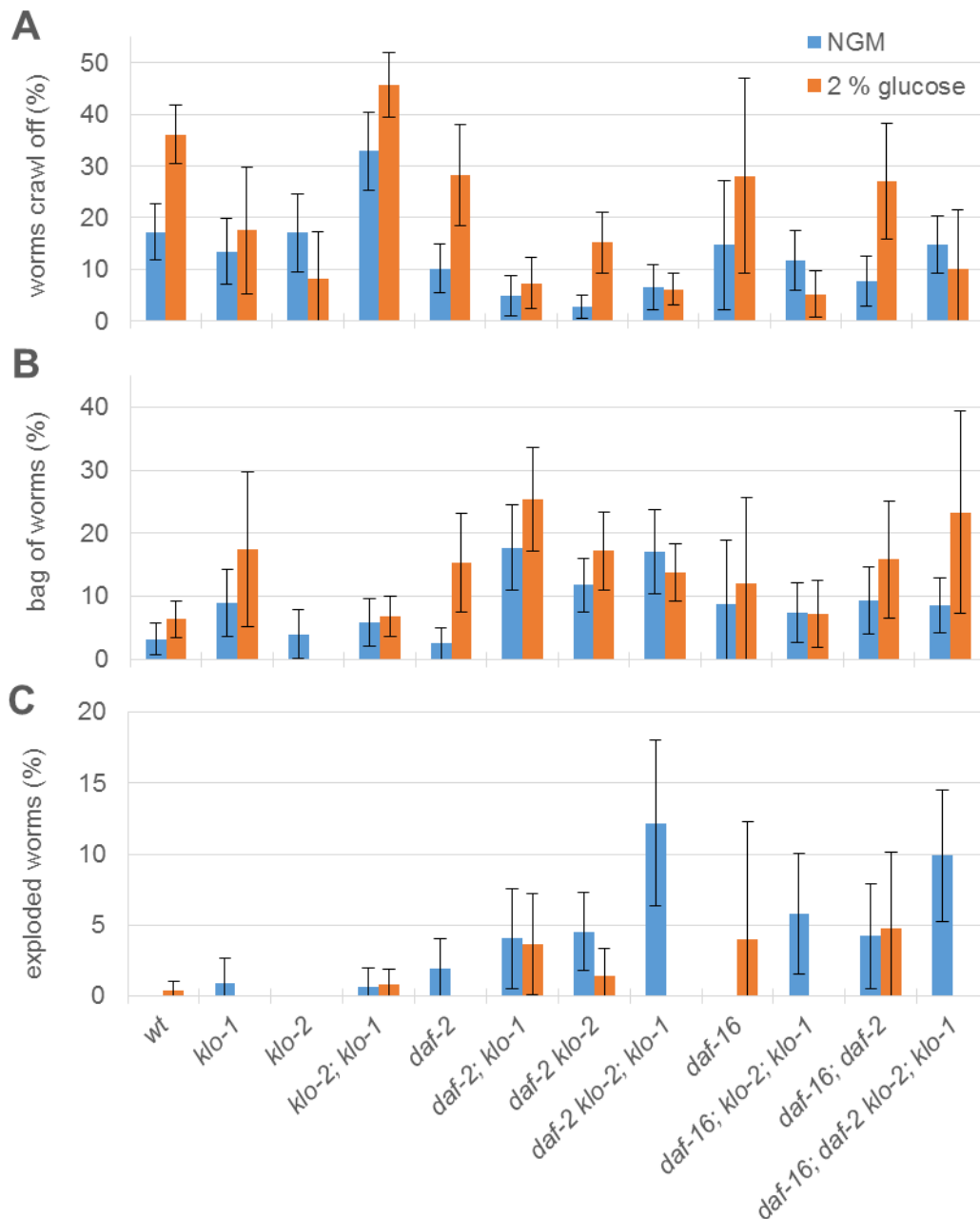


Figure 13 Percentage of censored worms in lifespan assay presented in the Figure 9 and Table 2.

Each worm strain was grown in standard NGM (blue bars) or 2 % glucose (orange bars). Error bars represent 95 % C.I.. Tukey's test was used to analyse the data. A: worms that crawled outside the NGM and died dehydrated in the plastic side of the plate. B: worms that became bag of worms (own progeny hatched inside and eat the mother). C: worms that exploded through the vulva.

3.2 Health of *Klotho* mutant worms

The fact that *Klotho* and DAF-2 act synergistically to extend lifespan does not necessarily imply that the worms lived healthier for longer. To observe if the long-lived worms were also healthier, the health of *Klotho* mutants and *daf-2 – daf-16 – Klotho* mutants was assessed by analysing the morphology and functionality of the pharynx, and the ability of the worm to crawl and to bend. Pharynx, intestine and hypodermis were also assessed to elucidate the presence of cysts in *Klotho* mutant worms (Polanska et al., 2011; Xu et al., 2017).

3.2.1 Morphology and functionality of the pharynx in *Klotho* mutant worms

Worms have a strong pharyngeal muscle that pumps the food into the intestine (Doncaster, 1962). Pharyngeal pumping consists of a contraction and relaxation of the pharyngeal muscle that sucks in the liquid food, then expels the liquid, trapping the bacteria and other small particles (Leon Avery, 1993; Raizen & Avery, 1994).

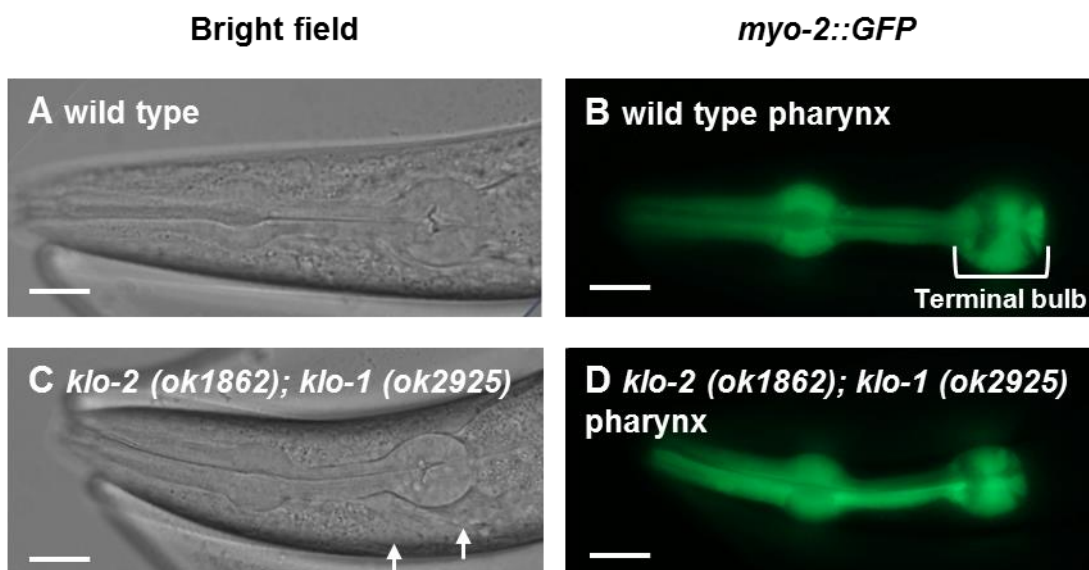


Figure 14 Pharynx morphology of young adult worms.

A: Pharynx of wild type. B: *myo-2::GFP* expression in the pharyngeal muscle of the same wild type adult as in A. C: Pharynx of *klo-2(ok1862); klo-1(ok2925)* worm. D: *myo-2::GFP* expression in the pharynx of the same *Klotho* double mutant as in C. 20 μ m scale bars. 100 worms were analysed for each strain.

Pharyngeal muscle of *Klotho* double mutant worms was analysed using *myo-2::GFP* reporter, which allows superficial observation of the pharynx morphology and muscle structure. 100 wild type and *klo-2(ok1862)*; *klo-1(ok2925)* mutant adult worms were scored, but no differences were found (Figure 14).

The pharynx functionality of *Klotho* mutant worms was also tested by comparing, the pumping rate (pumps / 30 s) of the pharynx at different developmental stages (24, 48 and 75 h). Wild type worms had a pumping rate of 80 pumps / 30 s at 24 h of development, 97 pumps / 30 s at 48 h of development and 115 pumps / 30 s at 72 h of development (Figure 15). *Klotho* mutant worms displayed very similar pumping rates compared to wild type at all three development points tested (Figure 15). No differences were found between any of the *Klotho* mutant strains and the pharynx morphology and functionality suggested a normal feeding activity.

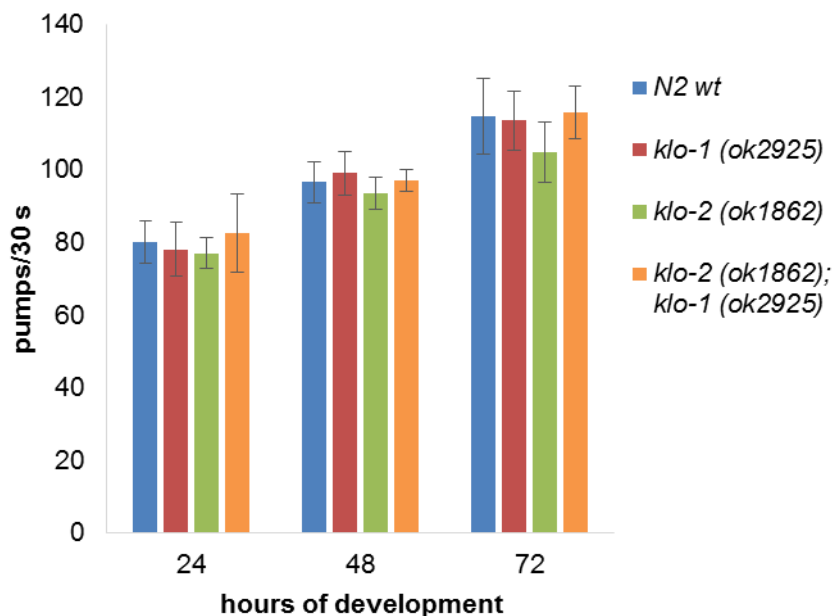


Figure 15 Pumping rate (pumps / 30 seconds) \pm 95 % C.I. of N2 wild type, *klo-1(ok2925)*, *klo-2(ok1862)* and *klo-2(ok1862); klo-1(ok2925)* double mutant worms at 24 h, 48 h and 72 h of development. Tukey's test was used to analyse differences between wild type and *Klotho* mutant worms ($\alpha = 0.05$).

Klotho has been shown to be involved in energy metabolism by interacting with insulin/IGFR (Kurosu et al., 2005) and, *Klotho* levels in plasma are be decreased in obesity (Amitani et al., 2013). Therefore, it was hypothesised that the slower development and longer lifespan of combined *daf-2* and *Klotho* mutant worms

could be caused by a slower metabolic rate. To confirm this hypothesis, the pharyngeal pumping rate (pumps / 30 s) of worms at 1st day of adult life was measured as an indicator of muscular activity related to food intake. As it was previously reported at 24, 48 and 72 h of development (Figure 15), wild type, *klo-1(ok2925)* and *klo-2(ok1862)* worms had similar pumping rates at 1st day of adult life, respective rates of 142, 140 and 145 pumps / 30 s (Figure 16).

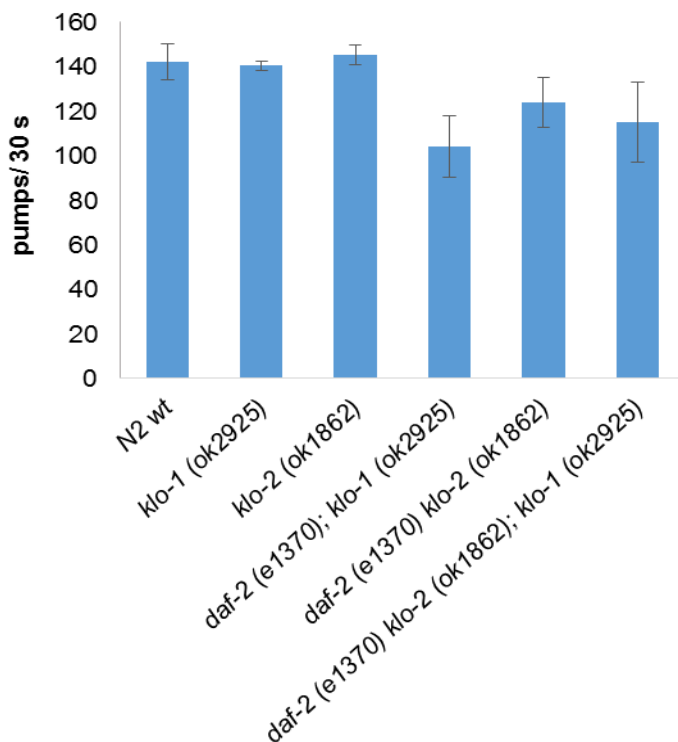


Figure 16 Pumping rate (pumps / 30 seconds) \pm 95 % C.I. of N2 wild type, *klo-1(ok2925)*, *klo-2(ok1862)* and *daf-2(e1370)* *Klotho* mutant worms at one day of adult life (10 worms per strain). Tukey's test was used to analyse differences between wild type and *Klotho* mutant worms ($\alpha = 0.05$).

In contrast, *daf-2(e1370)* *Klotho* mutants displayed a significant lower pumping rate. The pumping rate was reduced to 104 pumps / 30 s in *daf-2(e1370); klo-1(ok2925)* mutant worms as compared to *klo-1(ok2925)* mutants ($p < 0.0001$); and to 123 in *daf-2(e1370) klo-2(ok1862)* mutant worms as compared to *klo-2(ok1862)* mutant worms ($p = 0.0008$; Figure 16). *daf-2(e1370)* double *Klotho* mutant worms displayed similar pumping rate of 115 pumps / 30 s, as compared to single *Kloths* with *daf-2(e1370)* (Figure 16). Despite the differences of pumping rates between the different *Klotho* mutations with *daf-2(e1370)*

background mutation, those were not statistically significant. Altogether, suggested that with *daf-2(e1370)* background mutation the mutant worms feed slower, however, it cannot be concluded that this is only caused by *daf-2 (e1370)* or if this is another case of synergistic effect between *daf-2 (e1370)* and *Klotho* mutations because the pumping rate of *daf-2 (e1370)* single mutants was not assessed.

3.2.2 Movement of worms as an indicator of food sensitivity and metabolic rate

Motility can be used as an indicator of food preference or food sensing (Hahm et al., 2015). Because *klo-2(ok1862); klo-1(ok2925)* double mutant worms tend to crawl off the plate more often than wild type worms, it was hypothesised that *Klotho* mutant worms could have a defect with food sensing. Also, movement is an indicator of the metabolic rate of an organism (Gaglia & Kenyon, 2009; Tucker, 1970) which in turn is related to development, brood size and lifespan. The motility of *Klotho* mutant worms was analysed by measuring the distance covered by worms in 2 h at various temperature (Figure 17A - B).

Wild type worms crawled an average distance of 10.6 ± 2.1 cm (95 % C.I.) at 20 °C and 9.5 ± 1.9 cm at 25 °C (Figure 17C). When wild type worms were exposed to a heat shock by transferring them from 20 °C to pre-warmed NGM plates and incubated for 2 h at 25 °C they crawled 10.9 ± 2.5 cm (Figure 17C), suggesting that shift to higher temperature did not alter significantly the foraging behaviour of wild type worms.

Klotho double mutant worms crawled similar distance to wild type at 20 °C, an average of 10.2 ± 3.0 cm. At 25 °C *Klotho* mutants crawled 8.0 ± 3.5 cm, less than wild type at this temperature and less than the mutants did at 20 °C, suggesting an altered behaviour in response to heat. Wild type and *Klotho* double mutant worms crawled less at 25 °C than at 20 °C, but the differences were not statistically significant (Figure 17.C). In stressing conditions of heat shock, when transferred from 20 °C to pre-warmed NGM plates at 25 °C, wild type and *Klotho* double mutant worms crawled a slightly longer distance than at constant temperatures of 20 °C or 25 °C, but no significant differences were observed. From these results, no effect was observed in the locomotor ability or food sensitivity of *Klotho* mutant.

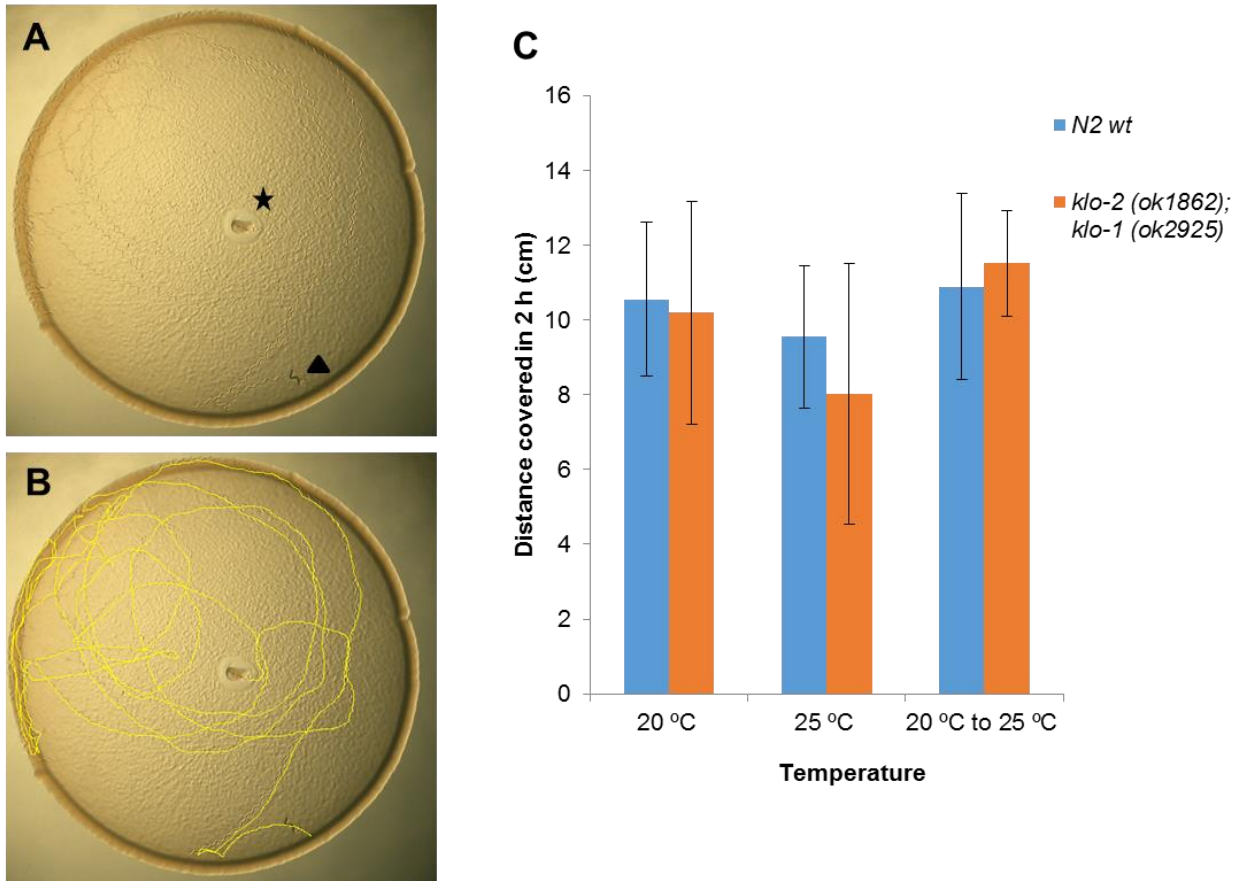


Figure 17 Worm motility at different temperatures and upon temperature upshift.

A: Each young adult worm was transferred to the centre of a circular food lawn and after 2 h of incubation at specific temperature, a picture was taken. Centre point where worm was transferred is next to star icon and worm is next to triangle icon. B: Crawled path was measured with ImageJ software. C: Mean distance covered (cm) in 2 h for wild type and *klo-2(ok1862); klo-1(ok2925)* mutant worms in three different conditions: “20 °C” means worms and test NGM plates were preconditioned at 20 °C and then incubated for 2 h at 20 °C (n = 10, for both worm strains); “25 °C” means worms and plates were preconditioned at 25 °C and then incubated for 2 h at 25 °C (n (wild type) = 10; n (*klo-2(ok1862); klo-1(ok2925)*) = 8); and “20 °C to 25 °C” means that worms were preconditioned at 20 °C, transferred to NGM test plates preconditioned at 25 °C and then incubated for 2 h at 25 °C (n = 11, for both worm strains). Error bars represent 95 % C.I.. Tukey test was used to analyse the data and not significant differences were found ($\alpha = 0.05$).

3.2.3 Healthy worms moving at 16 and 28 days of adult life

Healthspan means that the animals are healthy during the lifespan. To confirm that the worms living two or three times longer than wild type were also healthy for longer, the ability of the worms to crawl by bending

their body were used as health indicators (adapted from (Keith et al., 2014)). The number of healthy adult worms grown in standard NGM and in 2 % glucose was measured at 16 and 28 days of adult life.

At 16 days of adult life, 33 % of wild type worms were considered healthy as assessed by the ability to crawl. *Klotho* single and double mutants displayed a very similar percentage of healthy individuals as compared to wild type. All *daf-2(e1370)* and *daf-2(e1370) Klotho* mutant worms were able to crawl at day 16 of adult life. In contrast, none of the *daf-16(mu86)* mutant worms (N= 6) were able to crawl at day 16.

The addition of glucose to the medium increased the percentage of healthy animals at day 16 in all strains. In wild type (N2), glucose increased the percentage of healthy animals to 54 % and to similar values in *klo-1(ok2925)* (58 %), *klo-2(ok1862)* (50 %) and *klo-2(ok1862); klo-1(ok2925)* double mutant worms (50 %) (Figure 18A). *daf-16(mu86)* mutant worms were also affected by glucose but, despite the increased percentage of healthy animals the change was not significant due to the small number of live animals. The remaining living worms were healthy until 1 - 2 days before their death (Figure 18A).

The percentage of healthy animals was also quantified at 28 days for the *daf-2(e1370)* and *daf-2(e1370) Klotho* mutant worms only, because almost all wild type worms, *Klotho* mutants and worms containing *daf-16(mu86)* mutation were dead at this time. 97 % of *daf-2(e1370)* mutant worms were healthy at 28 days of adult life and similar values were observed for *daf-2(e1370) Klotho* mutant worms (Figure 18A). Although at 28 days only 3 – 6 worms were alive for *daf-2(e1370) Klotho* mutant strains grown in 2 % glucose, almost all of them were able to crawl/bend.

These results suggest that *daf-2(e1370) Klotho* mutant worms with prolonged lifespan, also had prolonged healthspan as they were all able to crawl at 28 days of adult life, while none of the few wild type and *Klotho* mutant worms could crawl until the last day of life (Figure 18). At the same time, the presence of glucose decreased significantly the lifespan (Figure 9).

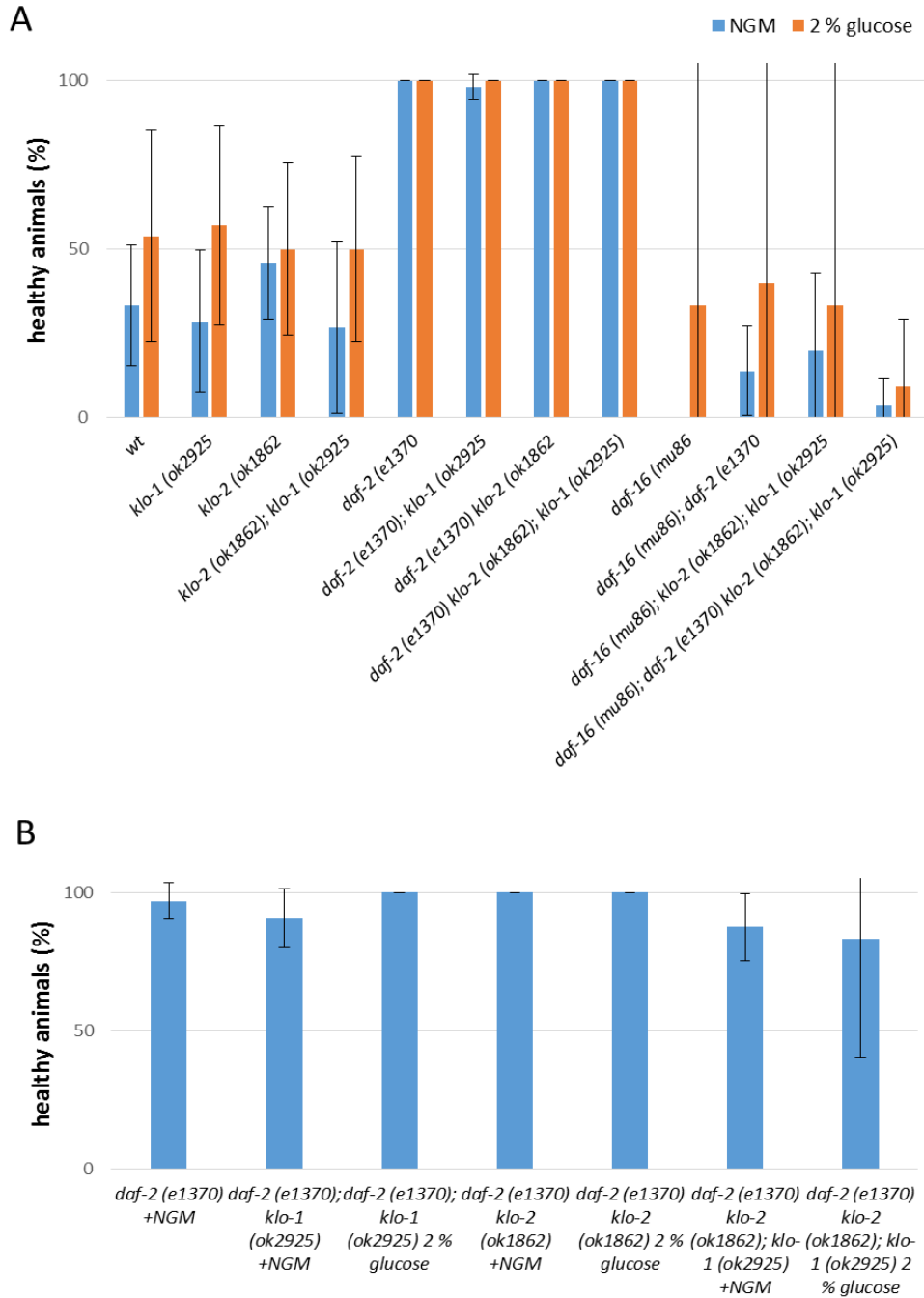


Figure 18 Worms with *daf-2 (e1370)* mutation are healthier for longer time.

Healthy animals (%) \pm 95 % C.I. is calculated as the percentage of animals that bend their bodies or crawl when gently tapped. A: healthy animals at 16 days of adult life when grown in standard NGM (blue bars) and in 2 % glucose NGM (orange bars). B: healthy animals at 28 days of adult life in NGM and in 2 % glucose. Only *daf-2(e1370)* and *daf-2(e1370) Klotho* mutant worms were living after 28 days.

Table 6. Healthy animals at 16 and 28 days of adult life.

Worms grown in standard NGM and 2 % glucose NGM. Number of animals (n) corresponds to the total number of living animals at this time used for lifespan assays. At 16 days the amount of living animals on glucose NGM is lower because of the shorter lifespan and higher percentage of censoring (crawled off, bag of worms or exploded). Tukey's test was used to analyse differences between strains ($\alpha = 0.05$) and results are presented as p-values against wild type grown in NGM. No significant differences were found on any strain when grown either on standard NGM or 2 % glucose NGM.

Worm strain	Treatment	16 days			28 days		
		n	healthy worms (%) ± 95 % C.I.	p value	n	healthy worms (%) ± 95 % C.I.	p value
<i>wt</i>	NGM	30	33 ± 17.9				
	glucose	13	54 ± 31.4	0.95			
<i>klo-1 (ok2925)</i>	NGM	21	29 ± 21.1	1.00			
	glucose	14	57 ± 29.7	0.77			
<i>klo-2 (ok1862)</i>	NGM	37	46 ± 16.8	0.99			
	glucose	18	50 ± 25.6	0.98			
<i>klo-2(ok1862); klo-1 (ok2925)</i>	NGM	15	27 ± 25.3	1.00			
	glucose	16	50 ± 27.5	0.99			
<i>daf-2 (e1370)</i>	NGM	48	100 ± 0.0	<0.001	31	18 ± 6.6	
	glucose	13	100 ± 0.0	<0.001			
<i>daf-2(e1370); klo-1 (ok2925)</i>	NGM	54	98 ± 3.7	<0.001	32	30 ± 10.7	0.06
	glucose	37	100 ± 0.0	<0.001	3	0 ± 0.0	0.14
<i>daf-2(e1370) klo-2 (ok1862)</i>	NGM	30	100 ± 0.0	<0.001	39	0 ± 0.0	0.06
	glucose	28	100 ± 0.0	<0.001	4	0 ± 0.0	0.13
<i>daf-2(e1370) klo-2(ok1862); klo-1(ok2925)</i>	NGM	38	100 ± 0.0	<0.001	32	34 ± 12.1	0.06
	glucose	30	100 ± 0.0	<0.001	6	41 ± 42.8	0.11
<i>daf-16 (mu86)</i>	NGM	6	0 ± 0.0	0.74			
	glucose	3	33 ± 143.4	1.00			
<i>daf-16(mu86); daf-2 (e1370)</i>	NGM	29	14 ± 13.3	0.73			
	glucose	5	40 ± 68.0	1.00			
<i>daf-16(mu86); klo-2(ok1862); klo-1 (ok2925)</i>	NGM	15	20 ± 22.9	1.00			
	glucose	3	33 ± 143.4	1.00			
<i>daf-16(mu86); daf-2(e1370) klo-2(ok1862); klo-1(ok2925)</i>	NGM	26	4 ± 7.9	0.07			
	glucose	11	9 ± 20.3	0.86			

3.2.4 Cysts in *Klotho* mutant worms

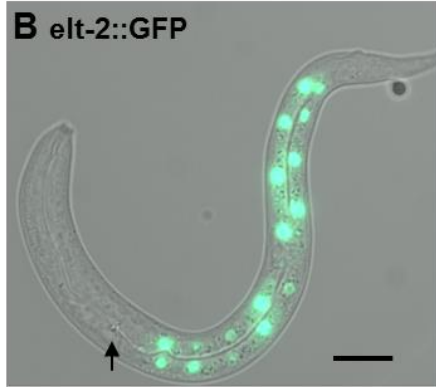
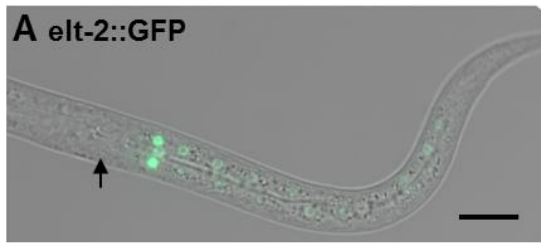
klo-2; klo-1 double mutant worms develop cysts within the body cavity. It has been suggested that these cysts are due to water retention and around one third of *Klotho* (gain of function) mutant worms (Polanska et al., 2011) and *klo-2; klo-1* double loss-of-mutant worms (Xu et al., 2017) present them. In this thesis, it was confirmed that *Klotho* (loss of function) mutant worms presented cysts (Figure 19C - D).

3.2.4.1 Presence of cysts and malformation of digestive tract

The *C. elegans* digestive tract consists mainly of the pharyngeal muscle and the intestine. The pharyngeal muscle of *klo-2(ok1862); klo-1(ok2925)* mutant worms did not have any obvious morphological defects compared to wild type worms (Figure 14) and it was fully functional (Figure 15; Figure 16). EGL-15 (FGF-like receptor tyrosine kinase) has been shown to be involved in the development of the intestine (Hoffmann, Segbert, Helbig, & Bossinger, 2010) and to assess whether *klo-1* and *klo-2* may play a role in the intestinal development, the intestine was analysed at different developmental stages. *ajm-1* encodes for an apical junction protein, and *ajm-1*-reporter is thus expressed in all cell boundaries containing apical junctions (Bulow et al., 2004; Mohler et al., 1998) and was used to visualise intestinal cells in embryos. No differences were found between the intestinal tube of *klo-2(ok1862); klo-1(ok2925)* mutant embryos and wild type embryos (Figure 19E - F).

The intestine was also analysed at L1 larval stage, but in this case, the expression of *elt-2::GFP* was used to observe the nuclei of intestinal cells. The *elt-2* reporter allowed analysis of the number of nuclei of intestinal cells in *Klotho* mutant worms. At L1 stage, wild type worms had 20 nuclei, one in each intestinal cell (Figure 19A - B). In contrast, in 10 % of *klo-2(ok1862); klo-1(ok2925)* L1 larvae, the *elt-2::GFP* was not confined to the nuclei but was more diffuse (Figure 19D), particularly in the worms with cysts (Figure 19C). This suggests that the worms with cysts are not only potentially retaining liquid but also have defects in tissue integrity and or degradation.

Wild type



klo-2 (ok1862); klo-1 (ok2925)

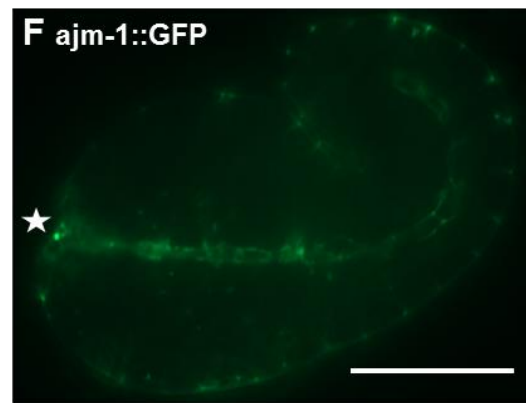
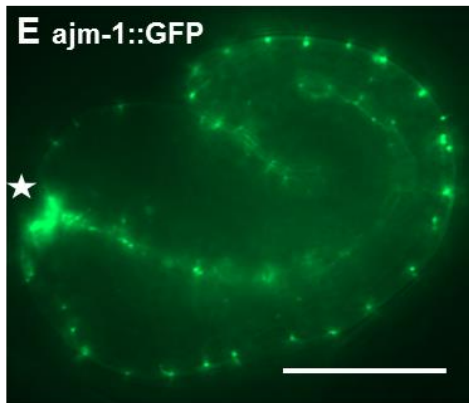
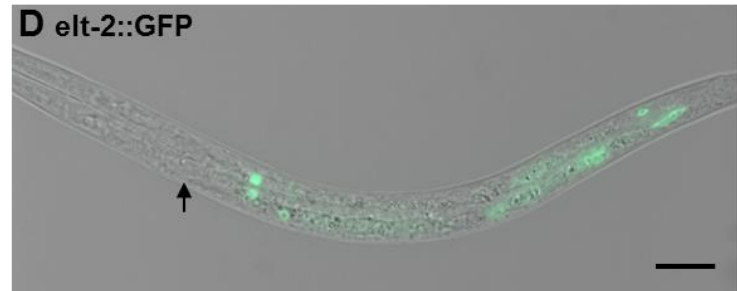
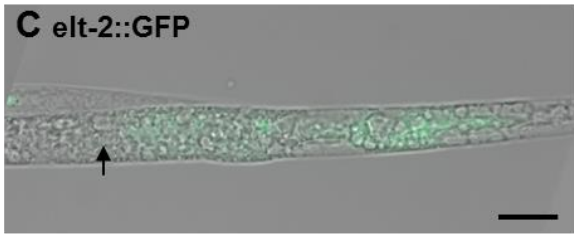


Figure 19 Assessment of digestive tract of wild type and *klo-2 (ok1862); klo-1 (ok2925)* worms at embryo and larvae stages.

A-B: *elt-2::GFP* expression in the nuclei of intestinal cells of wild type L1 larva. C-D: *elt-2::GFP* expression in *klo-2(ok1862); klo-1(ok2925)* L1 larva with cysts (C). The GFP expression is not confined to the nucleus. E-F: *ajm-1::GFP* expression on intestinal cells junctions of wild type (E) and *klo-2(ok1862); klo-1(ok2925)* (F) embryo. Star symbol indicates the mouth. G-H: *ajm-1::GFP* expression on seam cells junctions of wild type (G) and *klo-2(ok1862); klo-1(ok2925)* (H) L2 larva. Seam cells are visible from pharynx bulb to the tail. Arrow indicates the pharynx bulb. 20 μ m scale bars. 100 worms were analysed for each strain and representative images are shown.

3.2.4.2 The development of seam cells

Another hypothetical cause for the cysts could be a developmental problem of the seam cells of the hypodermis. Seam cells are epithelial cells, arranged in two longitudinal rows at each lateral side of the worm hypodermis (Singh & Sulston, 1978). Seam cells are required for the formation of stage specific cuticle, through synthesis of secreted collagens (Thein et al., 2003). The development of seam cells was followed from recently laid embryos (approximately 300 min post fertilisation) until L4 larval stage by observing the expression of *ajm-1::GFP* on cellular junctions (Figure 19G - H). No differences in the morphology and number of seam cell were observed between wild type and *klo-2(ok1862); klo-1(ok2925)* worms.

3.3 Stress resistance

Klotho has been suggested to be involved in stress resistance through the interaction with Insulin/IGF-1 signalling (Mitobe et al., 2005; Yamamoto et al., 2005). Having found the synergistic effects of *daf-2(e1370)* with *klo-1* and *klo-2* in the elongation of lifespan and in the slowing down of development, the effect of Klotho in response to oxidative stress, temperature stress and osmotic shock was assessed.

3.3.1 Oxidative stress

The theory of oxidative damage caused by high levels of reactive oxygen species (ROS) has been claimed as one of the main causes of cellular stress and ageing (Van-Raamsdonk, Hekimi, Van Raamsdonk, & Hekimi, 2010), although a number of studies dispute this theory (Gems & Doonan, 2009). The herbicide paraquat induces production of superoxide-anions and is thus a widely used experimental oxidative stress agent (Ishii et al., 1990; Vanfleteren, 1993).

3.3.1.1 Survival on exposure to high concentration of paraquat

Survival to oxidative stress was measured in L4 larvae submerged in M9 buffer containing 300 mM paraquat (Keith et al., 2014). Control worms were incubated in parallel in M9 buffer. The assay was stopped after 9 h and at this time all control worms were still alive.

In paraquat, wild type worms had a mean survival of 2.5 h and a maximum survival of 5 h (Table 7). *klo-1(ok2925)* single mutants had a significant increase in the mean survival to 5.4 h (Table 7) and one quarter of worms were still alive after 9 h of paraquat treatment (Figure 20A). *klo-2(ok1862)* single mutants and *klo-2(ok1862); klo-1(ok2925)* double mutants displayed a small, but not significant, prolonged mean survival (Figure 20A; Table 7).

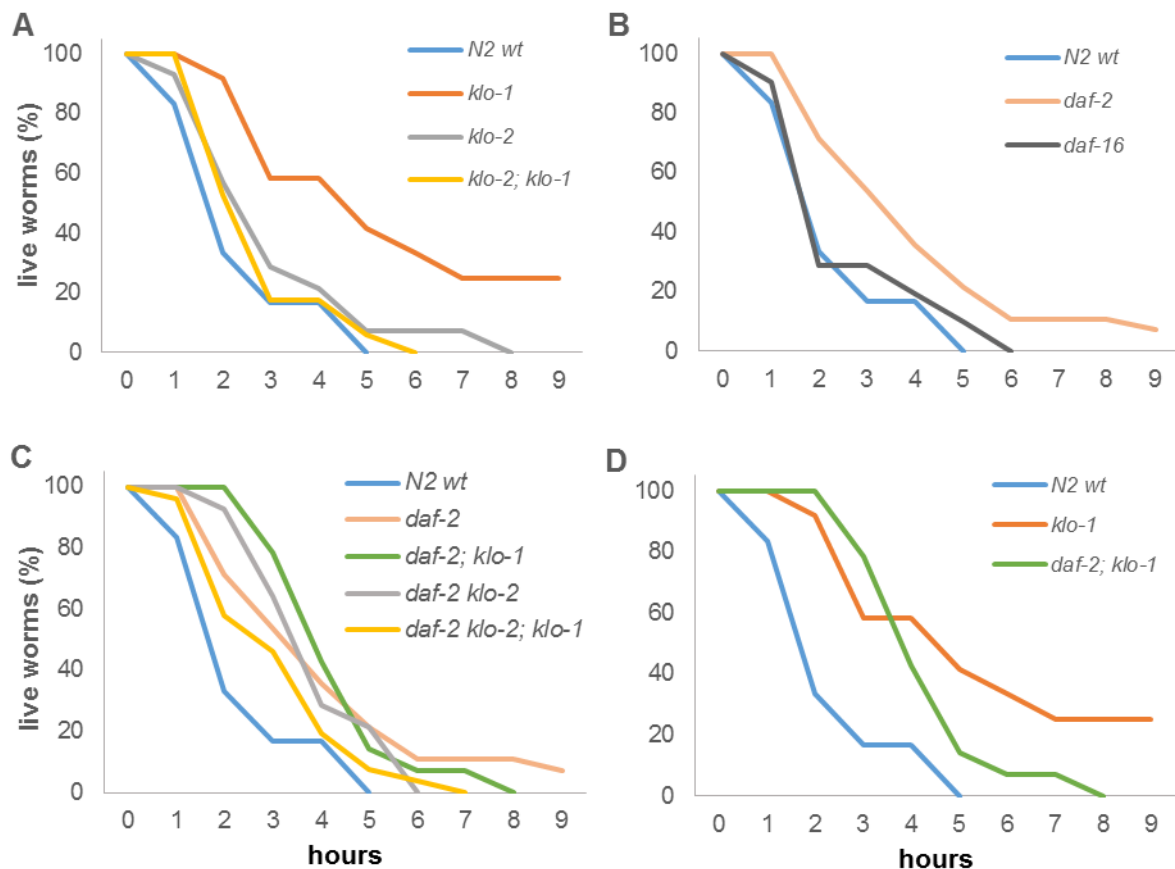


Figure 20 Survival of L4 larvae in 300 mM paraquat after 9 h.

A: *klo-1(ok2925)* worms have a longer mean lifespan than wild type, *klo-2(ok1862)* and *klo-2(ok1862); klo-1(ok2925)* mutant worms. One quarter of *klo-1(ok2925)* animals were still alive after 9 h in 300 mM paraquat. B: *daf-2(e1370)* worms have a longer mean lifespan than wild type. Lifespan is not affected in *daf-16(mu86)* worms compared to wild

type. C and D: *daf-2(e1370)*; *klo-1(ok2925)* and *daf-2(e1370) klo-2(ok1862)* double mutant worms have significantly longer mean lifespan than wild type worms, but no difference as compared to *daf-2(e1370)* single mutant worms. Triple mutant worms *daf-2(e1370) klo-2(ok1862)*; *klo-1(ok2925)* have a significant shorter mean lifespan than *daf-2(e1370)*; *klo-1(ok2925)* worms, but no difference when compared to wild type worms. n animals = 14-24. Equal number of animals per strain was assessed in parallel in M9 buffer as control. The survival of worms in control media (no paraquat) was 100 %. Data is the mean of at least two independent experiments per strain.

Compared to wild type, *daf-2(e1370)* mutant worms had a significantly longer mean survival of 4.3 h (Table 7; Figure 20B). Neither *klo-1(ok2925)* nor *klo-2(ok1862)* mutations in conjunction *daf-2(e1370)* genetic background altered the mean survival of *daf-2(e1370)* mutants alone (mean survival 4.6 and 4.0 h, respectively (Figure 20C)), suggesting *daf-2* being the determining factor (Table 7). However, simultaneous removal of both *klo-1* and *klo-2* in the *daf-2(e1370)* genetic background (in *daf-2(e1370) klo-2(ok1862)*; *klo-1(ok2925)* triple mutants) suppressed the survival benefit of *daf-2(e1370)* (mean survival in paraquat 3.0 h.

Table 7 Survival of worms in 300 mM paraquat.

Total number of animals includes observed animals and censored animals that crawled outside the paraquat solution. Logrank (Kaplan-Meier) statistical analysis was used to assess significant differences between worm strains, presented as p-values ($p < 0.05$). Other pairwise comparisons are presented in the first column from the right as follows ^a: compared to *klo-1(ok2925)*; ^b: compared to *daf-2(e1370)*; ^c: compared to triple mutant *daf-2(e1370) klo-2(ok1862)*; *klo-1(ok2925)*.

Worms in 300 mM paraquat	Mean Lifespan \pm SEM (hours)	Total Animals	p-value against N2 wild type	p-value other comparisons	
N2 wild type	2.5 \pm 0.37	14			
<i>klo-1(ok2925)</i>	5.4 \pm 0.73	15	0.001		
<i>klo-2(ok1862)</i>	3.2 \pm 0.48	15	0.317	0.012 ^a	
<i>klo-2(ok1862)</i> ; <i>klo-1(ok2925)</i>	3.1 \pm 0.31	23	0.133	0.005 ^a	
<i>daf-2(e1370)</i>	4.3 \pm 0.45	24	0.006		
<i>daf-2(e1370)</i> ; <i>klo-1(ok2925)</i>	4.6 \pm 0.35	17	0.001	0.841 ^b	0.012 ^c
<i>daf-2(e1370) klo-2(ok1862)</i>	4.0 \pm 0.34	17	0.009	0.660 ^b	0.115 ^c
<i>daf-2(e1370) klo-2(ok1862)</i> ; <i>klo-1(ok2925)</i>	3.0 \pm 0.36	22	0.363	0.029 ^b	
<i>daf-16(mu86)</i>	2.7 \pm 0.32	22	0.652	0.006 ^b	

Because DAF-16 is needed for transcription of genes with antioxidant activity (Honda & Honda, 1999) it was expected that *daf-16(mu86)* worms had a shorter mean survival. However, *daf-16(mu86)* animals had a mean survival of 2.7 h, almost identical to wild type worms (Figure 20B).

3.3.1.2 Superoxide dismutase gene expression is not altered in *Klotho* mutants upon oxidative stress response.

sod-3 (superoxide dismutase) is a target gene of DAF-16/FOXO (Honda & Honda, 1999) and it is activated in stress situations to protect against oxidative stress (Fukai, Folz, Landmesser, & Harrison, 2002). The expression of *psod-3::GFP* reporter gene (Essers et al., 2005; Honda & Honda, 1999) was measured to observe differences between wild type and *Klotho* mutant strains in standard NGM and in the presence of the herbicide paraquat known to lead to oxidative stress (Essers et al., 2005; Ishii et al., 1990).

3.3.1.2.1 *psod-3::GFP* expression on larvae grown in the presence of paraquat

Worms were synchronised by egg laying and grown for 48h at 20 °C in NGM plates with or without 0.25 mM paraquat. *psod-3::GFP* intensity was measured in the 1st and 3rd set of intestinal cells (Figure 21.A and B) and values were normalised to wild type worms grown in standard NGM. No increase in *psod-3::GFP* expression were observed in any of the strains analysed (Figure 21C - D) grown in paraquat, which is in contrast to previously published data (Essers et al., 2005). The only exception was the 3rd set of intestinal cells measured for the *Klotho* double mutant worms in the presence of paraquat where an increase of 35 % ± 16 % (95 % C.I.) ($p < 0.002$) in *psod-3::GFP* expression was observed (Figure 21D;

Table 8).

The error bars for the *psod-3::GFP* expression levels for *daf-16(mu86)* mutants are wider than for the other worm strains (Figure 21C - D), which is due to the high variation of GFP expression in *daf-16* mutant worms compared to wild type (Figure 21E) or *Klotho* mutant worms. These results suggest that DAF-16 regulates *sod-3* expression but is not necessary for it, which could explain why some *daf-16* larvae have 90 % less *psod-3::GFP* expression while others have three times higher expression than wild type in NGM.

Larvae grown in paraquat grew slower than larvae grown in standard NGM, and this developmental delay was particularly notable for *daf-16(mu86)* mutant worms (Figure 22).

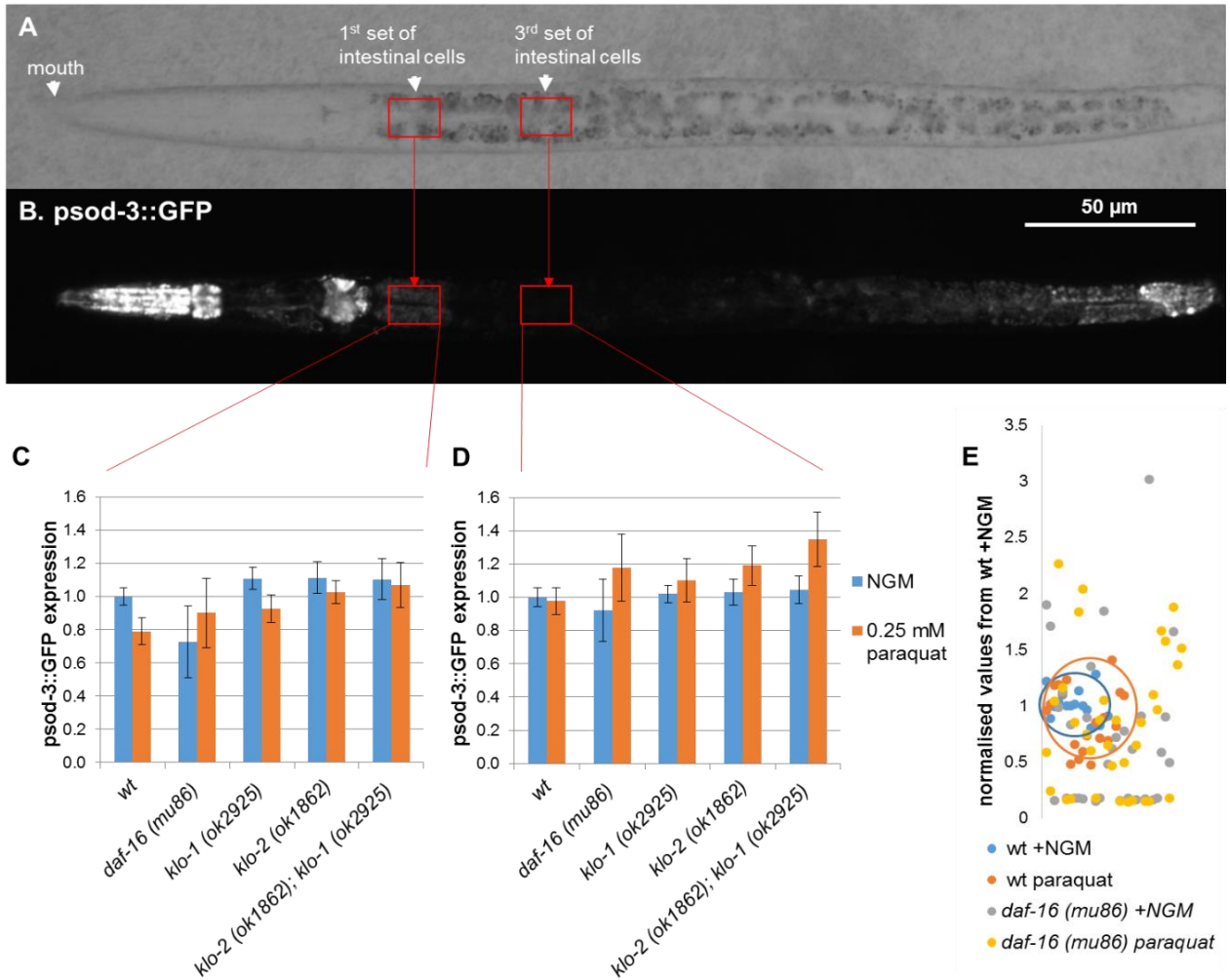


Figure 21 *psod-3::GFP* expression in L3 stage worms grown in NGM with or without 0.25 mM paraquat.

A: Wild type larvae at 48 h of development. Squares drawn represent the area of the intestine selected to quantify the average GFP intensity. The same sized area was analysed for all strains. White arrow indicates mouth. Scale bar is 50 μ m. B: *psod-3::GFP* expression pattern of the same wild type larva as in (A). C, D: *psod-3::GFP* mean intensity of each worm strain grown on NGM control plates (blue bars) or 0.25 mM paraquat plates (orange bars). Values were normalised to wild type (wt) on NGM and at least 38 individuals from two independent tests were used. Error bars represent 95 % C.I.. Values from 1st set of intestinal cells (C) and from 3rd set of intestinal cells (D) are shown. E: Dispersion of *psod-3::GFP* intensities in 1st set of intestinal cells. *psod-3::GFP* expression is more dispersed in *daf-16 (mu86)* compared to wt. GFP intensity of *psod-3::GFP* in wild type worms on NGM are inside the blue circle and in 0.25 mM paraquat inside the orange circle.

Table 8. Values of *psod-3::GFP* expression in larvae grown in NGM with or without 0.25 mM paraquat for 48 h. Tukey's analysis of data from two independent assays ($\alpha = 0.05$). Values are represented as the mean normalised values \pm 95 % C.I.

Strain	Treatment	n	1st set of intestinal cells		3rd set of intestinal cells	
			mean GFP intensity \pm 95 % C.I.	p value	mean GFP intensity \pm 95 % C.I.	p value
wt	NGM	43	1.00 \pm 0.05		1.00 \pm 0.06	
	0.25 mM paraquat	41	0.79 \pm 0.08	0.301	0.98 \pm 0.08	1.000
<i>daf-16(mu86)</i>	NGM	38	0.73 \pm 0.21	0.059	0.92 \pm 0.19	0.997
	0.25 mM paraquat	40	0.90 \pm 0.21	0.979	1.18 \pm 0.20	0.559
<i>klo-1(ok2925)</i>	NGM	40	1.11 \pm 0.06	0.959	1.02 \pm 0.05	1.000
	0.25 mM paraquat	43	0.93 \pm 0.08	0.997	1.10 \pm 0.13	0.973
<i>klo-2(ok1862)</i>	NGM	43	1.11 \pm 0.09	0.944	1.03 \pm 0.08	1.000
	0.25 mM paraquat	38	1.03 \pm 0.07	1.000	1.19 \pm 0.12	0.473
<i>klo-2(ok1862); klo-1(ok2925)</i>	NGM	41	1.10 \pm 0.12	0.970	1.05 \pm 0.08	0.999
	0.25 mM paraquat	44	1.07 \pm 0.13	0.998	1.35 \pm 0.16	0.002

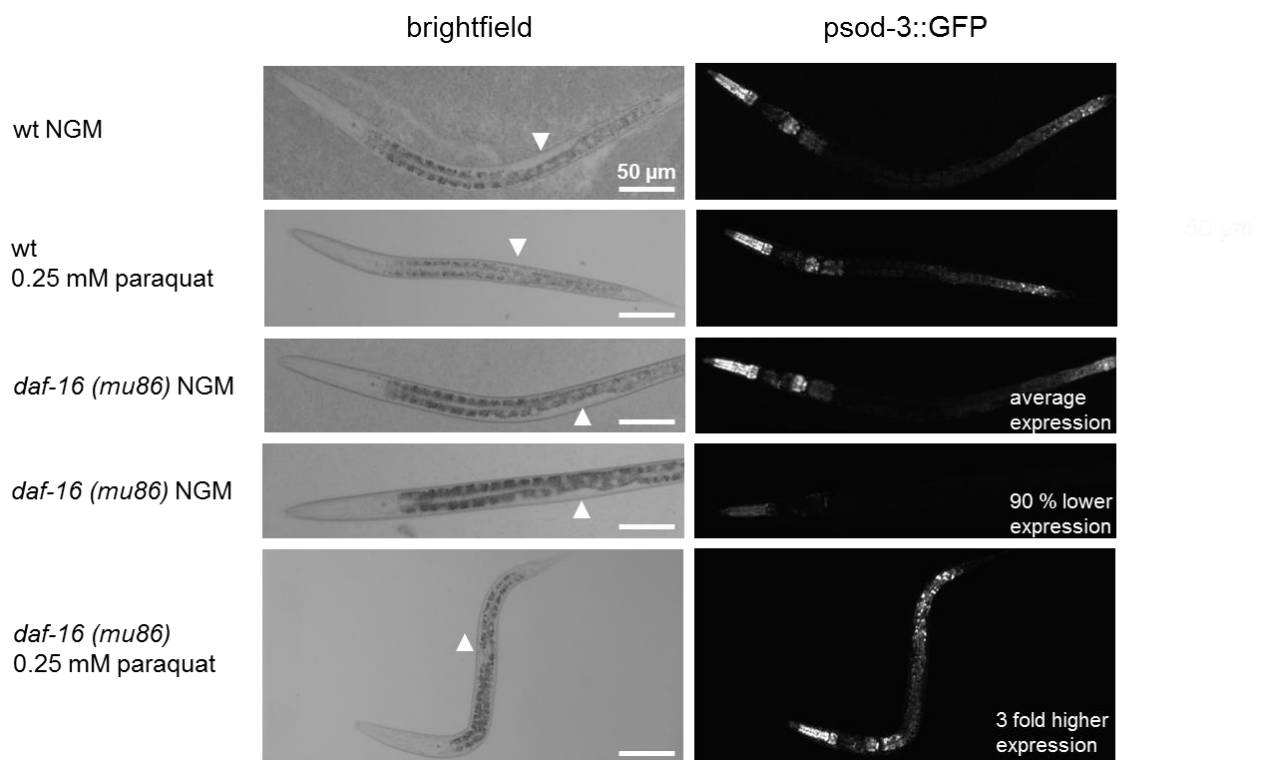


Figure 22 *psod-3::GFP* expression in larvae grown 48 h on NGM with or without 0.25 mM paraquat.

Scale bars represent 100 μm in all the pictures. White arrows point to developing vulva and gonad. Paraquat slowed down the development of wild type and *daf-16(mu86)* worms. *psod-3::GFP* expression did not change in wild type worms grown in paraquat. *psod-3::GFP* expression in *daf-16(mu86)* mutants displayed great variability.

3.3.1.2.2 *psod-3::GFP* expression in adults stressed with paraquat for 30 minutes

psod-3::GFP expression was also measured in the pharynx of one day old adult worms (Figure 23A) which were soaked in 100mM paraquat in M9 for 30 min and then allowed to recover for 3 h on NGM plates containing food (An & Blackwell, 2003). Control worms were soaked in M9 buffer for 30 min prior to recovery on NGM plates. GFP expression was normalised to wild type worms soaked in M9 and no difference was observed in comparison to *Klotho* mutants in M9 (Figure 23B). However, *daf-16(mu86)* worms had significantly less GFP than all other strains in control conditions (Figure 23B).

In the presence of 100 mM paraquat, *psod-3::GFP* was significantly reduced in wild type *C. elegans*. Similar to wild type worms, in both *klo-1(ok2925)* and *klo-2(ok1862)* single mutants, the expression of *psod-3::GFP* was decreased 3 h after exposure to 100 mM paraquat in comparison to worms incubated in M9. However, 100 mM paraquat did not cause a significant change in *psod-3::GFP* expression in *Klotho* double mutants 3 h after exposure (Figure 23B). The reduction of *psod-3::GFP* expression 3 h after paraquat exposure was somewhat unexpected (Figure 23B), and contradicts previous findings (Essers et al., 2005)

Table 9. *psod-3::GFP* values of one day old adult worms treated with 100 mM paraquat for 30 min followed by 3 hours recovery in standard NGM with food.

Mean GFP intensity \pm 95 % C.I. were normalised to wild type in M9. Tukey's analysis of data from two independent assays was used ($p = 0.05$). Statistic differences are presented as p values against wild type in M9 and p values of same worm strain treated with M9 or 100 mM paraquat.

Strain	Treatment	n	mean GFP intensity \pm 95 % C.I.	p value against wt M9	p value same strain different treatment
<i>wt</i>	M9	38	1.00 \pm 0.07		
	100 mM paraquat	41	0.73 \pm 0.07	0.0000	
<i>daf-16(mu86)</i>	M9	30	0.70 \pm 0.10	0.0000	
	100 mM paraquat	29	0.54 \pm 0.10	0.0000	0.1635
<i>klo-1(ok2925)</i>	M9	48	1.08 \pm 0.05	0.7435	
	100 mM paraquat	42	0.75 \pm 0.08	0.0000	0.0000
<i>klo-2(ok1862)</i>	M9	47	0.93 \pm 0.04	0.8664	
	100 mM paraquat	52	0.64 \pm 0.06	0.0000	0.0000

<i>klo-2(ok1862); klo-1(ok2925)</i>	M9	41	1.00 ± 0.06	1.0000	
	100 mM paraquat	43	0.86 ± 0.06	0.0951	0.1046

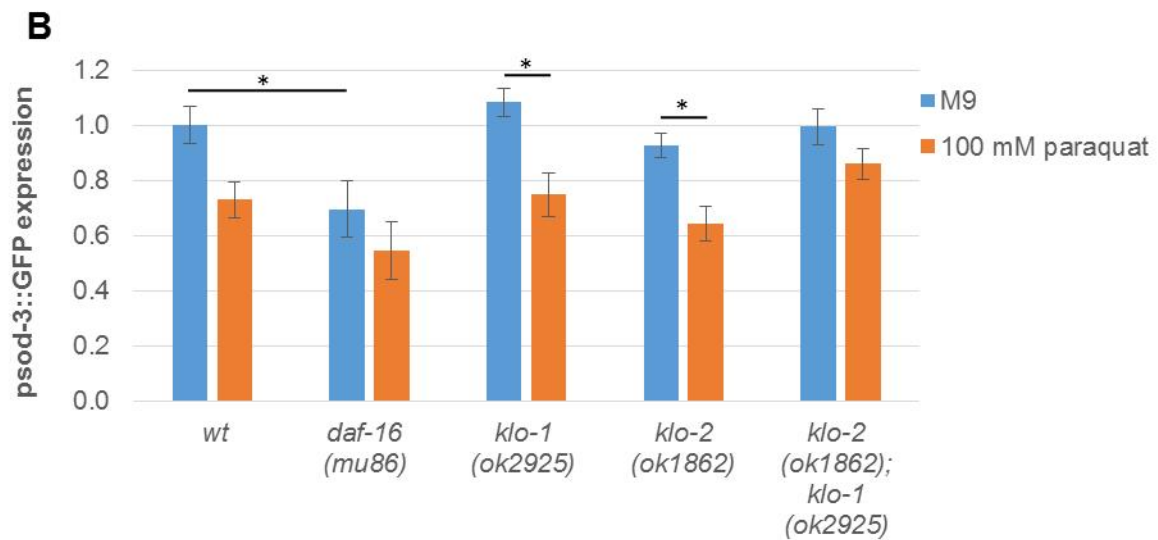
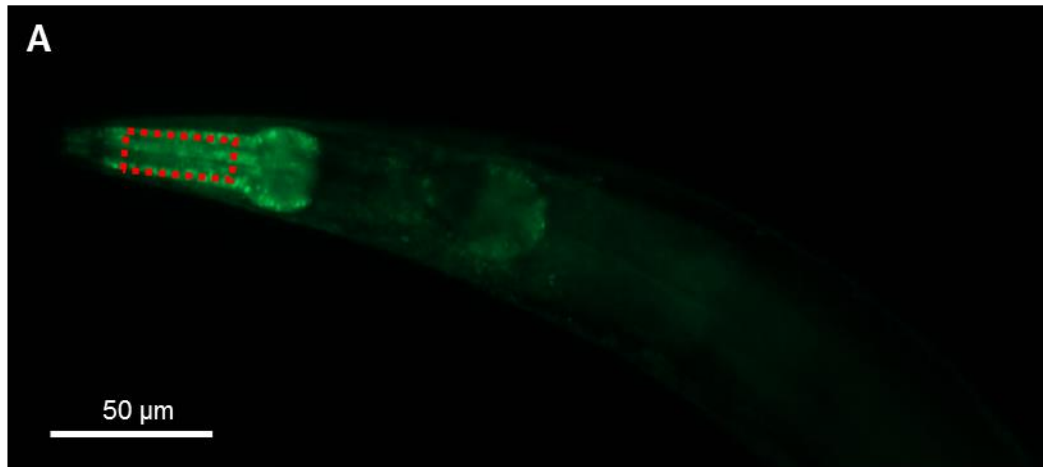


Figure 23 *psod-3::GFP* expression.

A: *psod-3::GFP* expression in the pharynx of one day adult wild type worm incubated in M9 control solution. Red dashed square represents the pharynx area selected to measure the expression. Same sized square was used to measure GFP expression in the pharynx of all worm strains treated with M9 or paraquat. B: *psod-3::GFP* expression in the pharynx of one day old adult worms treated with 100 mM paraquat for 30 min followed by 3 hours recovery in standard NGM with food. Control worms were soaked in M9 for 30min followed by the same recovery as the stressed worms. *psod-3::GFP* mean intensities of each worm strain were normalised to wild type (wt) in NGM. Error bars represent 95 % C.I..

3.3.2 Heat stress

Given the findings that genetic deletions of both *klo-1* and *klo-2* further prolong lifespan in the *daf-2(e1370)* mutant background, the effects of *Klotho* deletions to dauer formation and heat stress resistance were assessed.

3.3.2.1 Temperature dependent dauer formation of *Klotho* mutants

Dauer is an alternative larval stage facilitating energy conservation when environmental conditions are unfavourable (Cassada & Russell, 1975; Golden & Riddle, 1984).

3.3.2.1.1 Dauer formation at 27 °C for 72 h (genetic deletion of *klo-2* induces dauer formation at 27 °C)

At elevated temperatures of 27 °C wild type *C. elegans* progressed their development from eggs to adults as normal, with only 10% of worms entering the alternative dauer stage (as published by (Ailion & Thomas, 2000); Figure 24). Majority of *klo-1(ok2925)* worms also progressed normal life cycle, with only 15% entering dauer stage at 27 °C. In contrast, 68% of *klo-2(ok1862)* mutants entered dauer stage when grown at 27 °C ($p < 0.001$; Table 10). Intriguingly, genetic deletion of *klo-1* in *klo-2* mutant background suppressed the *klo-2* dauer formation phenotype, with only 18% of *klo-2; klo-1* double mutants entering dauer stage at 27 °C. However, this suppression is only partial and the penetrance of dauer phenotype in *klo-2; klo-1* double mutants is significantly higher than in wild type worms ($p < 0.0001$; Table 10).

e1370 is a constitutive dauer allele of *daf-2* which induces dauer formation in 100 % of the worms at temperatures of 25 °C or higher (Gottlieb & Ruvkun, 1994). All of the *daf-2(e1370)* entered dauer stage

when grown at 27 °C. Klotho mutations were not able to suppress the *daf-2(e1370)* dauer phenotype (Figure 24).

daf-16(mu86) is a dauer defective allele, which is resistant to dauer formation (Lin, Hsin, Libina, & Kenyon, 2001b). Consistently, none of the *daf-16(mu86)* worms entered dauer state at 27 °C. *daf-16(mu86)* is only able to partially suppress dauer formation in *daf-2(e1370)* with 22 % of *daf-16(mu86); daf-2(e1370)* double mutants entering dauer state at 27 °C. In contrast, *daf-16(mu86)* mutation was able to completely suppress *klo-2(ok1862)* induced dauer formation suggesting that dauer formation in *klo-2(ok1862)* mutants is dependent on DAF-16.

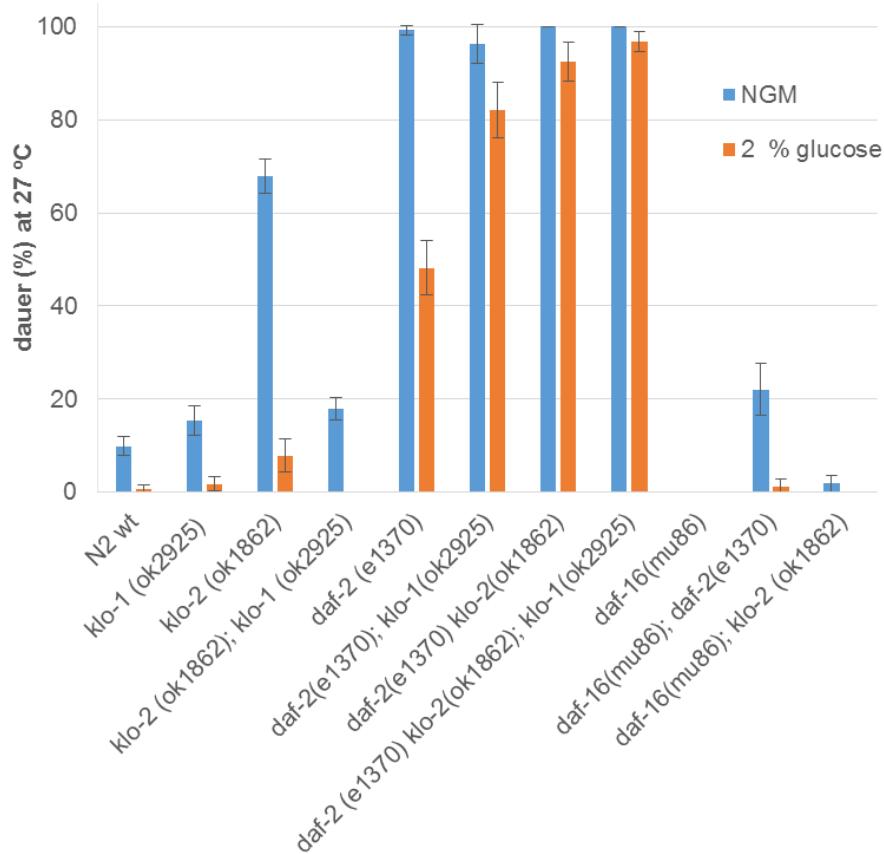


Figure 24 Dauer formation at 27°C.

Bars represent percentage of live animals at dauer state after 72 h incubation at 27 °C in standard NGM (blue bars) or 2 % glucose in NGM (orange bars). Error bars represent 95 % C.I.. Tukey's test was used to analyse the data and is presented in Table 10.

Excess energy in the form of 2% glucose provided in the growth media has been shown to shorten lifespan (Figure 9) and to reduce dauer formation of wild type and *daf-2(e1370)* mutant worms (Lee et al., 2009).

To assess the effect of glucose on *Klotho* worms, animals were grown in 2 % glucose containing NGM at 27 °C for 72 h and dauers were counted.

Table 10 Percentage of animals entering dauer state at 27 °C.

p values were calculated using Tukey's method and compared each strain either to wild type (N2) grown in standard NGM (2nd column from the right) or each strain grown on NGM compared to 2 % glucose containing media (1st column from the right) ($\alpha = 0.05$). Non-dauer animals were L3 or older. n = total number of animals counted.

Strain	Treatment	n	dauer (%) \pm 95 % C.I.	p value against wt NGM	p value NGM vs 2 % glucose
N2 wt	NGM	767	10 \pm 2.1		
	2 % glucose	292	1 \pm 1.0	0.0020	
<i>klo-1(ok2925)</i>	NGM	518	15 \pm 3.1	0.1573	
	2 % glucose	275	2 \pm 1.6	0.0250	<0.0001
<i>klo-2(ok1862)</i>	NGM	623	68 \pm 3.7	<0.0001	
	2 % glucose	228	8 \pm 3.5	1.0000	<0.0001
<i>klo-2(ok1862); klo-1(ok2925)</i>	NGM	966	18 \pm 2.4	<0.0001	
	2 % glucose	332	0 \pm 0.0	0.0001	<0.0001
<i>daf-2(e1370)</i>	NGM	255	99 \pm 1.1	<0.0001	
	2 % glucose	278	48 \pm 5.9	<0.0001	<0.0001
<i>daf-2(e1370); klo-1(ok2925)</i>	NGM	80	96 \pm 4.3	<0.0001	
	2 % glucose	167	82 \pm 5.9	<0.0001	0.0798
<i>daf-2(e1370) klo-2(ok1862)</i>	NGM	116	100 \pm 0.0	<0.0001	
	2 % glucose	159	92 \pm 4.2	<0.0001	0.9146
<i>daf-2(e1370) klo-2(ok1862); klo-1(ok2925)</i>	NGM	316	100 \pm 0.0	<0.0001	
	2 % glucose	252	97 \pm 2.2	<0.0001	0.9998
<i>daf-16(mu86)</i>	NGM	140	0 \pm 0.0	0.0568	
	2 % glucose	61	0 \pm 0.0	0.6664	1.0000
<i>daf-16(mu86); daf-2(e1370)</i>	NGM	222	22 \pm 5.5	<0.0001	
	2 % glucose	234	1 \pm 1.5	0.0238	<0.0001
<i>daf-16(mu86); klo-2(ok1862)</i>	NGM	213	2 \pm 1.8	0.0868	
	2 % glucose	62	0 \pm 0.0	0.6520	1.0000

The presence of 2 % glucose in the growth media almost completely suppressed dauer formation of wild type, *klo-2* and *klo-1* single mutants and *klo-2; klo-1* double mutants, and partially suppressed dauer formation of *daf-2(e1370)* (Figure 24; Table 10). Percentage of dauers in the presence of glucose was

reduced in *klo-2(ok1862)* and *daf-2(e1370)* mutants from 68 % to 8 % and from 99 % to 48 %, respectively. Intriguingly, glucose did not suppress dauer formation of *daf-2* in combination with *Klotho* mutations (either as double or triple mutations) (Figure 24; Table 10), suggesting that with reduced DAF-2/insulin receptor function and in the absence of KLO-1, KLO-2 or both, additional glucose is unable to provide the environmental growth advantage to escape the high temperature induced dauer state.

3.3.2.1.2 *klo-2(ok1862)* induces dauer formation at 25 °C

Since heat stress at 27 °C lead to dauer formation of *klo-2(ok1862)* mutants, temperatures below 27 °C, but above 20 °C were tested for heat induced dauer formation. After 72 h incubation at 25 °C all wild type worms progressed with the normal life cycle. Almost all *klo-1(ok2925)* worms also progressed with the normal life cycle with only 7 % entering dauer state (Figure 25; Table 11). In contrast, 34 % of *klo-2(ok1862)* worms entered dauer state at 25 °C. Surprisingly, double *Klotho* mutant animals proceeded normal life cycle at 25 °C (Figure 25; Table 11). This is consistent to findings at 27 °C, where *klo-1(ok2925)* mutation suppressed the high temperature induced dauer formation of *klo-2(ok1862)* mutation.

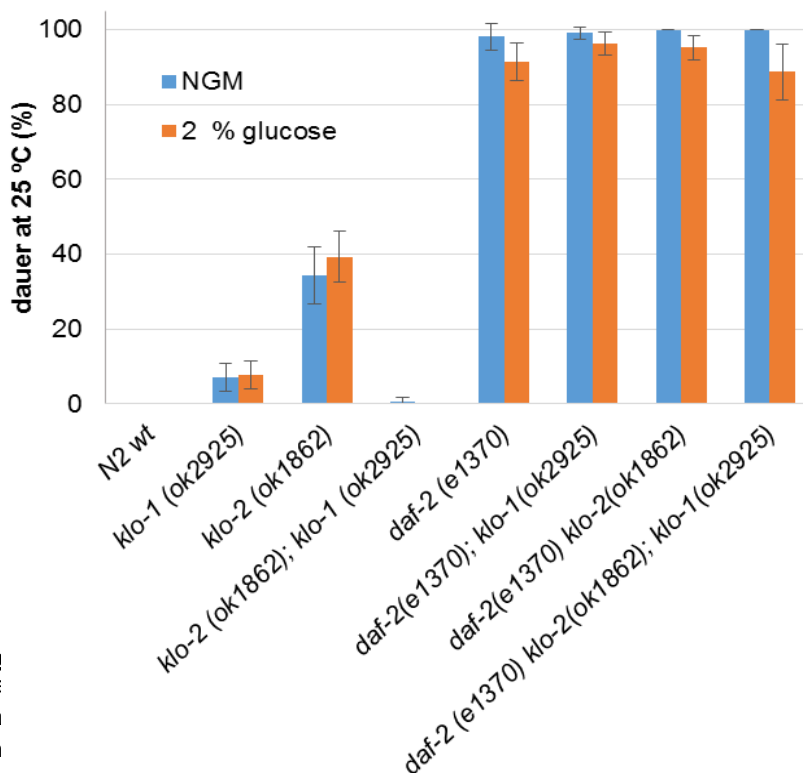


Fig. 25
B
ba
an

tion at 25 °C in standard NGM (blue bars) and 2% glucose (orange bars). Student's t-test was used to analyse the data.

All *daf-2(e1370)* worms and *daf-2(e1370)* *Klotho* mutant worms (double or triple mutant combinations) entered dauer state after 72 h incubation at 25 °C (Figure 25; Table 11). Consistent with findings at 27 °C, *Klotho* mutations did not have any effect in the dauer formation of *daf-2(e1370)* mutants.

Surprisingly, at 25 °C there was no effect of the presence of glucose in the media as it was observed when the stress assay was performed at 27 °C.

Table 11 Percentage of animals entering dauer state at 25 °C.

p values were calculated using Tukey's method and compare each strain either to wild type (N2) grown in standard NGM (2nd column from the right) or each strain grown on NGM compared to 2 % glucose containing media (1st column from the right) ($\alpha = 0.05$). Non-dauer animals were L3 or older. n = total number of animals counted.

Strain	Treatment	n	dauer (%) \pm 95 % C.I.	p value against wt NGM	p value NGM vs 2 % glucose
N2 wt	NGM	193	0 \pm 0.0		
	2 % glucose	167	0 \pm 0.0	1.0000	
<i>klo-1(ok2925)</i>	NGM	184	7 \pm 3.7	0.2251	
	2 % glucose	208	8 \pm 3.7	0.0904	1.0000
<i>klo-2(ok1862)</i>	NGM	151	34 \pm 7.7	<0.0001	
	2 % glucose	201	39 \pm 6.8	<0.0001	0.8768
<i>klo-2(ok1862); klo-1(ok2925)</i>	NGM	277	1 \pm 1.0	1.0000	
	2 % glucose	277	0 \pm 0.0	1.0000	1.0000
<i>daf-2(e1370)</i>	NGM	55	98 \pm 3.6	<0.0001	
	2 % glucose	128	91 \pm 4.9	<0.0001	0.9282
<i>daf-2(e1370); klo-1(ok2925)</i>	NGM	120	99 \pm 1.7	<0.0001	
	2 % glucose	138	96 \pm 3.2	<0.0001	0.9999
<i>daf-2(e1370) klo-2(ok1862)</i>	NGM	124	100 \pm 0.0	<0.0001	
	2 % glucose	170	95 \pm 3.2	<0.0001	0.9534
<i>daf-2(e1370) klo-2(ok1862); klo-1(ok2925)</i>	NGM	67	100 \pm 0.0	<0.0001	
	2 % glucose	71	89 \pm 7.5	<0.0001	0.2813

3.3.2.1.3 Dauer formation at 23 °C and 20 °C

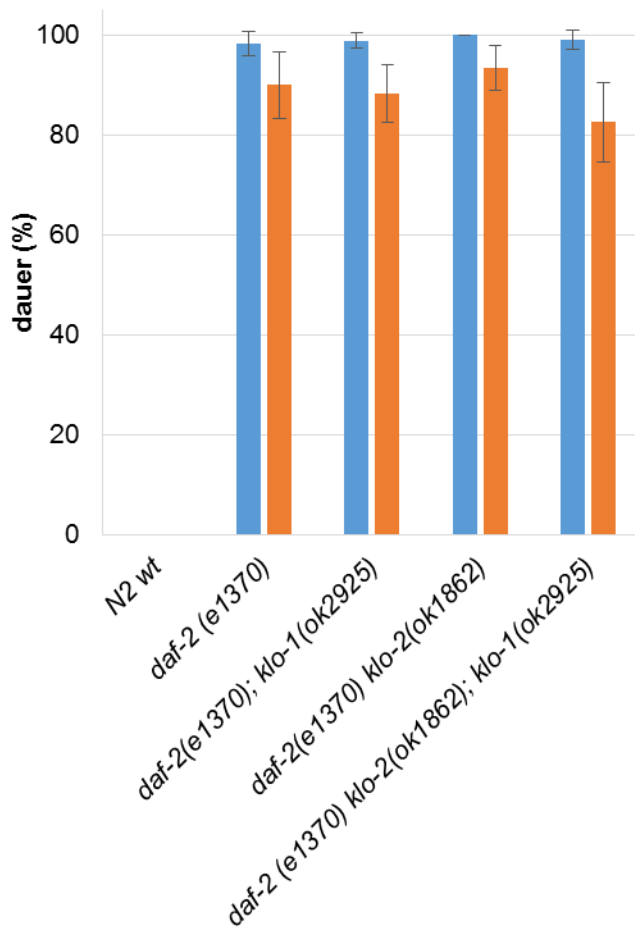
In an attempt to find a temperature where effects of *Klotho* mutation on *daf-2(e1370)* background would be seen, dauer formation was assessed at 23 °C and 20 °C.

At 23 °C wild type worms proceed normal life cycle and do not enter dauer state (Figure 26A) All *daf-2(e1370)* mutants enter dauer state already at the moderate temperature of 23 °C. *Klotho* mutations do not alter the dauer behaviour of *daf-2(e1370)* mutants and all *Klotho* mutants in *daf-2(e1370)* genetic background enter the dauer state (Figure 26A).

At 20 °C, however, none of the strains analysed displayed significant dauer phenotype with only 3% of *daf-2(e1370)* and *daf-2(e1370) klo-2(ok1862); klo-1(ok2925)* triple mutants becoming dauers (Figure 26B).

The presence of 2 % glucose had a minor suppression of dauer formation at 23 °C (Figure 26A). However, this reduction in dauer formation was significant in *daf-2(e1370) klo-2(ok1862)* (from 99% to 88%) and in *daf-2(e1370) klo-2(ok1862); klo-1(ok2925)* mutants (from 99% to 83%) (Figure 26A). Intriguingly, although at 27 °C the presence of excess glucose suppressed the dauer formation of *daf-2(e1370)* mutants, at 25 °C and 23 °C the glucose induced suppression of dauer formation of *daf-2(e1370)* was not significant (Table 12).

A. 23 °C



B. 20 °C

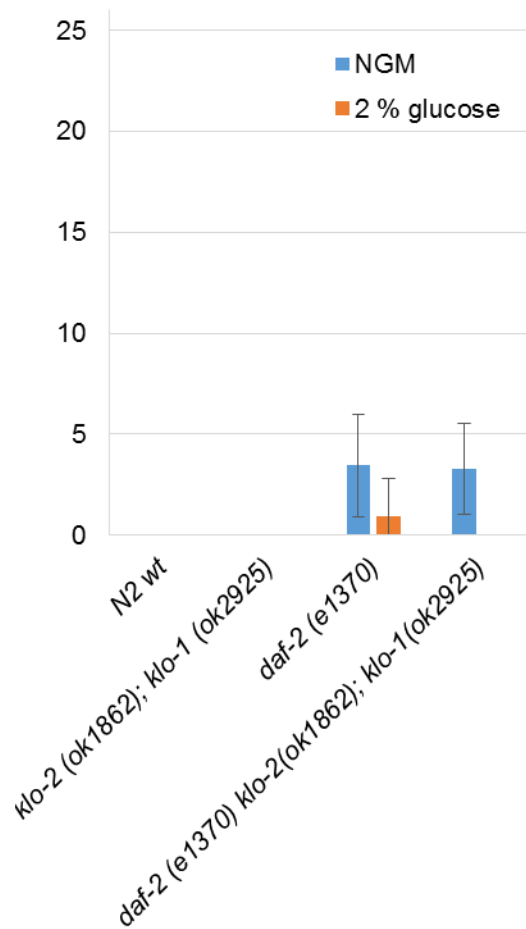


Figure 26 Dauer formation at 23 °C and 20 °C.

Bars represent percentage of live animals at dauer state after 72 h incubation at 23 °C (A) and 20 °C (B) in standard NGM (blue bars) or 2 % glucose in NGM (orange bars). Error bars represent 95 % C.I.. Tukey's test was used to analyse the data and is presented in Table 12. A: at 23 °C wild type worms did not entered dauer state but all worm strains with *daf-2(e1370)* were dauers at this temperature. 2 % glucose had a dauer suppressing effect in *daf-2(e1370)*; *klo-1(ok2925)* and *daf-2(e1370) klo-2(ok1862); klo-1(ok2925)* only. B: at 20 °C wild type worms did not entered dauer state, neither did *Klotho* mutants, and only 3 % of *daf-2(e1370)* and *daf-2(e1370) klo-2(ok1862); klo-1(ok2925)* entered dauer state.

Table 12 Percentage of animals entering dauer state at 23 °C and 20 °C.

p values were calculated using Tukey's method and each strain grown on NGM was compared to 2 % glucose containing media (1st column from the right) ($\alpha = 0.05$; NS = not significant difference). Non-dauer animals were L3 or older. n = total number of animals counted.

Strain	Treatment	n	dauer (%) \pm 95 % C.I.	p value NGM vs 2 % glucose
23 °C				
N2 wt	NGM	222	0 \pm 0.0	
	2 % glucose	188	0 \pm 0.0	1.0000
<i>daf-2(e1370)</i>	NGM	114	98 \pm 2.4	
	2 % glucose	80	90 \pm 6.7	0.0624
<i>daf-2(e1370); klo-1(ok2925)</i>	NGM	188	99 \pm 1.5	
	2 % glucose	120	88 \pm 5.8	<0.0001
<i>daf-2(e1370) klo-2(ok1862)</i>	NGM	131	100 \pm 0.0	
	2 % glucose	121	93 \pm 4.5	0.1153
<i>daf-2(e1370) klo-2(ok1862); klo-1(ok2925)</i>	NGM	107	99 \pm 1.9	
	2 % glucose	92	83 \pm 7.9	0.0000
20 °C				
N2 wt	NGM	156	0 \pm 0.0	
	2 % glucose	96	0 \pm 0.0	NS
<i>klo-2(ok1862); klo-1(ok2925)</i>	NGM	82	0 \pm 0.0	
	2 % glucose	138	0 \pm 0.0	NS
<i>daf-2(e1370)</i>	NGM	202	3 \pm 2.5	
	2 % glucose	106	1 \pm 1.9	NS
<i>daf-2(e1370) klo-2(ok1862); klo-1(ok2925)</i>	NGM	245	3 \pm 2.2	
	2 % glucose	159	0 \pm 0.0	NS

3.3.2.2 Resistance to heat stress of larvae

Worms become stressed at high temperatures and to avoid death they enter the dauer state (Golden & Riddle, 1984). Genetic background plays an important role in temperature sensitivity as also seen in the temperature dependent differences with dauer formation.

3.3.2.2.1 Lethality at 27 °C of non-dauer larvae

Although wild type *C. elegans* are dauer resistant at 27 °C, 20 % of all wild type larvae die at the elevated temperature of 27 °C (Figure 27). Similar larval lethality was observed for the *klo-1(ok2925)* and *klo-2(ok1862)* single mutant and *klo-2(ok1862); klo-1(ok2925)* double mutant animals (Figure 27). Thus, these larvae are unable to enter the dauer state for survival.

In contrast, 43% of *daf-2(e1370)* larvae died at 27 °C (Figure 27) and 99% of the surviving larvae entered dauer state (Figure 24). Genetic elimination of *klo-1(ok2925)* in *daf-2(e1370)* background resulted in a slight increased larval lethality of 55 % (Figure 27). In contrast, genetic elimination of *klo-2(ok1862)* or both *Klotho* in the *daf-2(e1370)* background resulted in a slight reduced larval lethality, 38% and 35% respectively (Figure 27; Table 13). *daf-16(mu86)* mutation did not lead to larval lethality at 27 °C and was able to suppress the *daf-2(e1370)* caused larval lethality from 43% to wild type levels, 23% ($p < 0.001$) (Figure 27).

Glucose had no effect on the heat (27 °C) induced lethality of wild type, *klo-2* single mutant and *klo-2; klo-1* double mutant animals. However, in the presence of glucose, *klo-1(ok2925)* worms had a significant increase of lethality from 15 % to 25 % (Figure 27; Table 13). In contrast, glucose was able to significantly suppress the heat induced lethality of *daf-2(e1370)* single mutants (from 43 % to 17% in the presence of 2% glucose) and the *daf-2(e1370); klo-1(ok2925)* double mutants (from 55% to 19%) as well as the *daf-2(e1370) klo-2(ok1862); klo-1(ok2925)* triple mutants (from 35% to 20%; Figure 27). However, glucose had no effect on the larval lethality of *daf-2(e1370) klo-2(ok1862)* animals at 27 °C.

In the presence of glucose, the percentage of dead larvae *daf-16(mu86); daf-2(e1370)* was not significantly decreased (Figure 27; Table 13). Because, *daf-16(mu86)* and *daf-16(mu86); klo-2(ok1862)* were not tested

on 2 % glucose, it was not possible to conclude any relation between *daf-16* and the potential lethality reduction in the presence of glucose.

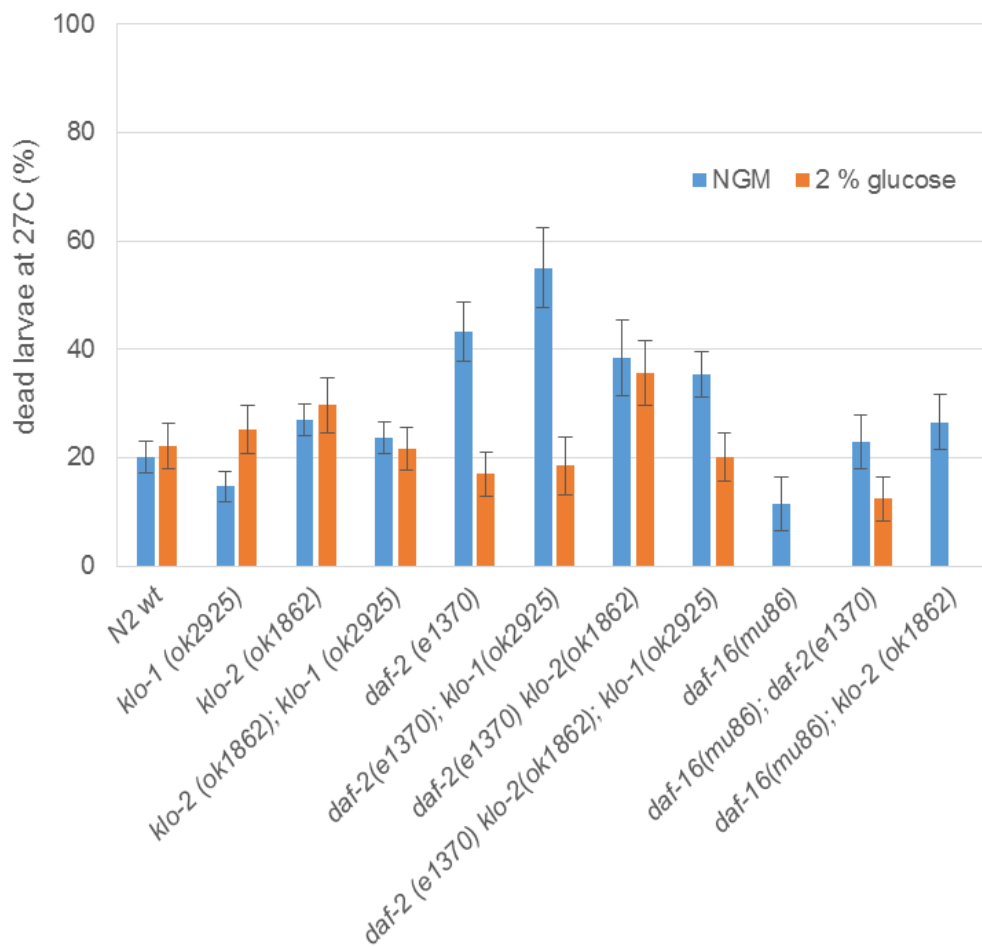


Figure 27 Dead larvae at 27 °C.

Bars represent percentage of dead animals after 72 h incubation at 27 °C in standard NGM (blue bars) or 2 % glucose NGM (orange bars). Error bars represent 95 % C.I.. Tukey's test was used to analyse the data and is presented in Table 13.

Table 13 Percentage of dead larvae after 72 h at 27 °C.

Tukey's analysis results are shown as p values of comparisons between each strain compared to either to wild type (N2) grown in standard NGM (2nd column from the right) or each strain grown on NGM compared to 2 % glucose containing media (1st column from the right) ($\alpha = 0.05$). n = total number of animals counted. Data collected from at least two independent trials. No data was collected for *daf-16(mu86)* and *daf-16(mu86); klo-2(ok1862)* in glucose.

Strain	Treatment	n	deads (%) \pm 95 % C.I.	p value against wt NGM	p value NGM vs 2 % glucose
N2 wt	NGM	751	20 \pm 2.9		
	2 % glucose	375	22 \pm 4.2	1.0000	
<i>klo-1(ok2925)</i>	NGM	607	15 \pm 2.8	0.6987	
	2 % glucose	367	25 \pm 4.5	0.9551	0.0288
<i>klo-2(ok1862)</i>	NGM	853	27 \pm 3.0	0.1294	
	2 % glucose	324	30 \pm 5.0	0.0849	1.0000
<i>klo-2(ok1862); klo-1(ok2925)</i>	NGM	828	24 \pm 2.9	0.9833	
	2 % glucose	423	22 \pm 3.9	1.0000	1.0000
<i>daf-2(e1370)</i>	NGM	315	43 \pm 5.5	<0.0001	
	2 % glucose	335	17 \pm 4.0	0.9999	<0.0001
<i>daf-2(e1370); klo-1(ok2925)</i>	NGM	178	55 \pm 7.4	<0.0001	
	2 % glucose	205	19 \pm 5.4	1.0000	<0.0001
<i>daf-2(e1370) klo-2(ok1862)</i>	NGM	188	38 \pm 7.0	<0.0001	
	2 % glucose	247	36 \pm 6.0	0.0001	1.0000
<i>daf-2(e1370) klo-2(ok1862); klo-1(ok2925)</i>	NGM	489	35 \pm 4.3	<0.0001	
	2 % glucose	315	20 \pm 4.4	1.0000	0.0001
<i>daf-16(mu86)</i>	NGM	158	11 \pm 5.0	0.7019	
	2 % glucose				
<i>daf-16(mu86); daf-2(e1370)</i>	NGM	288	23 \pm 4.9	1.0000	
	2 % glucose	267	12 \pm 4.0	0.5351	0.2727
<i>daf-16(mu86); klo-2(ok1862)</i>	NGM	290	27 \pm 5.1	0.8029	
	2 % glucose				

3.3.2.2.2 Survival of L4 larvae from a heat shock at 37 °C

Survival at higher temperature was measured as the percentage of L4 larval stage animals that survive at 37 °C. Number of animals was counted every 2 h until a maximum of 8 h incubation time.

After 8 h incubation at 37 °C, 44% of wild type worms were alive. *klo-1(ok2925)* mutation caused a minor reduction in survival (34% of animals alive), while *klo-2(ok1862)* mutation significantly enhanced survival rates compared to wild type. 72% of *klo-2* mutants were still alive after 8h at 37 °C ($p < 0.001$; Figure 28;

Table 14). Intriguingly, *klo-2(ok1862); klo-1(ok2925)* worms had a significantly reduced survival rate compared to wild type or either of the single mutants with only 12% of worms being alive after 8h at 37 °C ($p < 0.0001$; Figure 28;

Table 14).

daf-2(e1370) mutation did not increase survival percentage as compared to wild type, nor in conjunction with *klo-1(ok2925)* mutation. In contrast, a significantly higher percentage of both *daf-2(e1370) klo-2(ok1862)* mutants and *daf-2(e1370) klo-2(ok1862); klo-1(ok2925)* triple mutants survived 8 h incubation at 37 °C (91 % and 69 % respectively) (

Table 14, Figure 28B).

DAF-16 increases survival (Lin, Dorman, et al., 1997; Ogg et al., 1997) and it was confirmed that *daf-16(mu86)* mutant worms were less resistant to high temperatures. Only 23 % of *daf-16(mu86)* worms survived after 8 h incubation at 37 °C (Figure 28B), which was significantly less than wild type (44 %).

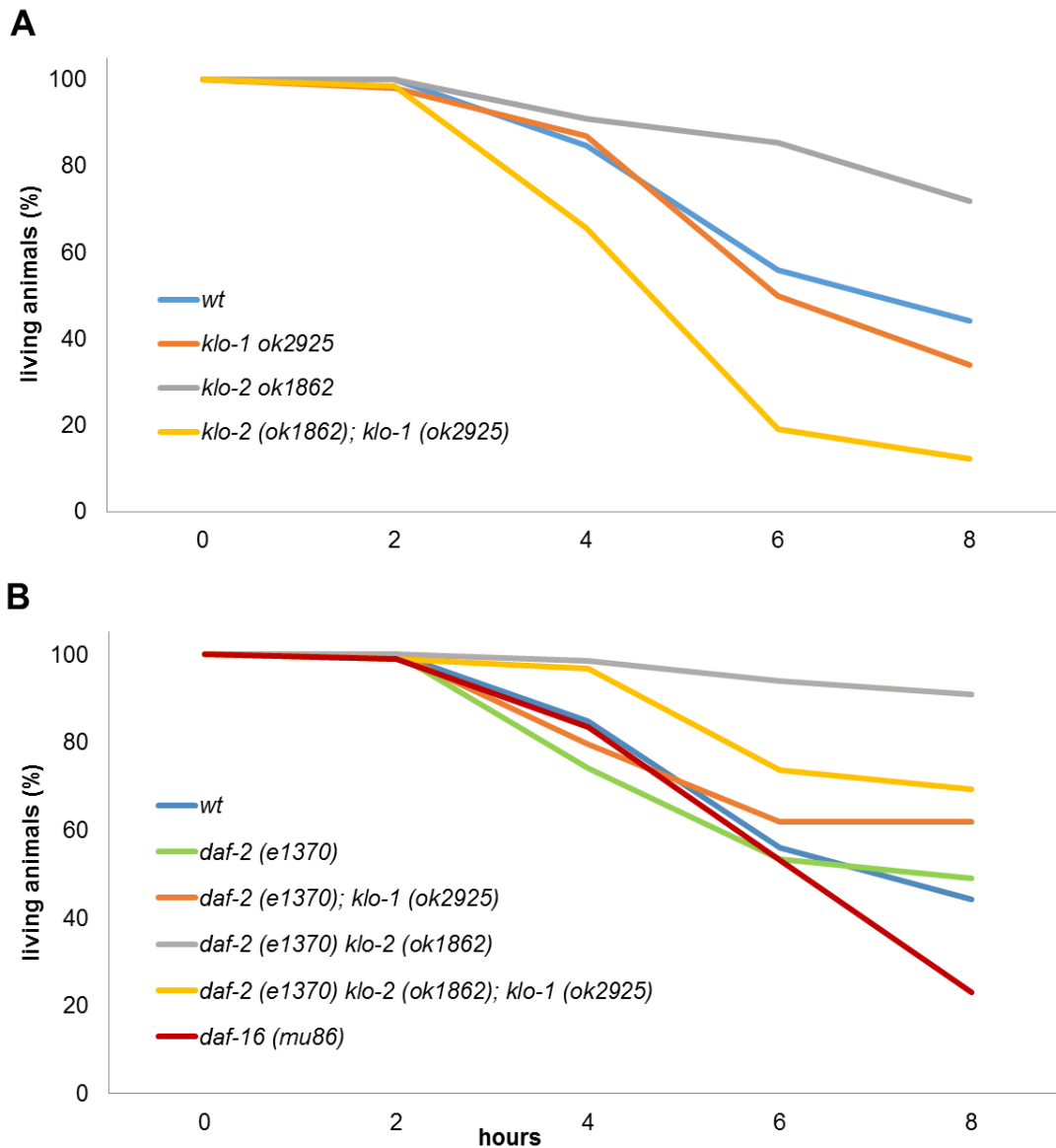


Figure 28 Survival of Klotho mutants at 37 °C.

Percentage of live animals at 37 °C was counted every 2 h for a maximum of 8 h. The survival curves represent the average of at least two independent experiments. The log-rank (Kaplan-Meier) test results are shown in

Table 14. A: Wild type and *klo-1(ok2925)* mutants had similar survival rate. *klo-2(ok1862)* mutant worms had survival advantage at elevated temperature, while double *Klotho* mutants were less resistant. B: *daf-2(e1370)* responded to elevated heat similarly to wild type. Both *klo-1* and *klo-2* mutants had better survival in *daf-2(e1370)* genetic background. *daf-2 klo2; klo-1* triple mutants had significantly increased survival compared to *klo-2; klo-1* double mutants. *daf-16 (mu86)* mutants were less resistant to heat stress than wild type.

Table 14 Percentage of living animals after 8 h incubation at 37 °C.

Log-rank (Kaplan-Meier) test was used to analyse the hypothesis that survival of different worm strains was equal. Analysis results are presented as p value ($\alpha = 0.05$) against N2 wild type worms, *daf-2(e1370)* mutants and *daf-2(e1370) klo-2(ok1862); klo-1(ok2925)* triple mutants.

Strain	n	Living animals 8 h at 37C \pm SE (%)	p value against		
			N2 wt	<i>daf-2(e1370)</i>	<i>daf-2(e1370) klo-2(ok1862); klo-1(ok2925)</i>
N2 wt	59	44 \pm 6.5			
<i>klo-1(ok2925)</i>	100	34 \pm 4.7	0.3079		
<i>klo-2(ok1862)</i>	89	72 \pm 4.8	0.0003		
<i>klo-2(ok1862); klo-1(ok2925)</i>	73	12 \pm 3.8	<0.0001		
<i>daf-2(e1370)</i>	92	49 \pm 5.2	0.9116		
<i>daf-2(e1370); klo-1(ok2925)</i>	34	62 \pm 8.3	0.2069	0.2271	
<i>daf-2(e1370) klo-2(ok1862)</i>	65	91 \pm 3.6	<0.0001	<0.0001	0.2379
<i>daf-2(e1370) klo-2(ok1862); klo-1(ok2925)</i>	91	69 \pm 4.8	0.0012	0.0012	0.0015
<i>daf-16(mu86)</i>	96	23 \pm 4.3	0.0420		

3.3.3 Response to osmotic stress caused by ion depletion

Klotho has been shown to be involved in the regulation of ion balance through the interaction with FGF23 and FGFR in mammals (Araya et al., 2005; Kurosu et al., 2006; Kurosu & Kuro, 2009; Nakatani, Ohnishi, & Razzaque, 2009). The role of KLO-1 and KLO-2 together with EGL-15/FGFR in the regulation of ion balance in *C. elegans* has been supported by some studies (Polanska et al., 2011) and confronted by others (Château et al., 2010).

To study the relation between Klotho and the response to osmotic stress, the development time of worms was analysed in different ion depleted conditions. Age wild type and *Klotho* single and double mutant worm synchronised eggs were picked and transferred to standard NGM plates or ion (Ca^{2+} , Mg^{2+} and K^{+})

depleted NGM plates. To quantify how many worms were adults at each time point, they were counted every 12 h for a maximum of 108 h (Polanska et al., 2011).

In standard conditions (20 °C in standard NGM), almost all (99%) wild type *C. elegans* developed from eggs to reproductively mature adults in 72 h (Figure 29A). Genetic mutations in *klo-1(ok2925)* and *klo-2(ok1862)* did not alter the development time (Figure 29A). Development was only delayed when both *klo-1* and *klo-2* were deleted. At 72 hours, significantly less (90 %) *Klotho* double mutant worms had developed into adults (Figure 29A).

Wild type *C. elegans* can adapt to changes to its microenvironment and displayed no differences in developmental time when grown in conditions where cations Ca^{2+} , Mg^{2+} and K^{+} are removed (Figure 29B). The development of *Klotho* mutant worms was not significantly delayed by the depletion of divalent cations Ca^{2+} and Mg^{2+} . However, when K^{+} was depleted, *Klotho* mutant worms developed slower than in standard conditions. Development delay was observed in *klo-1(ok2925)* mutants with 79% of worms being adults at 60 h in 0 mM K^{+} conditions in comparison to 90 % in standard NGM (Figure 29C). In both conditions 97 – 98 % of worms were adults at 72 h of development. *klo-2(ok1862)* and *klo-2(ok1862); klo-1(ok2925)* double mutant worms were especially affected by K^{+} . As compared to standard NGM, at 72 h of development in K^{+} depleted media, the percentage of *klo-2(ok1862)* adult worms was reduced from 94 % to 90 %, and of *klo-2(ok1862); klo-1(ok2925)* double mutant worms from 90 % to 86 % (Figure 29D - E).

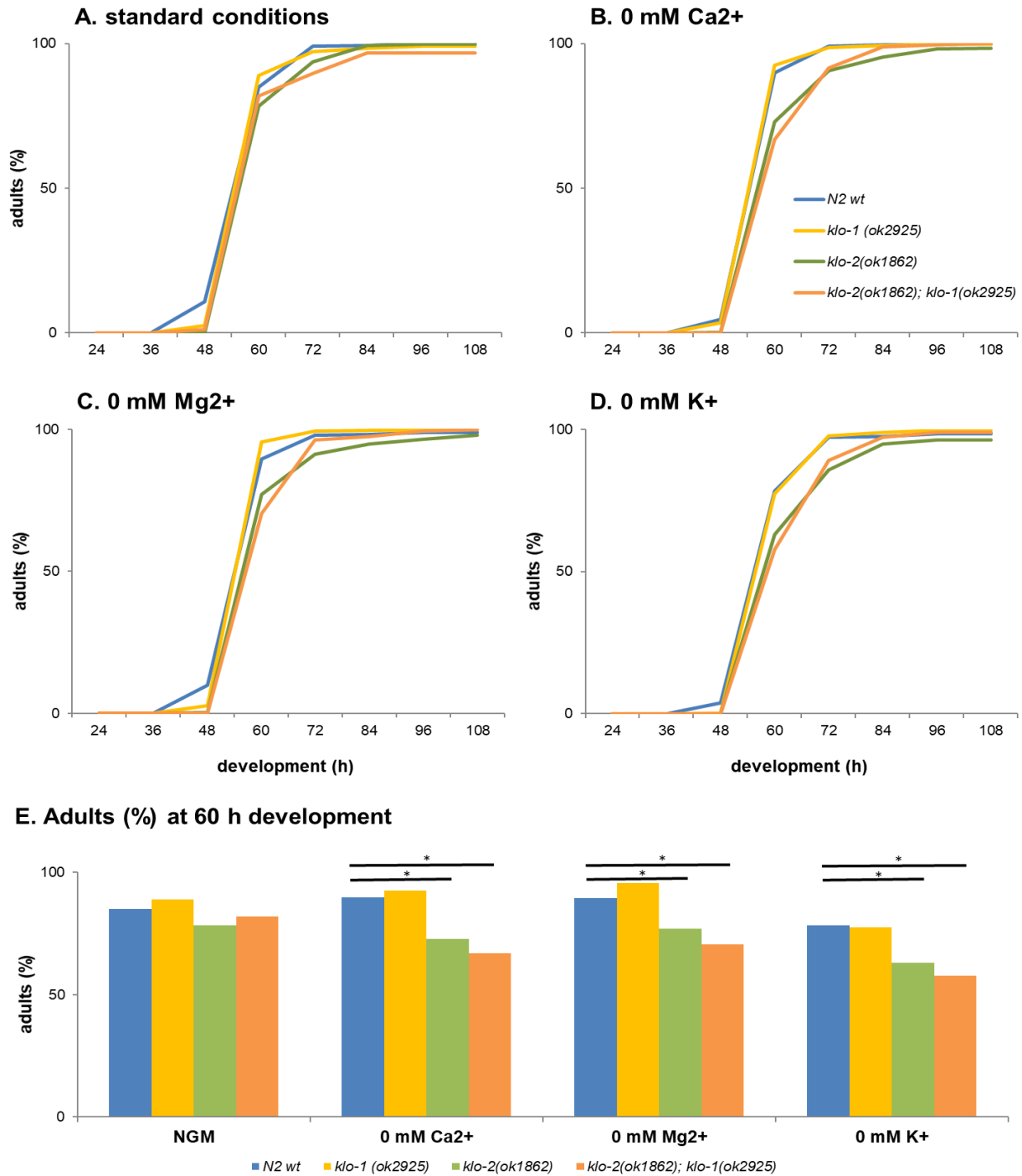


Figure 29 Percentage of adult worms at different time points (time 0 h corresponds to time of egg been lay). Strains analysed are: wild type, *klo-1(ok2925)*, *klo-2(ok1862)* and *klo-2(ok1862); klo-1(ok2925)* double mutant worms. Development time to reach adulthood is compared between strains when only one ion is depleted from the standard media (A): 0 mM Ca²⁺(B), 0 mM Mg²⁺ (C) and 0 mM K⁺(D). E: comparison of percentage of adults after 60 h of development after egg hatching with statistically significant differences are represented by a line connecting two values and a star ($p < 0.001$). Tukey's test was used to analyse the percentage of adult worms at 60 h and 72 h, and differences are presented in Table 15.

Table 15 Percentage of adult worms at 60 and 72 h of development in standard conditions (NGM) or ion depleted NGM (0 mM Ca²⁺, 0 mM Mg²⁺ and 0 mM K⁺).

At least two independent biological replicates are shown. Time 0 h corresponds to time of egg been lay. For each time point, the percentage of adults \pm 95 % C.I. was analysed with Tukey's test ($\alpha = 0.05$) and the results are presented as p-values. Each strain was compared against wild type on NGM or each strain grown on NGM compared to ion depleted media.

Strain	Treatment	N	60 h			72 h		
			Adults (%) \pm 95 % C.I.	p value against N2 NGM	p vale against same strain in NGM	Adults (%) \pm 95 % C.I.	p value against N2 NGM	p vale against same strain in NGM
N2 wt	NGM	651	86 \pm 2.7			99 \pm 0.7		
	0 M Ca ²⁺	663	89 \pm 2.4	0.97		99 \pm 0.7	1.00	
	0 M Mg ²⁺	442	90 \pm 2.9	0.95		98 \pm 1.3	1.00	
	0 M K ⁺	595	78 \pm 3.3	0.05		97 \pm 1.4	0.94	
<i>klo-1(ok2925)</i>	NGM	581	90 \pm 2.4	0.81		97 \pm 1.4	0.97	
	0 M Ca ²⁺	600	94 \pm 1.9	0.01	0.92	97 \pm 1.3	0.99	1.00
	0 M Mg ²⁺	575	95 \pm 1.7	0.0007	0.54	99 \pm 0.7	1.00	0.94
	0 M K ⁺	603	79 \pm 3.2	0.26	0.00	98 \pm 1.1	1.00	1.00
<i>klo-2(ok1862)</i>	NGM	320	78 \pm 4.6	0.25		94 \pm 2.6	0.05	
	0 M Ca ²⁺	238	68 \pm 6.0	<0.0001	0.15	93 \pm 3.3	0.006	1.00
	0 M Mg ²⁺	323	74 \pm 4.8	0.0006	0.99	97 \pm 1.9	0.96	0.97
	0 M K ⁺	287	59 \pm 5.7	<0.0001	<0.0001	90 \pm 3.5	<0.0001	0.72
<i>klo-2(ok1862)</i> <i>klo-1(ok2925)</i>	NGM	341	82 \pm 4.1	0.99		90 \pm 3.2	<0.0001	
	0 M Ca ²⁺	784	69 \pm 3.3	<0.0001	<0.0001	91 \pm 2.1	<0.0001	1.00
	0 M Mg ²⁺	676	77 \pm 3.2	0.003	0.84	91 \pm 2.2	<0.0001	1.00
	0 M K ⁺	644	62 \pm 3.8	<0.0001	<0.0001	86 \pm 2.7	<0.0001	0.31
Total		8323						

3.4 Klotho as a regulator of lipid metabolism and starvation

Klotho has been found to be involved in energy metabolism by interacting with insulin/IGFR (Kurosu et al., 2005). Klotho levels in plasma have been found to be decreased in anorexia and obesity and Klotho deficient mice have reduced amounts of adipose tissue (Amitani et al., 2013). *klo-1* and *klo-2* are both expressed in the intestine (Polanska et al., 2011) and *klo-1* is expressed in the excretory canal and *klo-2* is expressed in the hypodermis (Polanska et al., 2011). As *klo-1* and *klo-2* are expressed in tissues involved

in osmoregulation and energy metabolism of the worm, it is suggested that the function of Klotho in metabolism is evolutionary conserved from nematodes to mammals (Polanska et al., 2011).

3.4.1 Starvation effect on expression of Klotho gene reporter

In order to reveal the expression levels of *klo-1* and *klo-2* in starvation, worm strains with the extrachromosomal arrays *jtEx179* [*myo-2::GFP*; *pklo-1::RFP*] and *jtEx129* [*pklo-2::GFP*; *ptph-1::RFP*] were used to observe and quantify the expression of *klo-1* and *klo-2* respectively (Polanska et al., 2011).

Expression of *klo-1* and *klo-2* reporter genes (Polanska et al., 2011) was assessed in day 1 adult worms which were fed or starved (3 h). In normal feeding conditions, the expression of *klo-1* reporter gene was 98 ± 27 (SEM) % higher in the excretory canal and intestine of *Klotho* double mutant worms in comparison to wild type worms ($p = 0.01$; Figure 30A, B and E), suggesting an increased activation of *klo-1* promoter in *Klotho* deficient worms.

Expression of *klo-1* reporter after 3 h of starvation was increased in wild type worms and decreased in *Klotho* double mutant worms. However, due to the variation of the expression levels within the population analysed, neither of these changes were statistically significant when compared to the same strain in normal (fed) conditions. Interestingly, the level of expression for the *klo-1* reporter was similar for both wild type and double mutant worms under starvation (Figure 30E).

In wild type worms, starvation for 3 h caused a significant increase of *klo-2* reporter gene expression of 38 ± 13 (SEM) % in the intestine as compared to fed worms ($p = 0.01$; Figure 30C, D and F). The increased expression of *klo-1* and *klo-2* reporter genes upon starvation, although *klo-1* was not significant due to the high intrinsic variability, supported the hypothesis that Klotho is involved in lipid metabolism. Hypothetically, Klotho could be directly involved in regulation of lipid metabolism increasing in starvation as FGF21 (β -Klotho dependent) does in starved mammals (Uebanso et al., 2011).

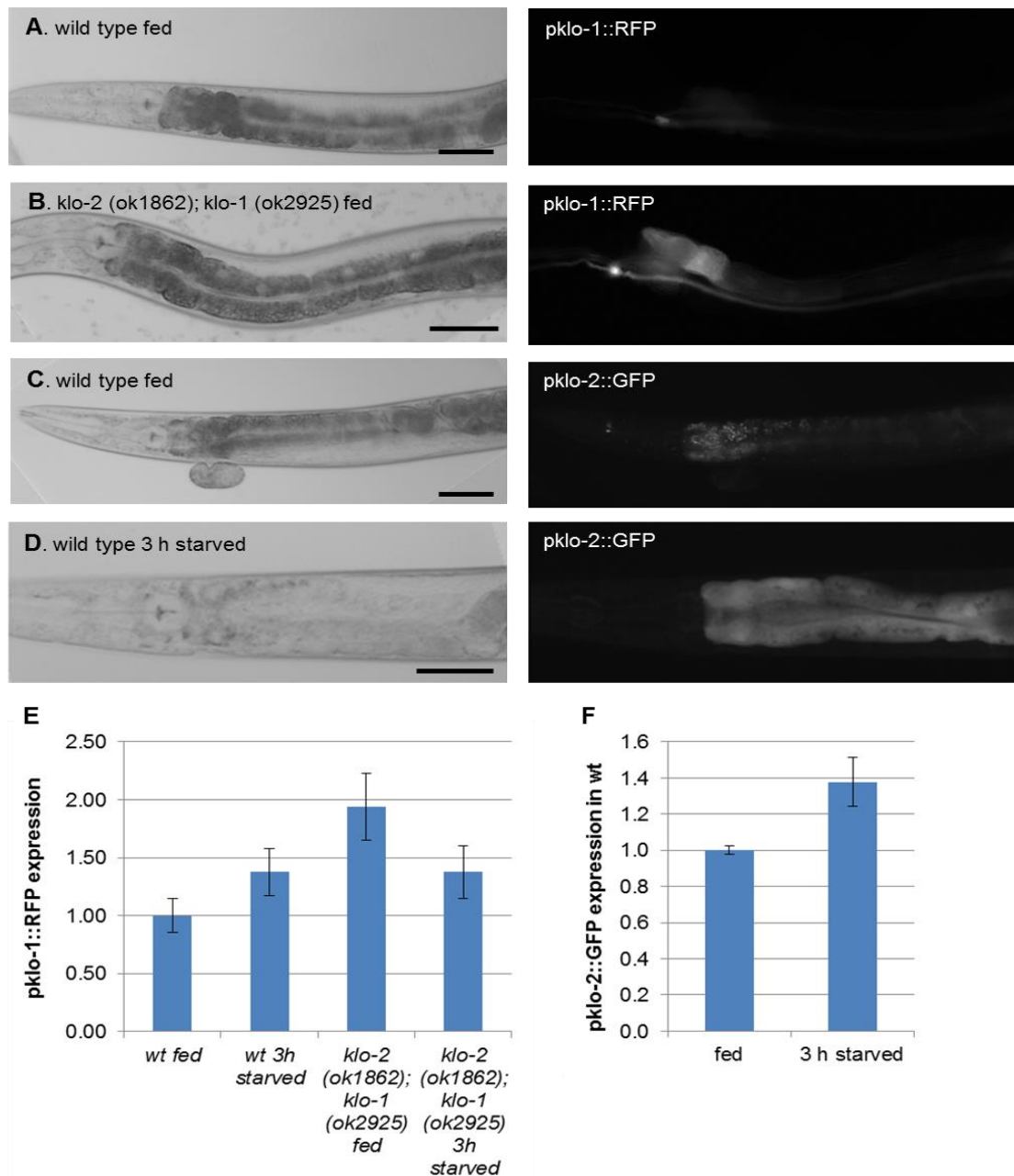


Figure 30 Expression of *pklo-1::RFP* and *pklo-2::GFP*.

A: *jtEx179* [*myo-2::GFP*; *pklo-1::RFP*] worm under bright field (left) and *pklo-1::RFP* expression of the same worm (right). B: *ok1862; ok2925; jtEx179* [*myo-2::GFP*; *pklo-1::RFP*] worm under bright field (left) and *pklo-1::RFP* expression of the same worm (right). C-D: *jtEx129* [*pklo-2::GFP*; *ptph::RFP*] worm under bright field (left) and *pklo-2::GFP* expression of the same worm (right), in normal fed conditions (C) or after 3 h starvation (D). Scale bar is 50 μ m. E: *pklo-1::RFP* expression of wild type fed (n = 22) and 3 h starved (n = 11), double Klotho mutant worms fed (n = 11) and 3 h starved (n = 16). Values were normalised to wild type (wt) fed. F: *pklo-2::GFP* expression in wild type fed (n = 34) and 3 h starved (n = 23). Error bars represent SEM. T Student test ($\alpha = 0.05$) was used to analyse the data.

3.4.2 Lipid quantification

Whereas mammals have adipocytes, which are cells specifically dedicated to store fat, *C. elegans* store fat in droplets in the intestinal and hypodermal cells (Kimura et al., 1997). These droplets can be visualised under the microscope due to the fact that the body of *C. elegans* is transparent. Three different lipid stains have been used in this thesis work: Sudan Black B (SBB), Nile Red and Oil-red-O (ORO).

3.4.2.1 Nile red

Nile red was used as a lipid staining with the advantage that the dye was added onto the food lawn for worms to eat it, reducing significantly the steps of the procedure as compared to SBB staining and the consequent alteration of the results. Worms grown on plates containing the dye were used directly for fluorescent microscopy (Figure 31A). The values of the intensity of Nile red stained fats were normalised to wild type fed worms.

In standard culturing conditions of continuous feeding, wild type worms and single and double Klotho mutant worms had similar levels of Nile red stained fats (Figure 31C). Compared to wild type worms (1.00 ± 0.42 (95 % C.I.)), the relative quantity of Nile red stained fats of *klo-1(ok2925)* worms was 1.07 ± 0.24 (95 % C.I.), of *klo-2(ok1862)* worms was 1.30 ± 0.14 (95 % C.I.) and of double mutant *klo-2(ok1862); klo-1(ok2925)* worms was 1.24 ± 0.32 (95 % C.I.).

Using Nile red visualisation of lipids, not decreases in lipid quantities could be detected in starved worms. Even after 12 h of starvation, the amount of Nile red stained fats was not significantly decreased in wild type (reduction of 4 ± 22 (95 % C.I.) %) nor in *klo-2(ok1862); klo-1(ok2925)* double mutant worms (reduction of 34 ± 15 (95 % C.I.) %; Figure 31E).

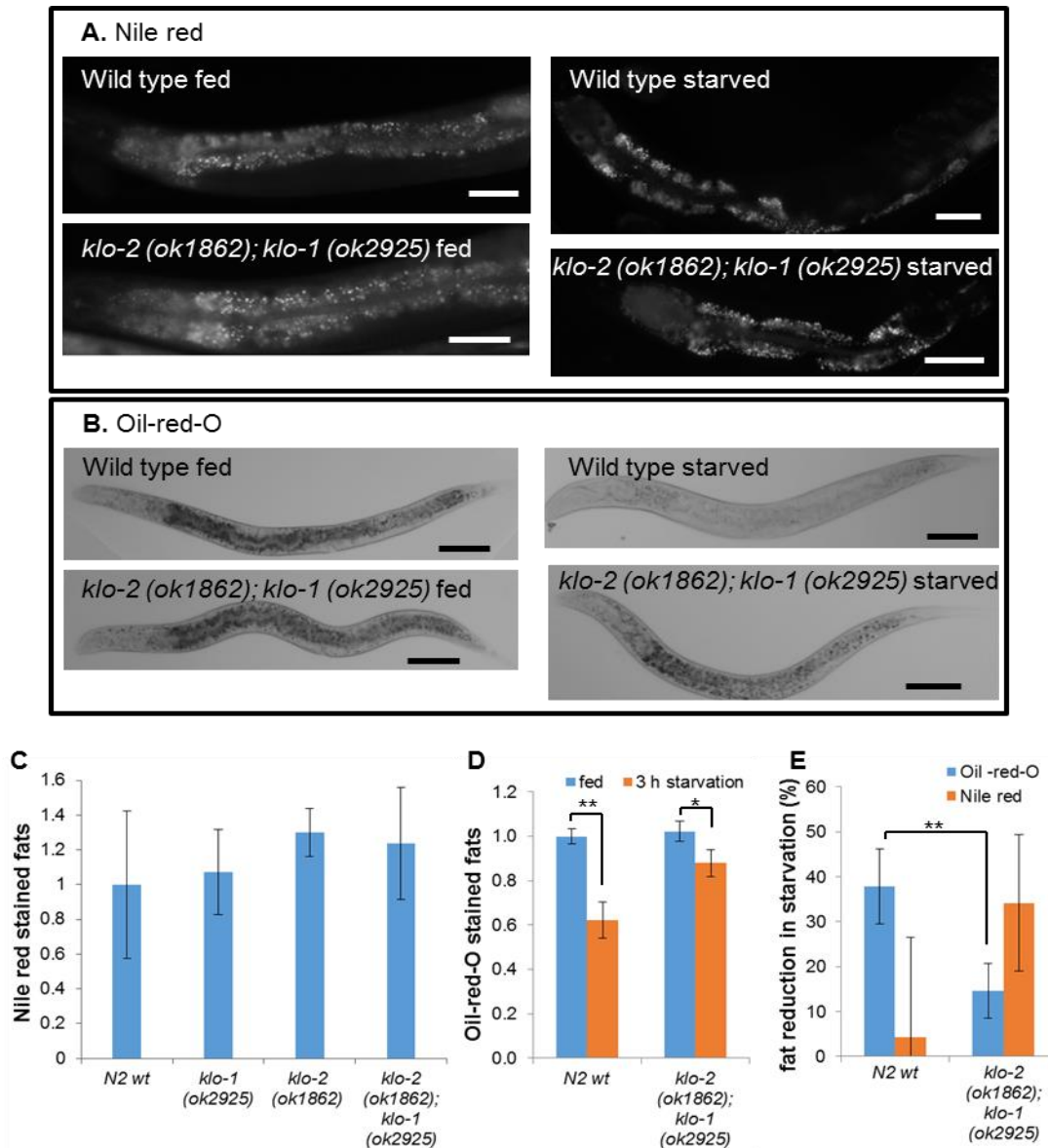


Figure 31 Lipid staining and quantification.

A: wild type and *Klotho* double mutant worms stained with Nile red in standard feeding conditions and after 12 h of starvation. B: wild type and *Klotho* double mutant worms stained with Oil-red-O in standard feeding conditions and after 3 h of starvation. C: Nile red stained fats relative values \pm 95 % C.I. n = 5 to 12. D: Oil-red-O stained fats relative values \pm 95 % C.I. in standard feeding conditions (blue bar) and after 3 h of starvation (orange bars). n = 35 to 45. E: fat reduction in starved worms (%) \pm 95 % C.I.. reduction of ORO stained fats after 3 h of starvation (blue bars; n = 35 to 45) and reduction of Nile red stained fats after 12 h of starvation (orange bars; n = 5 to 12). Student T-test analysis ($\alpha = 0.05$) was used for pairwise comparisons. * = 0.002; ** <0.0001.

3.4.2.2 Oil-red-O (ORO)

Oil red O (ORO) dye was used in PFA fixed worms and the stained lipids were observed under bright field. No differences were observed between wild type and *Klotho* double mutant worms in standard feeding conditions. Wild type worms displayed significantly less ORO stained fats after 3 h of starvation ($p < 0.0001$; Figure 31B and D). *Klotho* double mutant worms displayed also significantly less ORO stained fats upon starvation ($p = 0.002$; Figure 31B and D), although the fat reduction was significantly less pronounced in starved *Klotho* double mutants (15 ± 6 (95 % C.I.) % fat reduction; $p < 0.0001$) than in starved wild type worms (38 ± 8 (95 % C.I.) %; Figure 31E).

3.4.3 Expression of target proteins of DAF-16, involved in lipid homeostasis

The expression of proteins involved in lipid homeostasis was analysed in *Klotho* mutant worms and starvation. The adipose triglyceride lipase (ATGL-1) and the desaturase FAT-7 proteins were selected because are regulated by DAF-16.

3.4.3.1 *atgl-1::GFP* expression

Lipolysis signalling cascade is activated in starvation to provide the animal the energy from the stored lipids (Duncan, Ahmadian, Jaworski, Sarkadi-Nagy, & Sul, 2007; Zechner et al., 2012)). Short starvation periods increase cAMP levels, which activate protein kinase A (PKA) and, in consequence, activate the adipose triglyceride lipase (ATGL-1) to stimulate lipolysis (Granneman, Moore, Mottillo, Zhu, & Zhou, 2011; Miyoshi et al., 2007).

Transgenic worms containing an integrated array of *hjls67* [*atgl-1p::ATGL-1::GFP*] were used to quantify the levels of ATGL-1::GFP in the intestine (Figure 32A; (Zhang et al., 2010)). The effects of 8 hour starvation for ATGL-1::GFP expression were assessed in *Klotho* mutants and in wild type worms. After 8 h of starvation, expression of ATGL-1::GFP was not altered in wild type worms (Figure 32B), contrary to previously published data where ATGL-1::GFP was shown to be increased (J. H. Lee et al., 2014).

However, the same authors Lee et al. (2014) did not find any change in *atgl-1* mRNA levels during fasting.

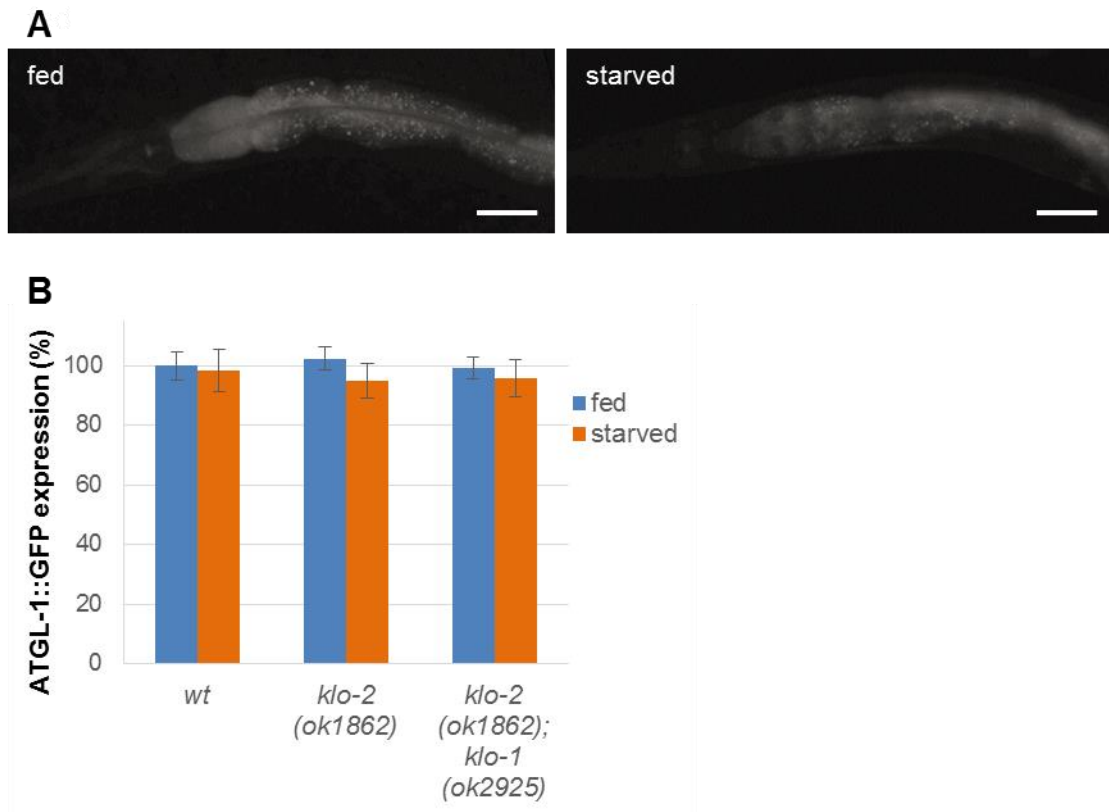


Figure 32 Expression of ATGL-1::GFP.

A: ATGL-1::GFP expression pattern in one day old adult wild type worms. No difference was seen between fed and starved worms. Scale bars are 50 μ m. B: ATGL-1::GFP mean expression (%) \pm 95 % C.I. of two independent experiments. Results normalised to GFP expression in wild type fed animals. ATGL-1::GFP expression was measured in fed worms (blue bars) and 8 h starved worms (orange bars). Student T-test was used for pairwise comparisons ($\alpha = 0.05$). At least 29 animals were used for each worm strain and treatment.

The absence of functional Klotho proteins in *klo-1* and *klo-2* mutants did not affect the expression of ATGL-1::GFP as compared to wild type (Figure 32.B). Also, the expression of ATGL-1::GFP was not altered in *klo-2(ok1862)* nor in *klo-2(ok1862); klo-1(ok2925)* double mutant worms after 8 h of starvation (Figure 32.B).

3.4.3.2 *fat-7::GFP* expression is altered in *Klotho* mutant worms

To further investigate the role of *Klotho* proteins in the regulation of lipid metabolism, a reporter for the desaturase enzyme *FAT-7* was used. *FAT-7* has been shown to be regulated by insulin signalling (*DAF-2* and *DAF-16*) (Horikawa & Sakamoto, 2010; Murphy et al., 2003) and the expression of *fat-7* reporter gene is decreased tenfold in fasting adult worms (Van Gilst, Hadjivassiliou, & Yamamoto, 2005).

The expression of *fat-7::GFP* was measured in worms carrying the integrated transgenic array *waEx15* [*fat-7::GFP* + *lin-15(+)*]. *fat-7::GFP* is only detected in the intestine and the expression was measured in the 1st and 2nd pair of intestinal cells called *int1* and *int2*, as reference cells for high and low expression of *fat-7::GFP*. In wild type worms, the average expression of *fat-7::GFP* in *int1* was 4-5 times higher than in *int2* in standard conditions of food and temperature. The expression intensities of *fat-7::GFP* in *Klotho* mutant worms were normalised to the intensity of wild type worms.

Overall, the expression of *fat-7::GFP* was more severely decreased in *klo-2(ok1862)* mutant worms as compared to wild type. *klo-2(ok1862)* mutant worms had significantly lower *fat-7::GFP* expression than wild type in *int1* cells (relative value of 0.72 ± 0.10 (95 % C.I.); $p = 0.001$). The expression of *fat-7::GFP* in *int2* cells was significantly reduced in *klo-1(ok2925)*, *klo-2(ok1862)* and *Klotho* double mutant worms, with respective relative values of 0.68 ± 0.12 (95 % C.I.), 0.57 ± 0.12 (95 % C.I.) and 0.75 ± 0.11 (95 % C.I.). Interestingly, expression of *fat-7::GFP* was more decreased when only one of the *Klotho* proteins was absent, suggesting a possible relation between *KLO-1* and *KLO-2* in the regulation of *FAT-7*. It could be hypothesised that the imbalance of *KLO-1/KLO-2* ratio caused a bigger decrease of *fat-7::GFP* than the absence of both *Klotho* proteins.

After 8 h of starvation the expression of *fat-7::GFP* was significantly decreased in all strains in *int1* cells but the decrease was not significant in *int2* cells. Wild type worms displayed a 83 ± 1.1 (95 % C.I.) % reduction in the expression of *fat-7::GFP* in *int1* cells and a 29 ± 3.7 (95 % C.I.) % reduction in *int2* cells. In *klo-1(ok2925)* mutant worms the 8h starvation caused a similar *fat-7::GFP* reduction to 82 ± 0.9 (95 % C.I.) % in *int1* cells. Interestingly, as compared to wild type, *klo-2(ok1862)* were significantly less affected by

starvation, while *Klotho* double mutants were significantly more affected by the 8 h of starvation, 79 ± 2.0 (95 % C.I.) % ($p = 0.002$) and 87 ± 1.0 (95 % C.I.) % ($p < 0.0001$) respectively.

A. fat-7::GFP expression

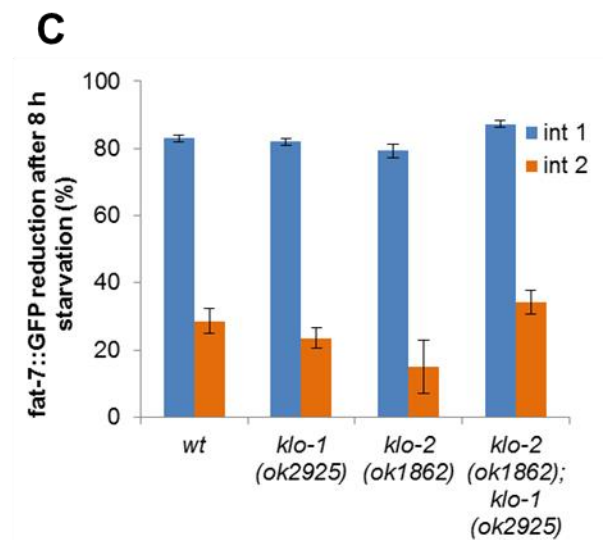
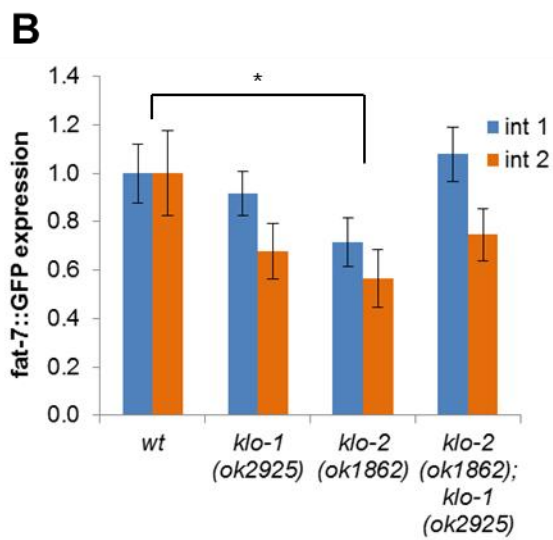
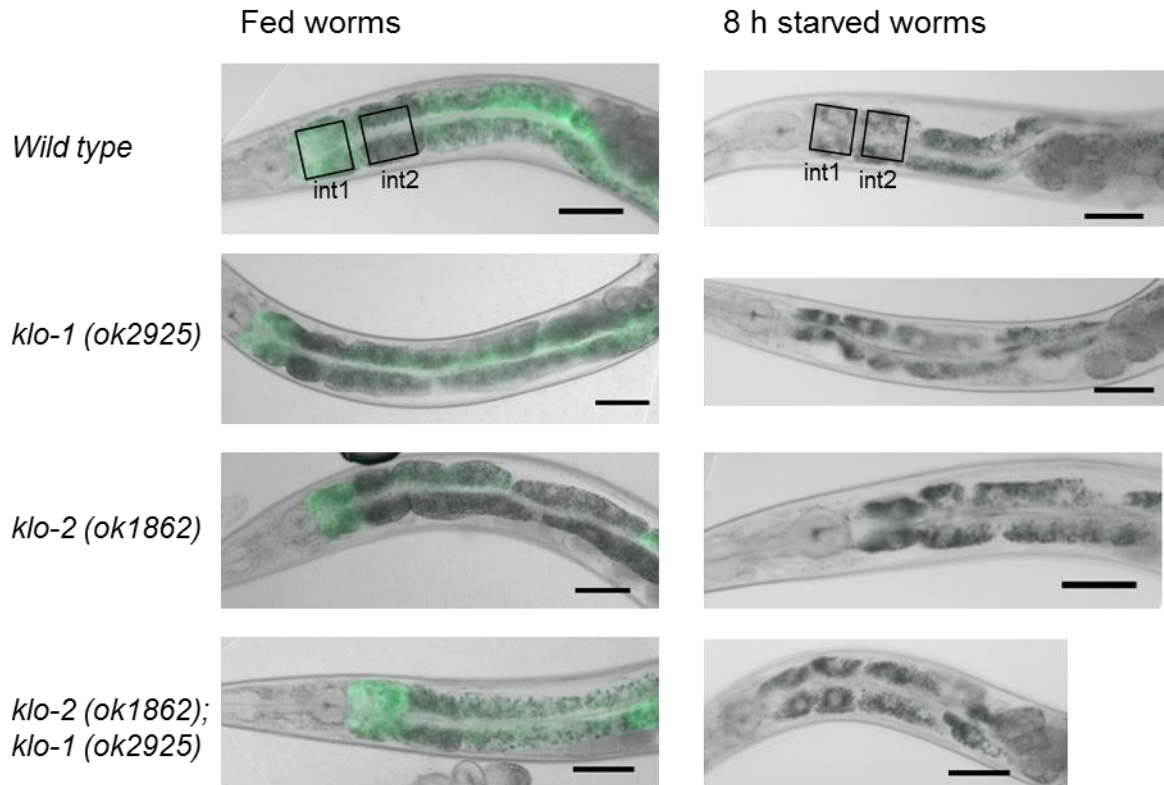


Figure 33 Expression and quantification of *fat-7::GFP*.

A: *fat-7::GFP* expression in wild type, *klo-1(ok2925)* mutant, *klo-2(ok1862)* mutant and *klo-2(ok1862); klo-1(ok2925)* double mutant worms one day adults. Pictures taken of worms grown in standard conditions of continuous feeding or after 8 h of starvation. *fat-7::GFP* expression was measured in int1 and int2 pairs of intestinal cells as represented by black squares. Scale bar is 50 μ m. All worms are heading to the left. B: mean *fat-7::GFP* expression measured in int1 (blue bars) and int2 (orange bars) pair of cells and normalised to wild type values. Error bars represent \pm 95 % C.I.. C: *fat-7::GFP* reduction after 8 h of starvation (%) \pm 95 % C.I.. Measured in int1 (blue bars) and int2 (orange bars) pair of cells. Tukey's test used for the statistical analysis ($\alpha = 0.05$). Between 37 and 50 worms were analysed in standard conditions of continuous feeding and 20 worms were analysed in starvation conditions for each strain.

3.4.4 Klotho regulation of cholesterol metabolism

Mouse FGF15 (human FGF19) interacts mainly with β -Klotho/FGFR complex to regulate cholesterol and suppress the synthesis of bile acids (Inagaki et al., 2005). In *C. elegans*, cholesterol has been shown to regulate DAF-16, therefore regulating lifespan and brood size (Matyash et al., 2004). Unlike humans, worms cannot synthesise cholesterol *de novo*, and hence it is essential for worms to obtain cholesterol from the diet (Cheong et al., 2011; Matyash et al., 2004; Merris et al., 2003; Merris, Kraeft, Tint, & Lenard, 2004; Shim, Chun, Lee, & Paik, 2002). Effect of cholesterol depleted diet on lifespan and viable progeny was measured by culturing Klotho mutant worms in 0 mM cholesterol NGM.

3.4.4.1 Cholesterol depletion shortens lifespan of wild type and lifespan Klotho defective worms

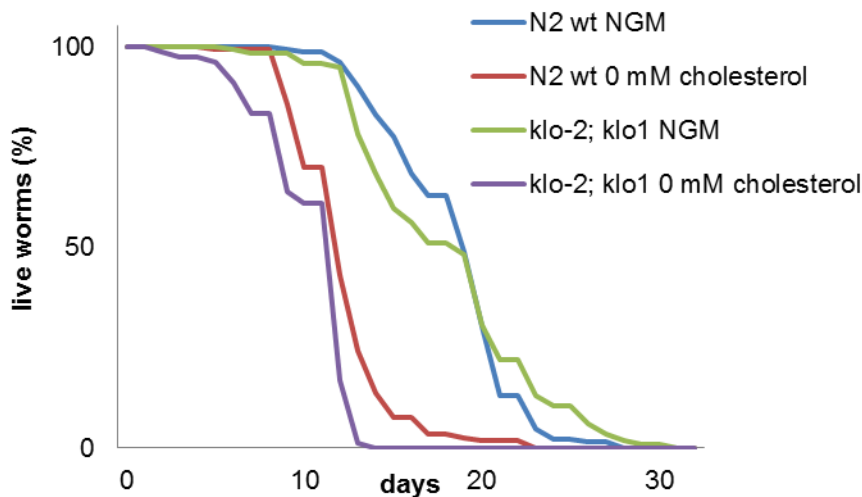
Lifespan of worms was measured from young adult stage until death. Worms were synchronised by egg laying on 0 mM cholesterol NGM or standard NGM in parallel. Mean lifespan was calculated and log-rank test was used to analyse differences between different worm strains and media conditions.

Cholesterol depletion reduced significantly mean lifespan of wild type and *klo-2(ok1862); klo-1(ok2925)* mutant worms, from 18.6 to 12.5 days and from 18.4 to 11.3 days respectively (Table 16; Figure 34). The mean lifespan of *Klotho* double mutants was more severely reduced by cholesterol depletion than the mean lifespan of wild type worms ($p < 0.0001$).

Table 16 Lifespan is reduced in cholesterol depleted NGM.

Two independent experiments are included per strain/treatment. Maximum lifespan corresponds to the death age of the most long-lived worm. Number of animals observed equals the number of total animals minus the censored. Animals were censored if they crawl off the plate, become bag of worms or explode at the time of the event; these worms were counted and included in the statistical analysis to avoid loss of information. Log-rank (Kaplan-Meier) test was performed to determine significant differences if p values were less than 0.05. Lifespan was significantly shortened ($p < 0.0001$) in *klo-2(ok1862); klo-1(ok2925)* worms as compared to wild type worms when grown in 0 mM cholesterol.

Strain	Treatment	Mean Lifespan \pm SEM (days)	Maximum Lifespan (days)	Number of Animals Observed/ Total Animals	P value NGM vs 0mM cholesterol
N2 wt	NGM	18.6 \pm 0.6	28	129 / 228	
	0 mM cholesterol	12.5 \pm 0.5	23	116 / 224	<0.0001
<i>klo-2(ok1862); klo-1(ok2925)</i>	NGM	18.4 \pm 0.9	31	114 / 219	
	0 mM cholesterol	11.3 \pm 0.4	14	77 / 214	<0.0001

**Figure 34 Effect of cholesterol depletion.**

N2 wild type was used as a control worm strain. The survival curves represent the sum of all animals examined in two independent experiments. The log-rank (Kaplan-Meier) test was used to test the hypothesis that means lifespan of different groups were equal. Worms were maintained at 20 °C with living *E. coli*. No FUdR was used and worms were transferred to new plates every two days until they stopped laying eggs. Worms were incubated in standard NGM and depleted (0 mM) cholesterol NGM in parallel. Total number of animals, mean lifespan \pm SEM (days), maximum lifespan and p values are presented in Table 16.

3.4.4.2 Cholesterol depletion effect on viable brood size

The role of cholesterol for the ability of *Klotho* mutants to produce viable progeny was also tested. The worms were grown in the absence of cholesterol (0 mM cholesterol) for one or two generations (F1 or F2) prior to analysis as previous evidence suggests that the progeny will acquire some cholesterol from their mothers (Merris et al., 2003). Young adult worms (P₀) were transferred from standard NGM (containing 12.9 μM cholesterol) to cholesterol depleted media before egg-laying started. The F1 generation was laid onto the cholesterol depleted NGM, so that the only cholesterol the F1 worms obtained was from the P₀ mother. The P₀ continued producing eggs for 5 days but because there was no cholesterol on the plate, the amount of cholesterol that incorporated into the eggs was, in theory, less every day. Hypothetically, the F1 produced on day 1 (F1D1) by the P₀ mother would have more cholesterol than the F1 produced on day 3 (F1D3) (Figure 35). The F2 brood size of F1D1, F1D2 and F1D3 mothers was analysed. Similar process was followed for the F2 progeny of F1D1 worms, to obtain mothers that were grown two generations without cholesterol. The F3 brood size of F2D1, F2D2 and F2D3 worms was analysed (Figure 35).

N2 wild type worms produced a mean viable progeny of 232 ± 15 (95 % C.I.) on standard NGM. In cholesterol depleted media, wild type F1 generation and F2D1 mothers produced similar mean viable progenies as in standard NGM. However, wild type F2D2 and F2D3 mothers produced significantly less viable progeny, 163 ± 39 (95 % C.I.) and 74 ± 18 (95 % C.I.) respectively (Figure 36A; Table 17). *klo-2(ok1862)*; *klo-1(ok2925)* mutants when grown in standard NGM produced a mean viable progeny of 211 ± 12 (95 % C.I.), whereas the brood size was reduced to 147 ± 31 (95 % C.I.) and 87 ± 128 (95 % C.I.) for F2D2 and F2D3 mothers, respectively (Figure 36A; Table 17).

The reduction of viable progeny was progressive in both N2 wild type and *Klotho* double mutant as the generations and days passed. The brood size of F1D3 was equal or less than of F2D1 worms, supporting the hypothesis that progeny laid at the end of the laying period were produced with less cholesterol than the first worms laid. Both strains respond similar to cholesterol depletion and the only difference was that *Klotho* double mutant mothers laid significantly less viable progeny at F2D1 than the F2D1 wild type worms, 151 ± 49 (95 % C.I.) and 222 ± 9 (95 % C.I.) respectively.

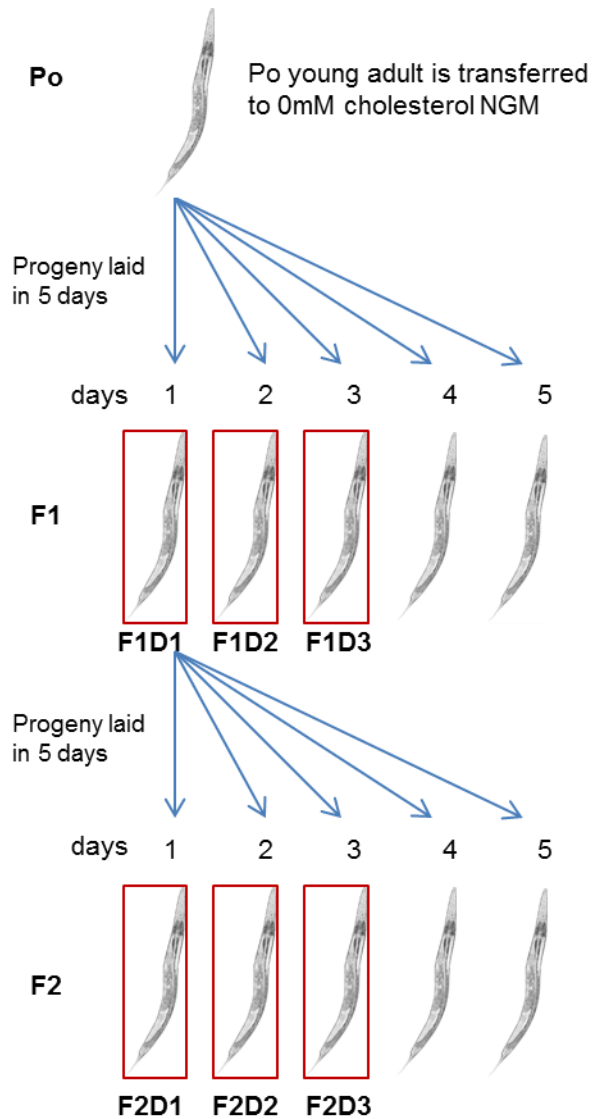


Figure 35 Explanation of the selected animals from worms grown in depleted (0 mM) cholesterol NGM for progeny quantification assay.

P₀ young adult was transferred from standard NGM to 0 mM cholesterol NGM. F₁ were laid on 0 mM cholesterol NGM, and the only cholesterol the F₁ progeny obtained was that provided by the P₀ mother during in utero development. P₀ was transferred to a new 0 mM cholesterol NGM plate every 24 hours. The F₁ progeny laid by P₀ on the 1st day of adult life was called F1D1. For the study, F₁ laid on day 2 (F1D2) and 3 (F1D3) were also used and transferred to a new plate at young adult stage to quantify their progeny (F₂). F1D1 young adult worms were transferred to new plates to separate their F₂ progeny laid every 24 hours. F₂ progeny laid by F1D1 on day 1 (F2D1), day 2 (F2D2) and day 3 (F2D3) were also used at the young adult stage to quantify their respective progenies (F₃).

The same progressive effect was seen in the increasing number of arrested larvae caused by the reduced amount of cholesterol available on cholesterol depleted media. F1D2 N2 wild type and *klo-2(ok1862)*; *klo-*

1(ok2925) worms had more larval arrested progeny than F1D1 and F1D3 even more, than F1D1 (Figure 36B; Table 17). Similarly, F2D3 progeny were more affected than F2D2 and F2D2 more affected than F2D1 (Figure 36B; Table 17). Interestingly, F1D1 had a mean arrested larval progeny similar to F2D1 mothers rather than to F1D3 mothers (Figure 36B; Table 17).

In standard NGM conditions, N2 wild type worms had a mean dead progeny of three worms, while *Klotho* double mutants had a similar mean dead progeny of five worms (Figure 36C; Table 17). Both strains had progressively more dead progeny when grown on cholesterol depleted media, with F2D2 mothers having the most of dead progeny, 14 dead progeny for wild type and 35 dead progeny for *Klotho* double mutant F2D2 mothers. The F2D2 *Klotho* double mutants had significantly increased lethality of their progeny (Figure 36C; Table 17). Surprisingly, F2D3 had much less dead progeny than F2D2, which could be explained by the fact that the total progeny of F2D3 is much lower too (Figure 36C; Table 17). Due to the high intrinsic variability between mothers, the increased quantities of dead progeny of F2D2 wild type mothers and F1D3 *Klotho* double mutant mothers were not significantly different.

Finally, N2 wild type worms in standard NGM produced a mean of 65 unfertilised eggs (Figure 36D). In cholesterol depleted NGM, wild type F1 worms produced similar quantities of unfertilised eggs (Figure 36.). However, N2 wild type F2D1 and F2D2 mothers laid significantly more unfertilised eggs, 138 and 124 respectively (Figure 36D; Table 17). No difference was observed in wild type F2D3 worms, which produced a mean of 64 unfertilised eggs, although the percentage was increased in relation to the smaller amount of viable progeny produce by these F2D3 worms (Figure 36D; Table 17). Similar results were seen in *klo-2(ok1862)*; *klo-1(ok2925)* worms, which laid a mean of 61 unfertilised eggs on standard NGM (Figure 36Table 17). F2D2 were the only *Klotho* double mutants that produced significantly more unfertilised eggs (175) on cholesterol than on standard NGM (Figure 36D; Table 17).

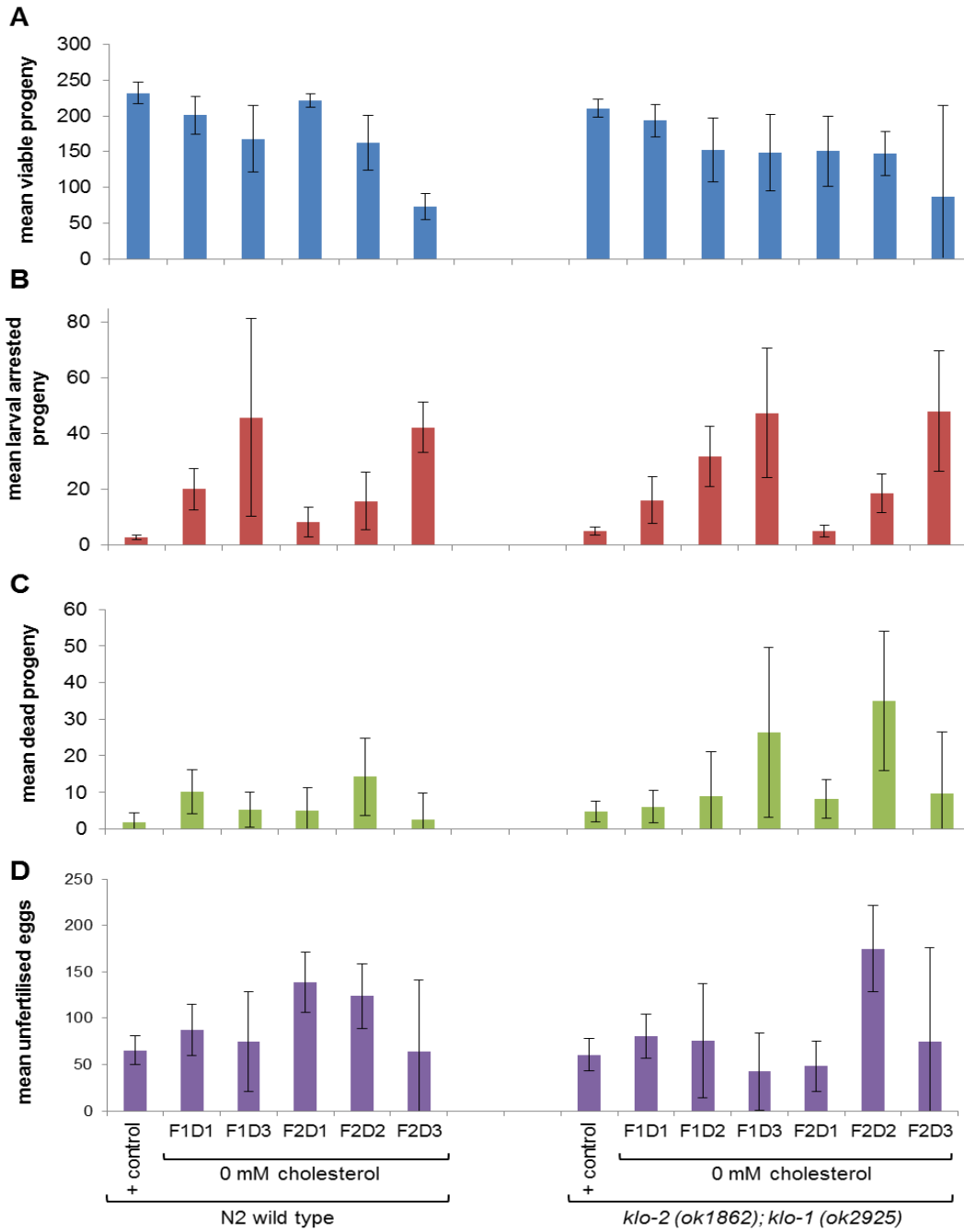


Figure 36 Mean progeny of N2 wild type and *klo-2(ok1862); klo-1(ok2925)* double mutant worms grown in standard NGM (+ control) or 0 mM cholesterol NGM.

Worm generation of the mother is expressed as F1 or F2 and the day on which the generation was laid as day 1 (D1), day 2 (D2) and day 3 (D3) (Figure 35). Error bars represent 95 % C.I.. A: mean viable progeny were the worms that developed into fertile adults. B: mean larval arrested progeny that were arrested as larvae after at least 5 days of development. C: mean dead progeny included the dead embryos and larvae. D: mean of unfertilised eggs laid. Tukey's test (Table 17Table 16Table 16).

Table 17 Mean progeny \pm 95 % C.I. of wild type and *klo-2(ok1862)*; *klo-1(ok2925)* worms grown in standard NGM or 0 mM cholesterol NGM.

Worm generation of the mother is expressed as F1 or F2 and the day on which the generation was laid as day 1 (D1), day 2 (D2) and day 3 (D3) (Figure 35). Tukey's analysis results are presented as p values of the comparisons between the mean progeny values of each generation of the mother grown in 0 mM cholesterol to standard NGM ($\alpha = 0.05$). NGM plates containing F1D2 wild type mothers were contaminated with mould and results were not included in the analysis.

Strain	Treatment	generation of the mother	N	viable progeny		larval arrested progeny		dead progeny		unfertilised eggs	
				mean \pm 95 % C.I.	p value	mean \pm 95 % C.I.	p value	mean \pm 95 % C.I.	p value	mean \pm 95 % C.I.	p value
N2 wild type	standard NGM		43	232 \pm 15		3 \pm 1		2 \pm 3		65 \pm 16	
	0 mM cholesterol	F1D1	19	201 \pm 26	0.65	20 \pm 7	0.001	10 \pm 6	0.82	87 \pm 28	0.98
		F1D3	8	168 \pm 47	0.09	46 \pm 36	<0.0001	5 \pm 5	1.00	75 \pm 54	1.00
		F2D1	9	222 \pm 9	1.00	8 \pm 5	1.00	5 \pm 6	1.00	138 \pm 32	0.05
		F2D2	20	163 \pm 39	0.0002	16 \pm 10	0.05	14 \pm 11	0.20	124 \pm 35	0.02
		F2D3	4	74 \pm 18	<0.0001	42 \pm 9	<0.0001	3 \pm 7	1.00	64 \pm 77	1.00
<i>klo-2(ok1862)</i> ; <i>klo-1(ok2925)</i>	standard NGM		42	211 \pm 12		5 \pm 1		5 \pm 3		61 \pm 17	
	0 mM cholesterol	F1D1	14	194 \pm 23	1.00	16 \pm 8	0.37	6 \pm 4	1.00	80 \pm 24	1.00
		F1D2	6	153 \pm 45	0.36	32 \pm 11	0.002	9 \pm 12	1.00	76 \pm 62	1.00
		F1D3	7	149 \pm 53	0.18	47 \pm 23	<0.0001	26 \pm 23	0.06	42 \pm 42	1.00
		F2D1	9	151 \pm 49	0.11	5 \pm 2	1.00	8 \pm 5	1.00	48 \pm 27	1.00
		F2D2	18	147 \pm 31	0.002	19 \pm 7	0.05	35 \pm 19	<0.0001	175 \pm 47	<0.0001
		F2D3	3	87 \pm 128	0.01	48 \pm 22	<0.0001	10 \pm 17	1.00	75 \pm 101	1.00

4 Discussion

4.1 Klotho regulation of ageing

The role of Klothos in ageing process in *C. elegans* was studied in this thesis. Previous studies have shown that defective Klotho leads to a premature ageing, while overexpression (OE) of Klotho extends lifespan in mice (Kuro-o et al., 1997; Kurosu et al., 2005) and *C. elegans* (Château et al., 2010; Polanska et al., 2011). The effects of *klo-1* and *klo-2* were tested in worm strains carrying genetic deletion mutations of these genes, *ok2925* and *ok1862*, respectively.

4.1.1 KLO-1 and KLO-2 in the regulation of lifespan

This is the first time that the lifespan of the deletion mutants of the *C. elegans* Klothos, *klo-1(ok2925)* and *klo-2(ok1862)*, were analysed. Surprisingly, genetic deletion of *klo-1* in the *ok2925* mutant, or deletion of both *klo-1* and *klo-2* in the *ok1862; ok2925* double mutant did not alter the mean lifespan as compared to wild type. Also, *klo-2(ok1862)* single mutants had one day longer mean lifespan than wild type worms ($p = 0.048$). *ok1862* allele leads to premature stop codon after Ile¹²⁹ (Polanska et al., 2011) thus deleting more than 70% of the wild type KLO-2 protein. *ok2925* deletion leads to an in-frame deletion of sequences encoding for Pro⁴ to Trp¹⁶⁴ after thus deleting 160 of the 479 amino acids of the KLO-1 protein (33%). Thus, both alleles are predicted to be a loss-of-function. This data thus suggests that genetic deletion of *klo-1* or *klo-2* or both in an otherwise wild type background does not alter worm lifespan.

Overexpression of *klo-1* (*klo-1* gain of function) in a wild type genetic background has been shown to prolong the mean lifespan by 1 to 2 days (Polanska et al., 2011). Given that *klo-2(ok1862)* mutant worms were found to have slightly longer lifespan (by 1 day) than wild type worms, one

could hypothesise that perhaps in the absence of *klo-2*, the expression of *klo-1* is upregulated, leading to prolonged mean lifespan. Another hypothesis could be that KLO-2 and KLO-1 proteins regulate the function of each other directly or most probably indirectly through another unidentified protein "X". This "protein X" has to be a protein that regulates DAF-16 activity, like DAF-2 or EGL-15 or any of the proteins downstream any of these 2 receptors. (Figure 37). However, this was not tested in this thesis and remains to be confirmed experimentally.

It has been suggested that Klotho regulates insulin receptor/DAF-2 signalling to prolong lifespan in mice and in *C. elegans* (Château et al., 2010; Kurosu et al., 2005). To elucidate the relation between Klotho and *daf-2/InsR* in worms, genetic mutants of *klo-1* and *klo-2* and components of *daf-2/InsR* pathway were analysed in combination. Partial loss-of-function mutation of *daf-2(e1370)* was used as a reference for long lived worms (Kenyon et al., 1993). *daf-2(e1370)* has been reported to have a mean lifespan of 42 days and a maximum lifespan of 75 - 80 days at 20 °C in comparison to mean lifespan of 20 days and a maximum of 30 days for wild type *C. elegans* (Kenyon et al., 1993). The results presented in this thesis are in agreement with those published previously by Kenyon et al (1993), with the mean lifespan for *daf-2(e1370)* measured as 46.2 days and 19.4 days for wild type *C. elegans*, and maximum lifespan measured 65 days for *daf-2(e1370)* and 30 days for wild type *C. elegans*. Surprisingly, it was discovered that *klo-1* and *klo-2* single mutations, and *klo-2; klo-1* double mutation in *daf-2(e1370)* genetic background further prolonged lifespan compared to long-lived *daf-2(e1370)* mutants. The synergistic lifespan promoting effect was particularly pronounced in *daf-2(e1370) klo-2(ok1862)* double mutant worms, which had a mean and maximum lifespan of 58.8 and 92 days respectively. This is three times longer than wild type worms and 25-50 % longer lifespan than *daf-2 (1370)* worms. Taken together, although the *C. elegans* Klotho mutations do not affect lifespan in otherwise wild type background, in combination with *daf-2(e1370)*, they significantly prolong lifespan as compared to *daf-2(e1370)* mutation only.

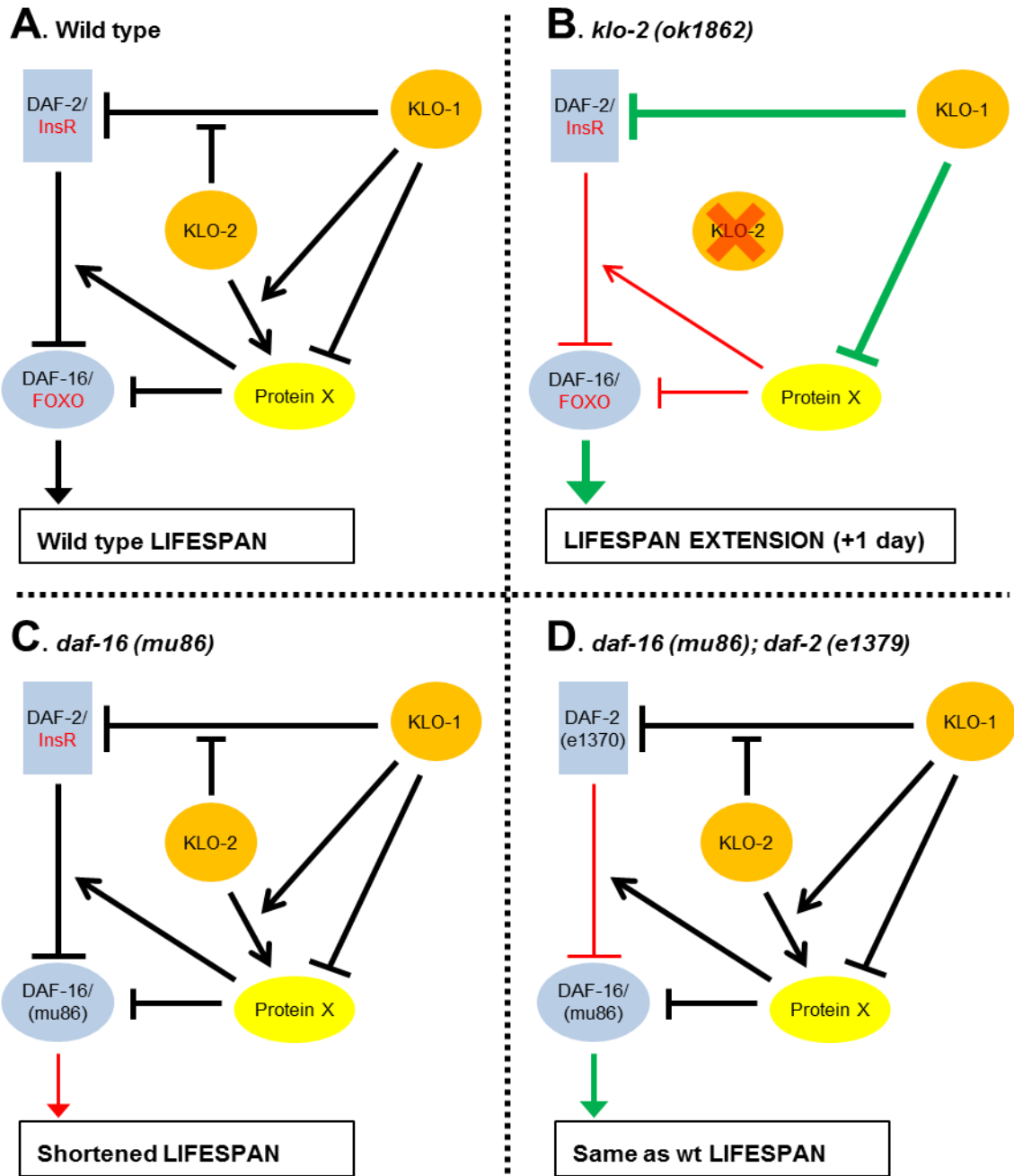


Figure 37 Proposed model of protein interactions between KLO-1, KLO-2, DAF-2 and DAF-16, including an unknown ageing mediator protein called "Protein X", which leads to alterations of lifespan.

A: model of protein interaction in wild type worms. B: Changes in signalling caused by *klo-2(ok1862)* mutation. C: alterations in lifespan caused by *daf-16(mu86)* mutation. D: alterations caused by *daf-16(mu86); daf-2(e1379)* mutations. Arrows indicate activation and "T" shaped lines indicate inhibition of mechanism of action. The protein interactions downregulated are shown by thinner red line/arrow and those upregulated are shown by a wider green line/arrow.

The effect of *daf-2(e1370)* is dependent on *daf-16/FOXO* (Kenyon et al., 1993), and the lifespan extension caused by *daf-2* downregulation in the *e1370* mutant is completely inhibited by *daf-16(mu86)* null allele (Figure 37D) (Lin, Dormanm, Rodan, & Kenyon, 1997). Similar results were found in this work, where *daf-16; daf-2* double mutants had a mean lifespan of 17.8 days and a max lifespan of 27 days. The lifespan regulation by *Klotho* is also dependent on *daf-16*, because *daf-16; klo-2; klo-1* triple mutants had a shorter lifespan than *klo-2; klo-1* mutants. Similarly, *daf-16(mu86)* shortened the lifespan of all *Klotho* mutants (single and double) in *daf-2(e1370)* genetic background suggesting that the lifespan prolonging effects of all these genes are mediated via DAF-16/FOXO (Figure 37D).

In the absence of functional KLO-2 the worms live longer. *klo-2(ok1862)* mutants lived an average of 1 day longer than wild type (Figure 37B) and *daf-2(e1370) klo-2(ok1862)* mutants lived three times longer than wild type (Figure 38D). Thus, KLO-2 may inhibit DAF-16, and in the absence of KLO-2 in *ok1862* mutants, this inhibition is abolished. On the other hand, the function of KLO-1 on lifespan regulation is less clear. Mean lifespan of *klo-1(ok2925)* single mutants was not significantly decreased as compared to wild type, but it was decreased as compared to *klo-2(ok1862)* single mutants. *daf-2(e1370); klo-1(ok2925)* mutants had a minor extension of mean lifespan as compared to *daf-2(e1370)* mutants (Figure 38A - B). Worms which only had KLO-1 protein (i.e. *klo-2(ok1862)* mutants) lived longer, but lifespan was not altered in worms which only had KLO-2 protein (i.e. *klo-1(ok2925)* mutants). Moreover, *klo-1* over expression extends lifespan even with functional KLO-2 (Polanska et al., 2011).

klo-2; klo-1 double mutants had a shorter mean lifespan than *klo-2(ok1862)* single mutants but longer than *klo-1(ok2925)*. Similarly, in *daf-2(e1370)* genetic background, *daf-2 klo-2; klo-1* triple mutants had shorter mean lifespan than *daf-2 klo-2* double mutants but longer than *daf-2; klo-1* double mutants. These results suggest that KLO-1 influences the activity of KLO-2 which is the main reason to propose an interaction's model with a mediator "protein X" regulated by both *Klotho* proteins (Figure 37A). KLO-1 and KLO-2 interact with each other to regulate lifespan, so

if both proteins are absent (Figure 38C) the mean lifespan is not extended as is the case when KLO-1 is functional in *klo2(ok1862)* mutants (Figure 38D). However, if both Klothos are absent, the lifespan is longer than if only KLO-2 is functional in *klo-1(ok2925)* mutants, which might imply that KLO-2 inhibits lifespan extension by activating the “protein X” which in turn inhibits DAF-16 (Figure 38C). Moreover, the model proposed is the better scenario to explain why in a *daf-2(e1370)* background mutation, double Klotho mutant worms have shorter lifespan than *klo-2(ok1862)* and longer than *klo-1(ok2925)* mutant worms.

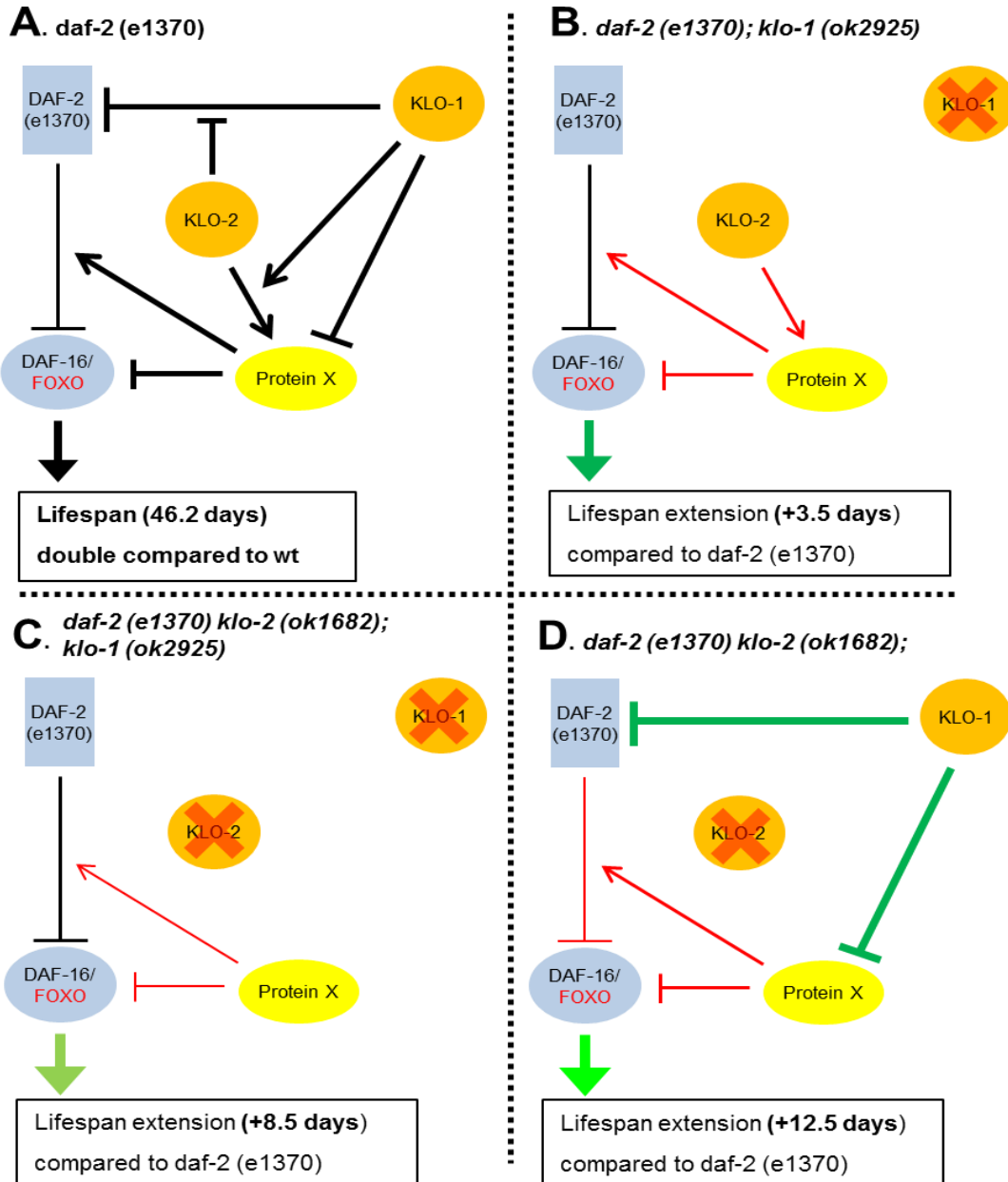


Figure 38 Proposed model of protein interactions between KLO-1, KLO-2, DAF-2 and DAF-16, including an unknown ageing mediator protein called “Protein X”, which leads to alterations of lifespan.

A: model of protein interactions in *daf-2(e1370)* hypomorphs. B: Alterations in signalling caused by *klo-1(ok2925)* mutation in *daf-2(e1370)* mutation background. C: alterations in protein interactions caused by *daf-2(e1370) klo-2(ok1862); klo-1(ok2925)* mutations. D: alterations caused by *klo-2(ok1862)* mutation in *daf-2(e1370)* mutation background. Arrows indicate activation and “T” shape lines indicate inhibition. The protein interactions downregulated are shown by thinner red line/arrow and the upregulated actions are shown by a wider green line/arrow. Up/downregulation of protein activities is compared to model A with only *daf-2(e1370)* mutation.

klo-1(ok2925) and *klo-2(ok1862)* mutations have a significant effect on lifespan only in *daf-2(e1370)* genetic background. Previous studies have shown that Klotho inhibits insulin and IGF-induced receptor autophosphorylation in cultured mammalian cells (Kurosu et al., 2005; Wolf et al., 2008) and represses directly or ligand-dependently the tyrosine kinase activity of DAF-2 (Château et al., 2010). It should be noted that in this thesis genetic deletion alleles were used, whereas Chateau et al used mixed RNAi to simultaneously knock-down both *klo-1* and *klo-2*. Chateau et al did not find any differences in the lifespan of *daf-2(e1370)* worms compared to the lifespan of *e1370* mutants treated with *klo-1/klo-2* hybrid RNAi. Chateau et al study suggested that simultaneous downregulation of *klo-1* and *klo-2* using mixed RNAi by feeding shortened the lifespan by almost 2 days (Château et al., 2010). The results of Chateau et al using RNAi thus differ from the results presented in this thesis. The probable explanation is that they used RNAi mixture which may not have completely knocked out both *klo-1* and *klo-2*, and hence they may have only observed the effects of *daf-2(e1370)* genetic mutation alone.

Moreover, the discrepancy between the data in this thesis using genetic mutant alleles versus gene knock-down by RNAi of Château (2010) is not unusual. Other genes have been shown to produce contradictory results when knocked down using RNAi or when studying genetic mutants. *fat-7*, which has also been studied in this thesis, is a target gene of DAF-16 and is involved in lipid metabolism. RNAi knock-down of *fat-7* induces fat reduction and shortens lifespan, in contrast to genetic mutants of *fat-7*, which have normal fat content and lifespan (Brock et al., 2006; Van Gilst et al., 2005).

The lengthiest maximum lifespan for *daf-2(e1370)* mutants that has been observed is around 80 days and a mean lifespan of 40-50 days (Chandler-Brown et al., 2015; Lee et al., 2009; Sutphin & Kaeberlein, 2008), which is longer than the lifespan of *daf-2(e1370)* mutants analysed for this thesis (mean lifespan of 46.2 ± 1.0 (SEM) days and maximum lifespan of 65 days). However, the previously published studies carried out the lifespan assays in the presence of 5-Fluoro-2'-deoxyuridine (FUdR) and UV-killed bacteria. FUdR is an inhibitor of DNA synthesis (Bell & Wolff,

1964; Cohen, Flacks, Barner, Loeb, & Lichtenstein, 1958) widely used in *C. elegans* lifespan assays because it inhibits the production and development of progeny (Mitchell, Stiles, Santelli, & Sanadi, 1979), resulting in easier worm maintenance conditions because the worms do not need to be transferred to fresh plates every couple of days during the egg laying period. A number of studies have shown that FuDR affects metabolism and in some genetic backgrounds extends lifespan and induces stress resistance (Anderson et al., 2016; Rooney et al., 2014). In some studies, *E. coli* OP50 is UV-killed to eliminate the potential harmful effects associated with the growth and proliferation of live bacteria in the worms (Garigan et al., 2002). However, the mean lifespan of worms grown on UV-killed bacteria is increased by 16 % (Gems & Riddle, 2000) or up to 40 % (Garigan et al., 2002) as compared to worms grown in live bacteria. The fact that FuDR and UV-killed bacteria could extend lifespan of worms was the main reason to discard their use in the lifespan experiments of this thesis, to avoid any potential synergistic effects.

Chateau et al report a mean lifespan reduction caused by simultaneous knock-down of *klo-1* and *klo-2* using mixed RNAi in worms (Château et al., 2010). However, they also report a reduced mean and maximum lifespans for wild type (17.5 and 29) and *daf-2(e1370)* (30.3 and 39 days). The findings of Château et al., 2010 study thus differ from a number of publications (Chandler-Brown et al., 2015; Dorman, Albinder, Shroyer, & Kenyon, 1995; Kenyon et al., 1993; Lee et al., 2009) and from the results presented in this thesis and is another factor to consider for the discrepancy of the results regarding *Klotho* mutations versus knockdown.

Because *klo-2(ok1862)* mutant worms (this thesis) and *klo-1* (gain of function) worms live longer (Polanska et al., 2011), KLO-1 is likely to be the Klotho protein downregulating DAF-2 activity, although further research should be done to confirm it. Moreover transcript levels of *klo-1* are increased 2.8 fold in *daf-2* loss of function mutant worms (McElwee, Schuster, Blanc, Thomas, & Gems, 2004).

The lifespan of *daf-2 klo-2* mutant worms is three times longer than wild type worms, which could be a consequence of two factors; first increased expression of *klo-1* caused by DAF-2 downregulation and second, the absence of functional KLO-2. The most plausible scenario could be the balance of KLO-1 and KLO-2 as the regulator of lifespan. Further analysis of lifespan of *klo-2* (gf) and also *klo-2* (gf); *klo-1* (gf) in *daf-2(e1370)* genetic background could clarify if the absence of KLO-2 is necessary for lifespan elongation effect of KLO-1.

4.1.2 Effect of glucose on lifespan

Glucose has been shown to shorten lifespan both in *C. elegans* and in mammals (Franco, Steyerberg, Hu, Mackenbach, & Nusselder, 2007; Kimura et al., 1997; Lee et al., 2009). Wild type, *daf-2* mutant and *klo-2* mutant worms cultured in NGM containing 2 % glucose had shorter mean lifespans than in standard NGM conditions. However, mean lifespan of *klo-1* single mutant worms was not affected by glucose. Similarly, glucose reduced the mean lifespan of *daf-2; klo-1* worms less than of *daf-2 klo-2* and *daf-2 klo-2; klo-1* triple mutant worms. These findings suggest that, KLO-1 is needed for the effects of glucose to shorten lifespan. Therefore, KLO-1 could be acting, in a yet unidentified way (specified in the model as an unknown “protein Y” from an unknown pathway), as a sensor for glucose to activate DAF-2 (Figure 39).

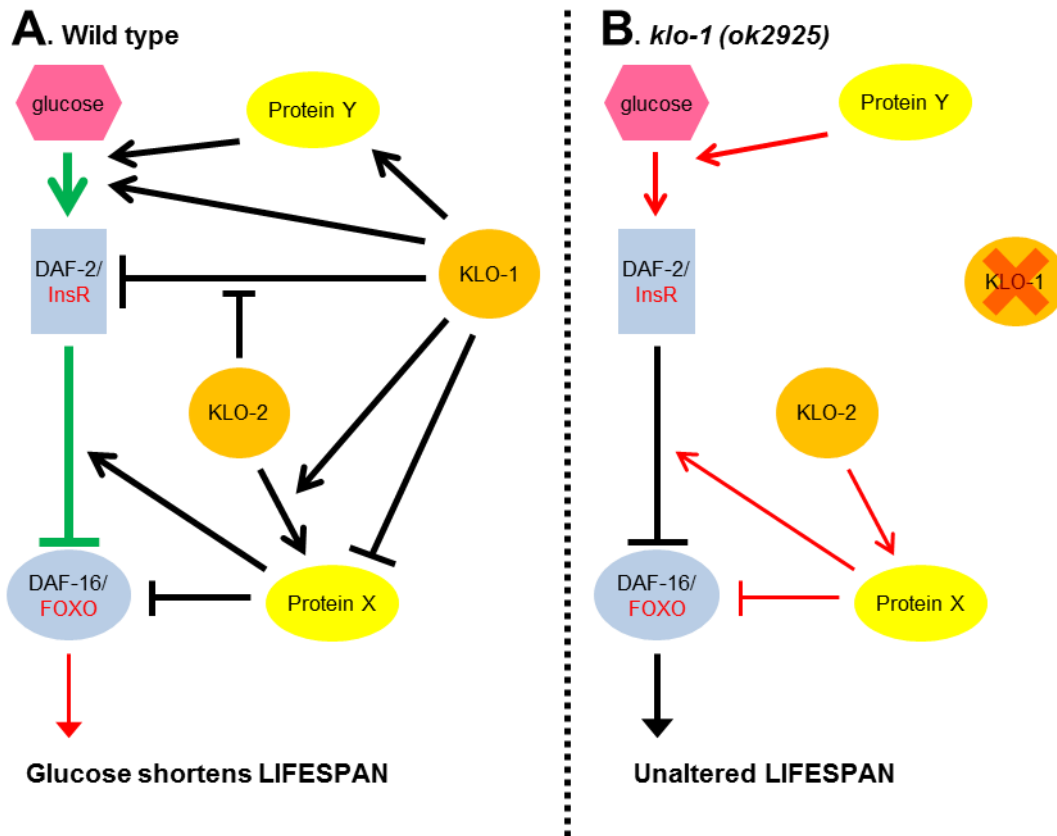


Figure 39 Proposed model of interactions between KLO-1 and glucose in the regulation of IIS pathway.

A: model interaction in wild type worms. KLO-1 controls the activity of glucose over DAF-2. B: alterations caused by *klo-1(ok2925)* mutation. Glucose does not activate IIS as in wild type phenotype, which is why the lifespan is unaltered. Arrows indicate activation and “T” shape lines indicate inhibition mechanism of action. The protein interactions downregulated are shown by thinner red line/arrow and the upregulated actions are shown by a wider green line/arrow.

4.1.3 Extended lifespan of *daf-2* and *klo-2* double mutants is not caused by a reduced brood size or retarded development

Life history theory claims that development time, brood size and lifespan of an animal are related (Hochberg, 2012; Roff, 1992; Stearns, 1976). It is common in nature that animals with higher metabolic rates have shorter lifespans as compared to animals with slower metabolic rates, and the shorter lifespan tends to correlate with bigger brood size and faster development. This is the case of *daf-2(e1370)* mutant worms which due to a downregulated insulin pathway, develop

slower, lay less progeny and have a longer mean lifespan than wild type *C. elegans* (Ruaud et al., 2011; Tissenbaum & Ruvkun, 1998). *a-Klotho* deficient mutant mice are infertile, have development retardation and shorter lifespans (Kuro-o et al., 1997), which do not align with the life history theory. However the premature ageing-like phenotype observed in *Klotho* deficient mice are primarily caused by the toxic effects of phosphate/ vitamin D excess (Kuro-o, 2009; Stubbs et al., 2007). *Klotho* mutant worms present some osmoregulation problems, like water retention cysts (Polanska et al., 2011; Xu et al., 2017) and retarded developed in the absence of potassium in their growth environment (Figure 29). Nevertheless, these osmotic alterations did not appear to significantly affect the development, brood size and lifespan of *Klotho* mutant worms.

The development of *daf-2(e1370)* mutants from eggs to adults was further slowed in *daf-2; klo-1* double mutants and *daf-2 klo-2; klo-1* triple mutant worms, although the difference was small. Surprisingly, *daf-2 klo-2* worms, which have the longest lifespan, did not develop slower than the *daf-2* mutants. The reduced brood size of *daf-2(e1370)* worms did not differ from the brood size of *daf-2 klo-2; klo-1* triple mutant worms, laying 60 % less viable progeny than wild type worms. Considering that there were no synergistic effects between *daf-2(e1370)* and *Klotho* mutations in the viable progeny number, and no difference was observed between the development time of *daf-2* and *daf-2 klo-2* mutants, the extended lifespan of *daf-2 klo-2* worms does not appear to be caused by delays in overall development or by reduced brood size.

As the single *daf-2(e1370)* mutants had a pronounced developmental delay, reduced brood size and extended lifespan indicating a slower metabolism (Ruaud et al., 2011; Tissenbaum & Ruvkun, 1998), only minor synergistic effects could be seen when mutations in *klo-1* and *klo-2* were introduced. The muscular activity, measured as the pharyngeal muscle pumping rate (number of contractions per minute of the pharyngeal muscle) of one day old *daf-2 klo-1* and/or *klo-2* mutant and *daf-2: klo-2* double mutant adults was significantly decreased compared to wild type and *Klotho* mutant worms, may indicate a reduced ingestion of food. In addition, all *daf-2(e1370)* and

daf-2 klo-1 and/or *klo-2* mutants were wider in shape as compared with wild type *daf-2*, which could be due to fat accumulation, as has been previously reported (Ashrafi et al., 2003; Kimura et al., 1997; O'Rourke et al., 2009). All these results together support the hypothesis that metabolism of *daf-2(e1370) klo-1* and/or *klo-2* worms was downregulated as compared to wild type. Lipid quantification, analysis of the activity of metabolic proteins and oxygen consumption of *daf-2 Klotho* mutants should be done in future investigations to confirm altered metabolic rate.

4.1.4 Glucose increases production of viable progeny

Glucose increases metabolic rate by inducing IIS pathway as previously described. The lifespan shortening effect of glucose is well known (Lee et al 2009) and has been successfully replicated in this thesis. However, the effects of over-activation of IIS pathway caused by glucose in relation to fertility remain to be investigated.

The reduced number of viable progeny and the slow development of *daf-2(e1370)* and *daf-2(e1370) Klotho* worms was restored to wild type levels if DAF-16/FOXO was absent (i.e. introduction of *daf-16(mu86)* mutation to the genetic background). Similar effect was observed when glucose was added to the worm plates. In the presence of 2 % glucose, all *daf-2(e1370) Klotho* mutants developed faster than in standard NGM, although the development was still slower than wild type worms.

Glucose activates DAF-2/Insulin Receptor cascade which in turn phosphorylates DAF-16 and prevents DAF-16 entering the nucleus to activate the transcription of the target genes (Kenyon et al., 1993). If DAF-2 is downregulated, less DAF-16 is phosphorylated and more DAF-16 enters the nucleus to induce lifespan extension, reduce brood size and slow down development. However, this is reversed if DAF-16 is downregulated (no DAF-16 activity in *daf-16(mu86)* mutants) or if worms are fed with glucose. This data thus suggests that together with DAF-2, KLO-1 and KLO-2 also regulate DAF-16 entry to the nucleus.

The brood size was also sensitive to the effect of added glucose. Because glucose shortens the lifespan of all strains tested, it was expected to increase the brood size. Surprisingly, all strains analysed laid a similar number of viable progeny in the presence of glucose i.e. glucose supplementation abolished any variation in the progeny numbers based on the genetic background. *daf-2(e1370)* and all *daf-2(e1370) Klotho* mutants had twice the number of viable progeny in the presence of glucose (>200 progeny on average) than in control conditions. In contrast, wild type and *daf-16(mu86); daf-2(e1370) Klotho* quadruple mutants had a reduction from an average number of 250 to around 200 viable progeny in the presence of glucose. The number of viable progeny was thus decreased in two opposite situations: in the excess stimulation of DAF-2 caused by glucose addition to wild type worms and in DAF-2 downregulation in hypomorphic *e1370* mutants in standard conditions. The absence of *Klotho* in *daf-2(e1370)* background did not produce any notable changes on the number of viable progeny after glucose addition compared to *daf-2(e1370)* worms. Therefore, it could be hypothesised that KLO-1 and KLO-2 regulation of DAF-16 does not affect the fertility of the worms. However, further experiments including the assessment of fertility of *Klotho* mutants in the presence of glucose need to be performed to claim an interaction between DAF-2 and *Klotho* proteins to regulate fertility.

The number of unfertilised eggs laid was not significant in *daf-2(e1370)* and *daf-2(e1370) klo-2(ok1862); klo-1(ok2925)* mutant worms, which only laid 2 and 3 unfertilised eggs respectively. In contrast, wild type and *daf-16(mu86); daf-2(e1370) Klotho* quadruple mutants laid a higher number of unfertilised eggs, 196 and 80 on average respectively. The addition of glucose did not alter the number of unfertilised eggs laid by *daf-2(e1370)* and *daf-2(e1370) Klotho* mutants. In *daf-2(e1370)* and *daf-2 Klotho* triple mutants, a higher percentage of DAF-16 may enter the nucleus and activate the transcription of target genes. However, when DAF-16 is normally regulated (in wild type worms) or is less active (*daf-16(mu86)* null mutants), addition of glucose almost completely abolished the production of unfertilised eggs.

In the presence of glucose, *daf-2(e1370)* and *daf-2(e1370) Klotho* triple mutants had twice the amount of viable progeny compared to normal condition. However, the overall brood size (including unfertilised eggs, dauer arrested larvae, dead larvae and viable progeny) was decreased when glucose was present. Importantly, dauer formation and larval lethality were completely suppressed by glucose. Glucose thus increased viable progeny and suppressed dauer formation and larval lethality of *daf-2* and of *daf-2 klo-2; klo-1* triple mutants. Similarly, in the presence of glucose, wild type worms and *daf-16; daf-2 klo-2; klo-1* quadruple mutants laid very few unfertilised eggs and almost all the eggs laid developed into fertile adults.

Overall, glucose increased the efficiency of reproduction as it increased the relative proportion of viable progeny with respect to the total number of eggs laid.

4.2 Health of *Klotho* mutant worms

4.2.1 *Klotho* effect in food behaviour does not depend on motility

Motility can be used as an indicator of food preference or food sensitivity (Hahm et al., 2015), in addition to being an indicator of the metabolic rate of an organism (Gaglia & Kenyon, 2009; Tucker, 1970) which in turn is related to development, brood size and lifespan. *klo-2(ok1862); klo-1(ok2925)* double mutant worms had a tendency to crawl off the plate more often than wild type worms. When carrying out lifespan assays it was counted that over 30 % of *klo2; klo-1* double mutant worms crawled outside the food plate, twice the number compared to wild type worms. It was hypothesised that *Klotho* double mutant worms have an alteration in food preference which would explain that worms crawl off the food as they are not so attracted to it. In mice, β -*Klotho* is involved in the action of administered FGF-21 to regulate sweet and alcohol preference (Talukdar, Owen, et al., 2016). Alternatively, it could be that *Klotho* mutant worms have a defective attraction to food which allows them to explore the plates beyond the food lawn.

However, when motility was specifically assessed, there was no difference in the distance crawled in 2 hours between *Klotho* double mutant worms and wild type worms. Other experiments showed that the same proportion of *Klotho* mutants and wild type worms were outside and inside the food at different developmental stages (Appendix 3). Also, the pharynx morphology and functionality (measured as the pumping rate) were similar for wild type and *Klotho* double mutant worms. In summary, further experiments would need to be carried out to explain the different behaviour of *Klotho* mutant worms.

Glucose also induced a higher proportion of wild type and *Klotho* double mutant worms to crawl off the plate. A similar effect of glucose was observed in *daf-2(e1370)* mutant worms. The *E. coli* OP50 on 2 % glucose NGM grew much faster than in standard conditions, and after few days the food lawn was so thick and dense that the worms could crawl under or over it. However, in these conditions, less than 10 % of the worms were in the middle of the food lawn, instead, they preferred to stay in the food lawn border, which could be the cause of almost 80 to 90 % of the worms crawling outside the food lawn and an increased number of them crawling off the plate and dying by desiccation.

Contrary to wild type and *Klotho* double mutant worms, the *klo-1(ok2925)* and *klo-2(ok1862)* single mutants did not crawl off the plate more in the presence of glucose. Moreover, the fact that higher number of worms crawled off the plate and die could be more related to the physical conditions of the food lawn (thickness) that related to specific molecular interactions of glucose with worm metabolism. Therefore, the relation of glucose and the tendency to crawl off the plate cannot be explained.

4.2.2 *Klotho* and DAF-2 act synergistically to increase healthspan and affect egg laying

Genetic elimination of worm *Kloths* and hypomorphic mutation of *daf-2* has a synergistic effect on lifespan extension. This synergy is especially strong between *klo-2(ok1862)* and *daf-2(e1370)*

mutations, with the double mutant worms living thrice the number of days than wild type worms and 25 - 50 % longer than *daf-2 (e1370)* hypomorphs. At the time point when all wild type and *Klotho* single and double mutant worms were dead, more than 95 % of *daf-2(e1370) Klotho* double/triple mutant worms (including either *klo-1* or *klo-2* or both *klothos*) were still moving and crawling. Similar findings have previously been reported for *daf-2(e1370)* worms (Garigan et al., 2002; Herndon et al., 2002; Kenyon et al., 1993). Clearly, these *daf-2 Klotho* double/mutants still moving at 28 days of adult life were not entering the normal decline and were, in fact, fully active animals. The *daf-2(e1370) Klotho* double/mutant worms had not only extended lifespan but, more importantly, their healthspan was also extended.

daf-2(e1370) mutants have been reported to lay progeny up to 50 days of adult life (Gems et al., 1998; Larsen, Albert, & Riddle, 1995) and the same extended fertility time was observed in *daf-2(e1370) Klotho* double/triple mutant worms. Wild type worms and *Klotho* mutant worms ceased to lay progeny completely after 8 days, although very few eggs were laid after 3 days of adult life. Wild type and *Klotho* mutants had a mean lifespan of 20 days, which is four times longer than the average fertility time. In contrast, equal mean lifespan and maximum fertility time are almost the same in worms with downregulated DAF-2 and in the absence of *Kloths*. All this data suggests that the synergistic relation between *Klotho* and DAF-2 extended the healthspan of the worms and not only the lifespan. Also, the extended fertility time in relation to lifespan could indicate that the *daf-2(e1370) Klotho* mutant worms were healthier for longer time in proportion to the respective lifespan. Further research needs to be done to investigate the specific relation of KLO-1 and KLO-2 with DAF-2 pathway in the ageing of gonad and other different tissues.

In contrast with the longer fertility, and better healthspan of the majority (85%) of the *daf-2 Klotho* double/triple mutants' worms, 15% of the triple mutants have a defect that affects egg laying. In consequence ~15 % of *daf-2(e1370) Klotho* mutant worms died because the larvae hatched inside the mother's gonad and started to eat her from inside. This egg laying defect was only seen in *daf-2 (e1370)* hypomorphs with *klo-2* and/or *klo-1* (double/triple mutants) also genetically

eliminated. Single *Klotho* mutants and *daf-2* single mutant worms were not different to wild type worms and presented very similar few cases (~5 %) of these deaths. This cause of death affected *daf-2 Klotho* double/triple worms only during first days of adult life when more eggs are fertilised and undergo embryonic and larval development. Therefore, *daf-2 Klotho* worms which survive the first days of adult life have a healthier and longer lifespan.

These results suggest that KLO-1 and KLO-2 might be necessary for the normal egg laying; however, the absence of KLO-1 and/or KLO-2 affects egg laying only when DAF-2 is downregulated. The synergistic effect on egg laying could be caused by defects in the vulval muscles or in the neurons that innervate the muscles and initiate egg-laying. The exact nature of these defects warrants a further study.

4.3 Stress resistance

4.3.1 *klo-2* controls dauer formation independently of *daf-2*, but dependent of *klo-1*

Klotho has been suggested to be involved in stress resistance through the interaction with Insulin/IGF-1 signalling (Mitobe et al., 2005; Yamamoto et al., 2005). In addition to the lifespan and healthspan extension, *daf-2 klo-2* double mutants tolerate heat stress better than *klo-2* and *daf-2* single mutants. It is well known that *daf-2* mutations enhance resistance to heat stress (Babar, Adamson, Walker, Walker, & Lithgow, 1999; Hsu, Murphy, & Kenyon, 2003; Lithgow, White, Hinerfeld, & Johnson, 1994; Lithgow, White, Melov, & Johnson, 1995; Walker et al., 2001) and induce dauer formation of all worms at 25 °C (Gottlieb & Ruvkun, 1994). *klo-2* (ok1862) mutation enhanced the formation of dauer at 25 °C in 34 % of cases. At higher temperature (27 °C), the absence of *klo-2* resulted in 68 % of worms entering the dauer state, while only 15 and 18 % of

klo-1 and *klo-2*; *klo-1* double mutants respectively and 10 % of wild type worms entered dauer state.

The induction of dauer formation in *klo-2* mutant worms did not happen if *klo-1* was also genetically eliminated. *klo-2(ok1862)* single mutation induced four times more dauers than *klo-2(ok1862)* with *klo-1(ok2925)*. The dependence of functional KLO-1 for the effect of KLO-2 deficiency for the induction of dauer was similar to the further lifespan extension of *daf-2 klo-2* mutants in comparison to *daf-2 klo-2 klo-1* triple mutants. However, for the induction of dauer formation, *klo-2* null mutation alone was enough without the synergistic relation with *daf-2(e1370)*. From these results it could be deduced that heat resistance was induced by KLO-1 and inhibited by KLO-2, which is the same model that was proposed for the extension of lifespan. Also, the induction of dauer formation of *klo-2* mutants was suppressed by *daf-16* mutation, indicating once more that the effects of KLO-1 were dependent on DAF-16 activity.

In conjunction with *daf-2(e1370)*, *Klotho* mutations did not change the fact that 95 – 100 % of the worms entered dauer stage at temperatures of 23 °C or higher. However, at 20 °C, less than 3 % of *daf-2* mutants and *daf-2 klo-2* mutants were dauers. Therefore, no synergic effects were observed between *daf-2* and *Klotho* (especially *klo-2(ok1862)*) at 20 °C. It should be considered, as described by (Ailion & Thomas, 2000) dauer assays are very variable due to multiple environmental conditions that regulate dauer induction and are difficult to control. Smaller than 0.5 °C changes have significant quantitative results on the formation of dauer. Further research should be done to establish the temperature between 20 and 23 °C at which *klo-2* mutation enhances the formation of dauers in the *daf-2(e1370)* genetic background.

β -Klotho has been shown to be involved in thermic regulation in mice (Chen et al., 2017; Somme et al., 2017). FGF21 activation of FGFR1/ β -Klotho complex stimulates brown fat thermogenesis. The effects of mammalian β -Klotho deficiency and worm *klo-2* deficiency appear to be

orthologous in the thermic regulation. Investigating the thermic response also in α -*Klotho* and double *Klotho* mutant mice would be of interest to elucidate the results observed in worm model.

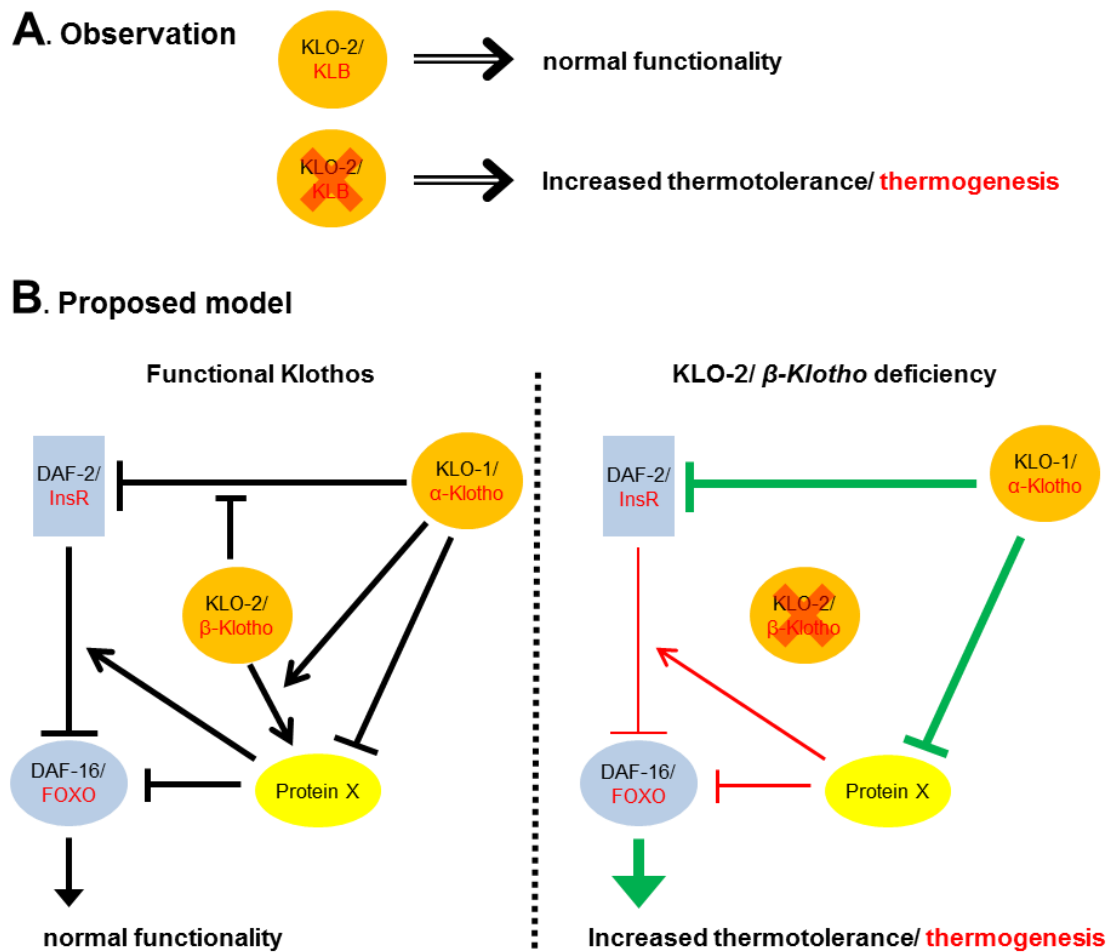


Figure 40 Phenotypic observations and proposed model for regulation of thermotolerance and thermogenesis.

A: Observed phenotype in wild type, *KLO-2* worms and β -*Klotho* mice. B: Proposed model of protein interactions between *kLO-1*, *KLO-2*, *DAF-2* and *DAF-16*, including an unknown ageing mediator protein called “Protein X”, which also regulates thermotolerance/thermogenesis. However, this “protein X” could be different to the one described in ageing. In β -*Klotho* deficient mice and *klo-2* deletion mutant worms the thermogenesis and thermotolerance have been shown to be increased respectively. Arrows indicate activation and “T” shape lines indicate inhibition. The protein interactions downregulated are shown by thinner red line/arrow and the upregulated actions are shown by a wider green line/arrow. Up/downregulation of protein activities are compared to wild type.

4.3.2 KLO-2 acts synergistically with DAF-2 to regulate heat stress response in a KLO-1 dependent manner

In addition to dauer formation, response to heat stress was also measured as the survival of L4 larvae to heat shock from 20 °C to 37 °C. Twice the number of *klo-2* mutants survived after 8 h at 37 °C compared to wild type and to *klo-1* mutant worms. *klo-2; klo-1* double mutants were severely defective in their ability to survive 8 h at 37 °C. This suggests that in the absence of KLO-2 (*klo-2(ok1862)* mutant worms), KLO-1 was able to protect against the heat stress. No effect was seen if only KLO-1 was mutated and KLO-2 was functional, which was the case of *klo-1(ok2925)* mutant larvae. Finally, in the case of both Klotho proteins being absent, the larval survival was four times lower than the survival if either KLO-2 only or both Klothos were functional. With these results, it is suggested that KLO-2 could be acting in maintaining normal (as in wild type) activation of DAF-16 and, somehow, inhibiting an over-activation of DAF-16 by KLO-1. This theory would explain that no change was observed in the heat stress survival when only KLO-1 was absent and that the heat survival was enhanced if only KLO-2 was absent. When both KLO-2 and KLO-1 are deficient, less DAF-16 is activated than in normal conditions and the survival to heat stress is reduced.

The heat stress protection effect caused by *klo-2* mutation is enhanced by *daf-2* mutation. The *daf-2* mutant worms used in this thesis were more resistant, although not statistically significant, to heat stress than wild type, as measured by the survival of L4 larvae at 27 °C for 8 h. This agrees with what has been previously published by others (Babar et al., 1999; Hsu et al., 2003; Lithgow et al., 1994, 1995; Walker et al., 2001). Nevertheless, in conjunction with *daf-2* mutation, *klo-1* and *klo-2* mutations enhanced the survival to greater extent than a single mutation alone. This would indicate once more, the synergic effect of DAF-2 downregulation and Klotho absence in the enhancement of health. Although in this case it cannot be confirmed that these effects were due to DAF-16 over-activation because no *daf-16(mu86)* Klotho mutants were used in the heat

shock experiments. However, given that dauer formation is a survival mechanism, the inhibition of dauer formation of *daf-16 klo-2* mutants would indicate so.

klo-2 mutation alone was enough to enhance the survival to heat stress, although the survival was enhanced in *daf-2 klo-2* mutant worms. *klo-2* mutation alone modifies the normal response to heat stress without been dependant on the *daf-2* dysfunction to show a synergistic effect. This is the main difference with respect to the effect on lifespan, development, brood size or egg laying. KLO-1 alone, without KLO-2 been present, is suggested to enhance the resistance to heat shock stress and the induction of dauer formation by inhibiting some DAF-16 inhibitor.

4.3.3 KLO-1 controls the response to oxidative stress independently of DAF-2, but dependent on KLO-2

Over-expression of *Klotho* has been shown to reduce DNA damage in mice and conferred more oxidative resistance in cultured mammalian cells (Yamamoto et al., 2005). Oxidative stress response is also mediated by DAF-16 and enhanced in *daf-2* mutant worms (Honda & Honda, 1999, 2002). It was hypothesised that *Klotho* mutations would affect survival to oxidative stress and would possibly have a synergistic effect with *daf-2* mutation to enhance even further the oxidative stress resistance. Paraquat was used to induce oxidative stress in worms and it was observed that *klo-2* mutant worms had similar sensitivity to high concentrations of paraquat (300 mM) than wild type worms. Surprisingly, *klo-1* mutation increased the survival to twice as long as compared to wild type worms.

daf-2 mutant worms were more resistant to oxidative stress, in agreement with previously published studies (Honda & Honda, 1999, 2002). However, the mean survival of *daf-2 klo-1* mutant worms was not different to the *daf-2* mutants. *klo-1* mutants had a longer mean survival time than *daf-2 klo1* mutants, although the difference was not significant. This result was completely unexpected considering all previous results, particularly, considering the heat stress protection observed in *klo-2* mutants. Instead, KLO-2 appears to be the Klotho protein inducing

the oxidative stress protection that only takes places if KLO-1 is not functional. This could explain why no enhancement of the survival was observed if both Klotho proteins were absent.

Neither *klo-1* nor *klo-2* mutations in combination with *daf-2* mutation influenced the mean survival to paraquat as compared to *daf-2* alone. However, the mean survival was significantly decreased in *daf-2 Klotho* triple mutants as compared to *daf-2* mutants, down to mean survival levels of wild type worms. This could indicate that DAF-2 downregulation might need the presence of at least one functional Klotho protein, KLO-1 or KLO-2, to enhance the survival of acute oxidative stress. Moreover, the further enhancement of survival of *klo-1* mutants in comparison to *daf-2 klo-1* mutants, may indicate that KLO-2 could be acting directly on DAF-2 as suggested previously (Château et al., 2010) or even in another parallel pathway independently of DAF-2 but dependent of DAF-16 activity (Figure 41). However, further analysis should be done to clarify the specific interactions of KLO-2 and KLO-1.

In addition to acute survival response to paraquat, the expression of *psod-3::GFP* (superoxide dismutase 3 reporter gene) was analysed in *Klotho* mutants in the presence of oxidative agent paraquat (Essers et al., 2005; Ishii et al., 1990). SOD-3 is a target gene of DAF-16 (Honda & Honda, 1999) and is activated in situations of oxidative stress (Fukai et al., 2002). *daf-2* mutants have increased levels of SOD-3 mRNA that protects them to oxidative stress (Honda & Honda, 1999).

Klotho mutants and wild type one day old adult worms had similar expression levels of *psod-3::GFP* reporter gene in standard conditions as measured in the pharyngeal muscle. Negative control *daf-16(mu86)* mutant worms had reduced levels of the reporter gene as compared to wild type and *Klotho* mutant worms. Contrary to previously published results (Essers et al., 2005; Ishii et al., 1990), the oxidative stress agent paraquat did not induce an increase in the expression of *psod-3::GFP*. Instead, 30 minutes exposure to 100 mM paraquat induced a significant 30 % reduction in the expression of the reporter gene in wild type, *klo-1* and *klo-2* mutant worms. The

psod-3::GFP expression was not significantly reduced in *Klotho* double mutants nor in *daf-16* mutants.

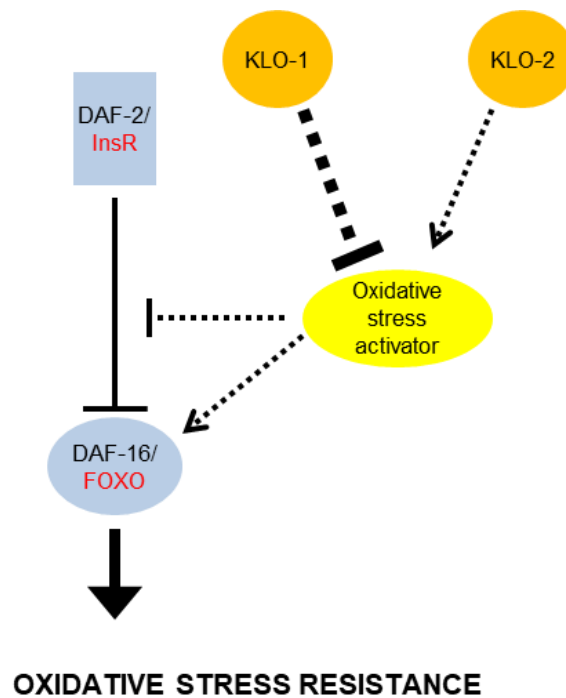


Figure 41 Proposed model of protein interactions between KLO-1, KLO-2, DAF-2 and DAF-16, including an unknown mediator protein called “Oxidative stress activator”. *klo-1(ok2925)* worms have increased survival to paraquat oxidative stress (independent of *daf-2(e1370)*). Arrows indicate activation and “T” shape lines indicate inhibition. The wider the line, the stronger the activity proposed by the model. Dashed lines indicate the proposed interactions and continue lines indicate proven protein relations.

Expression levels of *psod-3::GFP* were also similar in wild type and *Klotho* 48 h old larvae born and grown in the presence of 0.25 mM paraquat. Essentially, wild type, *Klotho* mutants and *daf-16* mutant larvae had similar expression levels of *psod-3::GFP* in standard conditions and only *klo-2; klo-1* double mutant larvae had 30 % increased expression in the presence of paraquat.

daf-16 mutant larvae at 48 h had similar mean expression levels of *psod-3::GFP* as compared to wild type worms, both in standard conditions and in the presence of paraquat. However, there was a broader range of expression levels of *psod-3::GFP* in the *daf-16* mutant larvae than in wild

type larvae. Some *daf-16* mutants had 90 % less *psod-3::GFP* expression than wild type, others had three times more than wild type. This intrinsic variability of *psod-3::GFP* expression levels in *daf-16(mu86)* larvae might be caused by the absence of DAF-16. In the absence of DAF-16, the transcription of *sod-3* is not controlled and some worms have ten times less SOD-3 while others have three times more. This dysregulation could also be the case of other superoxide dismutase proteins in the absence of DAF-16. Moreover, numerous studies have shown that the altered expression of oxidative stress protection genes (superoxide dismutases and catalases) have no effect in the lifespan of worms (Honda, Tanaka, & Honda, 2008; Matyash et al., 2004; Raamsdonk & Hekimi, 2009; Yang, Li, & Hekimi, 2007; Yen, Patel, Lublin, & Mobbs, 2009) and mice (Huang, Carlson, Gillespie, Shi, & Epstein, 2017; Pérez et al., 2009). However, the expression of *psod-3::GFP* should be analysed in *Klotho* mutations in combination with *daf-2* and *daf-16* mutations to reveal potential synergic relations observed in lifespan and stress resistance.

In addition, previous studies have found that levels of another superoxide dismutase, SOD-2, were not altered in *Klotho* deficient mutant mice nor in mice which had 1-fold increase in *Klotho* expression (Yamamoto et al., 2005), the same way that *Klotho* mutant worms studied in this thesis had no altered levels of *sod-3* reporter expression. Another study has shown that *sod-2* deletion extends lifespan in worms (Raamsdonk & Hekimi, 2009), contradicting the oxidative damage theory. Considering all the apparent contradictory studies relating the oxidative stress and lifespan, further research has to be done to unveil the role of oxidative protection genes in health and to redefine a new oxidative damage theory.

4.4 Klotho as regulator of lipid metabolism and starvation

4.4.1 Klotho proteins are needed for the utilization of lipids as energy source during fasting

In mice, Klotho has been shown to be involved in energy metabolism by interacting with insulin/IGFR (Kurosu et al., 2005) and regulated by PPAR γ (Zhang et al., 2008). In humans, Klotho levels in plasma have been found to be decreased in anorexia and obesity, and *Klotho* deficient mice have reduced amounts of adipose tissue and are resistant to high-fat diet induced obesity (Amitani et al., 2013; Razzaque, 2012). In *C. elegans*, *klo-1* and *klo-2* are both expressed in the intestine (Polanska et al., 2011), which is the major organ used by worms to store the lipid droplets. It was hypothesised that *Klotho* mutant worms might have dysregulation of lipid metabolism presenting higher or lower quantities of stored fats.

The expression of *pklo-1::RFP* and *pklo-2::GFP* reporters were increased upon starvation in wild type worms, indicating that the transcription of *Klotho* genes is induced in starvation and that Klotho is involved in the regulation of energy metabolism in a critical scenario of food deprivation.

For the observation and quantification of lipid droplets in intestine and hypodermis (Kimura et al., 1997) Sudan Black B (SBB) dye in paraformaldehyde fixed worms was used initially. SBB staining was repeated multiple times without consistent results and it was finally discarded as a possible method to quantify the amount of lipids in wild type and *Klotho* mutant worms. Also, the morphology of the worms was affected likely due to the fixation and permeabilization process.

Another two dyes were used for the staining of fats, Nile red and Oil-red-O. Nile red dye was simply added to the *E. coli* containing NGM media and the animals were observed alive, while Oil-red-O dye was used in paraformaldehyde fixed animals. Contrary to observations in mice (Razzaque, 2012), no differences in the fat content were observed between wild type and *Klotho* mutant worms irrespective of the staining procedure used.

However, food deprivation caused differences in the amount of lipids visualised by Oil-red-O and Nile red. Starved wild type worms presented a ~40 % reduction and starved *Klotho* double mutants a 15 % reduction of Oil-red-O stained fats. Upon starvation, the amount of Oil-red-O stained lipids was significantly reduced in both strains as compared to fed status. However, the reduction of Oil-red-O lipids was significantly less in *Klotho* double mutant worms than in wild type worms. These results indicate that KLO-1 and KLO-2 might be necessary for the utilisation of lipids as energy source in a situation when food is deprived.

The results using Nile red to detect lipids in starved versus fed worms contrasted the ones obtained with the use of Oil-red-O. Wild type worms had similar amount of Nile red staining in standard feeding conditions and after starvation. *Klotho* double mutant worms had a 30 % reduction of Nile red stained fats after starvation, although the difference was not statistically significant. The fact that Nile red staining was not decreased upon starvation in wild type worms was in conflict to the fact that the starved worms were thinner as compared to well fed worms (Figure 31). Previous studies have proposed that Nile red stains lysosome-related organelles which are not the main fat storage compartment (O'Rourke et al., 2009). This could explain why the Nile red staining was not affected by feeding status. Overall, the results using Oil-red-O are probably more reliable for the detection of lipids. Nevertheless, further research should be carried out to quantify the fat contents of the worms by HPLC or mass spectrometry.

4.4.2 Relation between *Klotho* and lipid metabolism proteins ATGL-1 and FAT-7

The expression of two key proteins involved in the lipid metabolism, ATGL-1 and FAT-7, was analysed to observe possible alterations of their expression in *Klotho* mutant worms and in conditions of food deprivation. The adipose triglyceride lipase (ATGL-1) was selected because it is expressed at the surface of lipid droplets allowing estimation of the quantities of these droplets and is involved in the utilisation of lipids in starvation (J. H. Lee et al., 2014; Villena, Roy, Sarkadi-

Nagy, Kim, & Sul, 2004). The desaturase FAT-7 protein was selected because it is regulated by insulin pathway (by DAF-2 and DAF-16) (Horikawa & Sakamoto, 2010; Murphy et al., 2003) and the expression of *fat-7* reporter gene is decreased tenfold in fasting adult worms (Van Gilst et al., 2005).

The levels of ATGL-1::GFP were not altered in single or double *Klotho* mutant worms compared to wild type. This result corroborates a previous study by Tomiyana et al., in which β -*Klotho* defective mice had no altered levels of ATGL-1 (Tomiyama et al., 2010), although in *fgf-21* defective mice the levels of ATGL-1 were reduced to half as compared to wild type mice (Hotta et al., 2009). This suggests that *Klotho* cofactor is not essential for the regulation of ATGL-1 by FGF21 in mammals or by EGL-17 and/or LET-756 in worms.

In contrast, *fat-7*::GFP levels were significantly decreased in *klo-1* mutant worms and a trend of reduction was observed in *klo-2* mutant worms, suggesting that Klothos regulate *fat-7* expression. As it has been previously discussed, DAF-16 is involved in the transcription regulation of several genes. This means that the increased activity of DAF-16 caused by *Klotho* knockout may not be the only factor regulating the transcription of *fat-7*, *atgl-1*, *sod-3*, genes for extension of lifespan, etc. Although DAF-16 is the key player, and thus it was the selected factor to study in this work, other factors have to be studied to understand the regulation of the metabolism discussed in this thesis.

The expression of *atgl-1* and *fat-7* was also studied in conditions of food deprivation. Previous study showed that in the absence of food, the levels of ATGL-1::GFP were increased (J. H. Lee et al., 2014). However, in this thesis work, no differences were observed in the levels of ATGL-1::GFP in starved wild type or *Klotho* mutant worms, although the intestine of the starved worms was evidently thinner. It is worth to consider that the same authors indicate that *atgl-1* mRNA levels are not affected in starvation (J. H. Lee et al., 2014). On the other hand, the levels of *fat-7*::GFP were significantly decreased up to 80 % in the int1 intestinal cells in starved worms without

differences between wild type and *Klotho* mutant worms. This is in agreement with previous study reporting significantly decreased levels of *fat-7* mRNA in starved worms (J. H. Lee et al., 2014). *Klotho* deficiency did not alter gene expression of *fat-7::GFP* in comparison to wild type worms in starved or fed conditions. The effect of *Klotho* deficiency should be assessed directly on the activity of FAT-7 and ATGL-1 proteins to know if there is a more direct metabolic interaction.

4.4.3 *Klotho* proteins help the worms to use cholesterol

In mice, β -*Klotho* facilitates FGF-15 (homolog to human FGF-19) activation of FGFR4 which initiates a signalling cascade that represses *Cyp7a* mRNA and the synthesis of bile acids from cholesterol (Inagaki et al., 2005; Ito et al., 2005; Jones, 2012). Worms are cholesterol auxotrophs and, unlike humans, they have to obtain cholesterol from the diet. Worms metabolise cholesterol into bile acid-like steroid, called the dafachronic acid, which has been shown to regulate DAF-12 (steroid hormone receptor) which in turn regulates DAF-16 (Groen & Kuipers, 2013; Magner et al., 2013; Matyash et al., 2004). Therefore, cholesterol interacts with components of Insulin/IGF-1 signalling to regulate dauer stage. It was hypothesised that KLO-1 and/or KLO-2 could also affect the metabolism of cholesterol in worms. In consequence, removal of cholesterol from the diet would affect the brood size, development of the progeny and lifespan of *Klotho* mutant worms less than that of wild type worms.

In the absence of cholesterol, viable progeny was highly reduced in *Klotho* mutant worms as compared to wild type worms. The F2D1 (second generation of worms laid on the first day of F1 fertile life) *Klotho* mutant mothers were especially affected and had a significantly reduced F3 brood size. As observed in this thesis and in previous studies, the worm cell membranes do not appear to need cholesterol in the same amounts as it is needed in cell membrane structure of mammals (Matyash et al., 2001, 2004). Instead, a few generations of worms are able to grow without any other source of cholesterol than the small proportion received from the original P₀ mother to the F1 at the embryo stage.

Lifespan was also measured in the absence of cholesterol and opposite to what was expected, *Klotho* mutant worms were more affected by cholesterol depletion. The lifespan of *Klotho* mutant worms was significantly more reduced than that of wild type worms. Previous study has shown that *Klotho* defective mice had increased and unregulated levels of bile acid synthesis (Ito et al., 2005). Hence it was expected that in the absence of cholesterol, *Klotho* mutants will be more efficient in utilising the remaining cholesterol of their body to produce other necessary sterols like dafrachronic acid. However, both progeny viability and lifespan suggest that *Klotho* mutations were not beneficial for the worms when external cholesterol is not available.

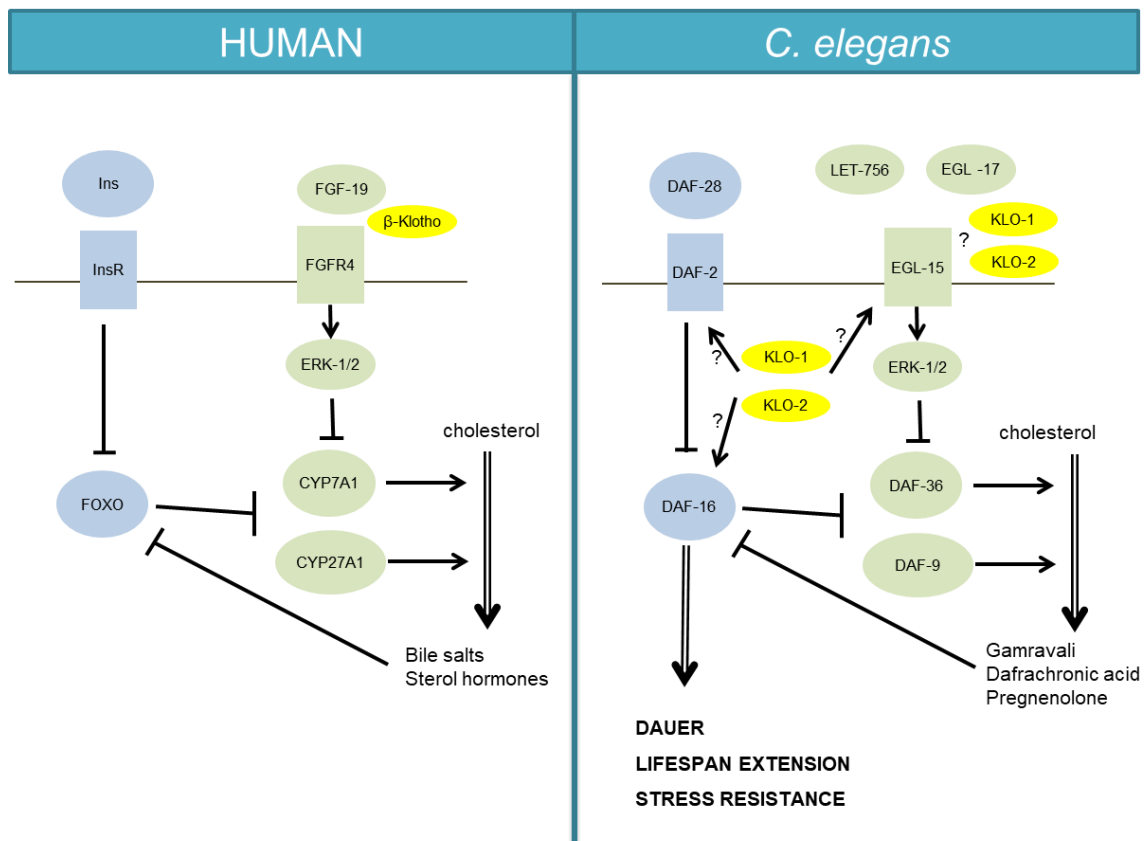


Figure 42 Human and worm metabolism of cholesterol.

β -Klotho is involved in the cross-talk interaction between FGF and IIS pathways to regulate cholesterol metabolism. Arrows indicate activation and "T" shape lines indicate inhibition. Double arrow indicates a transformation.

Recent studies have shown that β -*Klotho* deficiency in mice protects against obesity by inducing cholesterol metabolism (Somm et al., 2017). β -Klotho induces the production of sterol hormones because CYP7A1 and CYP8B1 are no longer repressed. The sterol hormones activate brown fat TGR5 receptor to enhance thermogenesis (Chen et al., 2017; Kolumam et al., 2015; Somm et al., 2017). Although this mechanism of burning calories prevents obesity, it also increases metabolic rate. A higher metabolic rate could explain why *Klotho* mutant worms have shorter lifespan than wild type worms in cholesterol free diets. However, the metabolic rate was not measured directly, and further research should be performed to prove this hypothesis.

4.5 Final conclusions and summary

Different phenotypic and physiological features have been assessed in this thesis work to provide a broader view of the role of *klo-1* and *klo-2* in the energy metabolism. The results obtained using deletion mutations of *klo-1* and *klo-2* individually, together or in combination with hypomorphic mutations of *daf-2* and *daf-16*, provide a better understanding. The phenotypic and physiological effects observed in the mutant worms suggest potential interactions between metabolic pathways affected by *klo-1* and *klo-2*.

The main phenotypic alterations observed in this work (summarised in the Table 18) caused by *klo-2* deficiency (*ok1862* mutation) were lifespan elongation and improved resistance to heat stress. Both parameters were also further improved in synergy between *klo-2(ok1862)* and *daf-2(e1370)* mutations. In the case of *klo-1* deficiency (*ok2925* mutation) the main phenotypic alteration caused was an improved survival to oxidative stress.

Lifespan extension and stress resistance caused by *Klotho* could be closely related supporting the extended theory that ageing is an oxidation process. Both cases could also be a consequence of a downregulated metabolism which has a better buffering effect for the reactive oxygen species

(ROS). This would not be because the quantity of antioxidants is increased (at least SOD-3 was not altered) in *Klotho* mutants, but because there were less ROS produced if the metabolism is downregulated causing the basal quantity of antioxidants used to be lower. In consequence, it would cause worms to have also an extended lifespan.

Other changes observed included synergistic effect of both *Kloths* with *daf-2* to extend lifespan, reduced progeny caused by *klo-2* and *klo-1* deficiency, delayed development of *daf-2 klo-1* mutants compared to *daf-2* mutants and shortened lifespan of *klo-2 klo-1* mutants in the absence of cholesterol. Moreover, glucose and hypomorphic *daf-16* mutation have been shown to regulate all the phenotypic alterations caused by *klo-1*, *klo-2* and *daf-2* mutations, strongly suggesting that the alterations are linked to IIS pathway and dependent of DAF-16/FOXO activity.

The findings observed by *klo-1(ok2925)* and/or *klo-2(ok1862)* deletion alleles, plus the synergic effects with *daf-2* deficiency, are similar to the effects caused by *rsks-1(ok1255)* deletion allele. *C. elegans* RSKS-1 (homolog to mammalian S6K) inhibits AAK-2 (homolog to mammalian AMPK α) to activate DAF-16/FOXO. *rsks-1(ok1255)* mutant worms have a mean lifespan extension of 1-2 days, however the main effect is observed in synergy with *daf-2(e1370)*, when *daf-2 rsks-1* double mutants have a mean lifespan more than four times longer than wild type and double than *daf-2* mutant worms (Chen et al., 2013). These results of *rsks-1* deletion mirror the observations of lifespan extension by one day caused by *klo-2(ok1862)* deletion and the extension of mean lifespan to triple in *daf-2 klo-2* mutants compared to wild type. Moreover, *rsks-1* deletion increases the resistance to oxidant agent paraquat (Chen et al., 2013), similarly to what was observed for *klo-1* deletion.

Table 18 Main phenotypic alterations observed

	phenotypic feature	strains performance	comments
lifespan	standard NGM	wt<klo-2<daf-2<daf-2 Klothos<daf-2 klo-2	synergistic effect of <i>daf-2(e1370)</i> and <i>klo-2(ok1862)</i> extends lifespan triple compared to wild type
	2% glucose	wt(NGM)=daf-2<daf-2 Klothos	any <i>Klotho</i> mutation in combination with <i>daf-2(e1370)</i> lived 28-30 days (wt in standard conditions live 20 days)
progeny	standard NGM	wt>Klothos>daf-2>daf-2 Klothos	reducing trend in <i>Klotho</i> double mutants
	2% glucose	wt=daf-2=daf-2 Klothos=daf-16	glucose regulates progeny production to ~200 eggs
development		wt=Klothos>daf-2=daf-2 klo-2>daf-2 klo-1	<i>Klotho</i> trend to retard development. Further development retardation in <i>daf-2 klo-1</i> double mutants
resistance to	oxidative stress	wt=klo-2=klo-2 klo-1=daf-16<daf-2 Klothos<daf-2=daf-2 klo-2=daf-2 klo-1<<klo-1	<i>klo-1</i> mutation enhances resistance to oxidation better than in combination with <i>daf-2</i> mutation
	heat stress	1. wt=klo-1=klo-2 klo-1<klo-2=daf-2<daf-2 klo-2	<i>klo-2</i> mutation enhances resistance to heat stress; synergistic effect of <i>daf-2(e1370)</i> and <i>klo-2(ok1862)</i> enhances resistance to heat stress
lipid storage		wt=Klothos	no differences observed
in cholesterol absence	lifespan	2. wt (NGM)>wt>klo-2 klo-1	cholesterol shortens lifespan of the worms; even shorter for <i>klo-2 klo-1</i> double mutants
	progeny	wt=Klothos	<i>klo-2 klo-1</i> double mutants less progeny than wt (no significant)

Mammalian *Klotho*s have been shown to interact with FGF/FGFRs to regulate the activity of AMPK α . The *C. elegans* orthologs EGL-15/FGFR and EGL-17 or LET756/FGFs also activate AAK-2/AMPK α . By homology to mammals and by phenotypic similarity to *rsks-1* deletion mutants it is suggested that KLO-1 and KLO-2 interact with EGL-15 protein directly or downstream the FGFR pathway and depend on the activity of AAK-2 to enhance lifespan extension and stress resistance (Figure 43 case 2). In addition, it is also possible that KLO-1 and/or KLO-2 interact downstream AAK-2, with SIR-2/SIRT-1 or HSF-1 which have been also shown to regulate lifespan and stress response by interacting with DAF-16/FOXO (Bamps, Wirtz, Savory, Lake, & Hope,

2009; Chau et al., 2010; Raynes, Leckey, Nguyen, & Westerheide, 2012; Tissenbaum & Guarente, 2001; Westerheide et al., 2009) (Figure 43 case 2).

During the discussion it has been proposed that effects caused by *klo-2(ok1862)* were KLO-1 dependant. To explain this relation between KLO-1 and KLO-2, it was proposed that KLO-1 was inhibiting an unknown “protein X” and inducing the activity of KLO-2 by activating the “protein X” that in turn inhibits DAF-16/FOXO (Figure 37). Because *rsk-1* inhibits the activity of DAF-16 and because of the effects observed in *rsk-1* deletion mutant worms, it may be possible that the “protein X” is in fact the protein RSKS-1 (Figure 43 case 3). Although, double and triple deletion mutants of *klo-1*, *klo-2* and *rsk-1* should be done to know if they work upstream or downstream the same pathway and direct protein-protein interaction should be confirmed.

Also, it is proposed that KLO-1 and KLO-2 interact directly with DAF-2/InsR, because it has been shown in mammals that Klotho regulates the autophosphorylation of InsR (Unger, 2006). The proposed model for the activity of KLO-1 and KLO-2 (Figure 37) was more complete and respond better to the phenotypes observed if there was a direct regulation of DAF-2 or its downstream pathway (Figure 43 case 1).

All the phenotypic alterations caused by *klo-1* and/or *klo-2* deletions have provided a broader view of all the possible relations that Klotho proteins could have out of the more studied relation with FGFs and FGFRs. It has not been possible to do an exact match between KLO-1 and KLO-2 worm proteins to the Klotho mammal proteins. The comparisons between worm and mammalian Klotho proteins done in this thesis have been done with α - and β -Klotho, because are the most studied ones. α -Klotho was the first of the Klotho proteins to be discovered and subsequently β -Klotho has been studied. However, KLO-1 and KLO-2 worm proteins are half the size of the mammal orthologs consisting of only one KL1 domain and not having a transmembrane domain. All these together may affect the functional disparity between these orthologs and it is proposed

that KLO-1 and KLO-2 may be more similar to alternatively spliced α -Klotho or the newly discovered γ -Klotho, the functions of which are largely unknown in mammals.

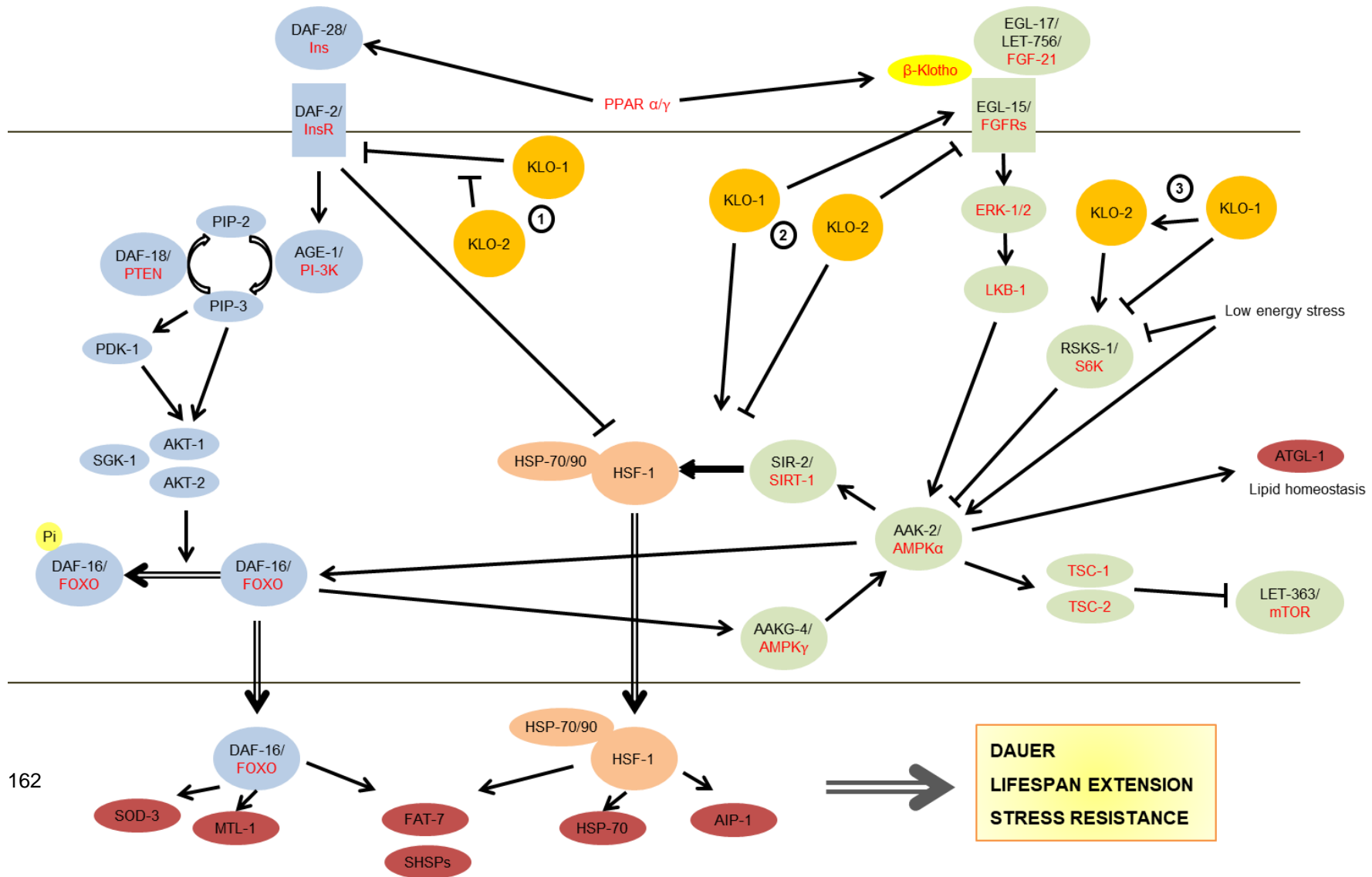


Figure 43 Summary of metabolic interactions described.

Proteins involved in IIS pathway are coloured in blue and proteins downstream β -Klotho/FGF/FGFR interaction are coloured in green. Both pathways regulate DAF-16 activity and the transcription of multiple target genes (coloured in garnet). HSF-1 could also be activated by FGF signalling to induce transcription of multiple genes, and together with DAF-16 could cause dauer formation, lifespan extension or stress resistance. Three proposed models for KLO-1 and KLO-2 activities are specified by numbers (1, 2 and 3). Arrows indicate activation and "T" shape lines indicate inhibition. Double arrow indicates a transformation.

Bibliography

- Ailion, M., & Thomas, J. H. (2000). Dauer Formation Induced by High Temperatures in *Caenorhabditis elegans*. *Genetics Society of America*, 156, 1047–1067.
- Amitani, M., Asakawa, A., Amitani, H., Kaimoto, K., Sameshima, N., Koyama, K. I., ... Inui, A. (2013). Plasma klotho levels decrease in both anorexia nervosa and obesity. *Nutrition*, 29(9), 1106–1109. <http://doi.org/10.1016/j.nut.2013.02.005>
- An, J. H., & Blackwell, T. K. (2003). SKN-1 links *C. elegans* mesendodermal specification to a conserved oxidative stress response. *Genes and Development*, 17, 1882–1893. <http://doi.org/10.1101/gad.1107803>
- Anderson, E. N., Corkins, M. E., Li, J. C., Singh, K., Parsons, S., Tucey, T. M., ... Hart, A. C. (2016). *C. elegans* lifespan extension by osmotic stress requires FUDR, base excision repair, FOXO, and sirtuins. *Mechanisms of Ageing and Development*. <http://doi.org/10.1016/j.mad.2016.01.004>
- Antebi, A. (2015). Nuclear receptor signal transduction in *C. elegans*. *WormBook*, Ed. *The C. Elegans Research Community*, *WormBook*. <http://doi.org/10.1895/wormbook.1>.
- Araya, K., Fukumoto, S., Backenroth, R., Takeuchi, Y., Nakayama, K., Ito, N., ... Fujita, T. (2005). A novel mutation in fibroblast growth factor 23 gene as a cause of tumoral calcinosis. *J Clin Endocrinol Metab*, 90, 5523–5527. <http://doi.org/10.1210/jc.2005-0301>
- Ashrafi, K., Chang, F. Y., Watts, J. L., Fraser, A. G., Kamath, R. S., Ahringer, J., & Ruvkun, G. (2003). Genome-wide RNAi analysis of *Caenorhabditis elegans* fat regulatory genes. *Nature*, 421, 268–272.
- Avery, L. (1993). Motor neuron M3 controls pharyngeal muscle relaxation timing in *Caenorhabditis elegans*. *The Journal of Experimental Biology*, 175, 283–97.
- Avery, L., & You, Y. J. (2012). *C. elegans* feeding. *WormBook*, 1–23. <http://doi.org/10.1895/wormbook.1.150.1>
- Avruch, J. (1998). Insulin signal transduction through protein kinase cascades. *Molecular and Cellular Biochemistry*, 182, 31–48. http://doi.org/10.1007/978-1-4615-5647-3_4
- Babar, P., Adamson, C., Walker, G. A., Walker, D. W., & Lithgo, G. J. (1999). PI3-kinase inhibition induces dauer formation, thermotolerance and longevity in *C. elegans*☆. *Neurobiology of Aging*, 20(5), 513–519. [http://doi.org/10.1016/S0197-4580\(99\)00094-9](http://doi.org/10.1016/S0197-4580(99)00094-9)
- Badman, M. K., Pissios, P., Kennedy, A. R., Koukos, G., Flier, J. S., & Maratos-Flier, E. (2007). Hepatic Fibroblast Growth Factor 21 Is Regulated by PPARα and Is a Key Mediator of Hepatic Lipid Metabolism in Ketotic States. *Cell Metabolism*, 5(6), 426–437. <http://doi.org/10.1016/J.CMET.2007.05.002>
- Bamps, S., Wirtz, J., Savory, F. R., Lake, D., & Hope, I. A. (2009). The *Caenorhabditis elegans* sirtuin gene, sir-2.1, is widely expressed and induced upon caloric restriction. *Mechanisms of Ageing and Development*, 130(11–12), 762–770. <http://doi.org/10.1016/j.mad.2009.10.001>
- Bartke, A. (2008). Insulin and aging. *Cell Cycle*, 7(21), 3338–3343. <http://doi.org/10.4161/cc.7.21.7012>

- Baxi, K., Ghavidel, A., Waddell, B., Harkness, T. A., & Carvalho, C. E. de. (2017). Regulation of lysosomal function by the DAF-16 Forkhead transcription factor couples reproduction to aging in *C. elegans*. *Genetics*, 207(September), Early Online. <http://doi.org/10.1534/genetics.117.204222>
- Bell, S., & Wolff, S. (1964). Studies on the mechanism of the effect of fluorodeoxyuridine on chromosomes. *Anal. Biochem. J. Mol. Biol*, 51(3), 66–161.
- Berglund, E. D., Li, C. Y., Bina, H. A., Lynes, S. E., Michael, M. D., Shanafelt, A. B., ... Wasserman, D. H. (2009). Fibroblast growth factor 21 controls glycemia via regulation of hepatic glucose flux and insulin sensitivity. *Endocrinology*, 150(9), 4084–4093. <http://doi.org/10.1210/en.2009-0221>
- Bloch, L., Sineshchekova, O., Reichenbach, D., Reiss, K., Saftig, P., Kuro-o, M., & Kaether, C. (2009). Klotho is a substrate for alpha-, beta- and gamma-secretase. *FEBS Lett*, 583, 3221–3224. <http://doi.org/10.1016/j.febslet.2009.09.009>
- Bluher, M., Kahn, B. B., & Kahn, C. R. (2003). Extended Longevity in Mice Lacking the Insulin Receptor in Adipose Tissue. *Science*, 299(5606), 572–574. <http://doi.org/10.1126/science.1078223>
- Brenner, S. (1974). The genetics of *Caenorhabditis elegans*. *Genetics*, 77, 71–94.
- Brock, T. J., Browse, J., & Watts, J. L. (2006). Genetic regulation of unsaturated fatty acid composition in *C. elegans*. *PLoS Genetics*, 2(7), 0997-1005. <http://doi.org/10.1371/journal.pgen.0020108>
- Brown-Borg, H. M., Borg, K. E., Meliska, C. J., & Bartke, A. (1996). Dwarf mice and the ageing process. *Nature*. <http://doi.org/10.1038/384033a0>
- Brunet, A., Park, J., Tran, H., Hu, L. S., Hemmings, B. A., & Greenberg, M. E. (2001). Protein kinase SGK mediates survival signals by phosphorylating the forkhead transcription factor FKHRL1 (FOXO3a). *Molecular and Cellular Biology*, 21(3), 952–65. <http://doi.org/10.1128/MCB.21.3.952-965.2001>
- Bulow, H. E., Boulin, T., & Hobert, O. (2004). Differential Functions of the *C. elegans* FGF Receptor in Axon Outgrowth and Maintenance of Axon Position. *Neuron*, 42(3), 367–374. [http://doi.org/10.1016/S0896-6273\(04\)00246-6](http://doi.org/10.1016/S0896-6273(04)00246-6)
- Burdine, R. D., Chen, E. B., Kwok, S. F., & Stern, M. J. (1997). egl-17 encodes an invertebrate fibroblast growth factor family member required specifically for sex myoblast migration in *Caenorhabditis elegans*. *Proc Natl Acad Sci U S A*, 94, 2433–2437.
- Byerly, L., Cassada, R. C., & Russell, R. L. (1976). The life cycle of the nematode *Caenorhabditis elegans*. I. Wild-type growth and reproduction. *Dev Biol*, 51, 23–33.
- C.Mello, C., M.Kramer, J., Stinchcomb, D., & Ambros, V. (1991). Efficient gene transfer in *C.elegans*: extrachromosomal maintenance and integration of transforming sequences. *The EMBO Journal*, 10(12), 3959–3970.
- Cassada, R. C., & Russell, R. L. (1975). The dauerlarva, a post-embryonic developmental variant of the nematode *Caenorhabditis elegans*. *Developmental Biology*, 46(2), 326–342. [http://doi.org/10.1016/0012-1606\(75\)90109-8](http://doi.org/10.1016/0012-1606(75)90109-8)
- Cha, S. K., Ortega, B., Kurosu, H., Rosenblatt, K. P., Kuro, O. M., & Huang, C. L. (2008). Removal of sialic acid involving Klotho causes cell-surface retention of TRPV5 channel via binding to galectin-1. *Proc Natl Acad Sci U S A*, 105, 9805–9810. <http://doi.org/10.1073/pnas.0803223105>

- Chalfie, M., Tu, Y., Euskirchen, G., Ward, W. W., & Prasher, D. C. (1994). Green fluorescent protein as a marker for gene expression. *Science*, 263, 802–805. <http://www.ncbi.nlm.nih.gov/pubmed/8303295>
- Chandler-Brown, D., Choi, H., Park, S., Ocampo, B. R., Chen, S., Le, A., ... Kaeberlein, M. (2015). Sorbitol treatment extends lifespan and induces the osmotic stress response in *Caenorhabditis elegans*. *Frontiers in Genetics*, 6(OCT), 1–9. <http://doi.org/10.3389/fgene.2015.00316>
- Chang, Q., Hoefs, S., van der Kemp, A. W., Topala, C. N., Bindels, R. J., & Hoenderop, J. G. (2005). The beta-glucuronidase klotho hydrolyzes and activates the TRPV5 channel. *Science*, 310, 490–493. <http://doi.org/10.1126/science.1114245>
- Château, M., Araiz, C., Descamps, S., & Galas, S. (2010). Klotho interferes with a novel FGF-signalling pathway and insulin/Igf-like signalling to improve longevity and stress resistance in *Caenorhabditis elegans*. *AGING*, 2(9).
- Chau, M. D. L., Gao, J., Yang, Q., Wu, Z., & Gromada, J. (2010). Fibroblast growth factor 21 regulates energy metabolism by activating the AMPK-SIRT1-PGC-1alpha pathway. *Proceedings of the National Academy of Sciences of the United States of America*, 107(28), 12553–8. <http://doi.org/10.1073/pnas.1006962107>
- Chen, Chang, J. C., Zavala-Solorio, J., Kates, L., Thai, M., Ogasawara, A., ... Sonoda, J. (2017). FGF21 mimetic antibody stimulates UCP1-independent brown fat thermogenesis via FGFR1/βKlotho complex in non-adipocytes. *Molecular Metabolism*, 6(11), 1454–1467. <http://doi.org/10.1016/j.molmet.2017.09.003>
- Chen, D., Li, P. W. L., Goldstein, B. A., Cai, W., Thomas, E., Chen, F., ... Kapahi, P. (2013). Germline Signaling Mediates the Synergistically Prolonged Longevity Produced by Double Mutations in *daf-2* and *rsks-1* in *C.elegans*. *Cell Reports*. <http://doi.org/10.1016/j.celrep.2013.11.018>
- Chen, Podvin, S., Gillespie, E., Leeman, S. E., & Abraham, C. R. (2007). Insulin stimulates the cleavage and release of the extracellular domain of Klotho by ADAM10 and ADAM17. *Proc Natl Acad Sci U S A*, 104, 19796–19801. <http://doi.org/10.1073/pnas.0709805104>
- Cheong, M. C., Na, K., Kim, H., Jeong, S.-K., Joo, H.-J., Chitwood, D. J., & Paik, Y.-K. (2011). A potential biochemical mechanism underlying the influence of sterol deprivation stress on *Caenorhabditis elegans* longevity. *The Journal of Biological Chemistry*, 286(9), 7248–56. <http://doi.org/10.1074/jbc.M110.189183>
- Clancy, D. J., Gems, D., Harshman, L. G., Oldham, S., Stocker, H., Hafen, E., ... Partridge, L. (2001). Extension of life-span by loss of CHICO, a *Drosophila* insulin receptor substrate protein. *Science*, 292(5514), 104–106. <http://doi.org/10.1126/science.1057991>
- Clark, S. G., Lu, X., & Horvitz, H. R. (1994). The *Caenorhabditis elegans* Locus *lin-15*, a Negative Regulator of a Tyrosine Kinase Signaling Pathway, Encodes Two Different Proteins. *Genetics Society of America*, 137, 987–997.
- Cohen, S. S., Flacks, J. G., Barner, H. D., Loeb, M. R., & Lichtenstein, J. (1958). The mode of action of 5-fluorouracil and its derivatives. *Proceedings of the National Academy of Sciences*, 44(10), 1004–1012.
- Corsi, A. K., Wightman, B., & Chalfie, M. (2015). A Transparent window into biology: A primer on *Caenorhabditis elegans*. *WormBook*, 1–31. <http://doi.org/10.1895/wormbook.1.177.1>
- Coskun, T., Bina, H. A., Schneider, M. A., Dunbar, J. D., Hu, C. C., Chen Moller, D. E., Y., & Kharitononkov,

- A. (2008). Fibroblast growth factor 21 corrects obesity in mice. *Endocrinology*, *149*, 6018–6027. <http://doi.org/10.1210/en.2008-0816>
- Culetto, E., & Sattelle, D. B. (2000). A role for *Caenorhabditis elegans* in understanding the function and interactions of human disease genes. *Human Molecular Genetics*, *9*(6), 869–877. <http://doi.org/10.1093/hmg/9.6.869>
- DeVore, D. L., Horvitz, H. R., & Stern, M. J. (1995). An FGF receptor signaling pathway is required for the normal cell migrations of the sex myoblasts in *C. elegans* hermaphrodites. *Cell*, *83*, 611–620. <http://www.ncbi.nlm.nih.gov/pubmed/7585964>
- Doncaster, C. C. (1962). Nematode Feeding Mechanisms. 1. Observations On Rhabditis and Pelodera. *Nematologica*, *8*(4), 313–320. <http://doi.org/10.1163/187529262X00125>
- Dong, J. Q., Rossulek, M., Somayaji, V. R., Baltrukonis, D., Liang, Y., Hudson, K., ... Calle, R. A. (2015). Pharmacokinetics and pharmacodynamics of PF-05231023, a novel long-acting FGF21 mimetic, in a first-in-human study. *British Journal of Clinical Pharmacology*, *80*(5), 1051–1063. <http://doi.org/10.1111/bcp.12676>
- Dorman, J. B., Albinder, B., Shroyer, T., & Kenyon, C. (1995). The age-1 and daf-2 genes function in a common pathway to control the lifespan of *Caenorhabditis elegans*. *Genetics*, *141*, 1399–1406.
- Duncan, R. E., Ahmadian, M., Jaworski, K., Sarkadi-Nagy, E., & Sul, H. S. (2007). Regulation of Lipolysis in Adipocytes. *Annual Review of Nutrition*, *27*(1), 79–101. <http://doi.org/10.1146/annurev.nutr.27.061406.093734>
- Essers, M. A. G., De Vries-Smits, L. M. M., Barker, N., Polderman, P. E., Burgering, B. M. T., & Korswagen, H. C. (2005). Functional Interaction Between b-Catenin and FOXO in Oxidative Stress Signaling. *Science*, *308*, 1181–1184. <http://doi.org/10.1126/science.1109083>
- Eswarakumar, V. P., Lax, I., & Schlessinger, J. (2005). Cellular signaling by fibroblast growth factor receptors. *Cytokine Growth Factor Rev*, *16*, 139–149. <http://doi.org/10.1016/j.cytogfr.2005.01.001>
- Fisher, F. M., Estall, J. L., Adams, A. C., Antonellis, P. J., Bina, H. A., Flier, J. S., ... Maratos-Flier, E. (2011). Integrated regulation of hepatic metabolism by fibroblast growth factor 21 (FGF21) in vivo. *Endocrinology*, *152*(8), 2996–3004. <http://doi.org/10.1210/en.2011-0281>
- Foltz, I. N., Hu, S., King, C., Wu, X., Yang, C., Wang, W., ... Li, Y. (2012). Treating diabetes and obesity with an FGF21-mimetic antibody activating the betaKlotho/FGFR1c receptor complex. *Sci Transl Med*, *4*, 162ra153. <http://doi.org/10.1126/scitranslmed.3004690>
- Franco, O. H., Steyerberg, E. W., Hu, F. B., Mackenbach, J., & Nusselder, W. (2007). Associations of diabetes mellitus with total life expectancy and life expectancy with and without cardiovascular disease. *Archives of Internal Medicine*, *167*(11), 1145–1151. <http://doi.org/10.1001/archinte.167.11.1145>
- Fukai, T., Folz, R. J., Landmesser, U., & Harrison, D. G. (2002). Extracellular superoxide dismutase and cardiovascular disease. *Cardiovasc Res*, *55*(2), 239–249. [http://doi.org/10.1016/S0008-6363\(02\)00328-0](http://doi.org/10.1016/S0008-6363(02)00328-0)
- Gaglia, M. M., & Kenyon, C. (2009). Stimulation of movement in a quiescent, hibernation-like form of *Caenorhabditis elegans* by dopamine signaling. *J Neurosci*, *29*, 7302–7314. <http://doi.org/10.1523/JNEUROSCI.3429-08.2009>

- Gaich, G., Chien, J. Y., Fu, H., Glass, L. C., Deeg, M. A., Holland, W. L., ... Moller, D. E. (2013). The Effects of LY2405319, an FGF21 Analog, in Obese Human Subjects with Type 2 Diabetes. *Cell Metabolism*, 18(3), 333–340. <http://doi.org/10.1016/J.CMET.2013.08.005>
- Garigan, D., Hsu, A. L., Fraser, A. G., Kamath, R. S., Abringet, J., & Kenyon, C. (2002). Genetic analysis of tissue aging in *Caenorhabditis elegans*: A role for heat-shock factor and bacterial proliferation. *Genetics*, 161(3), 1101–1112.
- Gems, D., & Doonan, R. (2009). Antioxidant defense and aging in *C. elegans*: Is the oxidative damage theory of aging wrong? *Cell Cycle*, 8(11), 1681–1687. <http://doi.org/10.4161/cc.8.11.8595>
- Gems, D., & Riddle, D. L. (2000). Genetic, behavioral and environmental determinants of male longevity in *Caenorhabditis elegans*. *Genetics*, 154(4), 1597–1610. <http://doi.org/10.1093/gerona/gls088>
- Gems, D., Sutton, A. J., Sundermeyer, M. L., Albert, P. S., King, K. V., Edgley, M. L., ... Riddle, D. L. (1998). Two pleiotropic classes of *daf-2* mutation affect larval arrest, adult behavior, reproduction and longevity in *Caenorhabditis elegans*. *Genetics*, 150(1), 129–155. <http://doi.org/10.1139/z78-244>
- Goetz, R., Ohnishi, M., Ding, X., Kurosu, H., Wang, L., Akiyoshi, J., ... Mohammadi, M. (2012). Klotho coreceptors inhibit signaling by paracrine fibroblast growth factor 8 subfamily ligands. *Mol Cell Biol*, 32, 1944–1954. <http://doi.org/10.1128/MCB.06603-11>
- Golden, J. W., & Riddle, D. L. (1984). The *Caenorhabditis elegans* dauer larva: Developmental effects of pheromone, food, and temperature. *Developmental Biology*, 102(2), 368–378. [http://doi.org/10.1016/0012-1606\(84\)90201-X](http://doi.org/10.1016/0012-1606(84)90201-X)
- Gottlieb, S., & Ruvkun, G. (1994). *daf-2*, *daf-16* and *daf-23*: Genetically Interacting Genes Controlling Dauer Formation in *Caenorhabditis elegans*. *Genetics*, 137(1), 107–120.
- Granneman, J. G., Moore, H.-P. H., Mottillo, E. P., Zhu, Z., & Zhou, L. (2011). Interactions of perilipin-5 (Plin5) with adipose triglyceride lipase. *The Journal of Biological Chemistry*, 286(7), 5126–35. <http://doi.org/10.1074/jbc.M110.180711>
- Groen, A. K., & Kuipers, F. (2013). Bile acid look-alike controls life span in *C. elegans*. *Cell Metabolism*, 18(2), 151–152. <http://doi.org/10.1016/j.cmet.2013.07.009>
- Hahm, J.-H., Kim, S., Diloreto, R., Shi, C., Lee, S.-J. V, Murphy, C. T., & Nam, H. G. (2015). *C. elegans* maximum velocity correlates with healthspan and is maintained in worms with an insulin receptor mutation. *Nature Communications*, 6. <http://doi.org/10.1038/ncomms9919>
- Hale, C., Chen, M. M., Stanislaus, S., Chinookoswong, N., Hager, T., Wang, M., ... Xu, J. (2012). Lack of overt FGF21 resistance in two mouse models of obesity and insulin resistance. *Endocrinology*, 153(1), 69–80. <http://doi.org/10.1210/en.2010-1262>
- Herndon, L. A., Schmeissner, P. J., Dudaronek, J. M., Brown, P. A., Listner, K. M., Sakano, Y., ... Driscoll, M. (2002). Stochastic and genetic factors influence tissue-specific decline in ageing *C. elegans*. *Nature*, 419(24), 808–814. <https://pdfs.semanticscholar.org/29de/30c9d05fb4021ff3f5ecb15999cf10730a99.pdf>
- Hochberg, Z. (2012). *Evo-devo of child growth: treatise on child growth and human evolution*. Wiley-Blackwell.
- Hoffmann, M., Segbert, C., Helbig, G., & Bossinger, O. (2010). Intestinal tube formation in *Caenorhabditis*

- elegans requires vang-1 and egl-15 signaling. *Developmental Biology*, 339(2), 268–279. <http://doi.org/10.1016/j.ydbio.2009.12.002>
- Honda, Y., & Honda, S. (1999). The daf-2 gene network for longevity regulates oxidative stress resistance and Mn-superoxide dismutase gene expression in *Caenorhabditis elegans*. *Journal of the Federation of American Societies for Experimental Biology*, 13(11), 1385–1393.
- Honda, Y., & Honda, S. (2002). Oxidative Stress and Life Span Determination in the Nematode *Caenorhabditis elegans*. *Annals of the New York Academy of Sciences*, 959(1), 466–474. <http://doi.org/10.1111/j.1749-6632.2002.tb02117.x>
- Honda, Y., Tanaka, M., & Honda, S. (2008). Modulation of longevity and diapause by redox regulation mechanisms under the insulin-like signaling control in *Caenorhabditis elegans*. *Experimental Gerontology*, 43(6), 520–529. <http://doi.org/10.1016/j.exger.2008.02.009>
- Horikawa, M., & Sakamoto, K. (2010). Polyunsaturated fatty acids are involved in regulatory mechanism of fatty acid homeostasis via daf-2/insulin signaling in *Caenorhabditis elegans*. *Mol Cell Endocrinol*, 323, 183–192. <http://doi.org/10.1016/j.mce.2010.03.004>
- Hotta, Y., Nakamura, H., Konishi, M., Murata, Y., Takagi, H., Matsumura, S., ... Itoh, N. (2009). Fibroblast growth factor 21 regulates lipolysis in white adipose tissue but is not required for ketogenesis and triglyceride clearance in liver. *Endocrinology*, 150, 4625–4633. <http://doi.org/10.1210/en.2009-0119>
- Hsin, H., & Kenyon, C. (1999). Signals from the reproductive system regulate the lifespan of *C. elegans*. *Nature*, 399.
- Hsu, A. L., Murphy, C. T., & Kenyon, C. (2003). Regulation of aging and age-related disease by DAF-16 and heat-shock factor. *Science*, 300, 1142–1145. <http://doi.org/10.1126/science.1083701>
- Hu, P. J. (2007). Dauer. *WormBook*, 1–19. <http://doi.org/10.1895/wormbook.1.144.1>
- Huang, T., Carlson, E. J., Gillespie, A. M., Shi, Y., & Epstein, C. J. (2017). Ubiquitous Overexpression of CuZn Superoxide Dismutase Does Not Extend Life Span in Mice, 55(1), 5–9.
- Iglesias, P., Selgas, R., Romero, S., & Diez, J. J. (2012). Biological role, clinical significance, and therapeutic possibilities of the recently discovered metabolic hormone fibroblastic growth factor 21. *Eur J Endocrinol*, 167, 301–309. <http://doi.org/10.1530/EJE-12-0357>
- Inagaki, Choi, M., Moschetta, A., Peng, L., Cummins, C. L., McDonald, J. G., ... Kliewer, S. A. (2005). Fibroblast growth factor 15 functions as an enterohepatic signal to regulate bile acid homeostasis. *Cell Metabolism*, 2(4), 217–225. <http://doi.org/10.1016/j.cmet.2005.09.001>
- Inagaki, T., Dutchak, P., Zhao, G., Ding, X., Gautron, L., Parameswara, V., ... Kliewer, S. A. (2007). Endocrine regulation of the fasting response by PPARalpha-mediated induction of fibroblast growth factor 21. *Cell Metab*, 5, 415–425. <http://doi.org/10.1016/j.cmet.2007.05.003>
- Ishii, N., Takahashi, K., Tomita, S., Keino, T., Honda, S., Yoshino, K., & Suzuki, K. (1990). A methyl viologen-sensitive mutant of the nematode *Caenorhabditis elegans*. *Mutation Research/DNAging*, 237(3–4), 165–171. [http://doi.org/10.1016/0921-8734\(90\)90022-J](http://doi.org/10.1016/0921-8734(90)90022-J)
- Ito, S., Fujimori, T., Furuya, A., Satoh, J., Nabeshima, Y., & Nabeshima, Y. I. (2005). Impaired negative feedback suppression of bile acid synthesis in mice lacking β Klotho. *Journal of Clinical Investigation*, 115(8), 2202–2208. <http://doi.org/10.1172/JCI23076>

- Ito, S., Fujimori, T., Hayashizaki, Y., & Nabeshima, Y. (2002). Identification of a novel mouse membrane-bound family 1 glycosidase-like protein, which carries an atypical active site structure. *Biochimica et Biophysica Acta (BBA) - General Subjects*, 1576.
- Ito, S., Kinoshita, S., Shiraishi, N., Nakagawa, S., Sekine, S., Fujimori, T., & Nabeshima, Y. I. (2000). Molecular cloning and expression analyses of mouse β klotho, which encodes a novel Klotho family protein. *Mechanisms of Development*, 98(1–2), 115–119. [http://doi.org/10.1016/S0925-4773\(00\)00439-1](http://doi.org/10.1016/S0925-4773(00)00439-1)
- Jones, S. A. (2012). Physiology of FGF15/19 (pp. 171–182). Springer, New York, NY. http://doi.org/10.1007/978-1-4614-0887-1_11
- Kaletta, T., & Hengartner, M. O. (2006). Finding function in novel targets: *C. elegans* as a model organism. *Nat Rev Drug Discov*, 5, 387–398. <http://doi.org/10.1038/nrd2031>
- Keith, S. A., Amrit, F. R. G., Ratnappan, R., & Ghazi, A. (2014). The *C. elegans* healthspan and stress-resistance assay toolkit. *Methods*, 68(3), 476–486. <http://doi.org/10.1016/j.ymeth.2014.04.003>
- Kenyon, C. J., Chang, J., Gensch, E., Rudner, A., & Tabtiang, R. (1993). A *C. elegans* mutant that lives twice as long as wild type. *Nature*, 366, 461–464.
- Kharitonov, A. (2009). FGFs and metabolism. *Curr Opin Pharmacol*, 9, 805–810. <http://doi.org/10.1016/j.coph.2009.07.001>
- Kharitonov, A., Dunbar, J. D., Bina, H. A., Bright, S., Moyers, J. S., Zhang, C., ... Shanafelt, A. B. (2008). FGF-21/FGF-21 receptor interaction and activation is determined by betaKlotho. *J Cell Physiol*, 215, 1–7. <http://doi.org/10.1002/jcp.21357>
- Kharitonov, A., Shiyanova, T. L., Koester, A., Ford, A. M., Micanovic, R., Galbreath, E. J., ... Shanafelt, A. B. (2005). FGF-21 as a novel metabolic regulator. *J Clin Invest*, 115, 1627–1635. <http://doi.org/10.1172/JCI23606>
- Kimura, K. D., Tissenbaum, H. A., Liu, Y., & Ruvkun, G. (1997). *daf-2*, an Insulin Receptor-Like Gene That Regulates Longevity and Diapause in *Caenorhabditis elegans*. *Science*, 277, 942–946. <http://doi.org/10.1126/science.277.5328.942>
- Klip, A., & Pâquet, M. R. (1990). Glucose transport and glucose transporters in muscle and their metabolic regulation. *Diabetes Care*, 13(3), 228–43. <http://doi.org/10.2337/DIACARE.13.3.228>
- Kolumam, G., Chen, M. Z., Tong, R., Zavala-Solorio, J., Kates, L., van Bruggen, N., ... Sonoda, J. (2015). Sustained Brown Fat Stimulation and Insulin Sensitization by a Humanized Bispecific Antibody Agonist for Fibroblast Growth Factor Receptor 1/ β Klotho Complex. *EBioMedicine*, 2(7), 730–743. <http://doi.org/10.1016/j.ebiom.2015.05.028>
- Kulkarni, R. N., Brüning, J. C., Winnay, J. N., Postic, C., Magnuson, M. A., & Kahn, C. R. (1999). Tissue-Specific Knockout of the Insulin Receptor in Pancreatic β Cells Creates an Insulin Secretory Defect Similar to that in Type 2 Diabetes. *Cell*, 96(3), 329–339. [http://doi.org/10.1016/S0092-8674\(00\)80546-2](http://doi.org/10.1016/S0092-8674(00)80546-2)
- Kuro-o, M. (2009). Klotho and aging. *Biochim Biophys Acta*, 1790, 1049–1058. <http://doi.org/10.1016/j.bbagen.2009.02.005>
- Kuro-o, M. (2010). Klotho. *Pflugers Arch*, 459(2), 333–343. <http://doi.org/10.1007/s00424-009-0722-7>

- Kuro-o, Matsumura, Y., Aizawa, H., Kawaguchi, H., Suga, T., Utsugi, T., ... Nabeshima, Y. (1997). Mutation of the mouse *klotho* gene leads to a syndrome resembling ageing. *Nature*, *390*, 45–51.
- Kurosu, H., Choi, M., Ogawa, Y., Dickson, A. S., Goetz, R., Eliseenkova, A. V., ... Kuro-o, M. (2007). Tissue-specific expression of betaKlotho and fibroblast growth factor (FGF) receptor isoforms determines metabolic activity of FGF19 and FGF21. *J Biol Chem*, *282*, 26687–26695. <http://doi.org/10.1074/jbc.M704165200>
- Kurosu, H., & Kuro, O. M. (2009). The Klotho gene family as a regulator of endocrine fibroblast growth factors. *Mol Cell Endocrinol*, *299*, 72–78. <http://doi.org/10.1016/j.mce.2008.10.052>
- Kurosu, H., Ogawa, Y., Miyoshi, M., Yamamoto, M., Nandi, A., Rosenblatt, K. P., ... Kuro-o, M. (2006). Regulation of fibroblast growth factor-23 signaling by *klotho*. *J Biol Chem*, *281*, 6120–6123. <http://doi.org/10.1074/jbc.C500457200>
- Kurosu, H., Yamamoto, M., Clark, J. D., Pastor, J. V, Nandi, A., Gurnani, P., ... Kuro-o, M. (2005). Suppression of aging in mice by the hormone Klotho. *Science*, *309*, 1829–1833. <http://doi.org/10.1126/science.1112766>
- Larsen, P. L., Albert, P. S., & Riddle, D. L. (1995). Genes that regulate both development and longevity in *Caenorhabditis elegans*. *Genetics*, *139*(4), 1567–1583.
- Lee, E.-Y., Jeong, P.-Y., Kim, S.-Y., Shim, Y.-H., Chitwood, D. J., & Paik, Y.-K. (2009). Effects of sterols on the development and aging of *Caenorhabditis elegans*. *Methods Mol Biol*, *462*, 167–179. http://doi.org/10.1007/978-1-60327-115-8_11
- Lee, J. H., Kong, J., Jang, J. Y., Han, J. S., Ji, Y., Lee, J., & Kim, J. B. (2014). Lipid droplet protein LID-1 mediates ATGL-1-dependent lipolysis during fasting in *Caenorhabditis elegans*. *Molecular and Cellular Biology*, *34*(22), 4165–76. <http://doi.org/10.1128/MCB.00722-14>
- Lee, Murphy, C. T., & Kenyon, C. (2009). Glucose shortens the life span of *C. elegans* by downregulating DAF-16/FOXO activity and aquaporin gene expression. *Cell Metab*, *10*, 379–391. <http://doi.org/10.1016/j.cmet.2009.10.003>
- Lemmon, M. A., & Schlessinger, J. (2010). Cell signaling by receptor tyrosine kinases. *Cell*, *141*(7), 1117–1134. <http://doi.org/10.1016/j.cell.2010.06.011>
- Lifestyles statistics team, H. and S. C. I. C. (2014). *Statistics on Obesity, Physical Activity and Diet: England 2014. Health and Social Care Information Centre.*
- Lin, K., Dorman, J. B., Rodan, A., Kenyon, C., Dormanm, J. B., Rodan, A., & Kenyon, C. (1997). *daf-16*: An HNF-3/forkhead Family Member That Can Function to Double the Life-Span of *Caenorhabditis elegans*. *Science*, *278*(5341), 1319–1322. <http://doi.org/10.1126/science.278.5341.1319>
- Lin, K., Dormanm, J. B., Rodan, A., & Kenyon, C. (1997). *daf-16*: An HNF-3/forkhead Family Member That Can Function to Double the Life-Span of *Caenorhabditis elegans*. *Science*, *278*(5341), 1319–1322. <http://doi.org/10.1126/science.278.5341.1319>
- Lin, K., Hsin, H., Libina, N., & Kenyon, C. (2001a). Regulation of the *Caenorhabditis elegans* longevity protein DAF-16 by insulin IGF-1 and germline signaling. *Nature Genetics*, *28*.
- Lin, K., Hsin, H., Libina, N., & Kenyon, C. (2001b). Regulation of the *Caenorhabditis elegans* longevity protein DAF-16 by insulin IGF-1 and germline signaling. *Nature Genetics*, *28*.

- Lin, Wang, M., Blackmore, C., & Desnoyers, L. R. (2007). Liver-specific activities of FGF19 require Klotho beta. *J Biol Chem*, *282*, 27277–27284. <http://doi.org/10.1074/jbc.M704244200>
- Lindhurst, M. J., Parker, V. E. R., Payne, F., Sapp, J. C., Rudge, S., Harris, J., ... Semple, R. K. (2012). Mosaic overgrowth with fibroadipose hyperplasia is caused by somatic activating mutations in PIK3CA. *Nature Genetics*, *44*(8), 928–933. <http://doi.org/10.1038/ng.2332>
- Lithgow, G. J., White, T. M., Hinerfeld, D. A., & Johnson, T. E. (1994). Thermotolerance of a Long-lived Mutant of *Caenorhabditis elegans*. *Journal of Gerontology*, *49*(6), B270–B276. <http://doi.org/10.1093/geronj/49.6.B270>
- Lithgow, G. J., White, T. M., Melov, S., & Johnson, T. E. (1995). Thermotolerance and extended life-span conferred by single-gene mutations and induced by thermal stress. *Proceedings of the National Academy of Sciences of the United States of America*, *92*(16), 7540–7544. <http://doi.org/10.1073/pnas.92.16.7540>
- Love, D. C., Ghosh, S., Mondoux, M. a, Fukushige, T., Wang, P., Wilson, M. a, ... Hanover, J. a. (2010). Dynamic O-GlcNAc cycling at promoters of *Caenorhabditis elegans* genes regulating longevity, stress, and immunity. *Proceedings of the National Academy of Sciences of the United States of America*, *107*(16), 7413–8. <http://doi.org/10.1073/pnas.0911857107>
- Magner, D. B., Wollam, J., Shen, Y., Hoppe, C., Li, D., Latza, C., ... Antebi, A. (2013). The NHR-8 nuclear receptor regulates cholesterol and bile acid homeostasis in *C. elegans*. *Cell Metabolism*, *18*(2), 212–224. <http://doi.org/10.1016/j.cmet.2013.07.007>
- Malone, E. A., & Thomas, J. H. (1994). A screen for nonconditional dauer-constitutive mutations in *Caenorhabditis elegans*. *Genetics*, *136*(3), 879–886. [http://doi.org/10.1016/0092-8674\(93\)90404-E](http://doi.org/10.1016/0092-8674(93)90404-E)
- Matsumura, Y., Aizawa, H., Shiraki-Iida, T., Nagai, R., Kuro-o, M., & Nabeshima, Y. (1998). Identification of the Human Klotho Gene and Its Two Transcripts Encoding Membrane and Secreted Klotho Protein. *Biochemical and Biophysical Research Communications*, *242*, 626–630.
- Matyash, V., Entchev, E. V., Mende, F., Wilsch-Bräuninger, M., Thiele, C., Schmidt, A. W., ... Kurzchalia, T. V. (2004). Sterol-derived hormone(s) controls entry into diapause in *Caenorhabditis elegans* by consecutive activation of DAF-12 and DAF-16. *PLoS Biology*, *2*(10). <http://doi.org/10.1371/journal.pbio.0020280>
- Matyash, V., Geier, C., Henske, A., Mukherjee, S., Hirsh, D., Thiele, C., ... Kurzchalia, T. V. (2001). Distribution and Transport of Cholesterol in *Caenorhabditis elegans*. *Molecular Biology of the Cell*, *12*, 1725–1736.
- McElwee, J. J., Schuster, E., Blanc, E., Thomas, J. H., & Gems, D. (2004). Shared transcriptional signature in *Caenorhabditis elegans* dauer larvae and long-lived *daf-2* mutants implicates detoxification system in longevity assurance. *Journal of Biological Chemistry*, *279*(43), 44533–44543. <http://doi.org/10.1074/jbc.M406207200>
- Merris, M., Kraeft, J., Tint, G. S., & Lenard, J. (2004). Long-term effects of sterol depletion in *C. elegans*: sterol content of synchronized wild-type and mutant populations. *Journal of Lipid Research*, *45*(11), 2044–51. <http://doi.org/10.1194/jlr.M400100-JLR200>
- Merris, M., Wadsworth, W. G., Khamrai, U., Bittman, R., Chitwood, D. J., & Lenard, J. (2003). Sterol effects and sites of sterol accumulation in *Caenorhabditis elegans*: developmental requirement for 4 α -methyl sterols. *Journal of Lipid Research*, *44*(1), 172–81. <http://doi.org/10.1194/JLR.M200323>

- Miraoui, H., Dwyer, A., & Pitteloud, N. (2011). Role of fibroblast growth factor (FGF) signaling in the neuroendocrine control of human reproduction. *Mol Cell Endocrinol*, *346*, 37–43. <http://doi.org/10.1016/j.mce.2011.05.042>
- Mitchell, D. H., Stiles, J. W., Santelli, J., & Sanadi, D. R. (1979). Synchronous Growth and Aging of *Caenorhabditis elegans* in the Presence of Fluorodeoxyuridine. *Journal of Gerontology*, *34*(1), 28–36. <http://doi.org/10.1093/geronj/34.1.28>
- Mitobe, M., Yoshida, T., Sugiura, H., Shirota, S., Tsuchiya, K., & Nihei, H. (2005). Oxidative stress decreases klotho expression in a mouse kidney cell line. *Nephron Exp Nephrol*, *101*, e67-74. <http://doi.org/10.1159/000086500>
- Miyoshi, H., Perfield, J. W., Souza, S. C., Shen, W.-J., Zhang, H.-H., Stancheva, Z. S., ... Greenberg, A. S. (2007). Control of adipose triglyceride lipase action by serine 517 of perilipin A globally regulates protein kinase A-stimulated lipolysis in adipocytes. *The Journal of Biological Chemistry*, *282*(2), 996–1002. <http://doi.org/10.1074/jbc.M605770200>
- Mohler, W. A., Simske, J. S., Williams-Masson, E. M., Hardin, J. D., & White, J. G. (1998). Dynamics and ultrastructure of developmental cell fusions in the *Caenorhabditis elegans* hypodermis. *Current Biology*, *8*(19), 1087–1090. [http://doi.org/10.1016/S0960-9822\(98\)70447-6](http://doi.org/10.1016/S0960-9822(98)70447-6)
- Muise, E. S., Azzolina, B., Kuo, D. W., El-sherbeini, M., Tan, Y., Mu, J., ... Wong, K. K. (2008). Adipose Fibroblast Growth Factor 21 is Up-Regulated by PPAR γ and Altered Metabolic states . <http://doi.org/10.1124/mol.108.044826>
- Murphy, C. T., McCarroll, S. A., Bargmann, C. I., Fraser, A., Kamath, R. S., Ahringer, J., ... Kenyon, C. (2003). Genes that act downstream of DAF-16 to influence the lifespan of *Caenorhabditis elegans*. *Nature*, *424*.
- Nakatani, T., Ohnishi, M., & Razzaque, M. S. (2009). Inactivation of klotho function induces hyperphosphatemia even in presence of high serum fibroblast growth factor 23 levels in a genetically engineered hypophosphatemic (Hyp) mouse model. *FASEB J*, *23*, 3702–3711. <http://doi.org/10.1096/fj.08-123992>
- Narbonne, P., Maddox, P. S., & Labbe, J.-C. (2015). daf-18/PTEN locally antagonizes insulin signalling to couple germline stem cell proliferation to oocyte needs in *C. elegans*. *Development*, 4230–4241. <http://doi.org/10.1242/dev.130252>
- Nishimura, T., Nakatake, Y., Konishi, M., & Itoh, N. (2000). Identification of a novel FGF , FGF-21 , preferentially expressed in the liver, *1492*, 203–206.
- O'Rourke, E. J., Soukas, A. A., Carr, C. E., & Ruvkun, G. (2009). *C. elegans* major fats are stored in vesicles distinct from lysosome-related organelles. *Cell Metab*, *10*, 430–435. <http://doi.org/10.1016/j.cmet.2009.10.002>
- Ogawa, Y., Kurosu, H., Yamamoto, M., Nandi, A., Rosenblatt, K. P., Goetz, R., ... Kuro-o, M. (2007). BetaKlotho is required for metabolic activity of fibroblast growth factor 21. *Proc Natl Acad Sci U S A*, *104*, 7432–7437. <http://doi.org/10.1073/pnas.0701600104>
- Ogg, S., Paradis, S., Gottlieb, S., Patterson, G. I., Lee, L., Tissenbaum, H. A., & Ruvkun, G. (1997). The fork head transcription factor DAF-16 transduces insulin-like metabolic and longevity signals in *C.*

- elegans. *Nature*, 389(6654), 994–999. <http://doi.org/10.1038/40194>
- Pan, D. A., Lillioja, S., Kriketos, A. D., Milner, M. R., Baur, L. A., Bogardus, C., ... Storlien, L. H. (1997). Skeletal muscle triglyceride levels are inversely related to insulin action. *Diabetes*, 46(6), 983–8. <http://doi.org/10.2337/DIAB.46.6.983>
- Patel, D. S., Garza-Garcia, A., Nanji, M., McElwee, J. J., Ackerman, D., Driscoll, P. C., & Gems, D. (2008). Clustering of genetically defined allele classes in the *Caenorhabditis elegans* DAF-2 insulin/IGF-1 receptor. *Genetics*, 178(2), 931–946. <http://doi.org/10.1534/genetics.107.070813>
- Pérez, V. I., Remmen, H. Van, Bokov, A., Epstein, C. J., Vijg, J., & Richardson, A. (2009). The overexpression of major antioxidant enzymes does not extend the lifespan of mice, 73–75. <http://doi.org/10.1111/j.1474-9726.2008.00449.x>
- Pierce, S. B., Costa, M., Wisotzkey, R., Devadhar, S., Homburger, S. A., Buchman, A. R., ... Ruvkun, G. (2001). Regulation of DAF-2 receptor signaling by human insulin and ins-1, a member of the unusually large and diverse *C. elegans* insulin gene family. *Genes Dev*, 15, 672–686.
- Polanska, U. M., Edwards, E., Fernig, D. G., & Kinnunen, T. K. (2011). The cooperation of FGF receptor and Klotho is involved in excretory canal development and regulation of metabolic homeostasis in *Caenorhabditis elegans*. *J Biol Chem*, 286, 5657–5666. <http://doi.org/10.1074/jbc.M110.173039>
- Polanska, U. M., Fernig, D. G., & Kinnunen, T. (2009). Extracellular interactome of the FGF receptor-ligand system: complexities and the relative simplicity of the worm. *Dev Dyn*, 238, 277–293. <http://doi.org/10.1002/dvdy.21757>
- Raamsdonk, J. M. Van, & Hekimi, S. (2009). Deletion of the Mitochondrial Superoxide Dismutase sod-2 Extends Lifespan in *Caenorhabditis elegans*, 5(2). <http://doi.org/10.1371/journal.pgen.1000361>
- Raizen, D. M., & Avery, L. (1994). Electrical Activity and Behavior in the Pharynx of *Caenorhabditis elegans* David, 12, 483–495.
- Raynes, R., Leckey, B. D., Nguyen, K., & Westerheide, S. D. (2012). Heat shock and caloric restriction have a synergistic effect on the heat shock response in a sir2.1-dependent manner in *Caenorhabditis elegans*. *The Journal of Biological Chemistry*, 287(34), 29045–53. <http://doi.org/10.1074/jbc.M112.353714>
- Razzaque, M. S. (2012). The role of Klotho in energy metabolism. *Nat Rev Endocrinol*, 8, 579–587. <http://doi.org/10.1038/nrendo.2012.75>
- Razzaque, M. S., & Lanske, B. (2007). The emerging role of the fibroblast growth factor-23-klotho axis in renal regulation of phosphate homeostasis. *J Endocrinol*, 194, 1–10. <http://doi.org/10.1677/JOE-07-0095>
- Roff, D. A. (1992). *The evolution of life histories : theory and analysis*. Chapman & Hall.
- Rooney, J. P., Luz, A. L., González-Hunt, C. P., Bodhicharla, R., Ryde, I. T., Anbalagan, C., & Meyer, J. N. (2014). Effects of 5'-fluoro-2-deoxyuridine on mitochondrial biology in *Caenorhabditis elegans*. *Experimental Gerontology*, 56, 69–76. <http://doi.org/10.1016/j.exger.2014.03.021>
- Roubin, R., Naert, K., Popovici, C., Vatcher, G., Coulier, F., Thierry-Mieg, J., ... Thierry-Mieg, D. (1999). let-756, a *C. elegans* fgf essential for worm development. *Oncogene*, 18, 6741–6747. <http://doi.org/10.1038/sj.onc.1203074>

- Ruaud, A. F., Katic, I., & Bessereau, J. L. (2011). Insulin/insulin-like growth factor signaling controls non-dauer developmental speed in the nematode *Caenorhabditis elegans*. *Genetics*, *187*(1), 337–343. <http://doi.org/10.1534/genetics.110.123323>
- Saltiel, A. R., & Kahn, C. R. (2001). Insulin signalling and the regulation of glucose and lipid metabolism. *Nature*, *414*(6865), 799–806. <http://doi.org/10.1038/414799a>
- Sharp, Z. D., & Bartke, A. (2005). Evidence for Down-Regulation of Phosphoinositide 3-Kinase/Akt/Mammalian Target of Rapamycin (PI3K/Akt/mTOR)-Dependent Translation Regulatory Signaling Pathways in Ames Dwarf Mice. *The Journals of Gerontology Series A: Biological Sciences and Medical Sciences*, *60*(3), 293–300. <http://doi.org/10.1093/gerona/60.3.293>
- Shim, Y.-H., Chun, J. H., Lee, E.-Y., & Paik, Y.-K. (2002). Role of cholesterol in germ-line development of *Caenorhabditis elegans*. *Molecular Reproduction and Development*, *61*(3), 358–366. <http://doi.org/10.1002/mrd.10099>
- Shimada, T., Kakitani, M., Yamazaki, Y., Hasegawa, H., Takeuchi, Y., Fujita, T., ... Yamashita, T. (2004). Targeted ablation of Fgf23 demonstrates an essential physiological role of FGF23 in phosphate and vitamin D metabolism. *Journal of Clinical Investigation*, *113*, 561–568. <http://doi.org/10.1172/jci200419081>
- Shimada, T., Mizutani, S., Muto, T., Yoneya, T., Hino, R., Takeda, S., ... Yamashita, T. (2001). Cloning and characterization of FGF23 as a causative factor of tumor-induced osteomalacia. *Proceedings of the National Academy of Sciences of the United States of America*, *98*(11), 6500–5. <http://doi.org/10.1073/pnas.101545198>
- Shiraki-Iida, T., Aizawa, H., Matsumura, Y., Sekine, S., Iida, A., Anazawa, H., ... Nabeshima, Y. (1998). Structure of the mouse *klotho* gene and its two transcripts encoding membrane and secreted protein. *Federation of European Biochemical Societies*, *424*, 6–10.
- Shtonda, B. B., & Avery, L. (2006). Dietary choice behavior in *Caenorhabditis elegans*. *J Exp Biol*, *209*, 89–102. <http://doi.org/10.1242/jeb.01955>
- Silverman, G. A., Luke, C. J., Bhatia, S. R., Long, O. S., Vetica, A. C., Perlmutter, D. H., & Pak, S. C. (2009). Modeling molecular and cellular aspects of human disease using the nematode *Caenorhabditis elegans*. *Pediatr Res*, *65*, 10–18. <http://doi.org/10.1203/PDR.0b013e31819009b0>
- Singh, R. N., & Sulston, J. E. (1978). Some Observations On Moulting in *Caenorhabditis Elegans*. *Nematologica*, *24*(1), 63–71. <http://doi.org/10.1163/187529278X00074>
- Somm, E., Henry, H., Bruce, S. J., Aeby, S., Rosikiewicz, M., Sykiotis, G. P., ... Pitteloud, N. (2017). β -Klotho deficiency protects against obesity through a crosstalk between liver, microbiota, and brown adipose tissue. *JCI Insight*, *2*(8), 1–16. <http://doi.org/10.1172/jci.insight.91809>
- Spieth, J., Lawson, D., Davis, P., Williams, G., & Howe, K. (2014). Overview of gene structure in *C. elegans*. *WormBook*, 1–18. <http://doi.org/10.1895/wormbook.1.65.2>
- Stearns, S. C. (1976). Life-History Tactics: A Review of the Ideas. *The Quarterly Review of Biology*, *51*(1), 3–47. <http://doi.org/10.1086/409052>
- Stiernagle, T. (2006). Maintenance of *C. elegans*. In *WormBook* (pp. 1–11). Caenorhabditis Genetics Center, University of Minnesota, Minneapolis, MN 55455, USA. [cgc@umn.edu. http://doi.org/10.1895/wormbook.1.101.1](http://doi.org/10.1895/wormbook.1.101.1)

- Stubbs, J. R., Liu, S., Tang, W., Zhou, J., Wang, Y., Yao, X., & Quarles, L. D. (2007). Role of hyperphosphatemia and 1,25-dihydroxyvitamin D in vascular calcification and mortality in fibroblastic growth factor 23 null mice. *Journal of the American Society of Nephrology: JASN*, 18(7), 2116–24. <http://doi.org/10.1681/ASN.2006121385>
- Sutphin, G. L., & Kaeberlein, M. (2008). Dietary restriction by bacterial deprivation increases life span in wild-derived nematodes. *Experimental Gerontology*, 43(3), 130–135. <http://doi.org/10.1016/j.exger.2007.10.019>
- Talukdar, S., Owen, B. M., Song, P., Hernandez, G., Zhang, Y., Zhou, Y., ... Kliwer, S. A. (2016). FGF21 regulates sweet and alcohol preference. *Cell Metabolism*, 23(2), 344–349. <http://doi.org/10.1016/j.cmet.2015.12.008>
- Talukdar, S., Zhou, Y., Li, D., Rossulek, M., Dong, J., Somayaji, V., ... Calle, R. A. (2016). A long-acting FGF21 molecule, PF-05231023, decreases body weight and improves lipid profile in non-human primates and type 2 diabetic subjects. *Cell Metabolism*, 23(3), 427–440. <http://doi.org/10.1016/j.cmet.2016.02.001>
- Tanaka, T., Ikita, K., Ashida, T., Motoyama, Y., Yamaguchi, Y., & Satouchi, K. (1996). Effects of growth temperature on the fatty acid composition of the free-living nematode *Caenorhabditis elegans*. *Lipids*, 31(11), 1173–8. <http://doi.org/10.1007/BF02524292>
- Taniguchi, C. M., Emanuelli, B., & Kahn, C. R. (2006). Critical nodes in signalling pathways: Insights into insulin action. *Nature Reviews Molecular Cell Biology*, 7(2), 85–96. <http://doi.org/10.1038/nrm1837>
- Tatar, M., Bartke, A., & Antebi, A. (2003). The endocrine regulation of aging by insulin-like signals. *Science*, 299, 1346–1351. <http://doi.org/10.1126/science.1081447>
- Teramoto, T., Lambie, E. J., & Iwasaki, K. (2005). Differential regulation of TRPM channels governs electrolyte homeostasis in the *C. elegans* intestine. *Cell Metab*, 1, 343–354. <http://doi.org/10.1016/j.cmet.2005.04.007>
- The *C. elegans* sequencing consortium. (1998). Genome Sequence Platform of the Nematode *C. elegans*: A Platform for Investigating Biology. *Science*, 282(5396), 2012–2018.
- Thein, M. C., McCormack, G., Winter, A. D., Johnstone, I. L., Shoemaker, C. B., & Page, A. P. (2003). *Caenorhabditis elegans* Exoskeleton Collagen COL-19: An Adult-Specific Marker for Collagen Modification and Assembly, and the Analysis of Organismal Morphology. *Developmental Dynamics*, 226, 523–539. <http://doi.org/10.1002/dvdy.10259>
- Tissenbaum, H. A., & Guarente, L. (2001). Increased dosage of a sir-2 gene extends lifespan in *Caenorhabditis elegans*. *Nature*, 410(6825), 227–230. <http://doi.org/10.1038/35065638>
- Tissenbaum, H. A., & Ruvkun, G. (1998). An Insulin-like Signaling Pathway Affects Both Longevity and Reproduction in *C. elegans*. *Genetics*, 703–717.
- Tohyama, O., Imura, A., Iwano, A., Freund, J. N., Henrissat, B., Fujimori, T., & Nabeshima, Y. (2004). Klotho is a novel beta-glucuronidase capable of hydrolyzing steroid beta-glucuronides. *J Biol Chem*, 279, 9777–9784. <http://doi.org/10.1074/jbc.M312392200>
- Tomiyama, K., Maeda, R., Urakawa, I., Yamazaki, Y., Tanaka, T., Ito, S., ... Nabeshima, Y. (2010). Relevant use of Klotho in FGF19 subfamily signaling system in vivo. *Proc Natl Acad Sci U S A*, 107, 1666–1671. <http://doi.org/10.1073/pnas.0913986107>

- Tomlinson, E., Fu, L., John, L., Hultgren, B., Huang, X., Renz, M., ... Stewart, T. A. (2002). Transgenic Mice Expressing Human Fibroblast Growth Factor-19 Display Increased Metabolic Rate and Decreased Adiposity. *Endocrinology*, *143*(5), 1741–1747. <http://doi.org/10.1210/endo.143.5.8850>
- Trošt, N., Peňa-Ilopis, S., Koirala, S., & Stojan, J. (2015). γ Klotho is a novel marker and cell survival factor in a subset of triple negative breast cancers, *7*(3).
- Tsujikawa, H., Kurotaki, Y., Fujimori, T., Fukuda, K., & Nabeshima, Y.-I. (2003). *Klotho*, a Gene Related to a Syndrome Resembling Human Premature Aging, Functions in a Negative Regulatory Circuit of Vitamin D Endocrine System. *Molecular Endocrinology*, *17*(12), 2393–2403. <http://doi.org/10.1210/me.2003-0048>
- Tucker, V. A. (1970). Energetic cost of locomotion in animals. *Comparative Biochemistry And Physiology*, *34*(4), 841–846. [http://doi.org/10.1016/0010-406X\(70\)91006-6](http://doi.org/10.1016/0010-406X(70)91006-6)
- Uebanso, T., Taketani, Y., Yamamoto, H., Amo, K., Ominami, H., Arai, H., ... Takeda, E. (2011). Paradoxical regulation of human FGF21 by both fasting and feeding signals: is FGF21 a nutritional adaptation factor? *PLoS One*, *6*(8), e22976. <http://doi.org/10.1371/journal.pone.0022976>
- Unger, R. H. (2006). Klotho induced insulin resistance: a blessing in disguise? *Nature Medicine*, *12*(1), 56–57. <http://doi.org/10.1038/nm0106-56>
- Urakawa, I., Yamazaki, Y., Shimada, T., Iijima, K., Hasegawa, H., Okawa, K., ... Yamashita, T. (2006). Klotho converts canonical FGF receptor into a specific receptor for FGF23. *Nature*, *444*, 770–774. <http://doi.org/10.1038/nature05315>
- Van-Raamsdonk, J., Hekimi, S., Van Raamsdonk, J. M., & Hekimi, S. (2010). Reactive oxygen species and aging in *Caenorhabditis elegans*: causal or casual relationship? *Antioxid Redox Signal*, *13*(12), 1911–1953. <http://doi.org/10.1089/ars.2010.3215>
- Van Gilst, M. R., Hadjivassiliou, H., & Yamamoto, K. R. (2005). A *Caenorhabditis elegans* nutrient response system partially dependent on nuclear receptor NHR-49. *Proc Natl Acad Sci U S A*, *102*, 13496–13501. <http://doi.org/10.1073/pnas.0506234102>
- Vanfleteren, J. R. (1993). Oxidative stress and ageing in *Caenorhabditis elegans*. *The Biochemical Journal*, *292* (Pt 2), 605–608.
- Villena, J. A., Roy, S., Sarkadi-Nagy, E., Kim, K.-H., & Sul, H. S. (2004). Desnutrin, an Adipocyte Gene Encoding a Novel Patatin Domain- containing Protein, Is Induced by Fasting and Glucocorticoids ECTOPIC EXPRESSION OF DESNUTRIN INCREASES TRIGLYCERIDE HYDROLYSIS*. <http://doi.org/10.1074/jbc.M403855200>
- Walker, G. a, White, T. M., McColl, G., Jenkins, N. L., Babich, S., Candido, E. P., ... Lithgow, G. J. (2001). Heat shock protein accumulation is upregulated in a long-lived mutant of *Caenorhabditis elegans*. *The Journals of Gerontology. Series A, Biological Sciences and Medical Sciences*, *56*(7), B281–B287. <http://doi.org/10.1093/gerona/56.7.B281>
- Wei, W., Dutchak, P. A., Wang, X., Ding, X., Wang, X., Bookout, A. L., ... Wan, Y. (2012). Fibroblast growth factor 21 promotes bone loss by potentiating the effects of peroxisome proliferator-activated receptor gamma. *Proc Natl Acad Sci U S A*, *109*(8), 3143–3148. <http://doi.org/10.1073/pnas.1200797109>
- Westerheide, S. D., Ankar, J., Stevens Jr., S. M., Sistonen, L., & Morimoto, R. I. (2009). Stress-inducible regulation of heat shock factor 1 by the deacetylase SIRT1. *Science*, *323*(5917), 1063–1066.

<http://doi.org/10.1126/science.1165946>

- White, K. E., Evans, W. E., O'Riordan, J. L. H., Speer, M. C., Econs, M. J., Lorenz-Depiereux, B., ... Strom, T. M. (2000). Autosomal dominant hypophosphataemic rickets is associated with mutations in FGF23. *Nature Genetics*, 26(3), 345–348. <http://doi.org/10.1038/81664>
- White, K. E., Jonsson, K. B., Carn, G., Hampson, G., Spector, T. D., Mannstadt, M., ... Econs, M. J. (2001). The Autosomal Dominant Hypophosphatemic Rickets (ADHR) Gene Is a Secreted Polypeptide Overexpressed by Tumors that Cause Phosphate Wasting. *The Journal of Clinical Endocrinology & Metabolism*, 86(2), 497–500. <http://doi.org/10.1210/jcem.86.2.7408>
- Wolf, I., Levanon-Cohen, S., Bose, S., Ligumsky, H., Sredni, B., Kanety, H., ... Rubinek, T. (2008). Klotho: a tumor suppressor and a modulator of the IGF-1 and FGF pathways in human breast cancer. *Oncogene*, 27, 7094–7105. <http://doi.org/10.1038/onc.2008.292>
- Wu, A. L., Coulter, S., Liddle, C., Wong, A., Eastham-Anderson, J., French, D. M., ... Sonoda, J. (2011). FGF19 regulates cell proliferation, glucose and bile acid metabolism via FGFR4-dependent and independent pathways. *PLoS ONE*, 6(3). <http://doi.org/10.1371/journal.pone.0017868>
- Wu, Ge, H., Gupte, J., Weiszmann, J., Shimamoto, G., Stevens, J., ... Li, Y. (2007). Co-receptor requirements for fibroblast growth factor-19 signaling. *J Biol Chem*, 282, 29069–29072. <http://doi.org/10.1074/jbc.C700130200>
- Wu, X., Lemon, B., Li, X., Gupte, J., Weiszmann, J., Stevens, J., ... Li, Y. (2008). C-terminal tail of FGF19 determines its specificity toward Klotho co-receptors. *J Biol Chem*, 283, 33304–33309. <http://doi.org/10.1074/jbc.M803319200>
- Xie, M.-H., Holcomb, I., Deuel, B., Dowd, P., Huang, A., Vagts, A., ... Gurney, A. L. (1999). FGF-19, A NOVEL FIBROBLAST GROWTH FACTOR WITH UNIQUE SPECIFICITY FOR FGFR4. *CYTOKINE*, 11(10), 729–735.
- Xu, C., Messina, A., Somm, E., Miraoui, H., Kinnunen, T., Jr, J. A., ... Pitteloud, N. (2017). KLB , encoding b -Klotho , is mutated in patients with congenital hypogonadotropic hypogonadism. *EMBO Molecular Medicine*, 1–19. <http://doi.org/10.15252/emmm.201607376>
- Yamamoto, M., Clark, J. D., Pastor, J. V., Gurnani, P., Nandi, A., Kurosu, H., ... Kuro-O, M. (2005). Regulation of oxidative stress by the anti-aging hormone klotho. *Journal of Biological Chemistry*, 280(45), 38029–38034. <http://doi.org/10.1074/jbc.M509039200>
- Yang, W., Li, J., & Hekimi, S. (2007). A measurable increase in oxidative damage due to reduction in superoxide detoxification fails to shorten the life span of long-lived mitochondrial mutants of *Caenorhabditis elegans*. *Genetics*, 177(4), 2063–2074. <http://doi.org/10.1534/genetics.107.080788>
- Yen, K., Patel, H. B., Lublin, A. L., & Mobbs, C. V. (2009). SOD isoforms play no role in lifespan in ad lib or dietary restricted conditions, but mutational inactivation of SOD-1 reduces life extension by cold. *Mechanisms of Ageing and Development*, 130(3), 173–178. <http://doi.org/10.1016/j.mad.2008.11.003>
- Zechner, R., Zimmermann, R., Eichmann, T. O., Kohlwein, S. D., Haemmerle, G., Lass, A., ... Zechner, R. (2012). FAT SIGNALS--lipases and lipolysis in lipid metabolism and signaling. *Cell Metabolism*, 15(3), 279–91. <http://doi.org/10.1016/j.cmet.2011.12.018>
- Zhang, Box, A. C., Xu, N., Le Men, J., Yu, J., Guo, F., ... Mak, H. Y. (2010). Genetic and dietary regulation of lipid droplet expansion in *Caenorhabditis elegans*. *Proc Natl Acad Sci U S A*, 107, 4640–4645.

<http://doi.org/10.1073/pnas.0912308107>

Zhang, H., Li, Y., Fan, Y., Wu, J., Zhao, B., Guan, Y., ... Wang, N. (2008). Klotho is a target gene of PPAR-gamma. *Kidney Int*, 74, 732–739. <http://doi.org/10.1038/ki.2008.244>

Appendix 1

Full list of all the strains obtained:

1. TC446 *klo-2(ok1862)* III; *klo-1(ok2925)* IV
2. TC510 *daf-2(e1370)* III *klo-2(ok1862)* III
3. TC528 *daf-2(e1370)* III; *klo-1(ok2925)* IV
4. TC489 *daf-2(e1370)* *klo-2(ok1862)* III; *klo-1(ok2925)* IV
5. TC520 *daf-16(mu86)* I; *daf-2(e1370)* III
6. TC515 *daf-16(mu86)* I; *klo-2(ok1862)* III
7. TC519 *daf-16(mu86)* I; *klo-1(ok2925)* IV
8. TC521 *daf-16(mu86)* I; *klo-2(ok1862)* III; *klo-1(ok2925)* IV
9. TC513 *daf-16(mu86)* I; *daf-2(e1370)* *klo-2(ok1862)* III; *klo-1(ok2925)* IV
10. TC516 *daf-16(mu86)* I; *daf-2(e1370)* *klo-2(ok1862)* III

Transgenic strains expressing jtEx179 [*myo-2::GFP*; *pklo-1::mCherry*]

11. TC474 jtEx179 [*myo-2::GFP*; *pklo-1::mCherry*]
12. *klo-1(ok2925)* jtEx179 [*myo-2::GFP*; *pklo-1::mCherry*]
13. TC475 *klo-2(ok1862)* III; *klo-1(ok2925)* IV; jtEx179 [*myo-2::GFP*; *pklo-1::mCherry*]
14. TC529 *daf-2(e1370)* III; *klo-1(ok2925)* IV; jtEx179 [*myo-2::GFP*; *pklo-1::mCherry*]

Transgenic strains expressing jtEx129 [*pklo-2::GFP*; *ptph::mCherry*]

15. TC391 jtEx129 [*pklo-2::GFP*; *ptph::mCherry*]

Transgenic strains expressing waEx15 [*fat-7::GFP* + *lin-15(+)*]

16. BX113 *lin-15B&lin-15A(n765)* X; waEx15 [*fat-7::GFP* + *lin-15(+)*]
17. TC506 *klo-1(ok2925)* IV; *lin-15B&A(n765)* X; waEx15 [*fat-7::GFP* + *lin-15(+)*]
18. TC507 *klo-2(ok1862)* III; *lin-15B&A(n765)* X; waEx15 [*fat-7::GFP* + *lin-15(+)*]
19. TC508 *klo-2(ok1862)* III; *klo-1(ok2925)* IV; *lin-15B&A(n765)* X; waEx15 [*fat-7::GFP* + *lin-15(+)*]

Transgenic strains expressing hjls67 [*atgl::ATGL-1::GFP* + *mec-7::RFP*]

20. VS20 hjls67 [*atgl-1p::atgl-1::GFP* + *mec-7::RFP*]

21. TC488 *klo-2(ok1862)* III; *hjls67 [atgl-1p::atgl-1::GFP + mec-7::RFP]*
22. TC511 *klo-2(ok1862)* III; *klo-1(ok2925)* IV; *hjls67 [atgl-1p::atgl-1::GFP + mec-7::RFP]*

Transgenic strains expressing *huls33[sod-3::GFP + rol-6(su1006)]*

23. KN259 *huls33[sod-3::GFP + rol-6(su1006)]*
24. KN478 *daf-16(mu86)* *huls33[sod-3::GFP + rol-6(su1006)]*
25. TC522 *klo-1(ok2925)* IV; *huls33[sod-3::GFP + rol-6(su1006)]*
26. TC523 *klo-2(ok1862)* III; *huls33[sod-3::GFP + rol-6(su1006)]*
27. TC526 *klo-2(ok1862)* III; *klo-1(ok2925)* IV; *huls33[sod-3::GFP + rol-6(su1006)]*

Transgenic strains expressing *rrls1 [elt-2::GFP + unc-119(+)] X*

28. TC476 *rrls1 [elt-2::GFP + unc-119(+)] X*
29. TC478 *klo-2(ok1862)* III; *rrls1 [elt-2::GFP + unc-119(+)] X*
30. TC479 *klo-1(ok2925)* IV; *rrls1 [elt-2::GFP + unc-119(+)] X*
31. TC477 *klo-2(ok1862)* III; *klo-1(ok2925)* IV; *rrls1 [elt-2::GFP + unc-119(+)] X*

Transgenic strains expressing *ncls13 [ajm-1::GFP]*

32. TC480 *nCIS13 [ajm-1::GFP]*
33. TC481 *klo-2(ok1862)* III; *nCIS13 [ajm-1::GFP]*
34. TC487 *klo-1(ok2925)* IV; *nCIS13 [ajm-1::GFP]*
35. TC485 *klo-2(ok1862)* III; *klo-1(ok2925)* IV; *nCIS13 [ajm-1::GFP]*
36. TC486 *ncls13 [ajm-1::GFP]; him-5 (e1490) V*
37. TC483 *klo-2(ok1862)* III; *nCIS13 [ajm-1::GFP]; him-5 (e1490) V*
38. TC482 *klo-1(ok2925)* IV; *nCIS13 [ajm-1::GFP]; him-5 (e1490) V*
39. TC484 *klo-2(ok1862)* III; *klo-1(ok2925)* IV; *nCIS13 [ajm-1::GFP]; him-5(e1490) V*

Appendix 2

Primer sequences:

TK166	ATGTCGCTGGCAACTAAATTC
TK175	TCACAGTTCTCCCTGTTAAG
TK176	TCAATGTCTTCCTGCGAATC
TK263	GTTCAAACCTTCTGGTATTCCATTC
TK264	ACCGATTTTTGAGAGAAGAGCAAC
TK265	GGTAATTTTTCTCTCATTGAGGCTG
TK280_klo1F	ATGTCTTTGCCAACTAAATTTCCAAAAAATTTCC
TK281_klo1R	CTACAAAAGATTATGATGCTTTTTAAATTCGCG
TK282_klo2F	ATGTCGCTGGCAACTAAATTCCCC
TK283_klo2R	TCAAATCCCATGAAAATCCTTGA ACTCC
TK311	ACGGTGACCATCTAGAGTCAC
TK312	CTAGGAGGAAAAGCCATTTGTC
TK313	CAATAGCTGGAGAAACACGAG
TK314	TCATCGGTGTCTCATCAATCG
TK315	GCGATGGTTGTGATGGAAATG

Appendix 3

Experiment methodology was explained in chapter 2.7 Figure 8. Basically, L1 stage worms grown on *E. coli OP50* were transferred to a new plate onto a spot equidistant from two food sources, *E. coli OP50* and *E. coli HB101* (more nutritious than *OP50* (L Avery & You, 2012)). There is no food preference along time. Worms stayed in the food lawn they first found and only after 2 days there was a relative increment in the *E. coli HB101* lawn. This is due to the better growth of the *HB101* strain, while *OP50* grows slower. After 2 days the *OP50* lawn was almost exhausted and worms searched for other food, causing the relative percentage increment of worms outside the food and worms in *E. coli HB101*. No food sensing differences could be observed between different *C. elegans* strains.

